FORMULATION AND CHARACTERISATION OF NOVEL FILMS FOR BUCCAL MUCOSA DRUG DELIVERY FOR PAEDIATRIC PATIENTS

SAJJAD KHAN [BSc (Hons), MSc (Pharm Sci.)]

A thesis submitted in partial fulfilment of the requirements of the University of Greenwich for the Degree of Doctor of Philosophy

FEBRUARY, 2015

DECLARATION

"I certify that this work has not been accepted in substance for any degree, and is not concurrently being submitted for any degree other than that of Doctor of Philosophy being studied at the University of Greenwich. I also declare that this work is the result of my own investigations except where otherwise identified by references and that I have not plagiarised the work of others".

SAJJAD KHAN (CANDIDATE)

……

PhD Supervisors

Dr Joshua Boateng ……..

Dr Vivek Trivedi …….

FEBRUARY, 2015

ACKNOWLWDGEMENTS

"In the name of Allah, most Gracious, most Compassionate"

Praise be to Allah, the most gracious the ever merciful, who gave me the strength, focus, knowledge and motivation to bring me to where I am today.

I would like to specially thanks and express my gratitude to my supervisors especially Dr Joshua Boateng (and as an older brother) for working with me, his assistance, guidance towards this project and for being patient and understanding when complications arose during the course of this project.

I would also like to thank Dr Laura Waters/Prof John Mitchell's who supported me to gain a PhD place in University of Greenwich. Also special thanks to Prof John Mitchell for guiding me through my PhD experience and when problems occurred guided me as a fatherly manner.

Thanks to all the academic staff in the school of Science for their help throughout my PhD and group members. I am also grateful for Dr Ian Slipper for all the SEM and XPD techniques, Devyani Amin for the HPLC analysis and Dr Samuel Owusu-Ware for helping me with DSC and TGA studies.

Finally, I am extremely and deeply grateful to my parents for being my support throughout my whole life and my study, also I would thank my brothers and sisters for supporting me and special thanks to my sister Salma Khan for her patience and support throughout my education.

ABSTRACT

The main aim of this project was to develop, formulate, characterise and optimise novel pre-formed thin polymer film that will deliver therapeutically relevant drugs via the buccal mucosa route of paediatric patients, using OME as model drug. The development focused on obtaining formulations with optimized drug loading, drug release and permeation, stability and low toxicity. Five different film forming polymers hydroxypropyl methylcellulose (HPMC), methylcellulose (MC), sodium alginate (SA), carrageenan (CA) and metolose (MET) were used initially and subsequently with polyethylene glycol (PEG 400) as plasticiser and L-arg (to stabilise OME). Polymeric gels (1% w/w) were prepared using water and ethanol (10% v/v and 20% v/v) as the casting solvents with PEG 400 at different concentrations (0 and 0.5 % w/w) and the films were obtained by drying the gels in an oven (40 °C). SA and MET films were chosen for drug loading and further investigation (OME stabilisation). These films showed a good balance between flexibility and toughness required for ease of transportation and patient handling. Drug loaded gels showed that OME was unstable, with gels turning red after 20 minutes and therefore required addition of L-arg. From the results obtained, plasticised (0.5 % w/w PEG 400) MET films prepared from ethanolic (20% v/v) gels and containing OME : L-arg ratio of 1:2 showed the most ideal characteristics (transparency, ease of peeling and flexibility) and was the formulation of choice for further investigation. Results obtained for the hydration and *in vitro* mucoadhesion studies showed that plasticised films had higher swelling capacity and mucoadhesivity than unplasticised films. In addition, BLK films showed higher swelling index and adhesion than DL films, whilst gelatine equilibrated with PBS showed higher values compared with simulated saliva (SS). Dissolution data from optimised DL MET films showed OME release was sustained over 1 hour. Fitting the release data to kinetic models showed that the Korsmeyer-Peppas equations best fit the dissolution data for both PBS and SS media. The permeability profile of optimised DL film using pig buccal tissue, showed that the amount of OME permeating over 2 hours was 275ug/cm^2 suggesting that pig buccal membrane is generally quite permeable and also that the OME is released from the films. Application of SCF caused significant changes to the functional and physical properties of the MET films and converted the original DL MET films from a sustained release formulation (1 hour) to a rapid release system, releasing > 90% of OME within 15 minutes and the release of OME from these films followed Higuchi kinetic model. Finally, incorporation of β cyclodextrin (βCD) into DL MET films containing OME:L-arg 1:1, improved the stability of the drug over

28 days under ambient conditions compared to 14 days for the corresponding DL MET films containing only L-arg at a higher loading (OME: L-arg 1:2). The optimised formulations have potential as paediatric buccal delivery system for OME.

CONTENTS

CHAPTER TWO: FORMULATION DEVELOPMENT, OPTIMIZATION AND PHYSICAL CHARACTERIZATION OF BLANK SOLVENT CAST FILMS

CHAPTER THREE: FORMULATION DEVELOPMENT AND OPTIMIZATION OF OMEPRAZOLE LOADED SOLVENT CAST FILMS AND DRUG STABILISATION USING L-ARGININE

LIST OF FIGURES

LIST OF TABLES

ABBREVIATIONS

FT-IR - (Fourier transform infrared)

AUC – Area under the curve

BLK - Blank

CA – Carrageenan

CD – Cyclodextrin

βCD – Beta cyclodextrin

γCD – Gamma cyclodextrin

DL – Drug loaded

DSC - Differential scanning calorimetry

EtOH – Ethanol

EuPFI - The European Paediatric Formulation Initiative's

GERD - Gastro-oesophageal reflux disease

GIT - Gastro-intestine tract

H2RAs - Histamine receptor 2 antagonists

HSM – Hot stage microscopy

HPLC – High-performance liquid chromatography

HPMC – Hydroxypropylmethylcellulose

ICH – International Conference on Harmonisation

L-arg – L-arginine

MC – Methylcellulose

MCGs - Membrane coating granules

MET – Metolose

MTT – 3 - (4,5-dimethylthiazol-2-yl)-2,5-diphenyltetrazolium bromide]

N – Newton

$N.mm^2$ – Newton per square millimetre

NSAID - Non-steroidal anti-inflammatory drugs

OME – Omeprazole

OTF – Oral thin film

PAF – Peak adhesive force

PEG – Polyethylene glycol

PBS – Phosphate buffered saline

PPIs – Proton pump inhibitors

SA – Sodium alginate

$scCO_2$ – Supercritical carbon dioxide

SCF – Supercritical fluid

SEM – Scanning electron microscopy

SS – Simulated saliva

TA – Texture analysis

T_g - Glass transition temperature

TGA – Thermogravimetric analysis

TWA – Total work of adhesion

v/v – Volume per volume

w/w – Weight per weight

WHO - World Health Organization

WOA – Work of adhesion

XRD – X-ray diffraction

LIST OF PUBLICATIONS

Sajjad Khan, Joshua S. Boateng, John Mitchell & Vivek Trivedi. (2015). Formulation, Characterisation and Stabilisation of Buccal Films for Paediatric Drug Delivery of Omeprazole. AAPS PharmSciTech DOI 10.1208/s12249-014-0268-7.

Joshua Boateng, Obinna Okeke, **Sajjad Khan**. 2015. Polyssacharide Based Formulations for Mucosal Drug Delivery. *Current Pharmaceutical Design* (Invited Review) In Press.

MANUSCRIPTS IN PREPARATION

Sajjad Khan et al., Hydration, *in-vitro* mucoadhesion, drug stability, *in-vitro* drug dissolution characteristics and release mechanisms of omeprazole loaded metolose (MET) films.

Sajjad Khan et al., *Ex-vivo*, permeation and mucoadhesion using pig buccal tissue, and cell toxicity of omeprazole loaded films.

Sajjad Khan et al., Fast dissolving film from slow release drug loaded metolose (MET) film using supercritical fluid (CO_2) technique.

CONFERENCE PROCEEDINGS

Sajjad Khan, Joshua Boateng. 2015. *In-vitro* buccal permeation and mucoadhesion studies of omeprazole loaded paediatric films using porcine tissue. European Conference on Pharmaceutics and Drug Delivery. Reims, France April 2015. (Accepted).

Sajjad Khan, Vivek Trivedi, John Mitchell, Joshua Boateng. 2014. Physico-chemical characterization of oral thin film for paediatric buccal drug delivery. Academy of Pharmaceutical Sciences UKPHARMSCI Conference, Hertfordshire University, UK.

Sajjad Khan, Vivek Trivedi, John Mitchell, Joshua Boateng. 2014. Formulation and Characterisation of Oral Thin Films for Buccal Mucosa Drug Delivery for Paediatric Patients. Annual International Conference on Pharmaceutical Sciences, Athens. (**Podium presentation**).

CHAPTER ONE: GENERAL INTRODUCTION AND LITERATURE REVIEW

1.1 Overview

Over the past few decades, there has been an increased interest in novel drug delivery systems to improve safety, efficacy and patient compliance, thereby increasing the product patent life cycle (Panda et al., 2012). The discovery and development of new chemical entities is not only expensive but also time consuming and pharmaceutical industries are focusing on the design and development of innovative drug delivery systems for existing drugs. An example of such a delivery system is the oral thin film (OTF), which has gained popularity among paediatric and geriatric patients. Oral thin films (Figure 1.1) present with many benefits and are largely risk free to paediatric and geriatric patients (Giovino et al., 2012).

Figure 1.1 Example of oral thin film. Available at - <http://www.romaco.com/uploads/tx_easynews/Strip_Tabs_03.jpg >[Accessed: 23/07/2013]

Oral drug delivery systems have always been an important means of drug administration; however, many paediatric patients are unwilling to take solid dosage forms due to many reasons including bitter taste and fear of choking. Due to the numerous advantages of buccal dosage forms, pharmaceutical companies have adopted various technologies to manufacture oral films on a large scale as an alternative to traditional dosage forms such as tablets and capsules (Siddhiqui et al., 2011). Generally, drug administration occurs via various routes with varying degrees of benefits and drawbacks (Kalani., 2011). Over the last few decades, administration of drugs in the human body has been the main area of research and different types of routes have been exploited as described in Table 1.1. The rejection rate of oral dosage forms is higher than other routes (topical, intravenous, intramuscular), due to the

unpleasant and bitter taste of the medicine (Panda et al., 2012) as previously noted. Administration of drug to paediatric patients' body is always a challenge as paediatric dosage forms require accurate doses based on the age and body weight (Gyllenhaal., 1993).

Table 1.1 Different routes of drug administration for paediatric patients.

Routes of administration	**Drug name**	**Dosage and frequency**	**Mechanism of action**
Oral cavity (tablets, capsules or syrups)	Paracetamol	10 – 500 mg per 4 hrs in 24 hrs	Inhibition of cycooygenase (COX) Analgesia and antipyretic effects.
Sublingual	Lorazepam	50 – 100 mg/kg 1 hr before procedure	Anti-anxiety agent with few side effects. Preanesthtic agent
Topical (skin)	Clotrimazole	2 – 3 times daily	Broad spectrum of antimycotic activity. It inhibits biosynthesis of the sterol membrane permeability and apparent disruption of enzyme systems bound to the membrane.
Parenteral (vein, subcutaneous)	Dipeptiven	300 – 400mg/kg daily	Clinical nutrition regimen in patient in hypercataabolic and hypermetabolic states.
Rectal (creams, solutions)	Codeine	0.5 – 1 mg/kg every 4 - 6 hrs max. 240mg daily 30 – 60 mg every 4-6 hrs max. 240 mg daily	An opoid analgesic similar to morphine but with less potent analgesic properties and mild sedative effects. It acts centrally to suppress cough.
Respiratory (inhalation, aerosols)	Budesonide	200 mg each nostril once daily	Glucocorticoid steroid for the treatment of asthma, COPD and infectious rhinitis.
Intrathecal (Lumbar or Ommaya reservoir)	Cytotoxic chemotherapy	Lumbar administration as required	Used for pain management and administration of cytotoxic chemotherapy drugs.
Conjunctival (Ointments)	Dexamethasone	Apply eye dropd 4 – 6 times daily	Anti-inflammator 9-fluro-gluococorticoid.
Vaginal (Cream, Emulsions)	Clotrimazole	Apply to anogenital area 2 – 3 times daily	Interacts with yeast
Intraocular (solutions, creams)	Alphagan P 0.1 %	Apply every 2 hrs as required	Is a route of eye medication that's approved for lowering high eye pressure in patient with angle glaucoma or ocular hypertension

Oral mucosa (buccal) thin films offer easy administration and handling, can provide rapid disintegration and dissolution or sustained release, bypasses first-pass metabolism, enhanced stability and taste masking for bitter drugs, local and systematic drug delivery, rapid onset action, and no trained or professional person is required for paediatric administration (Bala et al., 2013).

In 2007, the WHO launched an initiative "Make medicine child size" with the aim to raise awareness and accelerate action on providing access to child – specific medicines. The model formulary for children (WHO, 2010) provides independent prescriber information on dosage and treatment guidance for medicines based on the WHO model list of essential medicines for paediatrics. The desirable features that are essential and need to be taken into consideration when designing paediatric dosage forms include:

- Convenient, reliable administration
- Preferably ready-to-use formulations
- Minimal manipulation by health care professionals, parents or caregivers
- Dose and dose volume/weight adjusted to the intended age group
- Acceptable and palatable dosage form
- Minimum dosing frequency
- Minimal impact on life style
- Minimum, non-toxic excipients
- Transportable and low bulk/weight
- Easy to produce and stable in as variety of climates
- Affordable
- Commercially viable

Some of the above features are considered for certain paediatric drugs such as dose and dosage volume, while others such as transport, weight and affordability address end–user needs in developing countries.

As discussed previously, the design and selection of new pharmaceutical dosage forms involves the careful consideration and a balance between quality target product profile versus technical challenges and development feasibility. Paediatric dosage forms present particular complexity due to the diverse patient population, compliance challenges and safety

consideration amongst this vulnerable population. The paediatric population is divided into six groups such as; pre-term new-born, infant, term new-born infants, infants/toddlers, pre-school children, school children and adolescents (Hans et al., 1999). Further challenges include size and physiological and biological maturation, difficulties and low tolerance to unacceptable taste, specific concerns associated with required excipients (Bowles et al, 2010). These are discussed in detail in subsequent sections below.

Drug therapy plays a vital role in disease management for paediatric populations suffering from a variety of acute and chronic diseases. The majority of drugs approved for adults, however, have not been approved for use in children though such medicines are commonly used in paediatric populations. One of the most important impediments for their application however, is the lack of suitable alternative paediatric dosage forms. Nahata, (1999) reported that many drugs used in paediatric populations are not available in suitable dosage forms such as thin films and must be prepared extemporaneously, while using appropriate excipients. However, it is essential to determine the stability of various drugs at clinically important concentrations and safe practical storage conditions.

1.2 Gastro-oesophageal reflux

Gastro-oesophageal reflux refers to the excessive flow of gastric acid proximally into the oesophagus. It occurs in the majority of infants and presents with a wide range of symptoms, from infants with occasional physiological reflux (happy spitters) to infants with haematemesis, oesophageal stricture formation, apnoea, or even sudden infant death syndrome. Most infants have physiological gastro-oesophageal reflux with no definite anatomic, metabolic, neurological, or infectious cause and no serious associated complications (Choonara et al., 1999). Furthermore, studies assessing outcome with early therapy have indicated that as many as 55% of infants are symptom free by 10 months of age and 81% by 18 months (Lind et al., 1983). However, it is important to determine which infants have significant gastro-oesophageal reflux-associated disease to use the safest and most effective therapy for treating the symptoms (Missaghi., 2006).

Although simple measures such as positioning, feed changes, feed thickeners and alginate preparations, may be effective in the majority of cases, an effective therapeutic option is required for infants who do not respond to these measures or who have symptoms suggestive

of high levels of supine nocturnal percentage acid reflux time (complicated reflux) (Sachs, 1995).

Cisapride, the non-dopamine receptor blocking, non-cholinergic pro-kinetic drug with 5HT-4 antagonist properties, improves pH metric variables and has been the drug of first choice in gastro-oesophageal reflux (Ameen, et al., 2006). However, because of concerns regarding cardiac dysrhythmias associated with its use, it is now not generally available for prescription. H_2 receptor blockers can improve oesophagitis in older children, and high-dosage ranitidine (20 mg · kg^{-1} · day^{-1}) has been shown to be effective in refractory reflux oesophagitis, but rebound nocturnal acid secretion has been reported (Madanick., 2011). Trials and recent work with proton pump inhibitors (PPIs) (omeprazole, lansoprazole, pantoprazole etc.) suggested that they are safer and an effective therapeutic strategy in reflux oesophagitis in older children. However, a higher dosage per kilogram may be required than those used in adult studies (e.g. 0.7-2.0 mg · kg^{-1} · day^{-1}), with symptom and histological improvement of 100% and 40% of patients respectively. Indeed, they have been proposed as the treatment of choice in children with neurological compromise (Vandenplas et al., 2009).

1.3 Issues related to paediatric dosage forms

The adoption of the paediatric regulation (EC) No. 1901/2006 and consequent demand for greater consideration of medicines for children has strengthened the focus on a need for development of age-appropriate formulations. This is quite challenging, given the fact that there are still many unanswered questions such as the requirement for proper infant test culture to test drugs for paediatric use, additional machinery and cost involved in carrying out such operations for all relevant bodies including pharmaceutical, academic and the regulatory stakeholders (Nibha & Pancholi., 2012). It is clearly known that, paediatric medicine development is complex and resource and time intensive (Kristensen., 2012). European paediatric regulation has had a significant, positive impact in achieving this goal and paediatric strategy and data are now required to be part of every drug development programme, unless a wavier is appropriate. Development of new dosage forms for human/animals is very time consuming and it requires many human and financial resources. However, after development, it is required to be tested on animals and humans. This is the

main concern about the development of a dosage form for infants and small children as it is currently not routine to test paediatric dosage forms in children for clinical trials.

The European Paediatric Formulation Initiative's (EuPFI) 2nd conference on 'Formulating Better Medicine for Children' 2010, organised by the International Association for Pharmaceutical Technology on 21st and 22nd September 2010 in Berlin, Germany, shed light on gaps in knowledge by providing an overview of the main challenges and issues related to development of paediatric formulations. These include, appropriateness of dosage form, use of excipients, taste masking and assessment, administration devices, extemporaneous formulations, and new developments for the global market (Salunke et al., 2011).

Liu and co-workers in a review address the formulation factors affecting the acceptability of oral medicines (tablets, capsules, liquid, chewable table and orally dispersible tablets) in children including dysphagia (difficulty in swallowing) and acceptability of tablets and liquid formulations and flexibility of oral dosage forms. The review concluded that paediatric populations will benefit from novel formulations (including films) that overcome these challenge, such as getting the right formulation for the right age group, taste, smell and palatability. It also highlighted the need for fundamental research to support pharmaceutical development and clinical practice (Liu et al., 2014).

1.4 Adult formulations for paediatric use

Many medicines prescribed for children have not been specifically licensed for use by children, but rather have been originally tested and formulated for adults. This varies according to the setting in which the medicines are prescribed (Narang., 2011). For example, whereas only 10-20% of medicines prescribed for children by general practitioners have not even been licensed for use by children, this number rises to about 45% for medicines used in general paediatric wards and over 90% of those used in neonatal intensive care units. Doctors may prescribe adult formulations, or use licensed adult medicines in an unlicensed way (for example crushed in drinks to enable children to take them as shown in Figure 1.2) (Kalyan et al., 2012). However, doctors prescribing such medicines for children have to take responsibility for such unlicensed (off-label) use.

Figures 1.2 Different ways of administering drugs to paediatric patients. Available at - <http://assets.babycenter.com/ims/2013/04apr/growproj2_baby_given_meds2.jpg?width=280&height=200&pad=true> [Accessed:23/07/2013]

Because a child's body does not function in the same way physiologically as a small adult, it is not possible to make a simple extrapolation from the adult data. For some medicines, this lack of information and unavailability of appropriate formulations may expose children to side effects, over-dosing (potential toxicity) or under-dosing (lack of efficacy). As a result, the World Health Organization (WHO) launched a campaign *"Make medicine child size"* on 6th December 2007 for five years to raise awareness and accelerate action to address the need for improved availability and access to safe and effective child-specific medicines for all children under the age of 15 (Abdulla et al., 2009) as discussed in the overview above.

1.5 Oral thin films

Oral films are used in acute conditions such as pain, emesis, migraine and hypertension. Films are thin sheets, prepared from polymers and depending upon the type of application might be transparent or opaque. Oral dissolving films have gained popularity due to their availability in various sizes and shapes (Nunn & Williams., 2004). Most oral dissolving films are intended to disintegrate or dissolve within seconds and they offer advantages, such as administration without water, rapid onset of action and convenience of handling and dosing. For fast dissolving active pharmaceutical ingredients, absorption is possible through the oral (buccal and sublingual) mucosa and may improve bioavailability (Kalyan et al., 2012). Fast dissolving solid drug dosage forms for application onto the oral cavity for the paediatric population seem to be very appropriate, especially in pre-term and term time new-born infants.

Drug delivery through the oral mucosa offers many advantages including the fact that the oral mucosa is conveniently and easily accessible and therefore allows uncomplicated application of dosage forms such as films. The complete cellular structure of the buccal cavity is shown in Figure 1.3. Furthermore, the oral mucosa is robust against local stress or damage (epithelial cells) caused by drugs or particular delivery system at the site of the administration/attachment and shows rapid cellular recovery after such stress damage (Aggrawal et al., 2011). Active substances can be administered and systemic action can be achieved via drug permeation through the mucosal endothelium.

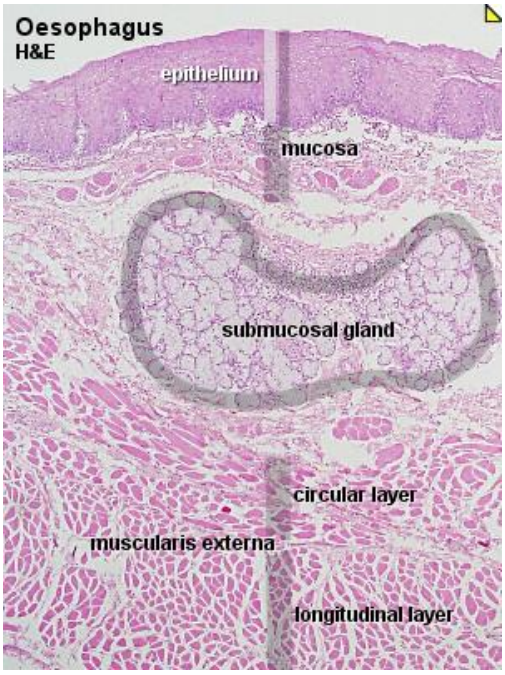

Figure 1.3 Cellular structure of buccal cavity. Available at - <http://www.iupui.edu/~anatd502/Labs.f04/digestive%20I%20lab/s47.20x.1.jpg> [Accessed: 23/07/2013]

Drug absorption through the buccal mucosa membrane depends on the drug concentration at the surface of the mucosa, the vehicle of delivery (delivery system), the contact time with the mucosa, the constitution of mucosal tissue, the degree of ionization of the drug, the pH of the absorption site, the size of the drug molecule and its relative lipid solubility (Schirm et al., 2003; Pankil et al., 2011). These main parameters need to be considered before formulating a dosage form for paediatric patients. Bioadhesive systems have long residence times in the oral cavity and may lead to an unpleasant mouth feel, therefore assumed inappropriate for use

in young children (Miller et al., 2005). However, the bioadhesion between the mucosa is an important factor to ensure the correct dose is available at the absorption site.

1.6 Film forming techniques

A combination of different methods/techniques can be used to form an oral thin film. The different films manufacturing methods have been explained below.

1.6.1 Solvent casting

In the solvent casting approach, water soluble (or swellable) polymers and other excipients are mixed together and dissolved in either aqueous or organic solvent (or mixture of both solvents together) to obtain a clear viscous solution. The solution is left to stand to remove all the air bubbles entrapped in the viscous solution (Boateng et al., 2009). The resulting clear and transparent solution is weighed in casting container such as a Petri dish and dried in an oven at a specified temperature depending on the polymer/drug properties. Once fully dried, the film is carefully removed, checked for any imperfections and cut according to the size required for testing. The samples are stored in a glass container maintained at temperatures ranging from 18-24±1°C and relative humidity of 60±5% until further analysis (Malke et al., 2009). Solvent casting is popular because it is simple, reproducible, cheap and a common process to develop thin films.

1.6.2 Semisolid casting

In semisolid casting, a solution of water soluble film forming polymer is first prepared. The resulting solution is added to another solution of acid insoluble polymer and approximate amount of plasticizer added according to the weight of the polymer or the volume of the solution so that a gel mass is obtained. The ratio of the acid insoluble polymers to the film-forming polymer should be about 1:4. Finally the gel mass is cast into the films or ribbon by using heat controlled drums with a final thickness of about 0.38- 1.27 inches. (Mishra et al., 2011).

1.6.3 Hot melt extrusion

Hot melt extrusion is a commonly used technique to prepare many dosage forms including granules, sustained released release tablets, trans-dermal patches and trans-mucosal films. This technique involves shaping a polymer into a film via a heating process without any solvent or liquid solution. In this method, the polymer and drug are mixed in a dry state to form a uniform powder blend. The mixture is placed in a hob, subjected to the heating process to produce a molten mixture of the blend, and then extruded out in a molten state which is then cast into a sheet of film using a casting mould. The films are cooled and cut to desired size and shape (Mishra et al., 2011). Advantages include improved bioavailability of poorly water-soluble compounds, no solvent required and fewer operation steps. Disadvantages include the importance of polymer flow properties, high energy input, excipients must be devoid of water or any other volatile solvent and heat sensitive drugs cannot be processed by this technique

1.6.4 Film casting by spraying

Here, a polymeric solution and other excipients are sprayed or coated onto a suitable sheet (e.g. Teflon) and incubated to allow solvent evaporation at a suitable temperature until the film is formed. Once the film is fully dried it can then be peeled off and stored (Mishra et al., 2011).

1.6.5 Solid dispersion extrusion

In solid dispersion extrusion, the polymer is dissolved in a suitable liquid solvent. Then the solution is incorporated into the melt of plasticizer, which is obtained below 70°C. Finally, the solid dispersions are shaped into films by means of dies (Mishra et al., 2011).

1.6.6 Rolling method

In the rolling method, a suspension or solution containing pre mix of film forming polymer, and polar solvent is rolled on a carrier without drug. Solvent mainly used is water or a mixture of water and alcohol. The mixture is fed via a first metering roller and controlled valve to either or both of the first or second mixtures. Then the drug is added according to the

required amount and blended with master batch premix to give a uniform matrix. A specific amount of the uniform matrix is then fed to the pan through the second metering roller. The matrix is then allowed to dry into films on the rollers and cut into desired shapes and sizes (Mishra et al., 2011).

1.7 Classification of oral drug release systems

Based on their dissolution or disintegration kinetics, dosage forms can be classified as quick, slow or non-dissolving delivery systems.

The *quick dissolution system* releases the drug into the oral cavity from a few seconds up to 1 minute and the delivery device disintegrates or dissolves in the saliva. This system is suitable for geriatric and paediatric patients, who experience difficulties in swallowing and for the other groups that may experience problems using conventional oral dosage forms such as tablets and capsules. They can be applied in supervised administration, buccal or sublingual absorption for systemic effect or local action within the oral cavity. The advantages include the case of swallowing and administration without with enhanced efficacy (Cilurzo et al., 2005).

The *slow dissolving delivery system* releases the drug into the oral cavity over a period of one to ten minutes and the drug carrier is generally dissolved in the oral cavity, such as chewable tablets, sublingual tablets and muco-adhesive tablets. Researchers have designed such combined bioadhesive and biodegradable polymeric delivery systems for drug delivery via the buccal mucosa (Cilurzo et al., 2005).

The *non-dissolving system* releases drug into the oral cavity over the period of ten minutes to about two hrs. The dosage form is not dissolved entirely when placed into the mouth and such systems are usually designed for controlled drug delivery. These dosage forms include chewing gums, buccal and gingival patches and periodontal fibres (Cilurzo et al., 2005).

1.8 Traditional paediatric routes of administration

There are currently few routes of drug administration employed for paediatric patients (Nahata et al., 1999).

1.8.1 Oral route

The oral route is the most commonly used for drug administration to children (Vipul et al., 2011). The main dosage forms employed are solutions, syrups, suspensions, emulsions, gels, powders, granules, capsules, tablets which are required to be swallowed and absorbed into the systemic circulation from the gastrointestinal tract (GIT). The various organs involved in the oral route of drug administration can be observed in Figure 1.4. Drugs administered by this route are easy to handle, no complicated procedures involved, dosage forms are cheap and can be self-administered. Further, no pain is involved in the administration and the route is very convenient. However, this route is fraught with several limitations and disadvantages. Paediatric patients have difficulty in swallowing; nausea and vomiting are common after administration and swallowing enhancers are sometimes needed as a result. It is unpredictable when the required clinical effect of the drug will be achieved because gastric emptying and the absorption rates differ from patient to patient. Other factors such as stomach and intestinal secretions and pH also play role to interfere with the absorption process. For example, peptides and proteins are destroyed by the GIT secretions, in particular the low pH in the stomach and most of the drug (60%) is removed by the liver before it reaches the systemic circulation by first pass metabolism. This process results in a higher metabolic load to the liver and kidney as they are required to eliminate higher amounts of drug.

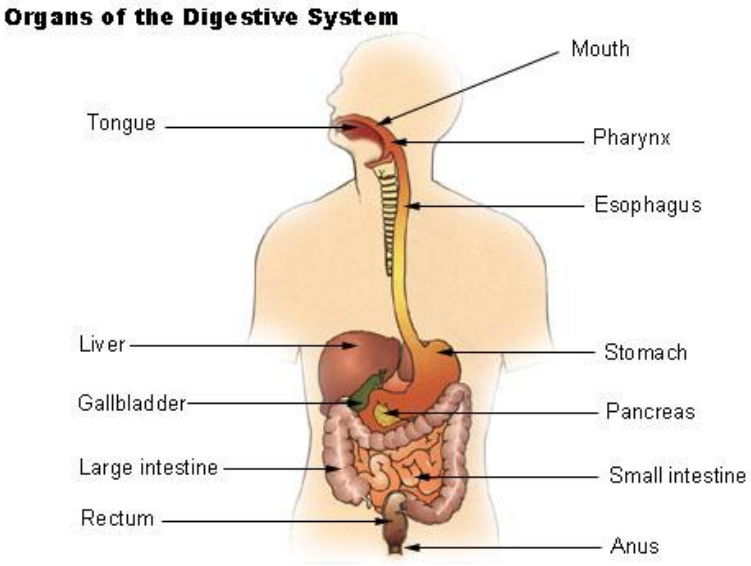

Figure 1.4 Anatomy of GIT. Available at -
<http://www.daviddarling.info/images/digestive_tract.jpg> [Accessed: 24/07/2013]

1.8.2 Injectable (parenteral) administration

Injectable dosage forms (mainly intravenous and intramuscular) are used for critical illness, where rapid onset action of drug is necessary or it is not compatible with any other routes. Different routes for injectable dosage forms are shown in Figure 1.5. It requires injecting medicine (in liquid form) directly into the veins and muscles (Therese et al., 2007). Its advantages are; first pass metabolism can be avoided, rapid onset action can be achieved with small doses compared to oral dosage form where large doses are required because of first pass metabolism and it is suitable for paediatric, aged and unconscious patients. However, it causes pain at the site of administration and there are chances for rejection of formulations such as vaccines and anti-biotic by the patient's body; trained professional is needed for drug administration and to avoid overdosing, repetition is needed which can cause increased stress levels in patients especially children

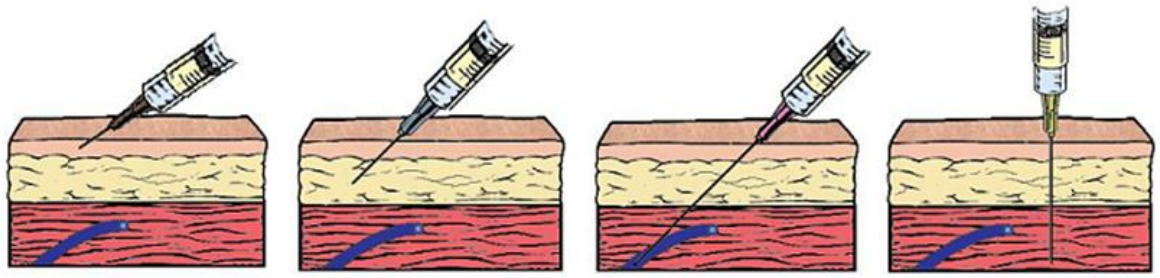

Figure 1.5 Different parenteral route of administration. Available at - <http://www.gpht.org/uploads/5/5/6/6/5566231/8527272.jpg?541 > [Accessed: 24/07/2013]

1.8.3 Topical routes

The topical route is generally for the dermatological administration of drugs. The commonly used preparations are ointments, creams and gels which are a very convenient means of delivering drugs locally to the skin surface. Patients do not need to be trained to apply the medication and is a very practical approach for local application to treat skin conditions. It is however, unsuitable in emergency situations and for systemic effects as absorption is slow. Also, due to the constant contact with air, there are chances for oxidation (e.g. hydroquinone creams) and contamination which can change the physical and chemical properties of the drug (Choonara et al., 1999).

1.8.4 Rectal route

Drugs administered by the rectal route may have a local effect (as for haemorrhoids) or a systemic effect (as in the prevention of nausea and vomiting). This route is convenient in children, unconscious patients or those feeling nausea or vomiting. The amount of drug absorbed via the rectal route is usually less than absorbed if given orally. The absorption of drugs rectally is also unpredictable and can vary among patients (Choonara et al., 1999). Drugs mostly used via these routes in the form of suppositories include benzocaine for haemorrhoids and nitro-glycerine for fissure.

1.9 Oral mucosa as a potential site for drug delivery

1.9.1 Anatomy of the oral mucosa

The oral cavity consists of two regions, the outer oral vestibule which is bounded by cheeks, lips, teeth and gingiva (gums) and the oral cavity proper which extends from the teeth and gums back to the faces with the roof comprising the hard and soft palates (Silvia et al., 2005). The oral epithelium consists of four anatomically distinct sites with unique tissue types, which include the palatal, gingival, sublingual, and buccal mucosa (Hans et al., 1999). The epithelium of the palate, the dorsum of the tongue and the parts of the gingivae attached to the teeth are keratinized. On the other hand, because their barrier is relatively thin and non-keratinized, the sublingual and buccal areas are the most commonly used for oral mucosal drug delivery (Viralkumar et al., 2012). The outer surface of the oral cavity is a mucous membrane consisting of an epithelium, basement and lamina propria overlying a sub mucosa containing blood vessels and nerves (Sudhakar et al., 2006). Table 1.2 provides data of the thickness of different parts of the oral cavity.

Table 1.2 Characteristics of adult human epithelia in the oral cavity

Location	**Thickness (μm)**	**Keratinisation**
Buccal	500–600	No
Sublingual	100–200	No
Gingival	200	Yes
Palatal	250	Yes

The surface area of the mucosal tissues of the adult human oral cavity is approximately 100 cm^2 (Figure 1.6), (the buccal mucosa make up about a third of this area), which is relatively small compared with that of the GIT (approximately 10,100cm^2) (Nair et al., 2013). The gingival tissues of children differ from those of adults in their clinical appearance and resistance to the development of gingivitis and periodontitis. The colour of the gingiva in children is more reddish because of an increased vascularity and a thinner, less keratinized and more translucent epithelium (Choonara et al., 1999). The gingival surface may be smooth or slightly stippled, and the tissues have a firm, resilient consistency (Nibha et al., 2012). However, due to the relatively low enzyme activity, less hostile environment, a better stability of drugs including proteins and peptides, and high vascular supply of the oral cavity; it is an attractive route for local absorption and ideal environment for initial dissolution of the dosage form. However, the constant production of saliva and mouth activities such as chewing and tongue movements can be variable and may have an impact on the performance of drug delivery systems, including film formulations. In situations where the salivary glands are stimulated, a more substantial amount of drug will be washed to the GIT and the drug will be subject to the same restrictions as conventional systems, for example, first-pass metabolism (Nair et al., 2013; Kumar et al., 2011; Andrews et al., 2009).

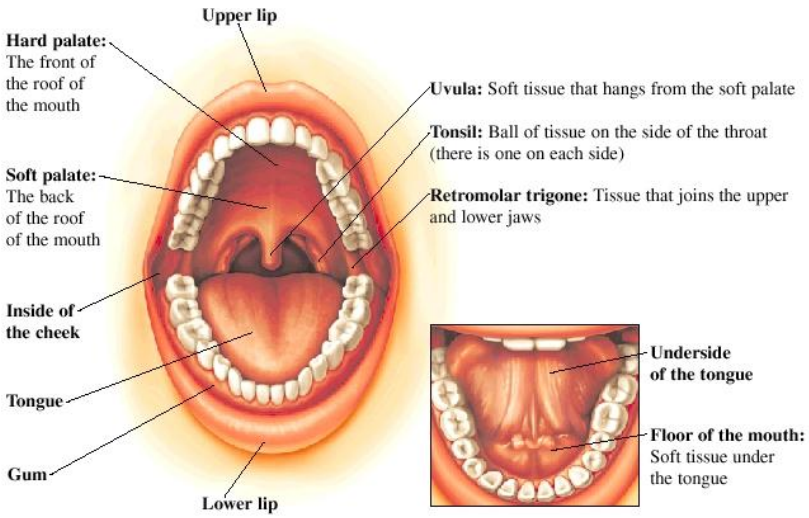

Figure 1.6 Anatomy of the oral mucosa (Yale Medical group, 2013).

The primary responsibility of the buccal mucosa is to protect the underlying structures from foreign materials such as food contaminated with toxic materials or inadvertently consuming some type of toxic materials. The surface of the buccal mucosa consists of stratified squamous epithelium, which is separated from the underlying connective tissue. It is supplied

with a rich amount of blood by the arteries derived from external arteries (Senel et al., 2001). The posterior alveolar artery and the intra-orbital artery, the facial blood suppliers and the buccal artery are the main sources of the blood supply to the lining of the cheek in the buccal cavity (Le Brun et al., 1989).

The barrier properties of the buccal mucosa have been attributed to the upper one-third to one-quarter of the buccal epithelium and the permeability barrier may be attributed to the materials extruded from membrane coating granules (MCGs). MCGs are found in almost all stratified squamous epithelia, regardless of whether the epithelium is keratinised or not (Aggrawal et al., 2011). The diameter of MCGs is 100-300 nm and found near the upper, distal, or the superficial border of the cells and to its opposite cell border. The barrier exists in the outermost 200 μm of the superficial layer. The MCGs discharge their neutral lipids into the intercellular space and form a barrier to the permeability of various compounds (Morales et al., 2011).

1.9.2 Mucus

Mucus is a gel type substance that is secreted in the mouth by the buccal cavity and lines the entire oral cavity. It lines the apical cell surface and provides a protective layer to underlying cells. It is a viscous-elastic hydrogel, made up of 95-99% of water and 1-5% of water insoluble glycoproteins. Generally, mucus is synthesized by specialized mucus secreting cells such as the goblet cells, however in the oral mucosa; it is secreted by the major and minor salivary glands as part of saliva. Other compounds such as proteins, enzymes, electrolytes and nucleic acids are also present in small quantities. At physiological pH, the mucus network carries a negative charge (due to sialic acid and sulphate residues) which may play a role in mucoadhesion. At this pH, mucus can form a strongly cohesive gel structure that will bind to the epithelial cell surface as a gelatinous layer. Because of this, it may sometimes show adverse effects on the absorption or actions of drugs administered by the oral mucosa routes (Chin 2000; Gupta et al., 2011; Nair et al., 2013).

1.9.3 Saliva

Saliva is a very dilute fluid, composed of more than 99% water and a variety of electrolytes, including sodium, potassium, calcium, magnesium, bicarbonate, and phosphates. Some other

components such as immune-globulins, proteins, enzymes, mucins and nitrogenous products (urea and ammonia) are also available in small quantities (Abruzzo et al., 2012). pH ranges between 6-7 and can be vary depending on variables such as low flow (5.3) and peak flow (7.8) (Nair et al., 2013).

Table 1.3 Salivary flow rates in different situations

Situation	**Salivary flow rate**
Unstimulated saliva normal flow	≥ 0.1 mL/min
Stimulated saliva normal flow	≥ 0.2 mL/min
Hypo functional unstimulated saliva flow	< 0.1 mL/min or 50% reduction in individualized base rate
Sleep	Nearly zero
Maximum stimulated flow rate	7 mL/min
Total daily flow of saliva	500 – 1500 mL
Summer	0.3 - 2.3 mL/min
Winter	0.2 - 1.5 mL/min
Average unstimulated flow rate during waking hrs (16 hrs)	0.3 mL/min

The secretion of saliva is controlled by a salivary centre composed of nuclei in the medulla, but there are specific triggers or stimuli for this secretion, including mechanical, gustatory, olfactory, psychic factors, certain types of medication and various local or systemic diseases such as sialadenitis affecting the glands themselves (Abruzzo et al., 2012; Dodds et al., 2005). An acidic excipient can stimulate the secretion of saliva, which is an important consideration in selecting formulation excipients (Won et al., 2001).

Buffering action is an important function of saliva through its components; bicarbonate, phosphate, urea and amphoteric proteins and enzymes, which work much more efficiently during stimulated high flow rates but are almost ineffective during periods of low flow with

unstimulated saliva (Dodds et al., 2005; Kalyan et al., 2012). Salivary bicarbonate is the most important buffering system followed by proteins. More than 90% of the non-bicarbonate buffering ability of saliva is attributed to low-molecular weight, histidine rich peptides. Urea provides buffering by releasing and increasing plaque pH). Phosphate is important as a buffer during unstimulated flow (Kalyan et al., 2012).

Saliva is an adverse, unpredictable factor in intraoral drug delivery due to its complicated composition and large variability between individuals. Therefore, it has a significant effect on polymer swelling and erosion, drug dissolution (including ionisation), release and absorption which all need to be taken into consideration during formulation design and development (Silvia et al., 2005). For fast-dissolving films, their physical and chemical properties in saliva are critical in controlling the quality and performance of the films. However, the properties are usually quite different from those in water and it is important but difficult for researchers to formulate an *in vitro* system which mimics closely the salivary environment and is reliable and facile (Le Brun et al., 1989; Alexander et al., 2011).

1.9.4 Intraoral delivery

There are various reasons for the formulation of drugs into appropriate dosage forms; one of which relates to accurate measurement of the dose. Many active drugs are very potent and only require milligram or microgram amounts to be administered to achieve the desired therapeutic effect. For children, the dose required varies with age and weight. In addition, the administration of drugs into children's bodies, are a very high risk and they vary from the adult dose.

1.9.4.1 Sublingual delivery

The sublingual route of drug administration is widely studied and known to be relatively permeable compared to other oral mucosal surfaces. The sublingual route can provide rapid absorption and easy accessibility to the drug for systemic delivery, especially for quick-dissolving dosage forms such as Buprenorphine as shown in figure 1.7. This route is surrounded by rich blood supply, however; the sublingual region lacks an expanse of smooth muscle or immobile mucosa and is constantly washed by saliva making it difficult for sustained drug delivery (Patel et al., 2012).

Figure 1.7 Sublingual drug administration of medicines. Available at- <http://medicala.12sistedtreatment.org/mediac/400_0/media/23howtotake.jpg > [Accessed: 13/05/2013]

1.9.4.2 Buccal drug delivery

The buccal mucosa has excellent accessibility, an expanse of smooth muscle and relatively immobile mucosa, hence suitable for the administration of retentive dosage forms. Direct access to the systemic circulation through the internal jugular vein bypasses hepatic first pass metabolism leading to high bioavailability (Figure 1.8). It has relatively low enzyme activity compared to the GIT, painless administration and easy dosage form withdrawal (Verma et al., 2010).

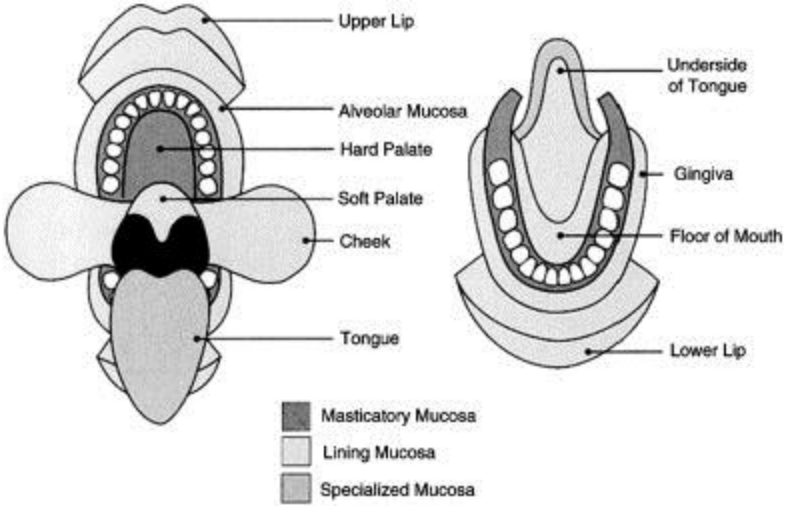

Figure 1.8 Schematic representation of the lining of different mucosal surfaces in the mouth. Available at- <http://origin-ars.els-cdn.com/content/image/1-s2.0-S0168365911000332-gr1.jpg > [Accessed: 16/05/2013]

It is suitable for those drugs which mildly or reversibly damage the mucosa, allows the use of permeation enhancers/enzyme inhibitors or pH modifiers in the formulation as well as provides versatility in designing multidirectional or unidirectional release systems for local or systemic actions (Sudhakar et al., 2006).

The buccal mucosa refers to the membrane lining the inside of the cheek, and the term "buccal drug delivery" refers to drug release, which can occur when a dosage form is placed in the outer vestibule between the buccal mucosa and gingiva. Buccal formulations have been developed to allow prolonged localised therapy and enhanced systemic delivery. The buccal mucosa, however, while avoiding first-pass effects, remains a significant barrier to drug absorption, especially for biopharmaceutical products (Aggrawal et al., 2011). The buccal route is typically used for extended drug delivery, therefore formulations that can be attached to the buccal mucosa for prolonged periods are favoured (Arya et al., 2010). As noted previously, paediatric patients always have difficulty in swallowing or chewing solid dosage forms such as tablets, due to the risk or fear of chocking (Chul et al., 2004). New approaches have already been considered, and the demand for oral dissolving film is growing as drug delivery system suitable for buccal delivery of drugs especially for paediatric and geriatric populations (Liu et al., 2014).

1.9.4.3 Commercial buccal dosage forms

Few buccal formulations are available on the market as shown in table 1.4. The size of the delivery system varies with the type of formulation, i.e., a buccal tablet may be approximately 5–8mm in diameter, whereas a flexible buccal patch may be as large as 10–15cm^2 in area. Mucoadhesive buccal patches with a surface area of 1–3 cm^2 are most acceptable. It has been estimated that the total amount of drug that can be delivered across the buccal mucosa from a 2-cm^2 system in one day is approximately 10–20 mg (Gupta et al., 2011). The shape of the delivery system may also vary, although for buccal drug administration, an ellipsoid shape appears to be most acceptable. The thickness of the delivery device is usually restricted to only 0.07 mm to 0.10 mm (Bobade et al., 2013). The location of the delivery device also needs to be considered. The maximal duration of buccal drug retention and absorption is approximately 4–6 h because food and/or liquid intake may require removal of the delivery device. The physiology of the mucus membrane in a disease

condition needs to be considered, for example, cancer patients suffer from oral candidiasis which decreases saliva production in the mouth. Different types of buccal formulations such as; tablets, patches and films, semisolids and powders are used depending upon the desirable pharmacological action (Chul et al., 2004).

Table 1.4 Oral thin film formulations already available in market for paediatric use

Prodcut name	Drug name	Dosage and frequency	Mechanism of action
Triaminic Thin Strips	Phenylephrine	4 to 5 years: 1 strip orally every 4 hrs not to exceed 6 doses daily. 6 to 11 years: 2 strips orally every 4 hrs not to exceed 6 doses daily.	Phenylephrine is a decongestant. It works by constricting (shrinking) blood vessels (veins and arteries). Constriction of blood vessels in the sinuses, nose, and chest allows drainage of these areas, which decreases congestion. Constriction of blood vessels also affects blood pressure.
Pedia-Lax Thin Strips	Senna	2 to 6 years: 1 strip (8.6 mg) orally per day, not to exceed 2 strips (17 mg) per day 6 to 12 years: 2 strips (17 mg) orally per day, not to exceed 4 (68 mg) strips per day	Causes local irritation in colon, which promotes peristalsis and bowel evacuation. Soften feces by increasing water and electrolytes in large intestine.
Theraflu Thin Strips	Diphenhydramine	Disintegrating strip: dissolve 2 strips on tongue every 6 to 8 hrs. Oral disintegrating strip: 15 to 30 mg orally every 6 to 8 hrs.	An antihistamine which blocks the effects of the naturally occurring chemical histamine, in the body.
Gas-x Thin Strips	Simethicone	2 to 12 years: 40 mg orally 4 times a day. For the 40 mg strips, allow 1 strip to dissolve on the tongue as needed after meals and at bedtime. Do not exceed 6 strips in 24 hrs except under the advice and supervision of a physician	Simethicone allows gas bubbles in the stomach and intestines to come together more easily, which allows for easier passage of gas.

1.9.5 Buccal absorption

A function of the oral cavity (buccal cavity) includes the analysis of potential food materials, mechanical processing, lubrication and digestion using the taste buds and other salivary glands. The oral cavity can be used for local and systemic therapy. The buccal route is of particular interest with regards to the systemic delivery of drugs that are subject to first-pass metabolism, or for protein and peptide administration. The absorption of drugs mainly occurs in two ways – (i) trans cellular (intracellular) and (ii) para cellular (intercellular) (Figure 1.9) (Sudhakar et al., 2006).

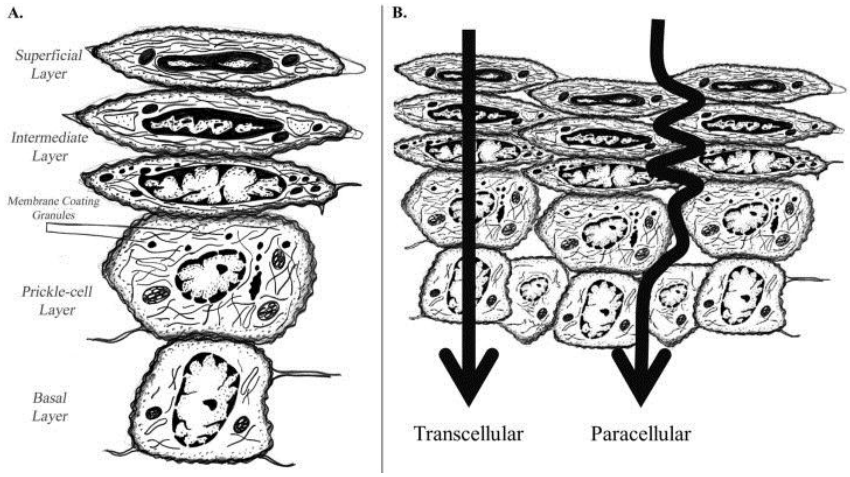

Figure 1.9 Intra and intercellular transportation of drug via the buccal route. Available at - <http://origin-ars.els-cdn.com/content/image/1-s2.0-S0168365999000322-gr1.gif > [Accessed: 20/05/2013]

Permeation across the buccal mucosa has been reported to occur mainly by the para-cellular route through the intercellular lipids produced by membrane-coating granules (MCGs) (Shojaei et al., 1998; Liu et al., 2010). As mentioned above, the buccal mucosa is a potential site for the controlled delivery of hydrophilic macromolecular therapeutic agents (biopharmaceuticals) such as peptides, oligonucleotides and polysaccharides. However, these high molecular weight drugs usually have low permeability leading to low bioavailability (Liu et al., 2010). The buccal mucosa also contains proteases that may degrade peptide-based drugs and the salivary enzymes may reduce stability (Pankil et al., 2011). The rate of absorption of hydrophilic compounds is a function of the molecular size with smaller molecules (75 - 100 Da) generally exhibiting rapid transport across the mucosa and permeability decreasing as molecular size increases. For hydrophilic macromolecules such as

peptides, absorption enhancers have been used to successfully alter the permeability of the buccal epithelium, causing this route to be more suitable for the delivery of larger molecules (Viralkumar et al., 2012). The buccal permeation enhancers act by inhibiting the various peptidases and proteases present within buccal mucosa, thereby overcoming the enzymatic barrier. Enzyme inhibitors, such as aprotinin, bestatin, puromycin and some bile salts stabilize protein drugs by different mechanisms, including change in the activities of enzymes, altering the conformation of the target drug (especially peptides or proteins) and/or rendering the drug less accessible to enzymatic degradation (Mitra et al., 2002).

The permeability for a given drug is also a direct function of their oil-water partition coefficients (Singh et al., 2011). The partition coefficient is a useful tool to determine the absorption potential of a drug. In general, increasing a drug's polarity by ionization or the addition of hydroxyl carboxyl, or amino groups, will increase the water solubility of any particular drug and cause a decrease in the lipid-water partition coefficient (Verma et al., 2010). Conversely, decreasing the polarity of a drug (e.g. adding methyl or methylene groups) results in an increased partition coefficient and decreased water solubility in saliva. The partition coefficient is also affected by pH at the site of drug absorption. With increasing pH, the partition coefficients of acidic drugs decrease, while that of basic drugs increases. The ionization of a drug is directly related to both its pKa and pH at the mucosal surface. Only the non-ionized form of many weak acids and weak bases exhibit appreciable lipid solubility, and thus the ability to cross lipid membranes. As a result, maximal absorption of these compounds has been shown to occur at the pH at which they are unionized, with absorbability diminishing as ionization increases (Pankil et al., 2011).

1.9.6 Advantages and limitations of buccal delivery systems

Buccal drug delivery systems present various advantages and limitations including the following:

Advantages

- Bypassing of the gastrointestinal tract and hepatic portal system, thus increasing the bioavailability of orally administered drugs that otherwise undergo hepatic first-pass metabolism.

- Improved patient compliance due to the elimination of pain associated with injections by just putting tablets/patches/films into the buccal cavity, which also increases the ease of drug administration.
- Extent of perfusion is greater than other oral dosage forms such as tables, capsules, and syrups, therefore quick and effective absorption because of the rich supply of the blood (2.0 mL/sec /cm^2) throughout the buccal cavity and allows sustained drug delivery.
- A relatively rapid onset of action can be achieved compared to the GI route and the formulation can be removed if therapy is required to be discontinued.
- Used in case of unconsciousness and less cooperative patients as these have difficulties in swallowing oral dosage form. Nausea and vomiting are avoided because medications do not interfere with the oesophagus and its functions.
- Drugs, which show poor bioavailability via the oral route, can be administered conveniently. For example, drugs such as pantoprazole sodium, which are unstable in the acidic environment of the stomach or are destroyed by the enzymatic or alkaline environment of the intestine.
- The large contact surface of the oral cavity contributes to rapid and extensive drug absorption (Reddy et al., 2011).

Limitations

- Drugs which irritate the oral mucosa, have a bitter taste, cause allergic reactions or discoloration of the teeth cannot be formulated for buccal delivery.
- If the formulation contains antimicrobial agents, it affects the natural microbes in the buccal cavity.
- The patient cannot eat/drink/speak normally and the swallowing of saliva can also potentially lead to the loss of dissolved or suspended drug
- Only those drugs which are absorbed by passive diffusion can be administered by this route.
- Drugs which are unstable at buccal pH cannot be administered by this route.
- The low permeability of the buccal membrane, specifically when compared to the sublingual membrane (Neelagiri et al., 2013).

1.10 Proton pump inhibitors

Proton pumps inhibitors (PPIs), are chemical compounds, which help to block secretion of excessive amounts of acid in the stomach, stimulated by any type of secretagogues (stimulates H/K ATPase) (Madanick and Ryan 2011). They are classified into two groups: (i) competitive and (ii) covalent. Drugs belonging to the competitive group exert reversible inhibition of PPIs in the stomach wall by binding to its extracellular surface as shown in Figures 1.10 and 1.11. The covalent class forms irreversible inhibition allowing a prolonged time for the secretion of other enzymes. The two drugs; 2-methyl-8-(phenyl-methoxy)-imidazo-1,2-pyridin-3-acetonitrile (SCH28080) and 3-butyryl-8-methoxy-4-(2-tolylamino) quinolone were used as PPIs in the early stages and latter groups mainly comprise derivatives of benzimidazole such as omeprazole, lansoprazole, rebeprazole and pantoprazole (Nishioka et al., 1999).

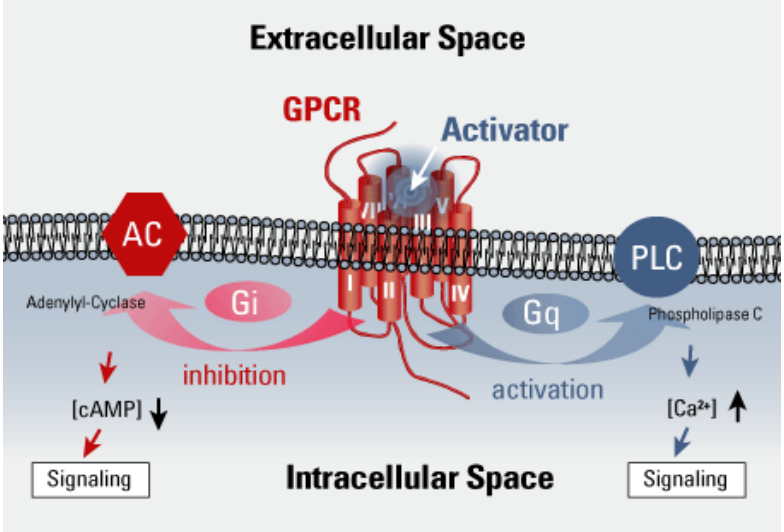

Figure 1.10 Extra/intracellular environment of stomach [(GPCR) - G protein-coupled receptor; (AC) - adenylyl-cyclase; (PLC) - phospholipase C; (Gi) - inhibitory regulative G-protein; (Gq) - heterotrimeric G protein]. Available at: -<http://www.yellowtang.org/images/proteins_embedded_w_c_la_784.jpg> [Accessed: 12/07/2013]

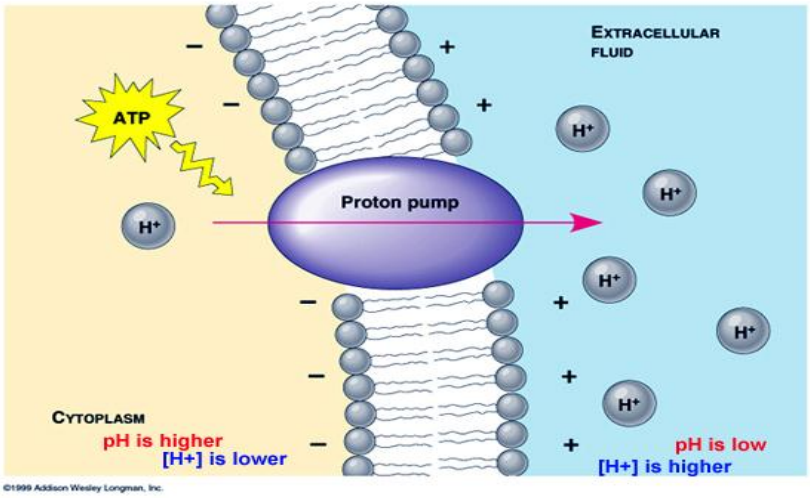

Figure 1.11 Proton pump pathway. Available at - <http://3.bp.blogspot.com/-HCGEB2oxTOQ/TZ5jAwJtEMI/AAAAAAAAABQ/mKqpzn85S28/s320/proton+pump.jpg> [Accessed: 23/07/2013]

1.10.1 Role of PPIs

Peptic ulcer leads to bleeding in the stomach which is painful for patients and could lead to significant morbidity and sometimes mortality. It has been shown that pharmacological tolerance of PPI is higher for this indication than histamine receptor 2 antagonists (H2RAs) such as Metiamide, Cimetidine and it significantly limits H2RAs' capability to sustain the acid imbalance in the high intra-gastric pH (Lin et al., 2010). PPIs block the hydrogen/potassium adenosine triphosphatase enzyme situated in the stomach wall thus inhibiting acid secretion, giving relief from ulcers of the oesophagus, stomach and duodenum and from gastro-oesophageal reflux disease (GERD). PPIs change their own chemical formula with the addition of H^+/K^+ adenosine triphosphatase enzyme in the parietal cells, resulting in the formation of active chemical derivative by gaining a proton (H^+), which increases the pH of the stomach and reduces acid secretion from the wall of the stomach. The chemical changes in the PPIs process is summarised in figure 1.12. The new protonated chemical compound also possesses the ability to bind with the parietal cells in the stomach wall, thus reducing further acid secretion (Chapman et al., 2011). Different PPIs with their chemical name and structures are given in table 1.5.

Table 1.5 Chemical name, structure of different type of proton pump inhibitor

Proton pump inhibitor	Molecular formula / chemical name	Chemical Structure
Omeprazole	$C_{17}H_{19}N_3O_3S$ 6-methoxy-2-{[(4-methoxy-3, 5-dimethylpyridin -2-yl)methyl]sulfinyl-1H-benzodiazole}	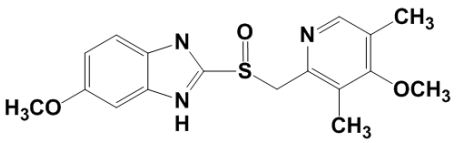
Lansoprazole	$C_{16}H_{14}F_3N_3O_2S$ 1H-Benzimidazole,2-[[[3-methyl-4-(2,2,2-trifluoroethoxy)-2-pyridinyl]methyl]sulfinyl]-, 2-[[[3-Methyl-4-(2,2,2-trifluoroethoxy)-2-pyridyl]-methyl]sulfinyl]benzimidazole	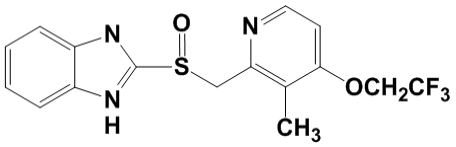
Pantoprazole	$C_{16}H_{15}F_2N_3O_4S$ 5-(difluoromethoxy)-2-[[(3,4-dimethoxy-2-pyridinyl) methyl] sulfinyl]-1H-benzimidazole	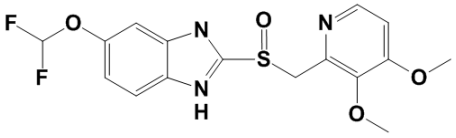
Rabeprazole	$C_{18}H_{21}N_3O_4S$ 2-[4-(3methoxypropoxy)-3-methyl-2-pyridinyl]-methyl]sulfinyl]-1H–benzimidazole	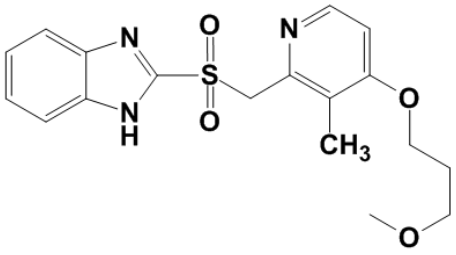
Esomeprazole	$C_{17}H_{19}N_3O_3S$ 5-methoxy-2-[(4-methoxy-3,5-dimethyl-pyridin-2-yl)methylsulfinyl]-3H-benzoimidazole	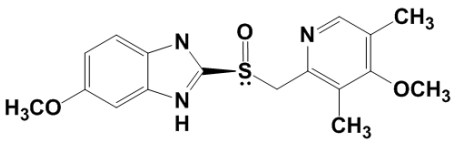

A PPI should be prescribed for the appropriate indication at the lowest effective dose for the shortest period of time due to potential side effects and the need for long-term treatment should be reviewed periodically (Thomson et al., 2010). The side effects of PPIs include headaches and gastrointestinal disturbance such as; nausea, vomiting, abdominal pain,

flatulence, diarrhoea and constipation. Less frequent side effects include dry mouth, peripheral oedema, dizziness, sleep disturbance, fatigue, paraesthesia, arthralgia, myalgia, rash and pruritus (Madanick 2011). Rare side-effects include taste disturbance, stomatitis, hepatitis, jaundice, hypersensitivity reactions and fever. By decreasing gastric acidity, PPIs may increase the risk of gastrointestinal infections. Rebound acid hyper secretion and protracted dyspepsia may occur after stopping prolonged treatment with PPIs (Nishioka et al., 1999).

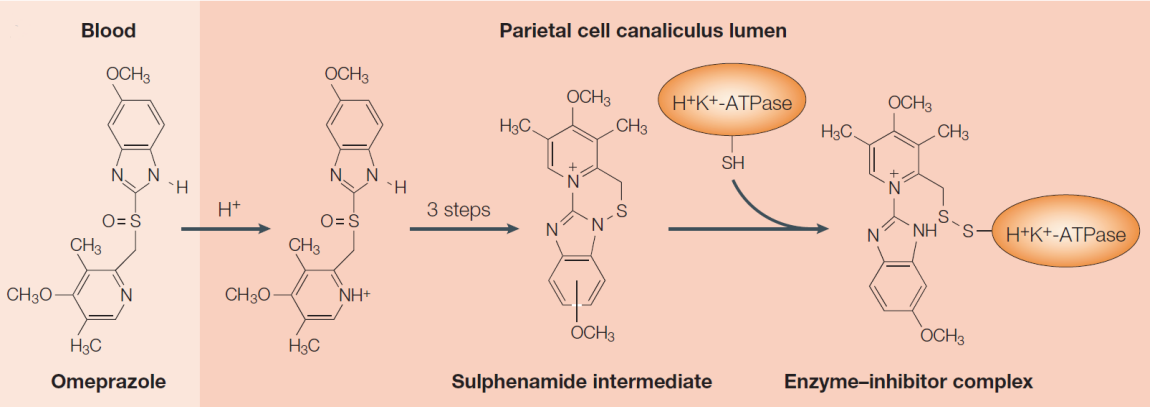

Figure 1.12 Mechanism of action of PPIs (Fass et al., 1998)

Formulation of PPI into oral solid dosage forms is a very challenging task for scientists because the drug molecules are acid-labile. OME is used for the treatment of over-acidity by inhibiting H^+/K^+/ATPase pump at the gastric partieal secretary cell (stomach). The main challange in the formulation of OME is to prevent degradation of API upon exposure to acidic enviroments or mositure (Mukharya et al.,2011).

1.11 Functional properties of buccal mucosa delivery systems

1.11.1 Bio-(muco) adhesion

The terms bioadhesion and mucoadhesion are sometimes used interchangeably though they mean slightly different things. Bioadhesion defines adhesion between two materials where at least one material is of biological origin as shown in Figure 1.13. It is generally used when interaction occurs between adhesive polymers and epithelial surface. Mucoadhesion on the other hand occurs when the adhesion occurs with the mucus layer covering a biological tissue. Mucoadhesion is also used to describe to in vitro adhesion tests carried out to simulate

bioadhesion using various artificial surfaces such as gelatine and agar equilibrated with simulated mucosal fluid such as simulated saliva (Ayensu et al, 2012, Kianfar et al., 2013).

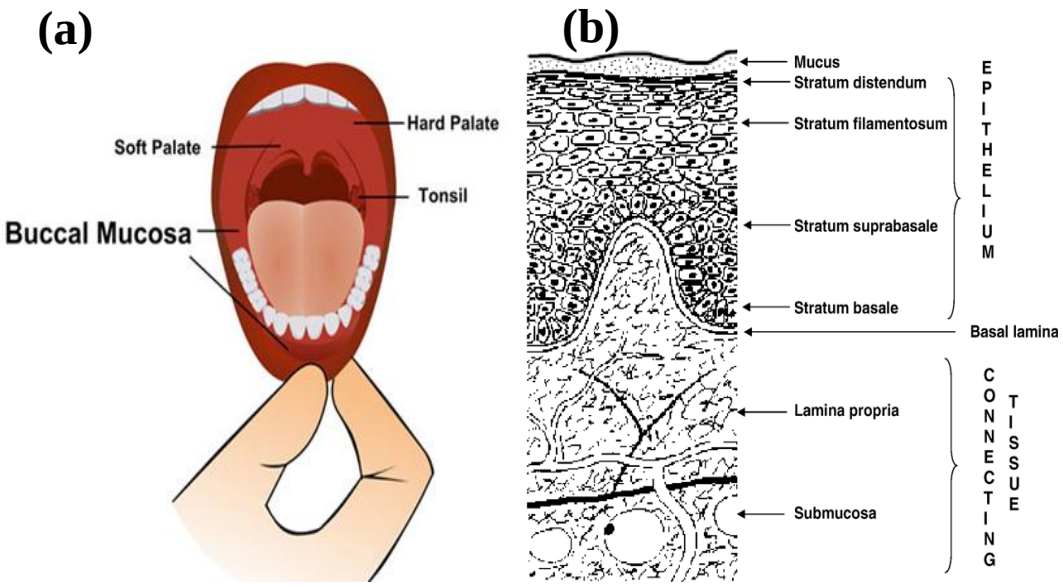

Figure 1.13 (a) Cartoon representation of the buccal mucosa (b) cross-section of the buccal mucosa structure. Available at < www.cedars sinai.edu/Patients/Programs and-Se.website.> [Accessed; 13/06/2013]

The adhesion force/bond is dependent on parameters such as hydrophilicity (progress bioadhesion), stage of hydration and rate of polymer erosion after being in contact with the hydrating surface. Apart from the function of increasing the retention time of the drug on the mucosal surface to enhance the bioavailability, some polymers can be used as an enzyme inhibitor and penetration enhancers. It has been proven that the presence of numerous polymers absorb the water from the epithelial cells to widen the tight junction (Viralkumar et al., 2012). In general, mucoadhesion is described as bonding between polymers and mucosal tissues or any biological surface as shown in figure 1.14.

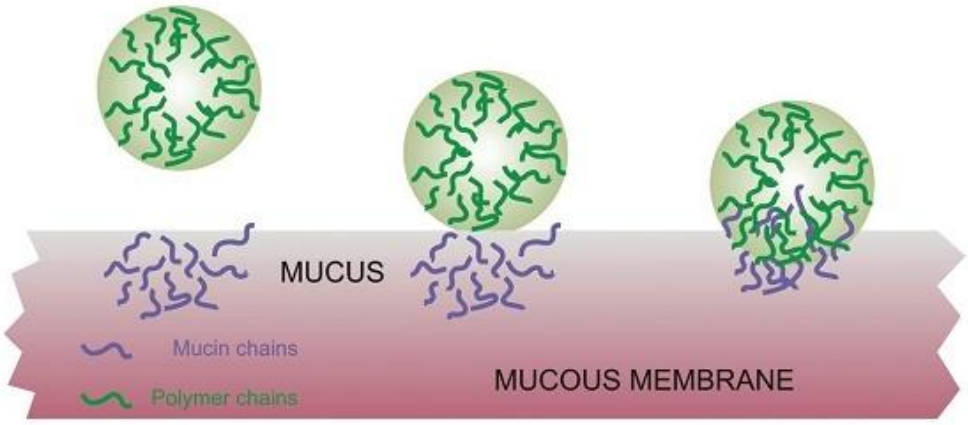

Figure 1.14 Adhesion process between polymer and mucous membrane. (Gupta et al., 2011).

In the adhesion process, the polymer is hydrated and swells when it comes into contact with the mucosal tissue and the polymer chains start to interpenetrate into the epithelium or entangle with the mucin chains. Finally, chemical or physical bonds are formed between the entangled chains. Mucoadhesion bond formation depends on the nature of the mucous membrane and mucoadhesive material, formulation type, the attachment procedure and the environment of the bond (figure 1.15). Mucoadhesion occurs because of various adhesive bonds at the interface of the mucosal membrane and mucoadhesive agent. These bonds include (1) ionic bonds: where two oppositely charged ions attract each other via electrostatic interactions and forms a strong bond; (2) covalent bond: which are very strong bonds in which electrons are shared in space, between the bonded atoms in order to fill the orbitals; (3) hydrogen bonds: a hydrogen atom, when covalently bonded to an electronegative atom such as an oxygen, fluorine or nitrogen, carries a slight positively charge and hence, is attracted to electronegative atoms. The mucosal membrane and mucoadhesive share the hydrogen atom, though this bond is usually weaker than ionic or covalent bonds; (4) van der Waal's forces: these are some of the weakest forms of interaction that arise from dipole-dipole attraction in polar molecules, and dispersion forces with non-polar substances: (5) hydrophobic forces: give rise to a hydrophobic effect and occur when non-polar groups are present in an aqueous solution.

Figure 1.15 Drug loaded bioadhesive delivery system. Available at-
<http://www.drbicuspid.com/user/images/content_images/nws_rad/2010_03_09_14_54_44_908_BioDelivery_Sciences_BEMA.jpg> [Accessed: 21/05/2013]

1.11.2 Mechanisms and theories of bioadhesion

A variety of factors affect the mucoadhesive properties of polymers, such as molecular weight, flexibility, hydrogen bonding capacity, cross-linking density, charge, concentration, hydration of a polymer and the environmental factors (Roy et al., 2010). The process involved in the formation of bioadhesive bonds has been described in three steps (i) wetting and swelling of polymer to permit intimate contact with biological tissue; (ii) interpenetration (entanglement) of bioadhesive polymer chains with mucin chains and (iii) formation of weak chemical bonds between the entangled chains (Sudhakar et al., 2006).

The mechanism of polymer attachment to a mucosal surface is not yet fully understood, however, certain theories of bioadhesion have been proposed suggesting that it might occur via physical entanglement and/or chemical interactions (Figure 16), such as electrostatic, hydrophobic, hydrogen bonding, and van der Waal's interactions (Bobade et al., 2013).The various theories proposed to explain the mechanisms of bio (muco) adhesion are briefly described below (Tangri, et al., 2011; Hans et al., 1999).

(1) Electronic theory: The electronic theory depends on the assumption that the bioadhesive material and the target biological surface have different electrical surface characteristics. Based on this, when two surfaces come in contact with each other, electron transfer occurs in an attempt to balance the electrical levels, resulting in the formation of a double layer of electrical charge at the interface of the bioadhesive and the biological surface. The

bioadhesive force is believed to be present due to the attractive forces across this double layer.

(2) Adsorption theory: This theory states that the bioadhesive bond formed between an adhesive substrate and the tissue is due to the weak van Der Waal's forces and hydrogen bond formation. It is one of the most widely accepted theories of bioadhesion.

(3) Diffusion theory: The concept of the interpenetration and entanglement of the bioadhesive polymer chains and mucus chains is supported by the diffusion theory. The polymer chains and mucus mix to a sufficient depth to create a semi-permanent adhesive bond. The bond strength increases with the increase in the degree of the penetration. This penetration is dependent on the concentration gradients and the diffusion coefficients.

(4) Wetting and fracture theories: The ability of bioadhesive or mucus to spread and develop intimate contact with its corresponding substrate is an important factor in bond formation. The wetting theory was developed predominantly concerning liquid adhesives and uses interfacial tensions to predict spreading and subsequently adhesion. The study of surface energy of polymers and tissues to predict mucoadhesive performance has been given considerable attention. The fracture theory attempts to relate the difficulty of separation of two surfaces after adhesion.

1.11.3 Mucoadhesive polymers

Buccal adhesive polymers include a large diverse group of molecules covering biodegradable grafted co-polymers and thiolated polymers and are used in bioadhesive formulations. These formulations are often water-soluble or swellable and when in dry form, they attract water from the biological surface and this water transfer results in a strong interaction (Sudhakar et al., 2006).

The ideal polymer should possess the following desirable characteristics (Punitha et al., 2010).

- It should be non-toxic, non-irritant and free from leachable impurities.

- It should possess good spreading ability, wetting, swelling, solubility and biodegradable properties.
- It should adhere to the target mucosa quickly and provide the required mechanical strength.
- It should demonstrate its bioadhesive properties in both dry and liquid state.
- pH should be biocompatible and should possess good viscoelastic properties.
- It should possess peel, tensile and shear strength at the bioadhesive range and have an adhesive active group.
- It should be readily available and cost should be reasonably cheap.
- It should demonstrate local enzyme inhibition and penetration enhancement properties and acceptable shelf life.
- It should have an optimum molecular weight and required spatial conformation.
- It should be sufficiently cross-linked but not to the degree of suppression of bind forming groups.
- It should not aid in development of secondary infections such as dental caries

1.11.3.1 Classification

Bioadhesive polymers are classified (Lehr., 2000) depending upon various characteristics such as (i) source (natural and synthetic polymers); (ii) aqueous solubility; (water soluble and insoluble, (iii) first and second generation (cationic, anionic and non-ionic polymer) and (iv) potential bioadhesive forces (electrostatic interactions, hydrogen bonds and covalent bonds) (Alexander et al., 2011).

Currently, polymers are classified as ‘first and second generation’. The older generation of mucoadhesive polymers is referred to as ‘off-the-shelf’ polymers (Kalani et al., 2011). They lack specificity and targeting capability and adhere to mucus non-specifically, and suffer short retention times due to the high turnover rate of mucus. The new generation of mucoadhesive polymers can adhere directly to the cell surface, rather than to mucus. They interact with the cell by means of specific receptor or covalent bonding instead of non-specific mechanism (Miller et al., 2005).

1.11.3.2 First generation mucoadhesive polymers

These have been divided into the following subsets;

1) **Anionic polymers:-**

Anionic polymers are the most widely employed mucoadhesive polymers for pharmaceutical formulation due to their high mucoadhesive functionality and low toxicity. Such polymers are characterised by the presence of carboxyl and sulphate functional groups that give rise to a net overall negative charge at pH values exceeding the pKa of the polymer (Abruzzo et al., 2012). Typical examples include polyacrylic acid (PAA) and its weakly cross-linked derivatives, sodium carboxymethylcellulose (NaCMC) and carrageenan (CA). PAA and NaCMC possess excellent mucoadhesive characteristics due to the formation of strong hydrogen bonding interactions with mucin (Miller et al., 2005). CA has been used to formulate wafers and films for buccal mucosal drug delivery (Kianfar et al., 2011). Another example of an anionic polymer is alginates that are negatively charged polysaccharides widely used in the production of micro-particles and are frequently reported as polyanionic mucoadhesive polymers.

2) **Cationic polymers:-**

Among the cationic polymers, chitosan is the most extensively investigated in recent years. Chitosan is a cationic polysaccharide, produced by the de-acetylation of chitin, the most abundant polysaccharide in the world, next to cellulose. The intriguing properties of chitosan have been known for many years with many examples of its use in agriculture, industry and medicine. Chitosan is gaining increasing importance due to its good biocompatibility, biodegradability and due to its favourable toxicological properties. Chitosan provides an improved drug delivery via mucoadhesion (Le Brun et al., 1989). The major benefit of using chitosan in pharmaceutical applications has been the ease with which various chemical groups may be added, in particular to the C-2 position allowing for the formation of novel derivatives with added and improved functionality (see section under second generation polymers below). Required pharmaceutical technological challenges can be overcome by tailoring chitosan's properties to the intended use (Andrews et al., 2009).

1.11.3.3 Second generation mucoadhesive polymers

The second-generation polymers adhere directly to the cell membranes rather than to the mucus covering these membranes. They are divided into the following categories depending on the adhesive activities.

1) **Lectin-mediated bioadhesive polymers-**

Lectins are naturally occurring proteins that play a fundamental role in biological recognition phenomena involving cells and highly heterogeneous proteins (Arya et al., 2010). They belong to a group of structurally diverse proteins and glycoproteins that can bind reversibly to specific carbohydrate residues. The possibility of developing a bioadhesive polymer which is able to selectively create specific molecular interactions with particular targets, such as cell membrane of specific tissues are very attractive potential for targeted delivery such as polyacrylic acids in the dry state, wheat germ agglutinin and concanavalin A (Dojo et al., 2001). For example, some Gram negative bacteria use lectins to attach themselves to the cells of the host organism during infection. After initial mucosal cell-binding, lectins can remain on the cell surface or in the case of receptor-mediated adhesion, possibly become internalised via a process of endocytosis. Such systems could offer duality of function in that lectin based platforms could not only allow targeted specific attachment but also additionally offer a method of controlled drug delivery of macromolecular pharmaceuticals via active cell-mediated drug uptake (Lehr., 2000).

2) **Bacterial adhesion**

The adhesive properties of bacterial cells, as a more complicated adhesion system, have recently been investigated. The ability of bacteria to adhere to a specific target is derived from particular cell-surface components or appendages, known as fimbriae that facilitate adhesion to other cells or inanimate surfaces (Nibha et al., 2012). Bacterial fimbriae adhere to the binding moiety of specific receptors. These are extracellular, long threadlike protein polymers of bacteria that play a major role in many diseases. A significant correlation has been found between the presence of fimbriae on the surface of bacteria and their pathogenicity (Miller et al., 2005). The attractiveness of this approach lies in the potential

increase in the residence time of the drug on the mucus and its receptor-specific interaction, similar to those of plant lectins (Sudhakar et al., 2006).

3) **Enzyme inhibiting and permeation enhancing bioadhesive polymers**

It has been shown that some mucoadhesive polymers can act as enzyme inhibitors. The particular importance of this finding lies in delivering therapeutic compounds that are specifically prone to extensive enzymatic degradation, such as proteins and polypeptide drugs (Lin et al., 2010). Investigations have demonstrated that polymers, such as poly (acrylic acid), operate through a competitive mechanism with proteolytic enzymes. This stems from their strong affinity to divalent cations (Ca^{2+}, Zn^{2+}). These cations are essential co-factors for metalloproteinase, such as trypsin. Circular dichroism studies suggest that Ca^{2+} depletion, mediated by the presence of some mucoadhesive polymers, causes the secondary structure of trypsin to change, and initiates a further auto degradation of the enzyme (Missaghi., 2006). The increased intestinal permeability of various drugs in the presence of numerous mucoadhesive polymers has also been attributed to their ability to open up the tight junctions by absorbing the water from the epithelial cells. The result of water absorption by a dry and swellable polymer is dehydration of the cells and their subsequent shrinking. This potentially results in an expansion of the spaces between the cells (Miller et al., 2005).

4) **Thiolated mucoadhesive polymers**

Thiolated polymers are capable of forming disulphide bonds with cysteine-rich subdomains of mucus glycoproteins covering mucosal membranes. These special class of multifunctional polymers also called thiomers (Schirm et al., 2003). Thiomers are capable of forming intra- and inter chain disulphide bonds within the polymeric network leading to strongly improved cohesive properties and stability of drug delivery systems such as matrix tablets. These hydrophilic macro-molecules exhibit free thiol groups on the polymeric backbone. These functional groups have enabled various features of well-established polymeric excipients such as poly (acrylic acid) and chitosan to be significantly improved (Bemkop., 2005). Due to the formation of strong covalent bonds with mucus glycoproteins, thiomers show the strongest mucoadhesive properties of all polymeric excipients via thiol-disulphide exchange reaction and an oxidation process (Punitha et al., 2010).

1.12 Controlled drug release systems

Controlled drug delivery is a complex process that delivers drugs at a rate which is determined by the specific need of the body over a specific period of time. Controlled release is helpful for maintaining a constant drug dissolution in target cells (Masaaki et al., 1998). There are several types of controlled drug release systems (Amidon et al, 1995) and briefly discussed below.

1.12.1 Dissolution controlled system

There are two types of dissolution controlled systems; matrix or encapsulation system (Chien 1991). Matrix systems are the most common and also referred to as monoliths (Zuleger 2001) where the drug is homogeneously dispersed throughout a medium. This utilizes waxes such as carnuba wax, which tightly control the rate of dissolution fluid penetration, into the matrix by altering the porosity. This is achieved by embedding (i.e. dispersing) the drug in a molten wax and congealing and granulating the same. In regards to the dissolution controlled system, the rate of controlling step is known as dissolution (Yie,. 1991).

1.12.2 Diffusion controlled system

Overall diffusion systems are characterized by the release rate of the drug which is dependent on its diffusion through inert water insoluble membrane barrier. The two types of diffusion are involved in this subdivision; reservoir controlled system and matrix controlled system.

1.12.3 Combined dissolution and diffusion controlled release system

In this system, the drug core is encased in a partially soluble membrane (Tamizharasi ,2008). Pores are thus created due to dissolution of parts of the membrane; which allows entry of the aqueous dissolution medium into the core and permit drug dissolution and allow subsequent diffusion of dissolved drug out of the system into the dissolution medium.

1.12.4 Water penetration and swelling controlled systems

The rate control in water penetration controlled delivery system is obtained by the penetration of water into the system. Initially, these systems are dry and when placed within the body, they absorb water. The swelling increases the aqueous solvent constant within the formulation, as well as, the polymer mesh size; therefore, this enables the drug to diffuse throughout the swollen network and into the external environment (Siepmann et al, .2012).

1.12.5 Osmotically controlled system

These systems are fabricated by encapsulating an osmotic drug core, containing an osmotically active drug within a semi permeable membrane, made from biocompatible polymer. As a result, a gradient of osmotic pressure is created which allows the drug solutes to be continuously pumped out over a prolonged period of time through the delivery orifice. This type of drug system dispenses drug solutes continuously at a zero order rate (Reddyet al., 2013).

1.12.6 Chemically controlled release system

This control system is known to change their chemical structure when exposed to biological fluid. Biodegradable polymers are designed to degrade as a result of hydrolysis of the polymer chains, into biologically safe and progressively smaller moieties. They are of two types; erodible and pendent chain systems. Within erodible systems, the mechanism of drug release occurs by erosion; bulk erosion polymer degradation may occur through bulk hydrolysis. Polymers such as polyorthoesters and polyanhydrides erode through degradation, only at the surface of the polymer. As a result, the release rate is proportional to the surface area of the delivery system (Dixit et al., 2013).

1.12.7 Ion-exchange resin controlled release systems

This controlled release system is designed to provide the controlled release of an ionic drug. The release system is achieved by an absorption of ionised drug onto an ion-exchange resin granules such as a codeine base with Amberlite; after, filtration from the alcoholic medium,

the drug resin complex granules are coated with a water permeable polymer (Srikanth et al., 2010).

1.13. Release kinetics

Release kinetics are mathematical models that are used to study and evaluate the kinetic and overall mechanism of drug release from dosage forms. The different models are then compared to the result, in order to obtain the model that best fits the release data and such model is selected based on the correlation coefficient (R^2) value. The model that produces the highest (R^2) value is then considered as the most appropriate to study and evaluate the release data (Dash 2010). The mathematical models are discussed briefly below:

1.13.1 Zero order

This model is derived directly from the equation on the dissolution plot for the time on x-axis and the cumulative percentage drug release on the y-axis and usually is a straight line. This typically depicts a system where the drug release rate is independent of concentration of the dissolved substance within the dissolution medium.

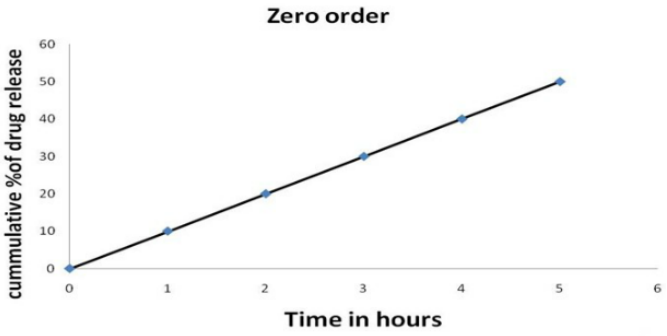

$Q_2 = Q_0 + k_0 t$ Equation 1.1

Where

Q_0 = the initial amount of drugs

Q_t = cumulative amount of drug release time t

K_0 = zero order release constant

t = time in hrs (or minutes)

Assumptions:

- The formulation does not disaggregate (no change in area)
- No equilibrium conditions are achieved

1.13.2 First order kinetic model

The first order kinetic model describes a system where the rate of drug release is dependent on the concentration of the dissolved substance in the dissolution medium. From the equation, a graph plotting time on x-axis and log cumulative percentage of the drug remaining to be released on y-axis; produces a straight line.

$$\text{Log } Qt = \text{Log } Q_0 + kt/2.303 \qquad \text{Equation 1.2}$$

Where

Q_0 = initial amount of drugs

Q_t = cumulative amount of drug release in time t

k = first order release constant

t = time in hrs

1.13.3 Higuchi kinetic model

This equation suggests that the drug is released mainly by diffusion through the matrix (non-degradable monolithic system) and is directly proportional to the square root of time. A graph

plotted between the square root of time on the x–axis and the cumulative percentage of drug release on the y–axis therefore, yields a straight line.

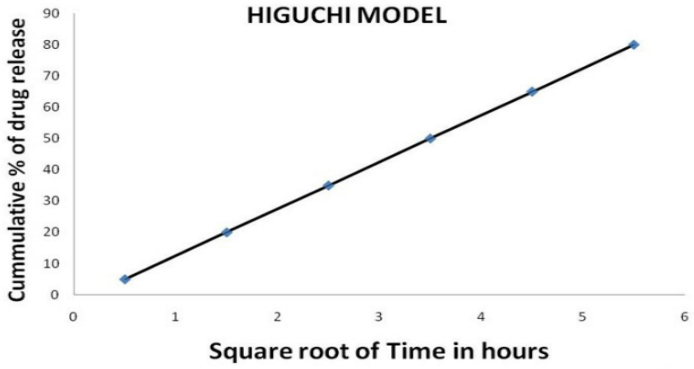

$Q = K_H t^{½}$ Equation 1.3

Q = cumulative amount of drug release in time (t)

K_H = Higuchi constant

t = time in hrs

The equation is based on the following assumptions:

- A pseudo steady state of the system
- The drug particles are small compared to the average distance of diffusion in the device
- There is constant diffusion coefficient
- Perfect sink conditions exist in the external medium such that the initial concentration of the drug in the system (C_o) is much higher than drug solubility (C_s) (Higuchi, 1961).

1.13.4 Korsmeyer-Peppas kinetic model

A graph is plotted between the log time taken on X-axis and the log cumulative percentage of drug release on y-axis and it gives a straight line.

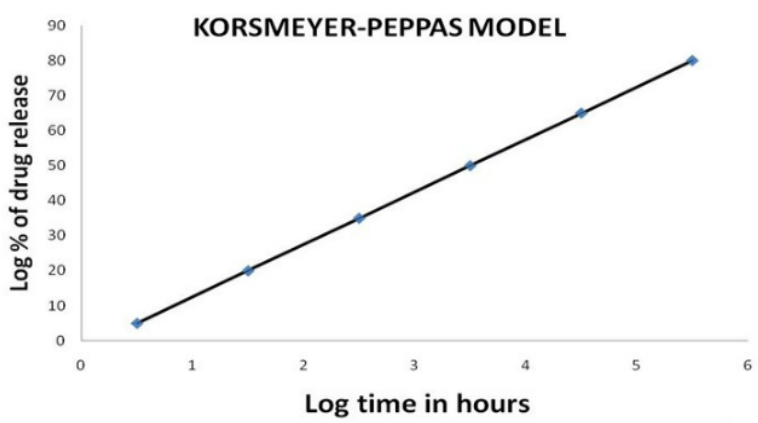

$F = (M_t/M) = K_m t^n$ Equation 1.4

F = fraction of drug release in time (t)

M_t = Amount of drug released at time (t)

M = total amount of drug in dosage from

K_m = kinetic constant

n = diffusion or release exponent

t = time in hrs

'n' is estimated from linear regression of log (M_t/M) versus log t.

Assumptions for this equation include:

- The equation applies to the first 60% of drug release
- The release system does not swell to more than 25% of its original volume in the dissolution medium
- It is also necessary that the release occurs in a one dimensional way
- The system width/thickness or length/thinkness ratio is at least 10

Table 1.6 Interpretation of diffusional release mechanisms from polymeric films (Korsmeyer et al., 1983).

Release exponent (n)	**Drug transport mechanism**	**Rate as a function of time**
0.5	Fickian diffusion	$t^{-0.5}$
$0.45 < n = 0.89$	Non – Fickian transport*	t^{n-1}
0.89	Case II transport**	Zero order release
Higher than 0.89	Super case II transport**	t^{n-1}

*Anomalous diffusion or non-Fickian refers to combination of both diffusion and erosion controlled rate release. **Case II transport or super case II transport refers to the erosion of the polymeric chain.

1.14 Materials used

1.14.1 Metolose (MET)

MET is non-ionic water-soluble cellulose ether that is derived from pulp with a chemical structure as shown in figure 1.16. MET comprises methylcellulose and three substitution types of HPMC each available in several grades with varying viscosities. Highly purified pulp is etherified with methyl or a combination of methyl chloride and propylene oxide to form a water soluble, non-ionic cellulose ether. It can produce transparent films by casting from their gel solutions. The film properties markedly depend on the moisture content (Roy et al., 2010).

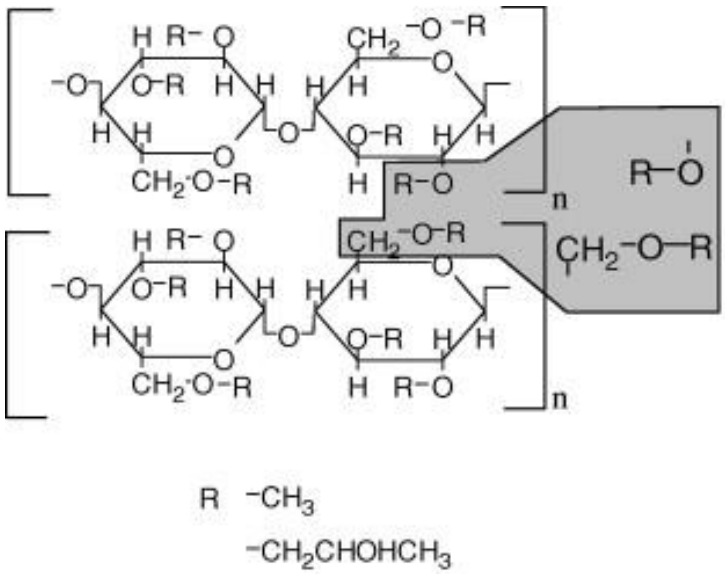

Figure 1.16 Chemical structure of MET.

Some of the key properties of MET include solubility in cold water and forms transparent solutions; it forms reversible gels during heating due to its viscoelastic properties and the formed gel maintains its shape during the heating. It achieves a very good miscibility with salts and sugars and has excellent water binding properties; is suitable for emulsification and stabilization of dispersions and it has a buffer capacity in a wide range of pH values (3-11).

1.14.2 Hydroxypropyl methylcellulose (HPMC)

HPMC is methylcellulose modified by treatment with alkali and propylene oxide by which a small number of 2-hydroxypropyl groups are attached through ether links to the anhydro-glucose units of the cellulose. HPMC is widely used as thickening and binding agents, emulsifiers and stabilizers in various oral pharmaceutical preparations e.g. Zanaflex (skeletal muscle relaxant), Adderll (CNS stimulants) and Valdecoxib topical gel (NSAID) (Setty et al., 2010). It is also used in the food industry as a gelling and stabilizing agent (Byun et al., 2012). HPMC possesses special characteristics for controlled release formulations and its applications based on four key features i.e. surface activity, film forming ability, the capacity to form thermal gels that convert to liquid on cooling and efficient thickness. These properties are mainly due to the strong hydrophobic zones of the methyl substitutes with a backbone of cellulose and hydroxypropyl group that are hydrophilic in nature (figure 1.17) (Papkov et al., 2007). HPMC has been used for edible coatings or as films for packaging.

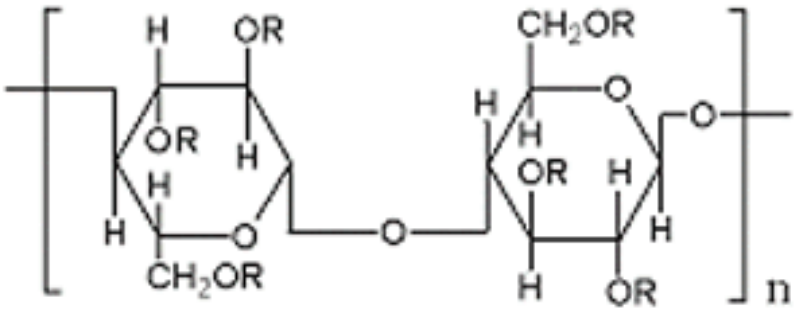

Figure 1.17 Chemical structure of HPMC

1.14.3 Methylcellulose (MC)

MC is the methyl ether of cellulose, prepared from wood pulp or cotton by treatment with alkali and methylation of the alkali cellulose with methyl chloride (figure 1.18). MC has a wide range of uses in general industrial settings, depending on viscosity depending upon molecular weight. They can be used as adhesives or thickening agents, viscosity control agents, or protection in paint formulations. Pharmaceutical grades have been used as thickeners, binders, emulsifiers, and stabilizers in a variety of cosmetic, pharmaceutical and food products (Kumar et al., 2012).

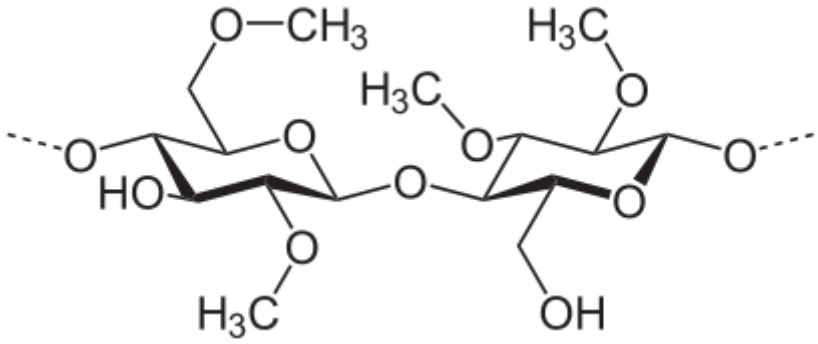

Figure 1.18 Chemical structure of MC

1.14.4 Sodium alginate (SA)

SA, the sodium salt of alginic acid, is a water soluble anionic polymer. Alginate comprises un-branched binary copolymers of alginic acid (1-4)-linked to b-D-mannuronic acid (M) and a-L-guluronic acid (G) residues as monomers, constituting M-, G-, and MG - sequential block structures (Figure 1.19) (Funami et al., 2009). SA and their derivatives are widely used in the food, cosmetics and pharmaceutical industries (Fan et al., 2001). As hydrophilic polymers, alginates have one important feature, that, its solution has relatively high viscosity that plays a vital role in drug stability and enables alginates to act as thickening and tackifying agents. Alginates have favourable film-forming properties (Fan et al., 2001) and also widely used to produce microspheres, beads, microcapsules and tablets for drug delivery systems and it shows prolonged effects of the active ingredient.

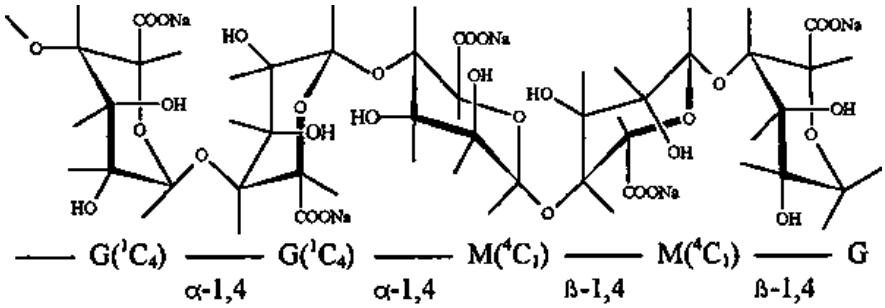

Figure 1.19 Chemical structure of SA (Nono, et al., 2012).

1.14.5 Carrageenan (CA)

CA is a high molecular weight material with a high degree of polydispersity. CAs are commercially important hydrophilic colloids (water-soluble gums) which occur as matrix

material in numerous species of red seaweeds (Rhodophyta) where they serve a structural function analogous to that of cellulose in land plants. Chemically they are highly sulphated galactans and they are strongly anionic polymers due to their half-ester sulphate moieties. It is linear, water-soluble and typically forms highly viscous aqueous solutions. Commercially, CA is available as stable sodium potassium and calcium salts or, most commonly, as a mixture of these. It comes in three grades; kappa, iota and lambda depending upon the position of the ester sulphate group (figure 1.20) (Nono et al., 2012). In aqueous solution, kappa and iota CA exhibit a thermo reversible sol-gel transition and retain pseudo-plastic properties with some degree of 'yield value' structure.

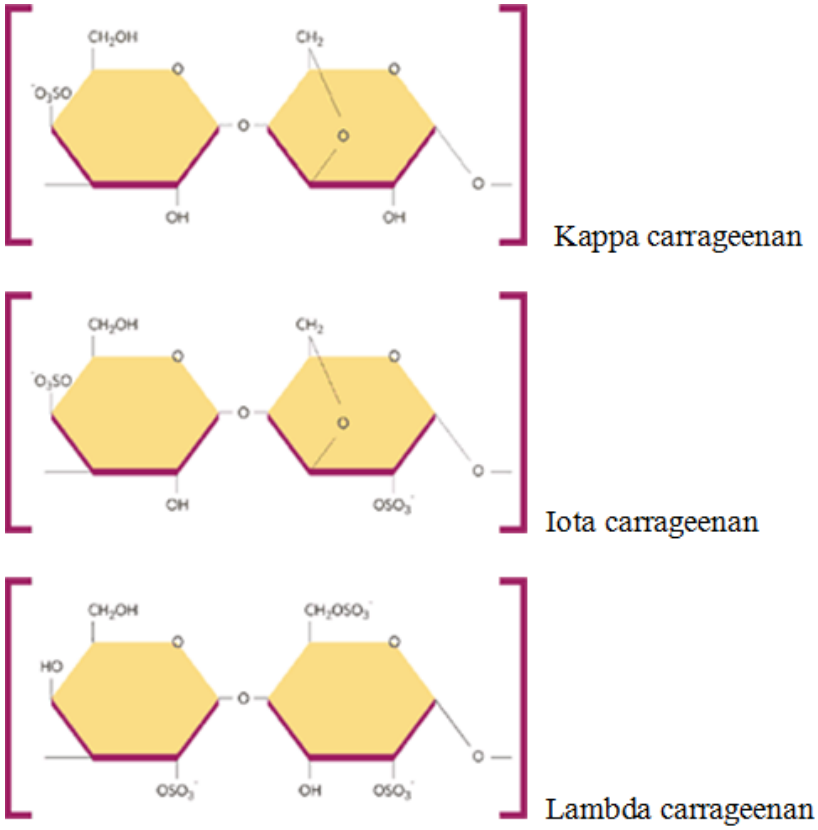

Figure 1.20 Chemical structure of kappa, iota and lambda CA (Nono et al., 2012)

1.14.6 Polyethylene glycol (PEG)

PEGs are a family of water-soluble linear polymers formed by the addition reaction of ethylene oxide (EO) with mono ethylene glycols (MEG) or diethylene glycol. There are many grades of PEGs depending on their average molecular weight (Abdulla et al., 2009). For example, PEG 400 consists of a distribution of polymers of varying molecular weights with

an average of 400, which corresponds to an approximate average number of repeating EO groups (n) of ≈ 9. PEG 400 is strongly hydrophilic and the partition coefficient between water and hexane is 0.000015 (Turton., 2008). The liquid PEG has broad use in preparation of parenteral drug delivery systems or filling for gelatine capsule where it functions as a plasticiser. Compatibility with the polymer, processing characteristics, desired thermal and mechanical properties, required amount of plasticization are the main factors affecting the selection of the grade of PEG as plasticisers (Zhou et al., 2013).

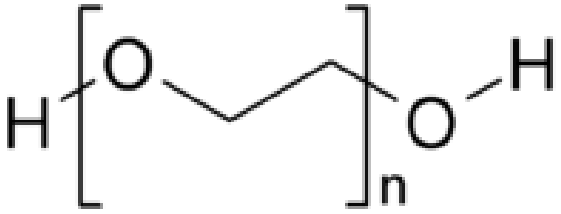

Figure 1.21 Chemical structure of PEG 400

1.14.7 L-Arginine (L-arg)

L-arg [(S)-2-Amino-5-guanidinopentanoic acid (Figure 1.22) is a basic amino acid naturally present in our diets and is particularly rich in certain food products, such as meats and nuts. Arginine was initially regarded as a non-essential amino acid. Thus, an initial classification of arginine as a semi-essential amino acid was given. Arginine prevented thymic involution after surgery and helps to increase the number of lymphocytes and a necessary agent for adequate wound healing. It also acts as an auxiliary substance by significantly increasing the aqueous solubility of other compounds at the molecular level (Alvares et al., 2012).

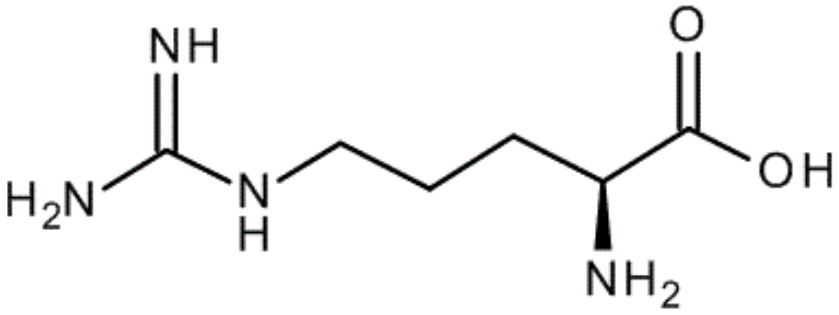

Figure 1.22 Chemical structure of L-arg (Fan et al., 2001)

1.14.8 Omeprazole (OME)

OME, 5-methoxy-2-[[(4-methoxy-3, 5-dimethyl-2-pyridinyl) methyl] sulfinyl]-1H-benzimidazole is an inhibitor of gastric acid secretion, developed by the Swedish firm Aktiebolaget Hassle. In the treatment of acid-related diseases, OME is superior to H2 – receptor antagonists such as Cimetidine. Omeprazole achieves its effects by blocking the final common pathways of acid secretion at the luminal surface of the parietal cell by binding the H^+K^+ -ATPase known as the 'acid pump' or the 'proton pump' thereby providing potent inhibition of gastric acid.

OME is an effective short-term treatment for gastric and duodenal ulcers and used in combination with antibiotics for eradication of *Helicobacter pylori* (Stroyer et al., 2006). An initial short course of OME is the treatment of choice in gastro-oesophageal reflux disease with severe symptoms; children with endoscopically confirmed erosive, ulcerative, or stricturing (narrowing or tightening) of oesophagus (Fass et al., 1998). OME is also used for the prevention and treatment of ulcers associated with non-steroidal anti-inflammatory drugs (NSAID). In children who need to continue NSAID treatment after an ulcer has healed, the dose of OME should not normally be reduced because asymptomatic ulcer deterioration may occur (Zimmermann et al., 2001). OME is effective in the treatment of Zollinger-Ellison syndrome and is used to reduce the degradation of pancreatic enzyme supplement in children with cystic fibrosis (Nishioka et al., 1999).

In aqueous solution its stability is entirely dependent on the initial pH and in acidic and neutral conditions, it is rapidly degraded, whereas in alkaline medium OME shows a greater stability. In the solid state OME is rapidly degraded in the presence of heat, light and humidity. (Ruiz M et al, 1998). To prevent degradation of the drug in the acid medium of the stomach, the drug is formulated as enteric-coated granules in capsule form (Lind et al., 1983). The mean time to attain maximum plasma concentrations (t_{max}) of OME is highly formulation dependent. It is a very well tolerated drug and its doses are 20 mg up to 80 mg. OME's terminal half-life is between 0.5 and 2 hrs (Dojo et al., 2001). Although OME is well absorbed from the gastrointestinal tract, its oral bioavailability in humans is about 40 to 50% suggesting pronounced first pass metabolism for this drug. After absorption, it is metabolized and three main metabolites; OME sulphone, OME sulphide and hydroxyl OME have been identified in human plasma (Naseri et al., 2006). Hydroxylation of OME at the 5-position is

subject to genetic polymorphism and the sulphone in plasma is cumulated in poor metabolizers of S-mephenytion 4' hydroxylation. Therefore, most individuals metabolize the drug normally, and only a small number might be expected to be poor metabolizers (Wagner et al., 2011).

OME is available in mainly two forms in the market such as tablet (20 mg) and capsule (10mg, 20mg and 40mg) as can be seen in Figure 1.23.

Figure 1.23 Omeprazole tablet (20mg) and capsule (10 mg). Available at - <http://upload.wikimedia.org/wikipedia/commons/thumb/1/13/Omeprazole_10mg_UK.jpg/220px-Omeprazole_10mg_UK.jpg > [Accessed: 13/05/2013]

1.14.8.1 Side effects of OME

Though OME is generally well tolerated, headache, diarrhoea, stomach ache, muscle weakness and rash have been reported. Other less common adverse reactions reported include constipation, cough, fatigue, sore throat and vomiting. It slows the elimination of several drugs that must be processed by the liver, including the anxiety medicine valium®, the anti-epileptic dilantin and the blood thinner coumadin (Caroet al., 2001; Mostafavi et al., 2004).

1.15 Experimental Techniques

Various analytical and preformulation techniques were employed in the characterisation of the formulations prepared as part of the development and optimization studies. These are briefly discussed in the supplementary information found in the appendix.

1.16 Aims and objectives

The main aim of this project was to develop, formulate, characterise and optimise novel pre-formed thin polymer film that will deliver therapeutically relevant drugs via the buccal mucosa route of paediatric patients, using OME as model drug. The development will be focused on obtaining formulations with optimized drug loading, drug release and permeation, stability and low toxicity

The main objectives include:

1. Pre-formulation studies, to select and characterise polymeric materials to be used in formulating films with potential to deliver OME via the buccal mucosa of paediatric patients. Work will range from basic formulation steps such as polymer gel preparation, film formation, by using model drug (OME), stabiliser (L-arg), polymers (MET, HPMC, MC, SA and CA) and plasticiser (PEG 400) in optimum ratios that will ensure product stability.
2. Physico-chemical and bio-analytical methods (TA, SEM, XRD, HSM, DSC, TGA, ATR-FT-IR, HPLC and SCF CO_2) will be used to characterise physicochemical properties of the raw materials, films with/ without plasticiser and films with/ without drug (OME) as part of the pre-formulation and preliminary formulation development.
3. Further formulation development using selected optimum polymeric systems characterised above, loaded with the drug to obtain an optimised thin film buccal drug delivery system.
4. Functional characterisation studies by *in vitro* mucoadhesion and swelling will be carried out on the optimised films (blank and drug loaded) using PBS and simulated saliva (pH 6.8±0.5).
5. Drug dissolution and release characteristics will be conducted for drug loaded films by using Franz diffusion cells and drug release kinetics will be evaluated to predict possible *in vivo* performance. Stability studies of the drug-loaded films based on the International conference on harmonization (ICH) guidelines will be conducted. These will cover drug and polymer stability with the help of HPLC technique respectively as well as formulation approaches for improving drug stability during development and storage.
6. *Ex vivo* drug permeation and bioadhesion studies of the films using pig buccal tissue and

cell viability studies using MTT assay to evaluate toxicity profile of model drug (OME), stabiliser (L-arg) and polymer (MET) and the optimised drug loaded films.

7. Investigate the effect of SCF on the properties of the optimised drug loaded films.

CHAPTER TWO: FORMULATION DEVELOPMENT, OPTIMIZATION AND PHYSICAL CHARACTERIZATION OF BLK SOLVENT CAST FILMS

2.1 INTRODUCTION

Many paediatric patients resist solid dosage forms such as tablets due to the bitter taste and fear of choking. Though sweetened liquid formulations are commonly used, they present many challenges including bitter after taste, unpleasant flavours, short half-lives once opened and generally bulky to handle and store. Oral thin films offer easy administration and handling, rapid disintegration and dissolution, enhanced stability and taste masking for bitter drugs, local and systematic drug delivery, rapid onset of action and no trained or professional person is required for paediatric administration (Dixit et al., 2009). Due to the numerous advantages of buccal dosage forms, a lot of pharmaceutical companies have adopted various technologies to manufacture oral films on a large scale as an alternative to traditional dosage forms such as tablets and capsules (Siddhiqui et al., 2011).

The development of paediatric dosage forms faces unique challenges, including the important differences between growing and developing children and adults; toxicity profiles, difference in rates of drug metabolism and different drug responses. These require specific clinical trials to ascertain the safety and efficacy of specific drugs and dosage forms in children (Schachter et al., 2007). This chapter aims to develop and optimise solvent cast films for potential buccal delivery in paediatric patients using various hydrogel polymers generally regarded as safe (GRAS) including hydroxypropylmethylcellulose (HPMC), methylcellulose (MC), sodium alginate (SA), carrageenan (CA) and metolose (MET) with polyethylene glycol (PEG 400) as plasticiser. Films have been produced using the solvent casting approach using different solvents (either aqueous or ethanolic). The films were characterised for tensile properties (texture analysis - TA), physical form (differential scanning calorimetry - DSC; X-ray diffraction -XRD; thermogravimetric analysis - TGA and hot stage microscopy - HSM) and surface topography (scanning electron microscopy - SEM). The characterisation results were then used to select optimised films for drug loading and further work.

2.2 MATERIALS AND METHOD

2.2.1 Materials

Table 2.1 List of materials used

Name	Batch Number	Purity	Company	Location
Ethanol	1405343	-	Fisher Scientific	Loughborough, UK
Hydroxypropylmethylcellulose (HPMC)	9004-65-3	97%	Sigma Aldrich	Gillingham, UK
Methylcellulose (MC)	9004-67-5	-	Sigma Aldrich	Gillingham, UK
Metolose (MET)	311615	-	Shin Etsu	Stevenage, Hertfordshire
Carrageenan (CA)	30207001	-	FMC Bio-Polymer	Cork, Ireland
Sodium alginate (SA)	LSL001301	-	FMC Bio-Polymer	Cork, Ireland
PEG 400	1405869	97%	Sigma Aldrich	Gillingham, UK

2.2.2 Consumables

Table 2.2 List of consumables

Consumable	Company	Location
Blue, white and yellow micropipette tips	Fisher Scientific	Loughborough, UK
100 mL beakers	Fisher Scientific	Loughborough, UK
Magnet stirrer	Fisher Scientific	Loughborough, UK
Tzero hermetic pans and lids	TA Instruments	Crawley, UK
SEM stubs	Agar Scientific	Essex, UK

2.2.3 Instruments

Table 2.3 List of instruments used

Instrument	Manufacturer/Supplier
Texture analyser TA HD plus	Stable Micro Systems, Surrey, UK
DSC Q2000	TA Instruments, Crawley, UK
Q5000-IR thermogravimetric analyser	TA Instruments, Crawley, UK
Mettler Toledo FP82HT	Greifensee, Switzerland
SEM. Hitachi SU 8030	Hitachi High-Technologies, Tokyo, Japan
D8 Advantage X-ray diffractometer	Bruker, Coventry, UK
Perkin Elmer spectrophotometer	Spectrum Two, Perkin Elmer, US
Tzero sample encapsulation press	TA Instruments, Crawley, UK
Micrometre screw gauge (0-25mm)	Fisher Scientific, Loughborough, UK

2.2.4 METHODS

2.2.4.1 Preparation of BLK solvent cast films

Solvent cast films were formulated by using different polymers (SA, HPMC, MC, CA and MET) which were chosen because of their hydrophilic nature.

Gel preparation

Aqueous and ethanolic gels of the different polymers were prepared prior to film casting as follows.

i. The preliminary gels were formulated by adding the required weight of polymers (0.5 g) to the relevant solvent (deionised water), (50 mL) at room temperature (22 °C). Further heating was not applied to dissolve any polymer as the polymers easily hydrated in cold water. Based on the total weight of polymers, plasticiser (PEG 400) was added in different quantities of (0.00 %, 0.10 %, 0.25 %, 0.50 %, 0.75 % and 1.00 % w/w) to the gels prepared above.
ii. The resulting gels were left on the water bath with regulated temperature of 40 ˚C (except CAR prepared at 70 ˚C) and continuous stirring was carried out by a mechanical stirrer for about 30 minutes to achieve a homogeneous dispersion.

iii. For ethanolic gels, the appropriate volume of ethanol was added to yield the target 1 % w/w gel as for water above and the solution was brought to room temperature and stirred again for 30 minutes. The final solution was left to stand overnight to remove all the entrapped air bubbles (Morales et al., 2011).

Drying procedure to obtain films

After removal of the air bubbles, 20 g of gel solution was poured into Petri dishes (86 mm diameter) and dried in an oven (60 °C) for 12 h and 18-24 h for the unplasticised and plasticised gels respectively as shown in figure 2.1 (Sudhakar et al., 2006). The dried films were carefully peeled off from the Petri dish and transferred into poly bags and placed in a desiccator over silica gel at room temperature until ready for analysis.

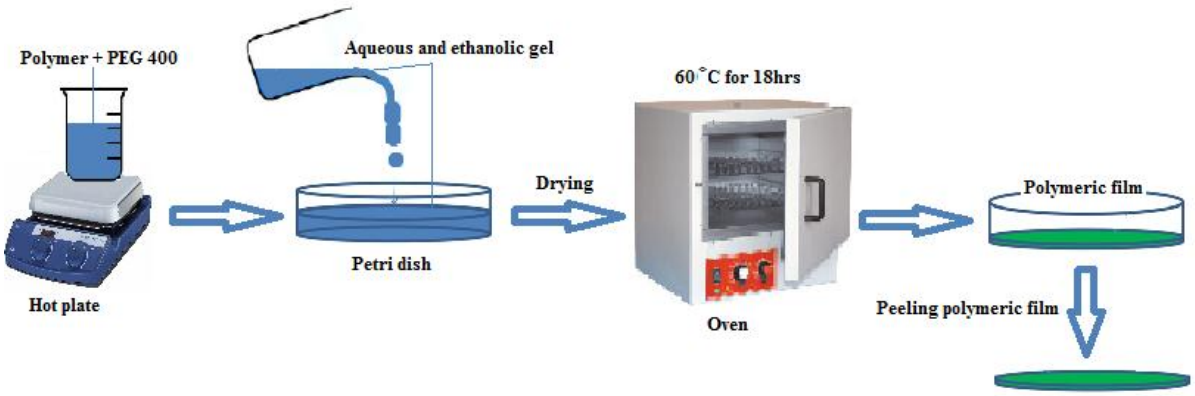

Figure 2.1 Schematic diagram representing preparation of BLK films using gels from different polymers and PEG 400 at different concentrations

2.2.4.2 Texture analysis

Texture analysis was used to characterise the tensile properties of the films (films plasticized with 0-1.0 % PEG 400). A texture analyser TA HD plus (Stable Micro System, Surrey, UK) equipped with 5 kg load cell was used to perform the experiment and data evaluation was performed by texture exponent-32 software program. The films free from any physical imperfection with the average thickness of (0.03 + 0.05 mm) were selected for testing (Boateng et al., 2013) and cut into dumb-bell shaped strips. The dumb-bell shaped films were fixed between two tensile grips positioned 30 mm apart and stretched to break point as shown

in figure 2.2. The peak force and elongation at break, elastic modulus of the films prepared with different polymers (SA, HPMC, MC, CA and MET) and PEG 400 as plasticiser (0-1.0 % w/w based on polymer's weight) (Ayensu et al., 2012) were determined when films broke. Three replicates were carried out for each type of film and the instrument settings used in the analyses are given in table 2.4.

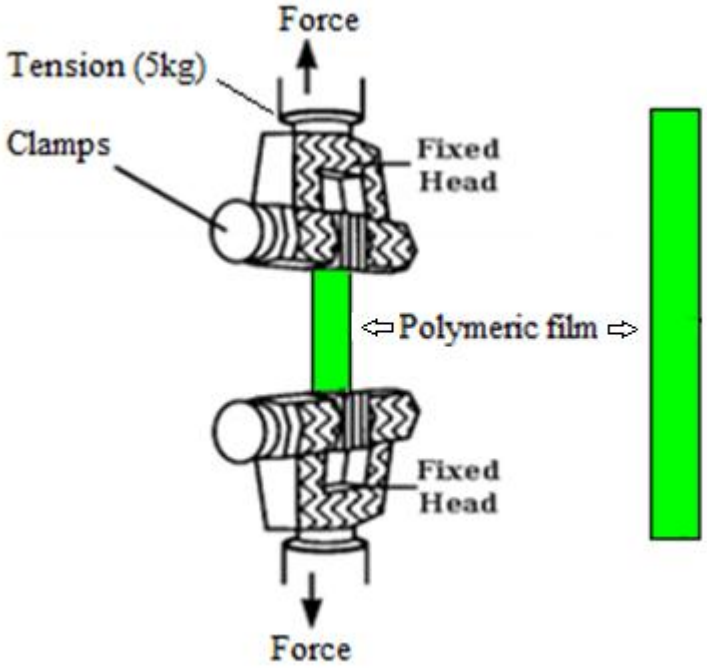

Figure 2.2 Schematic representation of texture analysis for the evaluation of mechanical (tensile) properties of the polymeric film.

Table 2.4 Texture analyser settings

Test parameter	**Value**	**Description**
Pre-test speed	0.1 mm/sec	Speed of probe before stretching
Test speed	1.0 mm/sec	Stretching speed during testing
Post-test speed	0.1 mm/sec	Speed at which probe returns to the starting position
Distance	50.0 mm	Distance to which grips separate from their starting position after stretching
Trigger type	Auto (Force N)	Force achieved before profile is plotted
Product length	30.0 mm	Length of film between clamps
Product width	10.0 mm	Width of the film
Contact area	300.0 mm^2	Total area of films between tow clumps

2.2.4.3 Hot stage microscopy (HSM)

The hot stage microscopy experiments were conducted on a Mettler Toledo FP82HT (Greifensee, Switzerland) with a Nikon Microphot. MET and SA films were placed on a glass slide, covered with a coverslip, and heated from ambient room temperature to 200 °C at 10 °C per minute. Changes in morphological behaviour during heating were collected as a video recording by using PixeLINK PL-A662 camera (PixeLINK, Ontario, US).

2.2.3.4 Differential scanning calorimetry (DSC)

Differential scanning calorimetry was used to characterise the thermal behaviour (glass transition point (T_g) and melting transition (T_m)) of MET and SA (pure materials and films) and changes in their properties with introduction of PEG within the films. Analysis of the films and starting materials were carried out on a Q2000 (TA Instruments) calorimeter. About 2.5 mg of each sample was placed into hermetically sealed Tzero aluminium pans with a pin hole in the lid and heated from -40°C to 180°C at a heating rate of 10 °C/min under constant purge of nitrogen (N_2) (100 mL/min) to evaluate the glass transition, melting, crystallisation and possible interaction between polymers and plasticisers (Boateng, et al., 2013).

2.2.3.5 Thermogravimetric analysis (TGA)

TGA studies were performed using a Q5000 (TA instrument) thermogravimetric analyser. About 1-2.5 mg of films and starting materials (MET and SA) was placed into hermetically sealed Tzero aluminium pans with a pin hole in the lid. Samples were heated under nitrogen (N_2) gas with a flow rate of 25 mL/min, from ambient temperature (20 °C) to 200 °C at a heating rate of 10 °C/min to evaluate the water content of the pure materials and films.

2.2.3.6 Scanning electron microscopy (SEM)

SEM was used to investigate the surface morphology of the films and to check for film uniformity and the presence of any cracks. The films were analysed using a Hitachi Triple detector CFE-SEM SU8030, (Hitachi High-Technologies, Japan) scanning electron microscope. Films were mounted onto Agar scientific G301aluminium pin-type stubs (12 mm diameter) with Agar scientific G3347N double-sided adhesive carbon tapes and chrome

coated (Sputter Coater S150B, 15 nm thickness). The coated films were analysed at 2 kV accelerating voltage (x200 magnification) (Engel et al., 1993; Frank et al., 2011).

2.2.4.7 X-ray diffraction (XRD)

D8 Advantage X-ray diffractometer was used to investigate the physical nature (crystalline or amorphous) of the films and starting materials (MET, SA, PEG 400). XRD patterns of films and starting materials were obtained with a DIFFRAC plus instrument (Bruker Coventry, UK) with an XRD commander programme. A Goebel mirror was used as monochromator which produced a focused monochromatic CuK$\alpha_{1\&2}$ primary beam (λ=1.54184 Å) with exit slits of 0.6 mm and a Lynx eye detector for performing the experiment. The operating conditions during the experiment were 40 kV and 40 mA. Samples were prepared by cutting 2cm^2 of films to fit the square tiles of the holder as shown in figure 2.3, mounted on the sample cell and scanned between 2 theta of 0° to 70° with counting time (0.1 second step size) (Brügemann, et al., 2004; Dittrich, et al., 2009).

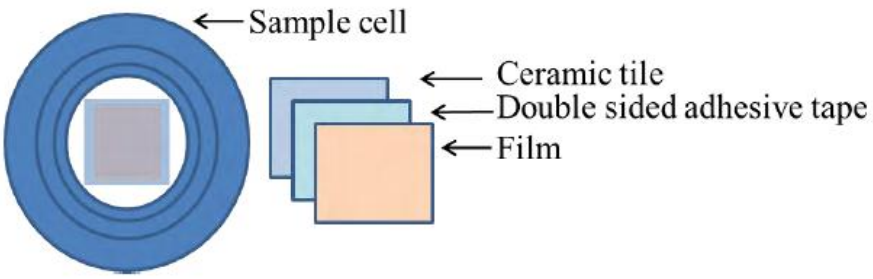

Figure 2.3 Representation of sample cell used for XRD analysis of polymeric film.

2.2.4.8 Fourier transform infrared (FT-IR) spectroscopy

FT-IR spectra were obtained using a Perkin Elmer spectrophotometer (Spectrum Two, Perkin Elmer, US) equipped with a crystal diamond universal ATR sampling accessory (UATR). Before each measurement, the ATR crystal was carefully cleaned with ethanol. During the measurement, the sample was in continuous contact with the universal diamond ATR top-plate. For each sample, an average of 4 scans per spectrum was recorded in the range of 4000-400 cm-1.

2.3 RESULTS AND DISCUSSION

2.3.1 Gel formulation

Different polymers such as HPMC, MC, SA, CA and MET were used for formulation because of their hydrophilic nature their desirable properties for formulating oral thin films (Papkov et al., 2007), (Siahboomi et al., 1993), (Boateng et al., 2009), (Kianfar et al., 2012). To obtain uniform gels, the gels were constantly stirred for 30 min which caused the formation of bubbles (Bemkop, 2005). Constant heat was provided (40 °C), while stirring to prevent formation of lumps which can occur through incomplete hydration especially for polymers with high viscosity. The heat (40 °C or 70 °C) reduced the viscosity of the final gels, which helped to facilitate the escape of entrapped air bubbles caused by stirring and also allowed ease of pouring into the casting Petri dishes. The removal of the air bubbles entrapped inside the gel was essential to avoid any empty gaps, which could lead to non-uniform distribution of drug and contents added in films formulation.

Drying time

Films formulated with the different polymers are shown in figure 2.4. The main reason behind keeping the gel for 18-24 hrs in an oven at 60 °C was for complete drying of the gel. During the drying process most of the solvent was evaporated. The drying process for unplasticised gels was shorter (12 hrs) compared to plasticised gels (18-24 hrs) due to the known water affinity of most plasticisers (Boateng et al., 2009). Formulated films were evaluated in terms of transparency, satisfactory elasticity and stability during handling and storage.

Visual evaluation of resulting films

Films prepared from MET and SA were transparent, uniform and easy to peel off from the Petri dishes. However, HPMC, MC and CA films were transparent but not uniform due to air bubbles and difficult to peel without damaging the films as shown in figure 2.4. CA films (both plasticised and unplasticised) showed the same characteristics and were all very brittle regardless of plasticiser concentration. On the other hand, HPMC and MC films (plasticised) showed too much elasticity at both low and high concentration of PEG 400 (elasticity of films increased with higher concentration of plasticiser). As a result, film formulation with

CA, HPMC and MC was discontinued as shown in table 2.7 and only MET and SA films were taken forward for further development in terms of plasticiser content and drug loading optimisation.

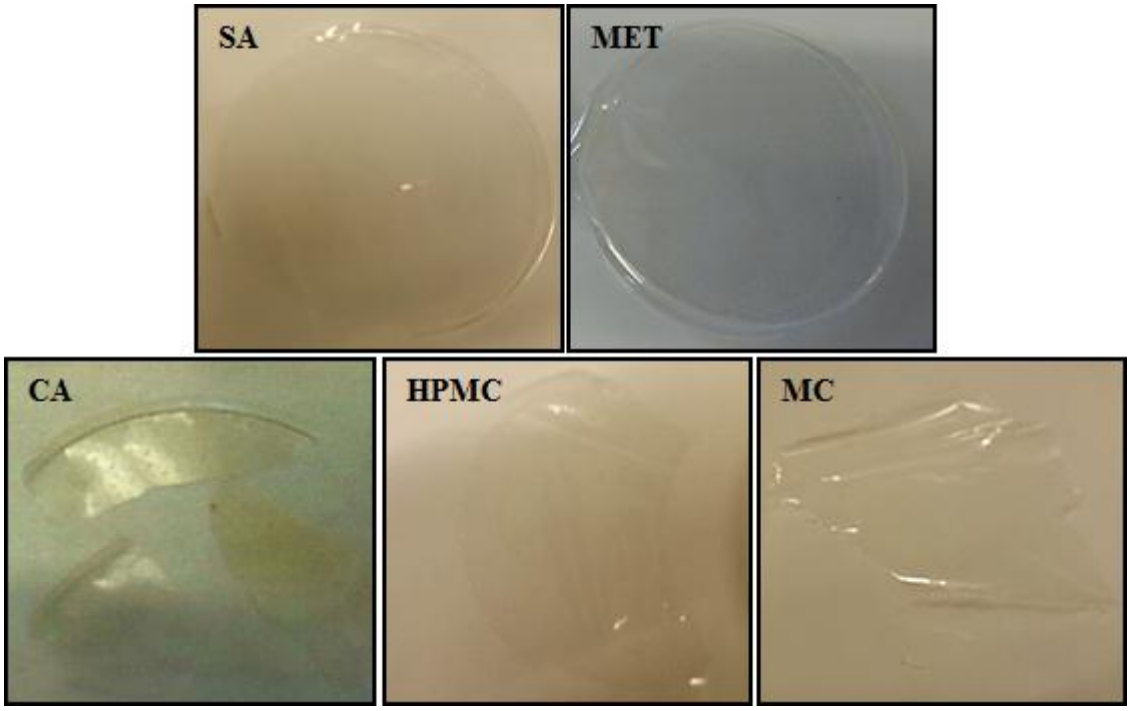

Figure 2.4 Physical appearances of oral films prepared with different polymers.

Further development of MET and SA films, during the preliminary experiments, involved preparing films with and without plasticiser and solvent used (pure H_2O and 10 and 20% v/v EtOH). The main purpose of using plasticiser is to provide flexibility and to overcome the brittleness in films, while EtOH was used to speed up the drying process and improve dissolution of some polymers. Un-plasticised films showed some elasticity but this was not flexible enough to satisfy the criteria (transparency, satisfactory elasticity and ability to incorporate drug (Bala et al., 2013)) of novel oral films. The films with PEG 400 plasticiser showed optimised results with desirable flexibility and reduced brittleness (Choi et al., 2000). Application of heat was not required to dissolve plasticiser (PEG 400) as it is hydrophilic in nature. The initial physical appearance and other properties of formulated films with MET and SA are summarised in tables 2.5 and 2.6. However, optimum plasticiser concentration(s) for further formulation development was evaluated by using texture analysis as below.

Table 2.5 Visual characteristics of different BLK MET films formulated from gels prepared with water, 10 % v/v and 20 % v/v EtOH.

Observation							
Polymer	**PEG % (w/w)**	**Texture**	**Colour**	**Bubbles**	**Sticky**	**Peels off easily**	**Thickness (rounded to two decimal places) (mm)**
Water							
MET	0.00	Smooth	Transparent	No	No	Yes	0.03
	0.25	Smooth	Transparent	No	No	Yes	0.03
	0.50	Smooth	Transparent	No	Yes	Yes	0.03
	0.75	Smooth	Transparent	No	Yes	Yes	0.03
	1.00	Smooth	Transparent	No	Yes	Yes	0.03
10% v/v EtOH							
MET	0.00	Smooth	Transparent	No	No	Yes	0.03
	0.10	Smooth	Transparent	No	No	Yes	0.03
	0.25	Smooth	Transparent	No	No	Yes	0.03
	0.50	Smooth	Transparent	No	Yes	Yes	0.03
	0.75	Smooth	Transparent	No	Yes	Yes	0.03
	1.00	Smooth	Transparent	No	Yes	Yes	0.03
20% v/v EtOH							
MET	0.00	Smooth	Transparent	No	No	Yes	0.03
	0.25	Smooth	Transparent	No	No	Yes	0.03
	0.50	Smooth	Transparent	No	No	No	0.03
	0.75	Smooth	Transparent	No	Yes	No	0.03
	1.00	Smooth	Transparent	No	Yes	No	0.03

Table 2.6 Visual characteristics of different BLK SA films obtained from gels prepared with water, 10% v/v and 20% v/v EtOH.

Observation							
Polymer	**PEG % (w/w)**	**Texture**	**Colour**	**Bubbles**	**Sticky**	**Peels off easily**	**Thickness (rounded to two decimal places) (mm)**
Water							
SA	0.00	Smooth	Transparent	Yes	No	Yes	0.03
	0.10	Smooth	Transparent	No	No	Yes	0.03
	0.25	Smooth	Transparent	No	No	Yes	0.03
	0.50	Smooth	Transparent	No	No	Yes	0.03
	0.75	Smooth	Transparent	No	No	Yes	0.03
	1.00	Smooth	Transparent	No	No	Yes	0.03
10% v/v EtOH							
SA	0.00	Smooth	Transparent	No	No	Yes	0.03
	0.10	Smooth	Transparent	No	No	Yes	0.03
	0.25	Smooth	Transparent	No	No	Yes	0.03
	0.50	Smooth	Transparent	No	No	Yes	0.03
	0.75	Smooth	Transparent	Yes	No	Yes	0.03
	1.00	Smooth	Transparent	No	No	Yes	0.03
20% v/v EtOH							
SA	0.00	Smooth	Transparent	No	No	Yes	0.03
	0.10	Smooth	Transparent	Yes	No	Yes	0.03
	0.25	Smooth	Transparent	Yes	No	Yes	0.03
	0.50	Smooth	Transparent	No	No	Yes	0.03
	0.75	Smooth	Transparent	No	No	Yes	0.03
	1.00	Smooth	Transparent	No	No	Yes	0.03

Table 2.7 Visual characteristics of different BLK films of HPMC, MC and CA formulated from gels prepared water, 10 % v/v and 20 % v/v EtOH and without drug.

Observation								
Polymer	**PEG % (w/w)**	**Texture**	**Colour**	**Bubbles**	**Sticky**	**Brittle**	**Peels off easily**	**Thickness (rounded to two decimal places) (mm)**
Water								
HPMC	0.00	Smooth	Transparent	Yes	No	No	Yes	0.03
	0.10	Smooth	Transparent	Yes	No	No	Yes	0.03
	0.25	-	-	-	-	-	No	-
	0.50	-	-	-	-	-	No	-
	0.75	-	-	-	-	-	No	-
	1.00	-	-	-	-	-	No	-
MC	0.00	Smooth	Transparent	Yes	Yes	No	Yes	0.03
	0.10	Rough	Transparent	No	Yes	No	Yes	0.02
	0.25	Smooth	Transparent	No	Yes	No	Yes	0.02
	0.50	-	-	-	-	-	No	-
	0.75	-	-	-	-	-	No	-
CA	0.00	Smooth	Transparent	Yes	No	Yes	Yes	0.03
	0.10	-	-	-	-	-	No	-
	0.25	Rough	Transparent	Yes	Yes	Yes	Yes	0.02
	0.50	Smooth	Transparent	No	Yes	Yes	Yes	0.02
	0.75	Smooth	Transparent	No	Yes	Yes	Yes	0.03
	1.00	Smooth	Transparent	No	Yes	Yes	Yes	0.03
10% v/v EtOH								
HPMC	0.00	Smooth	Transparent	Yes	No	No	Yes	0.03
	0.10	Smooth	Transparent	Yes	Yes	No	Yes	0.03
	0.25	-	-	-	-	-	No	0.03
	0.50	-	-	-	-	-	No	-
	0.75	-	-	-	-	-	No	-

	1.00	-	-	-	-	-	No	-
MC	0.00	Smooth	Transparent	Yes	No		Yes	0.03
	0.10	Smooth	Transparent	Yes	No		Yes	0.03
	0.25	Smooth	Transparent	Yes	No		Yes	0.03
	0.50	-	-	-	-	-	No	-
	0.75	-	-	-	-	-	No	-
	1.00	-	-	-	-	-	No	-
CA	0.00	Rough	Transparent	Yes	Yes	Yes	Yes	0.03
	0.10	Smooth	Transparent	No	Yes	Yes	Yes	0.03
	0.25	Smooth	Transparent	No	No	Yes	Yes	0.03
	0.50	Smooth	Transparent	No	No	Yes	Yes	0.03
	0.75	Smooth	Transparent	No	No	Yes	Yes	0.03
	1.00	Smooth	Transparent	No	No	Yes	Yes	0.03

Polymer	PEG % (w/w)	Texture	Colour	Bubbles	Sticky	Brittle	Peels off easily	Thickness (mm)
20% v/v EtOH								
HPMC	0.00	Smooth	Transparent	No	No	No	Yes	0.03
	0.10	Smooth	Transparent	No	No	No	Yes	0.03
	0.25	Smooth	Transparent	No	Yes	No	Yes	0.04
	0.50	Smooth	Transparent	No	Yes	No	Yes	0.04
	0.75	Smooth	Transparent	No	Yes	No	Yes	0.04
	1.00	Smooth	Transparent	No	Yes	No	Yes	0.04
MC	0.00	Smooth	Transparent	No	Yes	No	Yes	0.04
	0.10	Smooth	Transparent	No	Yes	No	Yes	0.04
	0.25	-	-	-	-	-	No	-
	0.50	-	-	-	-	-	No	-
	0.75	-	-	-	-	-	No	-
CA	0.00	Smooth	Transparent	No	No	Yes	Yes	0.04
	0.10	Smooth	Transparent	No	No	Yes	Yes	0.04
	0.25	Smooth	Transparent	No	No	Yes	Yes	0.04
	0.50	Smooth	Transparent	No	No	Yes	Yes	0.04
	0.75	Smooth	Transparent	No	No	Yes	Yes	0.04
	1.00	Smooth	Transparent	No	No	Yes	Yes	0.04

2.3.2 Texture analysis

TA was used to measure tensile properties such as tensile strength (brittleness of the film), elastic modulus (rigidity) and elongation (flexibility and elasticity). Thickness and width of the specimen were measured and stress and strain values were calculated based on these values. The initial linear portion of the stress-strain curve was used to estimate the elastic modulus and tensile strength was calculated by dividing the peak force at break by the initial cross-sectional area of the films specimen (Lehrsch et al., 2012). The films showed significant differences in the tensile strength (brittleness) based on the PEG 400 concentration. Figures 2.5 to 2.7 show results of the effects of PEG 400 on the tensile strength values of the films. Generally, physical properties of polymers play an important role in the formulation of the films. Soft and weak polymers have low tensile strength, low elastic modulus (young's modulus) and low elongation at break. On the other hand soft and strong polymers display acceptable strength, low elastic modulus and high elongation at break (Morales et al., 2011).

HPMC was not selected for future formulations because plasticised HPMC film was too elastic and sticky which made it difficult to handle. Texture analysis of HPMC was only possible for films prepared from gels containing with 0% and 0.1% w/w of PEG 400. Films prepared from MC also showed the same characteristics as HPMC and as a result, MC was also discontinued for further film formulation. On the other hand, films with CA were very brittle with very high elastic modulus, tensile strength and low elastic modulus irrespective of the concentration of PEG 400 added as shown above in table 2.7 (Abdulla et al., 2009).

This could cause film breakage and eventual loss of drug and therefore not suitable for paediatric administration.

However, the average percent elongation at break point should be within 30% to 60% which indicates good balance between flexibility and elasticity (Boateng et al., 2009) and MET produced films which satisfied this required criteria. The elongation at break point of MET gradually increased with increasing concentration of the PEG 400. MET films prepared from gels containing 0.5% w/w PEG 400, formulated with different solvents (water, 10% v/v and 20% v/v of EtOH) were within the required range as can be observed in Figures 2.5, 2.6 & 2.7. Films with water as the casting the solvent gave a very low percentage elongation at

break point but with EtOH (10% v/v and 20% v/v) the peaks steadily increased with higher concentration of plasticiser. At the concentration of 0.75% w/w of PEG 400, all the films showed elongation at break point of 55-58% (figure 2.6). On the other hand, tensile strength and elastic modulus decreased with increased concentration of PEG.

Based on these observations future gel formulations were prepared with only two concentrations (0% and 0.5% w/w) of PEG 400. Films containing 0% w/w of PEG 400 were prepared as the reference for films plasticised with 0.5% w/w PEG 400. SA films showed similar results as MET films as shown in figures 2.8, 2.9 and 2.10. However further SA films were formulated without plasticiser as the SA powder was already blended with PEG. Generally, plasticisers impart flexibility and gloss to the finished film product, therefore, the concentration of plasticiser should be optimized along with the polymer and other excipients to obtain an elegant film. Plasticisers such as PEG in the system increase the free volume between the polymeric chains and allow them to slide past each other and subsequently produce appropriate flexibility and consequent decrease in tensile strength and elastic modulus (Alexander et al., 2011).

TA results for MET

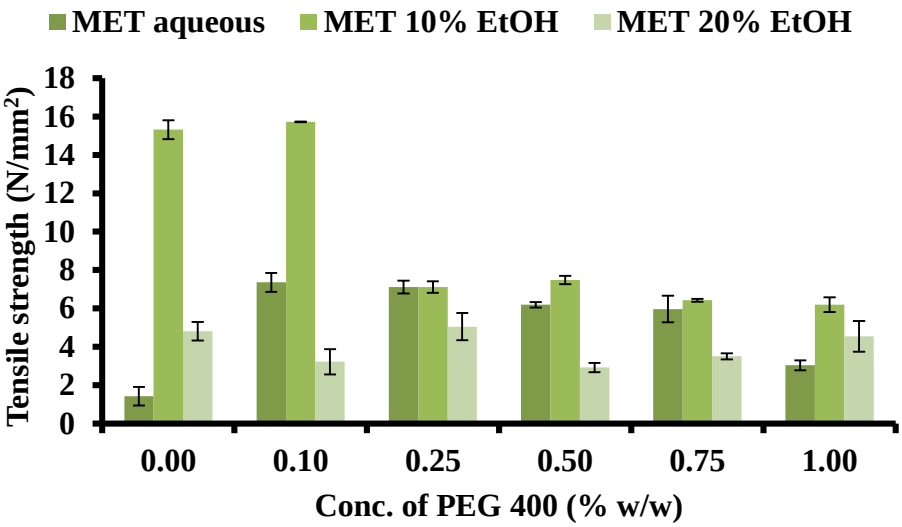

Figure 2.5 Mechanical properties (tensile strength) of MET films cast from aqueous and ethanolic (10% and 20% v/v EtOH) polymeric gels with increasing plasticizer (PEG 400) concentration (mean ± SD, (n=3))

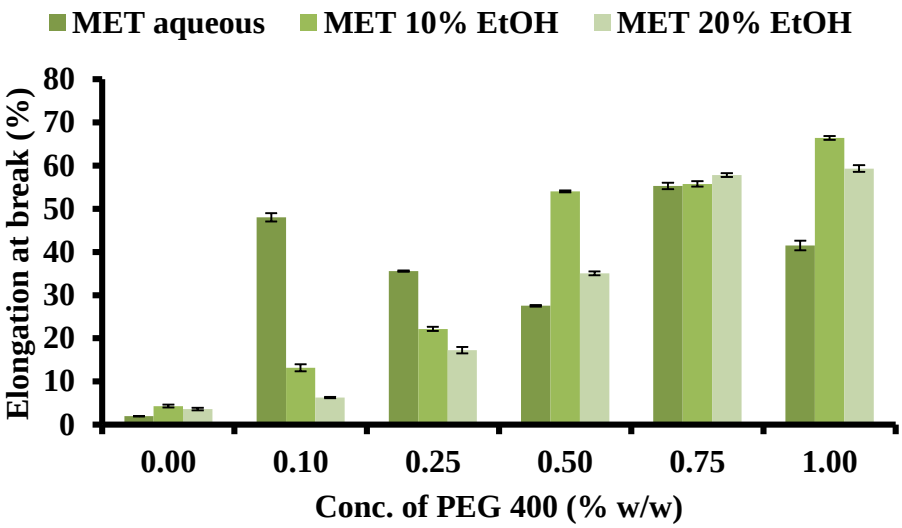

Figure 2.6 Mechanical properties (% elongation at break) of MET films cast from aqueous and ethanolic (10% and 20% v/v EtOH) polymeric gels with increase of plasticizer (PEG 400) concentration (mean ± SD, (n=3))

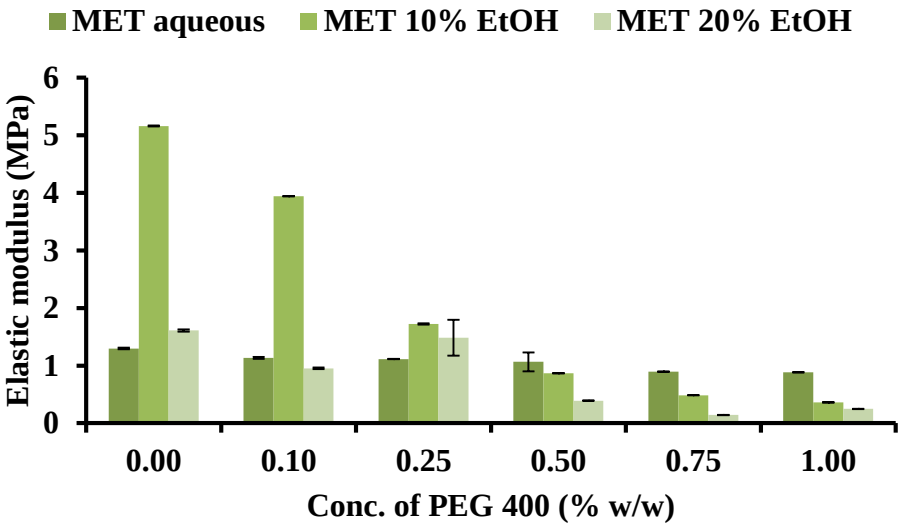

Figure 2.7 Mechanical properties (elastic modulus) of MET films cast from aqueous and ethanolic (10% and 20% v/v EtOH) polymeric gels with increase of plasticizer (PEG 400) concentration (mean ± SD, (n=3))

TA results for SA

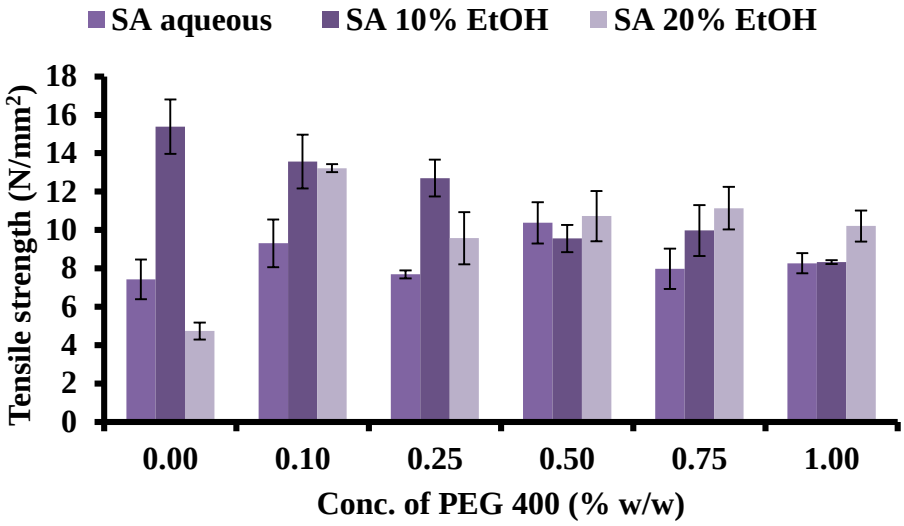

Figure 2.8 Mechanical properties (tensile strength) of SA films cast from aqueous and ethanolic (10% and 20% v/v EtOH) polymeric gels with increase of plasticizer (PEG 400) concentration (mean ± SD, (n=3))

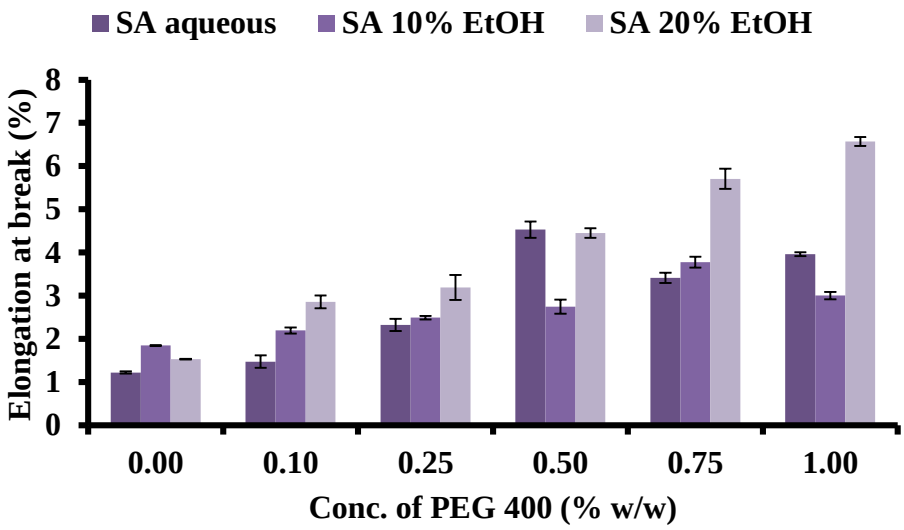

Figure 2.9 Mechanical properties (% elongation at break) of SA films cast from aqueous and ethanolic (10% and 20% v/v EtOH) polymeric gels with increase of plasticizer (PEG 400) concentration (mean ± SD, (n=3))

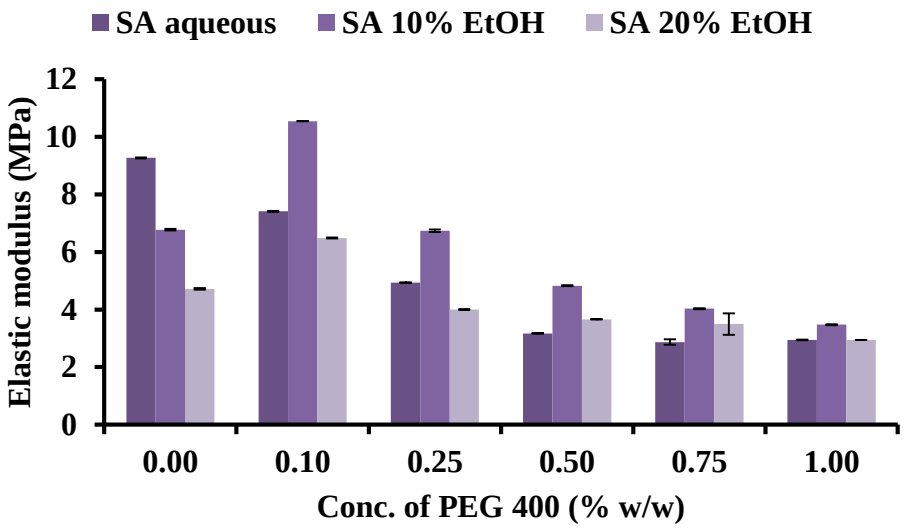

Figure 2.10 Mechanical properties (elastic modulus) of SA films cast from aqueous and ethanolic (10% and 20% v/v EtOH) polymeric gels with increase of plasticizer (PEG 400) concentration (mean ± SD, (n=3))

2.3.3 Hot stage microscopy (HSM)

HSM allows visual observation of the thermal processes occurring within the films. As such it is possible to processes that are not entirely obvious in DSC or TGA. The main characteristic analysed by the HSM was the melting point range which is entirely dependent on the purity of the film. This is important as the prepared BLK films contain (MET, SA), (aqueous and ethanolic (10% and 20 % v/v EtOH)) with different concentrations of PEG 400. The results of unplasticised films showed that as the temperature increased the films evaporation due to loss of water content as seen in figure 2.11.

Films containing PEG 400 (0.5% w/w) had bubbles (droplets) on the surface at the starting point of heating and as the temperature increased the bubbles disappeared as seen in figure 2.12. These droplets observed is excess PEG, which may be due to drastic change in viscosity (thinning out of the PEG bubbles, which spreads and coalesce together over a large area and transparent hence the disappearance of the bubbles). HSM results obtained helped in developing suitable methods for TGA and DSC analysis and determined the maximum temperature to which samples could be heated.

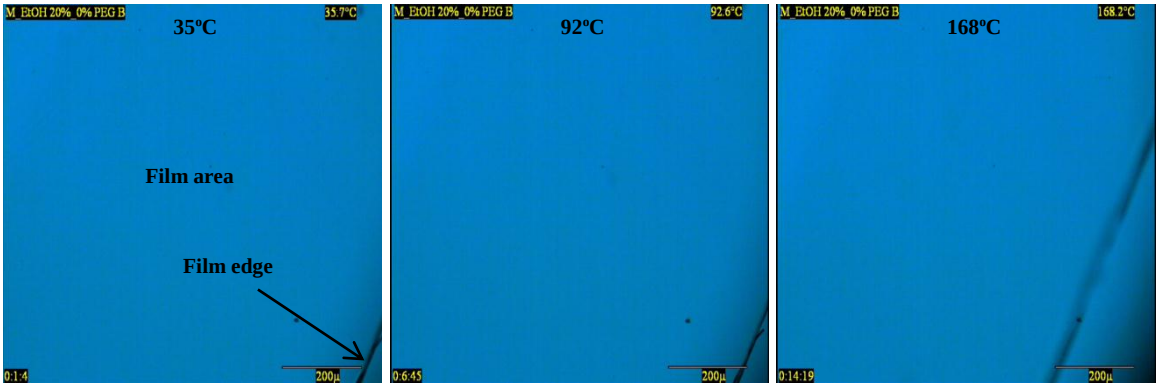

Figure 2.11 HSM results showing films prepared without any PEG 400 with heating

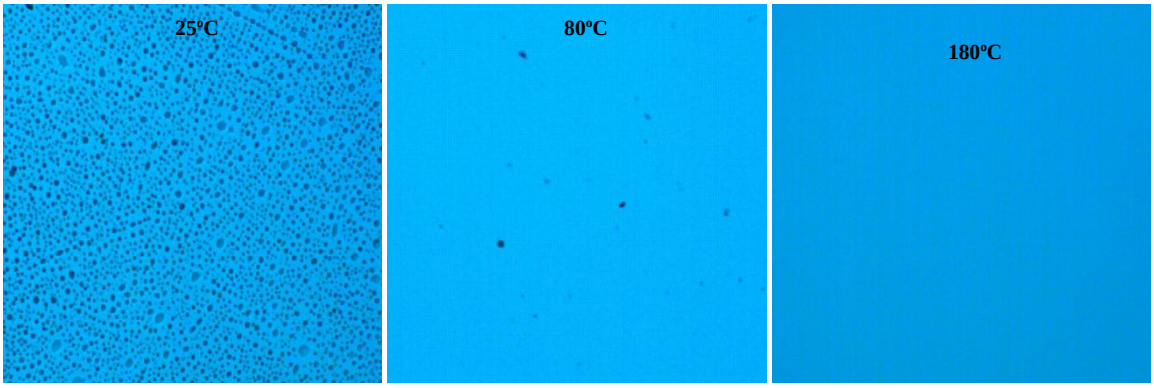

Figure 2.12 HSM results showing films prepared with PEG 400 as heated to higher temperature

2.3.4 Differential scanning calorimetry (DSC)

DSC was used to determine the interactions between the components within the film matrix. Pure MET and SA powder showed broad endothermic peaks at 67.07 °C and 72.80 °C. MET peak can be attributed to dehydration and no definite melt or glass transition peaks were observed as shown in figure 2.13 which was further confirmed with TGA as below. The thermograms of BLK MET films [aqueous and ethanolic (10% and 20% v/v EtOH)] was observed to exhibit broad endothermic transition between 50 – 65 °C as shown in figure 2.14 - 2.16 and table 2.8. However, plasticized films prepared from gels containing PEG 400 (0% and 0.5% w/w) also showed broad endothermic transition between 50 – 60 °C. The thermograms of SA BLK films [aqueous and ethanolic (10% and 20% v/v EtOH)], showed similar results to MET BLK films i.e. broad endothermic transition between 70 – 75 °C, as shown in figure 2.17 and table 2.8. All the films (MET and SA) can be characterized as amorphous because there is not melting peak (sharp endothermic peak) observed in any of the

films thermograms, as only the broad endothermic peak can be observed between 50 – 75 °C which is attributed to water loss.

DSC results for pure materials

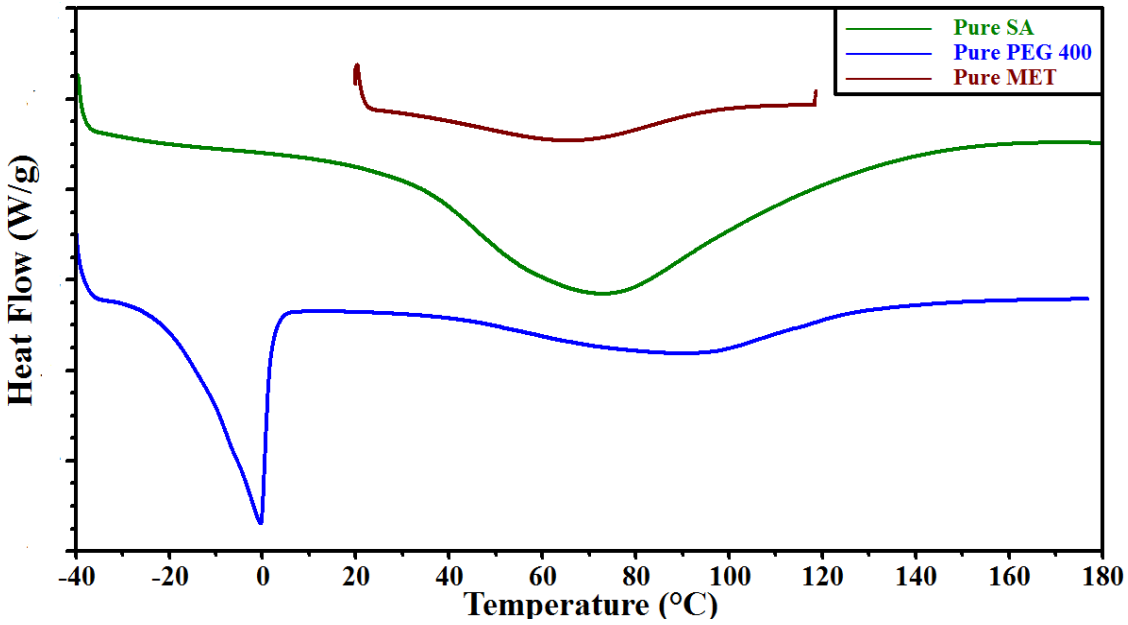

Figure 2.13 DSC thermogram of pure MET, SA and PEG 400 (W/g (Watts/gram))

DSC results for MET films

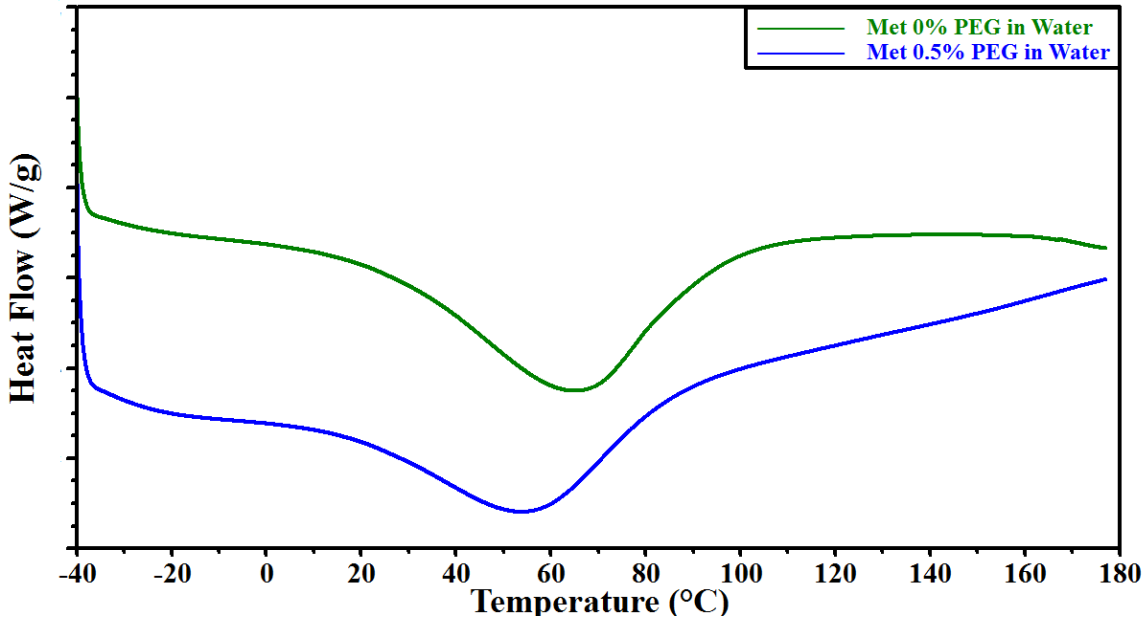

Figure 2.14 DSC thermograms of BLK films prepared from aqueous MET gels with PEG 400 (0% and 0.5% w/w) (W/g (Watts/gram))

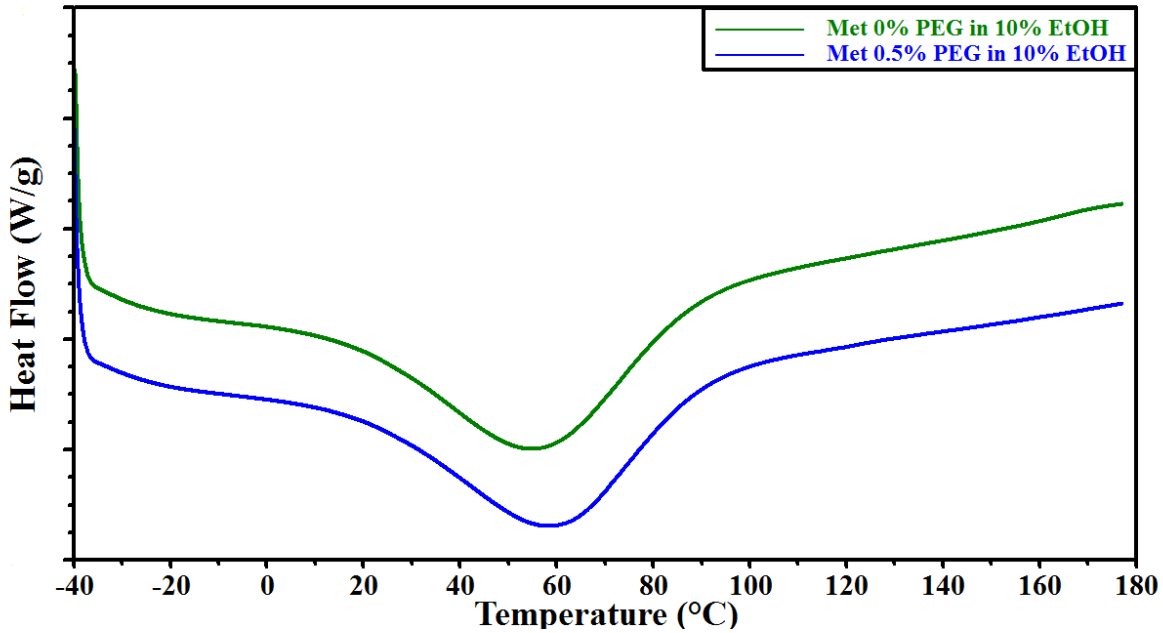

Figure 2.15 DSC thermograms of BLK films prepared from ethanolic (10% v/v EtOH) MET gels with PEG 400 (0% and 0.5% w/w) (W/g (Watts/gram))

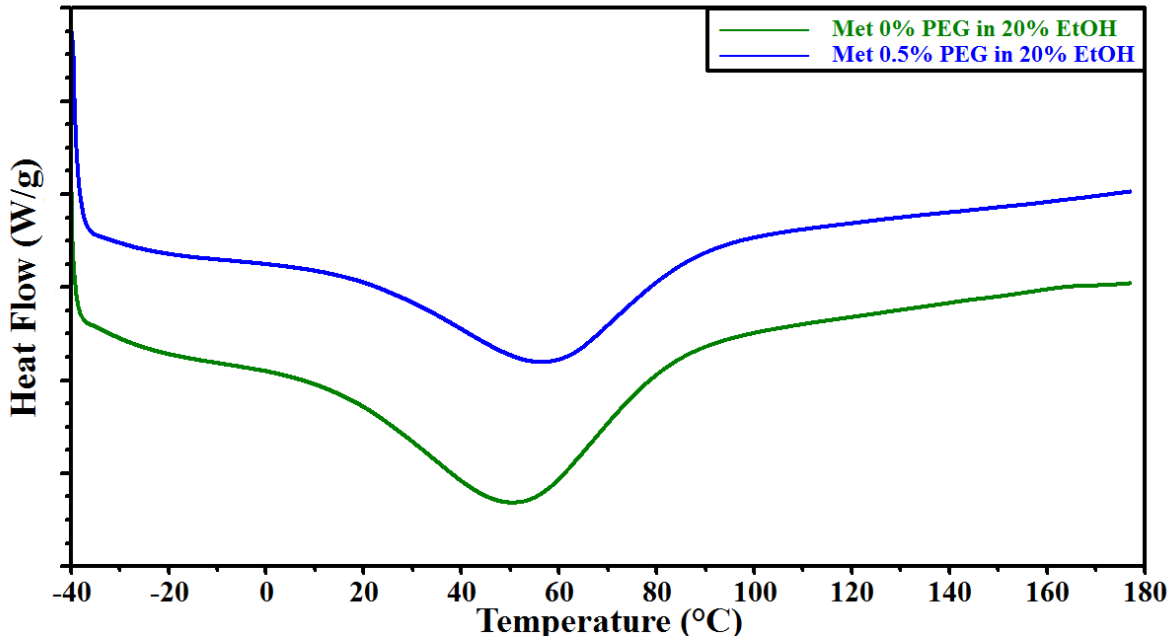

Figure 2.16 DSC thermograms of BLK films prepared from ethanolic MET gel (20% v/v EtOH) with PEG 400 (0% and 0.5% w/w) (W/g (Watts/gram))

DSC results for SA

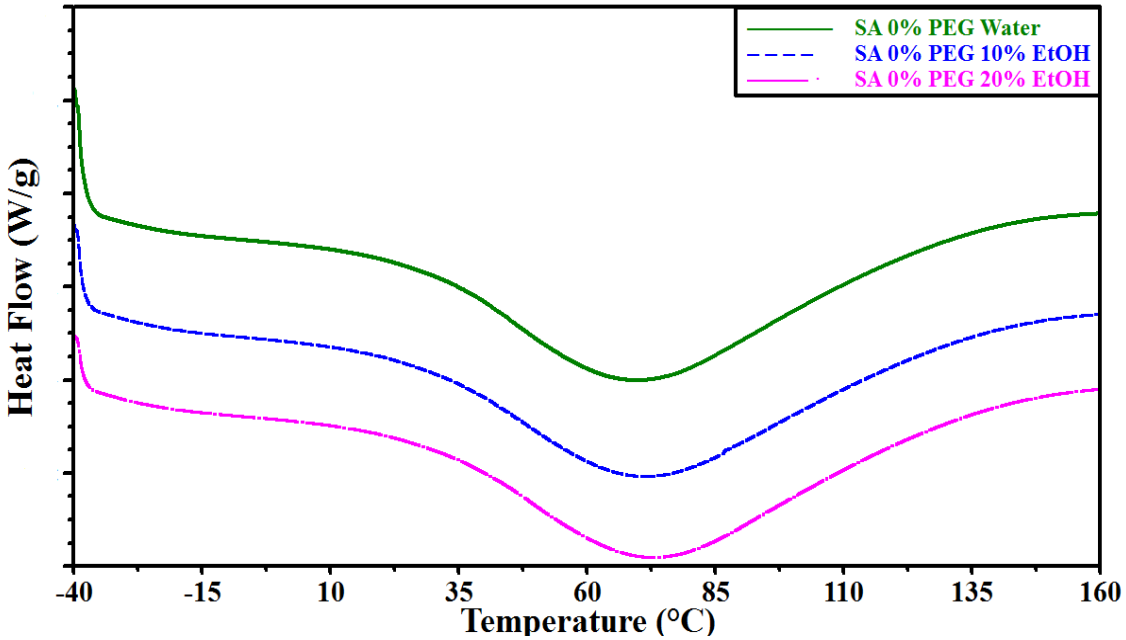

Figure 2.17 DSC thermogram of BLK films prepared from aqueous and ethanolic (10% EtOH and 20% v/v EtOH) SA gel without PEG 400 (W/g (Watts/gram))

As seen above from figures 2.13 to 2.17 there was no glass transition observed in any of the thermograms for the films which is attributed to possible suppression by the broad endothermic peak from water evaporation. However, if a glass transition was to be observed a heat-cool-heat cycle can be used. This will involve heating the sample to the highest temperature without degrading which will remove all residual moisture, cooling it down back to starting temperature and then heating it to observe a glass transition peak without any potential interference from a broad endothermic water peak.

Table 2.8 Temperature and heat changes observed for the endothermic transitions observed during DSC cycle for pure materials and films.

DSC results			
Pure materials/ gels	**Onset °C**	**Peak °C**	**ΔH (J/g)**
Pure materials			
Pure MET	25.89	67.07	71.05
Pure SA	25.94	72.80	328.10
PEG 400	-	0.00	-
MET films			
MET, 0.0% w/w PEG, aqueous	19.16	64.99	107.70
MET, 0.5% w/w PEG, aqueous	7.79	54.91	94.86
MET, 0.0% w/w PEG, 10% v/v EtOH	8.93	55.22	99.55
MET, 0.5% w/w PEG, 10% v/v EtOH	11.23	58.92	96.43
MET, 0.0% w/w PEG, 20% v/v EtOH	5.35	50.92	118.20
MET, 0.5% w/w PEG, 20% v/v EtOH	6.32	56.67	106.40
SA films			
SA, 0.0% w/w PEG, aqueous	20.43	70.27	365.10
SA, 0.0% w/w PEG, 10% v/v EtOH	18.67	71.99	383.40
SA, 0.0% w/w PEG, 20% v/v EtOH	22.45	73.45	374.80

2.3.5 Thermogravimetric analysis (TGA)

TGA was used to determine the residual moisture/water content (%) of the starting materials (MET, SA and PEG 400) and BLK films. Amorphous polymers which contain water molecules that are bonded to monomer chains or units have an impact on their glass transition temperature and these polymers therefore usually undergo spontaneous, though slow, transformation towards low energy equilibrium states. On the other hand characteristics such as mechanical properties are also affected by this phenomenon. This physical ageing is usually manifested in the relaxation phenomena (volume) indicating considerable structural changes in the materials and films. The plasticizer applied can modify the structure of the polymer films, causing the change in the mechanical properties of the polymeric binder (Hodi et al, 2006).

Table 2.9 Thermal transition with weight loss observed for MET and SA films from aqueous and ethanolic (10% and 20 % v/v EtOH) gels containing different concentrations of PEG 400 (0, 0.5 %w/w) by TGA.

Gels used	**Weight loss (%)**
MET, 0% w/w PEG, aqueous	2.77
MET, 0.5% w/w PEG, aqueous	2.03
MET, 0% w/w PEG, 10% v/v EtOH	2.26
MET, 0.5% w/w PEG, 10% v/v EtOH	2.12
MET, 0% w/w PEG, 20% v/v EtOH	2.64
MET, 0.5% w/w PEG, 20% v/v EtOH	1.99
SA, 0% w/w PEG, aqueous	10.59
SA, 0% w/w PEG, 10% v/v EtOH	8.83
SA, 0% w/w PEG, 20% v/v EtOH	10.44
Pure materials	
Pure MET	0.87
Pure SA	11.24
PEG 400	2.79

The TGA results of starting materials (MET, SA and PEG 400) are shown in table 2.9. The weight loss of MET, SA and PEG 400 from ambient temperature (20°C) to 100°C was of 0.87 %, 11.42 % and 2.79 % respectively. MET powder had low water content than its films, whilst SA had higher water content than its films. These differences in water contents observed between the pure components and their films could be due to the drying process when formulating the film.

The TGA results of MET and SA BLK films (aqueous and ethanolic) are shown in table 2.9 indicating the percentage loss with heating, attributed to residual water present within the film matrix. Due to PEG 400 having hydrophilic characteristic, it was expected that the residual moisture content will increase for films (plasticised) with increasing PEG 400 concentration. However, this was not the case except at higher concentrations (0.5 % w/w of PEG) where the % water content decreased. It also appears that the residual water was generally lower for films prepared using ethanolic gels than those from aqueous gels because when drying the film most of the water is evaporated with help of EtOH. In addition, the moisture content of less than 3% (MET film) was considered low enough to sustain drug stability during storage though this needed to be investigated with an accelerated stability study.

2.3.6 Scanning electron microscopy (SEM)

SEM was used to investigate the differences in the surface morphology and topography of the films and to check for film uniformity and the presence of any cracks. The surface SEM images of the MET films cast from gels prepared with different solvents (aqueous and ethanolic (10% and 20% v/v EtOH)) with or without PEG (0% - 0.5% w/w) are shown in figure 2.18 – 2.20. The microscopic appearance of all MET films, showed continuous sheets with relatively smooth and homogeneous surfaces and confirmed that all the components were uniformly mixed during gel formation. The plasticised films showed smooth and homogeneous surfaces whilst unplasticised films showed rougher surfaces with some lumps.

The surface topography of the SA films was dependent on the solvent used during gel preparation. Films prepared from aqueous gels showed considerably rougher surfaces than films prepared using 10% v/v EtOH, which in turn showed uneven surfaces than films prepared using 20% v/v EtOH as shown in Figure 2.21. This could be related to the more

rapid drying of ethanolic gels during film formation. Such differences in surface topography could influence could affect the subsequent functional performance of different formulations with respect to hydration capacity/swelling studies, mucoadhesion and drug release characteristics.

SEM results for MET films

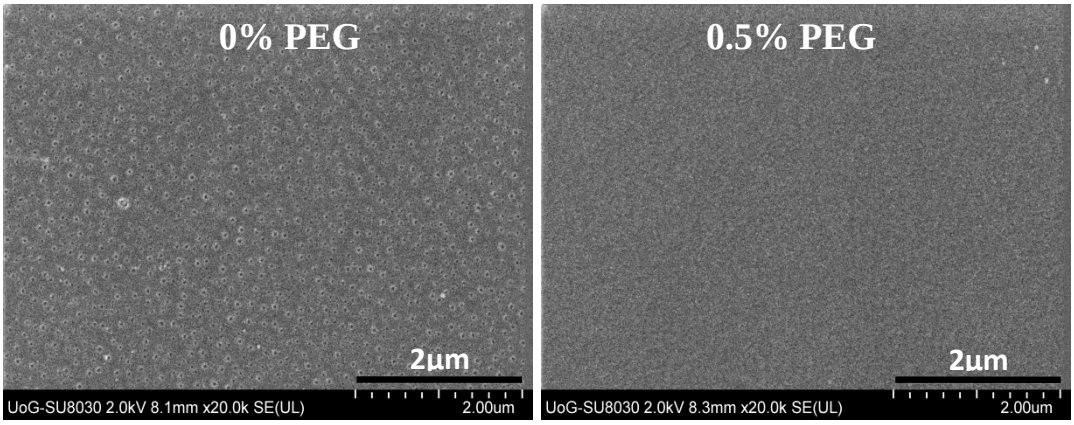

Figure 2.18 MET Films prepared from aqueous gels comprising 1% w/w MET + 0.0 % w/w PEG 400 or 0.5 % w/w PEG 400

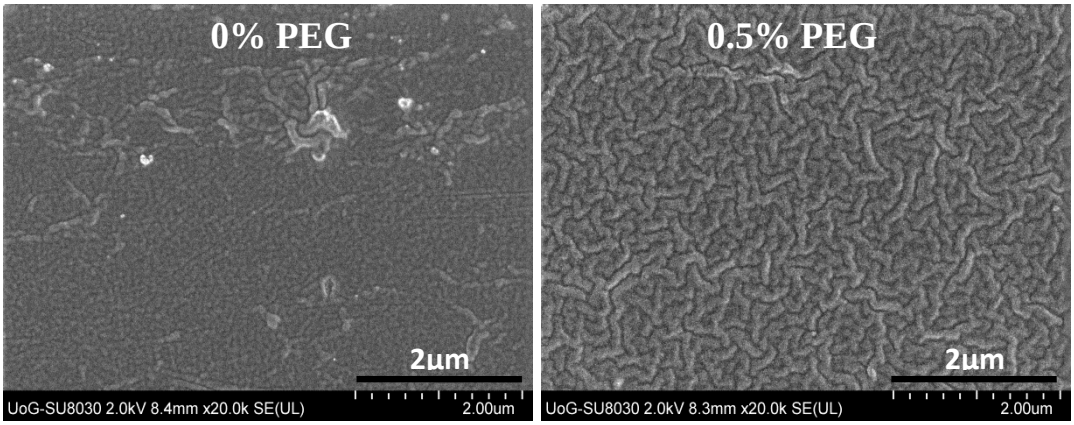

Figure 2.19 MET films prepared from gels comprising 10% v/v EtOH + 1% w/w MET + 0.0% w/w PEG 400 and 0.5% w/w PEG 400

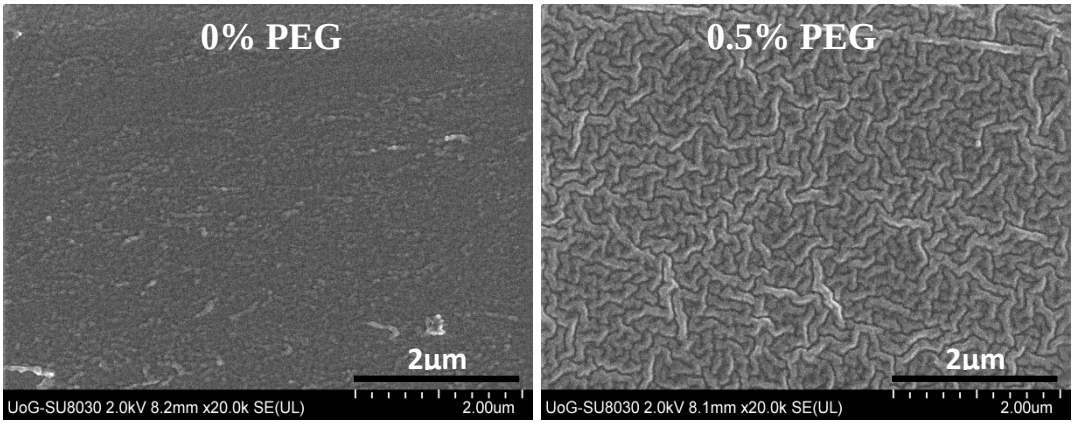

Figure 2.20 MET films prepared from gels (1 % w/w) comprising 20% v/v EtOH and different concentrations (0.0% w/w and 0.5% w/w) of PEG 400

SEM results for SA

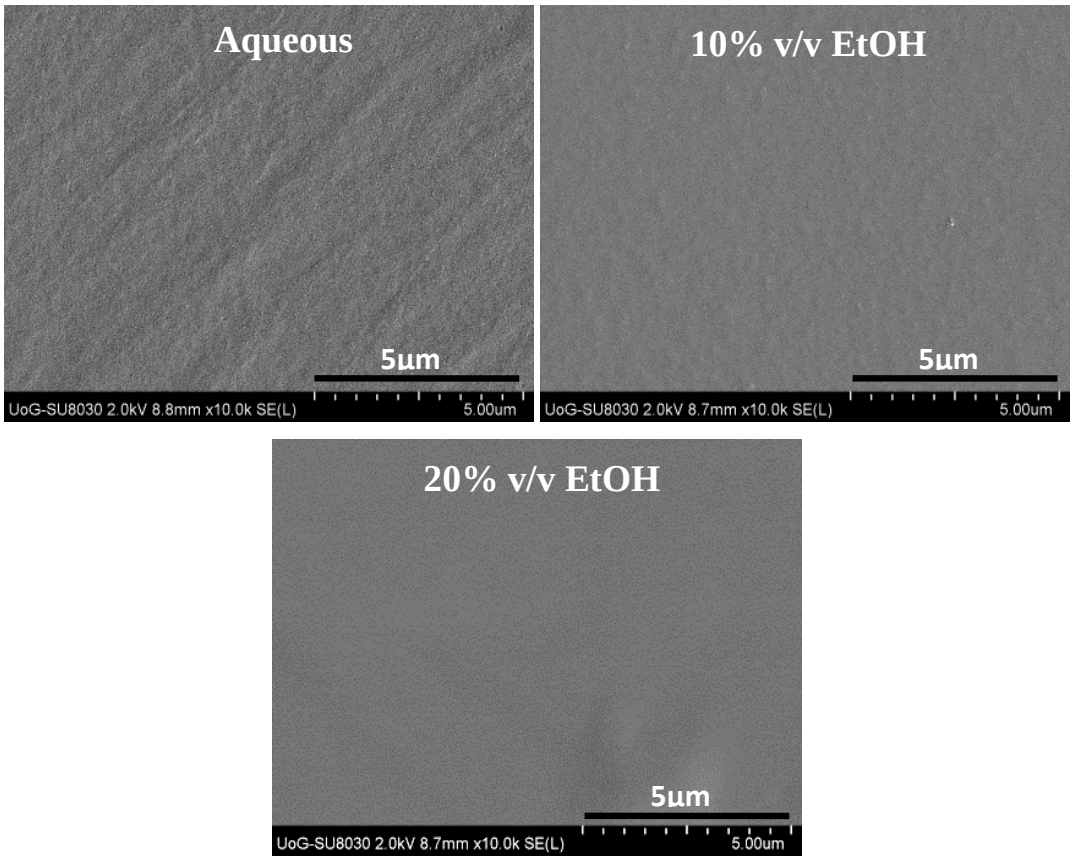

Figure 2.21 Unplasticised (0% w/w PEG) SA films prepared from aqueous and ethanolic (10% and 20% v/v EtOH) gels (1% w/w)

2.3.7 X-ray diffraction (XRD)

To investigate the crystalline/ amorphous characteristics of all starting materials and films XRPD was used. Amorphous compounds generally show very broad peaks, distinguishable in comparison to the sharp peaks belonging to the crystalline form. XRPD can also give information about the crystalline-amorphous ratios for the various starting materials and the formulated films (see in appendix for more information) (Kumar et al., 2012).

The limitation of detecting amorphous and crystalline forms in a film depends on the relative weight percentage of crystalline material in a film. Crystals in film can be seen under the SEM, but because they make up such a small weight in the total matrix, coupled with the largely amorphous nature of the film which scatters the X-rays, they are not readily detected in the film matrix. When diluted in the film which is largely amorphous material then the amorphous scattering takes over. Generally, XRD tends to use a >1% rule but if the crystalline material is a very good diffractor; it can be detected down to 0.2%. The general rule is that if any sharp peaks can be observed, then it implies some crystalline components may be present. However, if no peaks can be observed, then it could imply three things: (a) crystalline but below detection which is a sensitivity issue, (b) microcrystalline i.e scattering domain is too small to produce Bragg peaks and (c) complete absence of crystallinity.

Figure 2.22 shows XRPD diffractograms of pure polymers (MET and SA) and PEG 400, indicating the amorphous nature of both polymers and plasticiser. For MET powder, the results showed some peaks which indicated a small amount of crystallinity but was significantly amorphous which was reproducible before and after grinding (crystalline: amorphous, 1:99%). The results for SA powder showed that the crystalline- amorphous ratio was 0/100 (Refer to appendix B for working out).

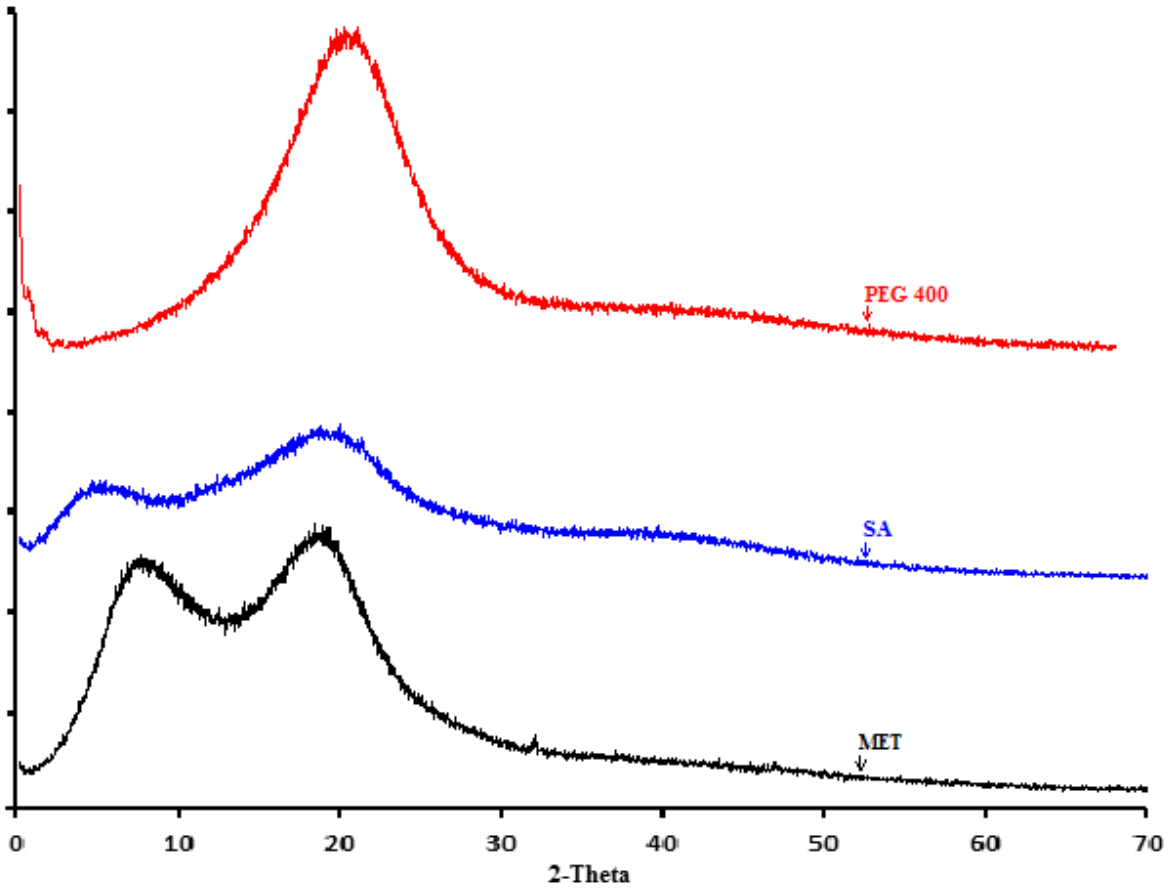

Figure 2.22 XRD diffractograms for pure MET, pure SA and PEG 400 (plasticiser).

Figures 2.23 - 2.25 show the diffractograms of non-DL MET films. The results demonstrated amorphous components present in the films with and without PEG 400. Figure 2.26 shows the diffractograms of SA films. The results demonstrated that there were more broad amorphous peaks in the unplasticised SA films compared to MET. In the XRPD diffractograms of MET and SA BLK films there were no sharp peaks which demonstrated possible amorphous nature. An amorphous film is advantageous in terms of better solubility; however, it is associated with stability challenges, which need to be further, investigated. The swelling capacity is also affected by amorphous nature, as it absorbs more liquid and thus the release of the drug is accelerated.

XRD results for MET films

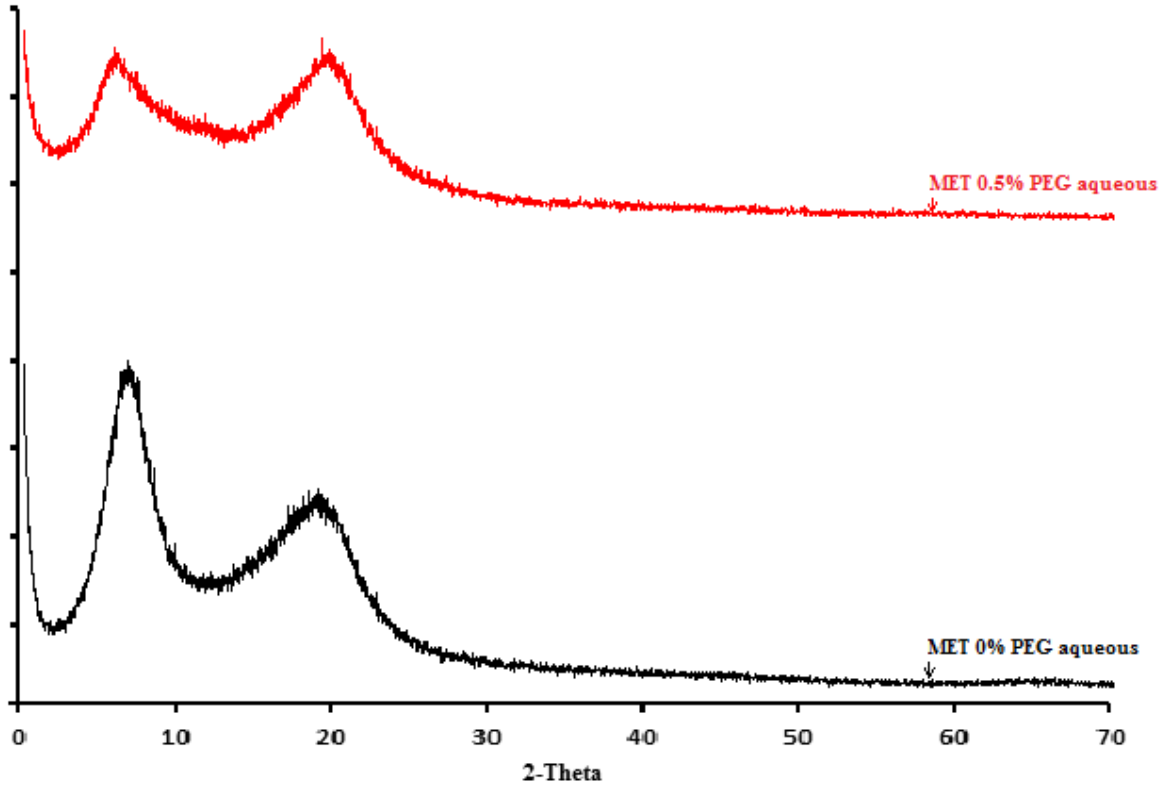

Figure 2.23 XRD diffractograms for MET films cast from aqueous polymer gels containing 0.0% w/w and 0.5% w/w PEG 400

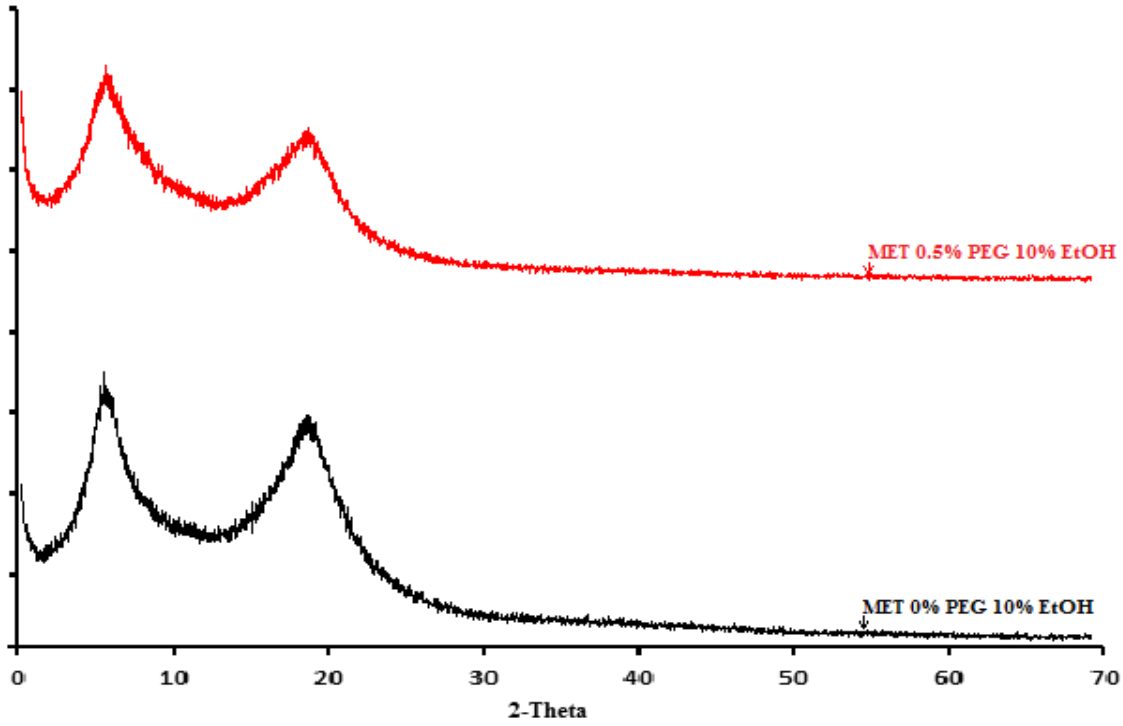

Figure 2.24 XRD diffractograms for MET films cast from ethanolic (10% v/v EtOH) gels containing 0.0% w/w and 0.5% w/w PEG 400

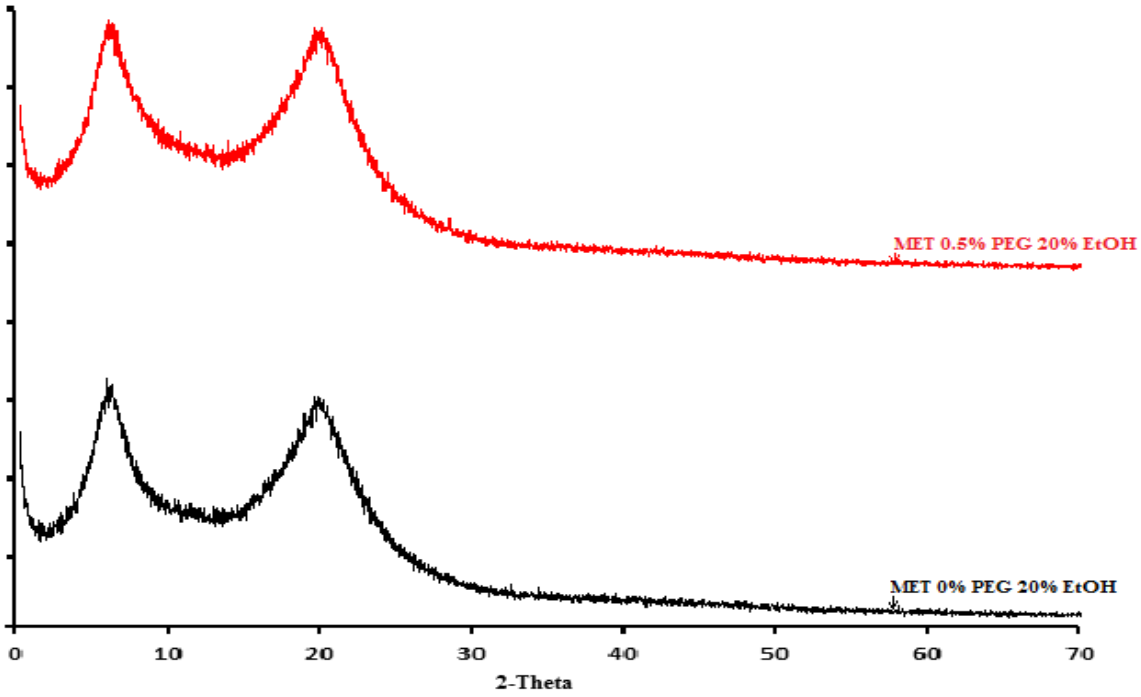

Figure 2.25 XRD diffractograms for MET films cast from ethanolic gels (20% v/v EtOH) containing 0.0% w/ and 0.5% w/w PEG 400

XRD results for SA

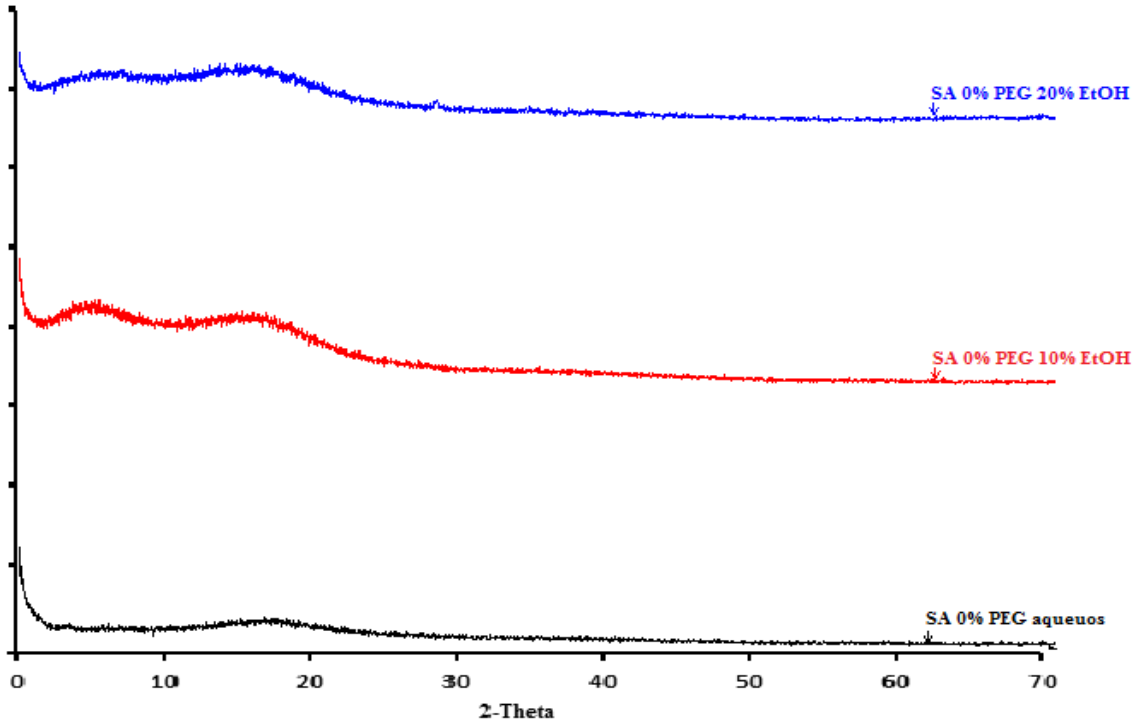

Figure 2.26 XRD diffractograms for unplasticised SA films cast from aqueous and ethanolic (10% v/v and 20% v/v EtOH) gels

2.3.8 Fourier transform infrared (FT-IR) spectroscopy

The FT-IR spectra shows the respective absorption peaks of MET, SA, PEG 400 and EtOH, which shows similar corresponding characteristics of peaks between 3447.40cm^{-1} to 880.21 cm^{-1} as discussed in table 2.10.

Table 2.10 The observed FTIR peaks (n=3) for pure polymers, plasticizer and solvent with their characteristic bands

Polymers	**Peaks (cm^{-1})**	**Peak assignment**
MET	944.61	=C-H out of plane bending vibration
	1053.73	C-O stretching
	1374.85	C-H bending
	1455.43	C-C stretching
	2890.24	C-H stretching
	3436.32	O-H stretching, H-bonded
SA	1029.19	C-C stretching
	1603.82	Asymmetric –COO^{-} stretching
	1733.24	C=O stretching
	3291.93	O-H stretching
PEG 400	940.79	=C-H out of plane bending vibration
	1092.10	C-O stretching
	1250.00	C-O stretching
	1352.01	C-O bending
	2865.10	O-H stretching
	3447.40	O-H stretching
Ethanol	880.21	=C-H out of plane bending vibration
	1045.93	C-O stretching
	1419.72	C-C stretching
	2973.03	C-H stretching
	3323.09	O-H stretching

The peaks in the region of 3500 cm^{-1} are attributed to bound or free hydroxyl groups in all pure materials. The presence of the hydrogen-bonded hydroxyl group causes a shift of absorption therefore lower frequencies are observed at 3200 cm^{-1} with increased as can be seen in table 2.10. The FTIR spectrum of MET- based films recorded between 4000 and 400 cm^{-1} can be seen in figures 2.27-2.29. The region of interest in the spectra of MET films was between 3700 and 3100 cm^{-1} and the spectra were interpreted in terms of hydroxyl stretching at 3453 cm^{-1} which was observed at between 3453 and 3436 cm^{-1} in all the films (with and without PEG 400) that were analysed. It can be concluded that the overall composition of the films had no effect at this peak position, but the symmetry of this band was observed to be distorted significantly relative to the pure materials (MET) 3436.32 cm^{-1}.

The other peak of interest was between 1000 and 1100 cm^{-1} as seen in figures 2.27-2.29, which describes the peak region as C-O stretching. This suggests that the groups within this region are crossed-linked through the activity of hydrogen bonding interaction of MET without causing any change in the chemical property of the plasticised and unplasticised films. The peaks obtained within the region of 940cm^{-1} correspond to O-H out of plane bending. Significantly no difference was observed between films prepared using different ethanol (10 and 20 %) concentrations with or without PEG 400. It was concluded that overall, ethanol concentration had no effect on the films. Its main effect was a reduction in drying time due to its low boiling point (78^{o}C) and does not remain in the film after drying, therefore no interaction and no consequent change in the polymeric matrix structure.

Figure 2.30 shows that SA films prepared from gels of all three solvents (aqueous and ethanolic (10 and 20% EtOH)) without any PEG 400 had no significant differences in peaks according to MET films.

FT-IR results for MET

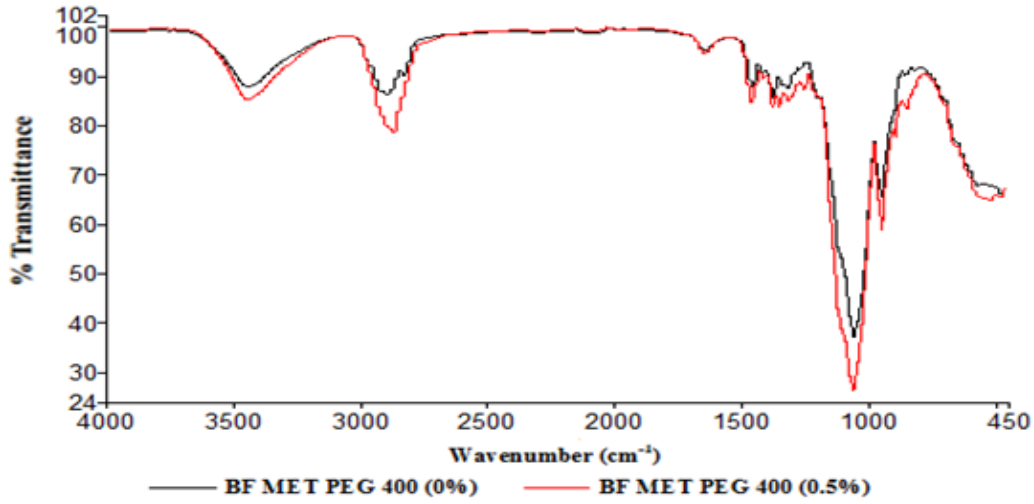

Figure 2.27 FT-IR spectra of MET films prepared from aqueous gels containing different concentrations of plasticiser (0.0% w/w or 0.5% w/w PEG 400),

Table 2.11 Major FTIR peaks of interests for BLK MET films prepared from aqueous gels

Peak No.	(cm^{-1})	(%T)	Peak No.	(cm^{-1})	(%T)	Peak No.	(cm^{-1})	(%T)
Unplasticised								
1	3453.54	88.65	2	2901.38	86.96	3	1455.06	88.38
4	1373.73	86.02	5	1051.53	36.94	6	945.25	65.54
Plasticised								
1	3448.95	85.78	2	2875.08	78.81	3	1454.93	85.00
4	1348.90	84.18	5	1056.35	25.85	6	944.96	59.08

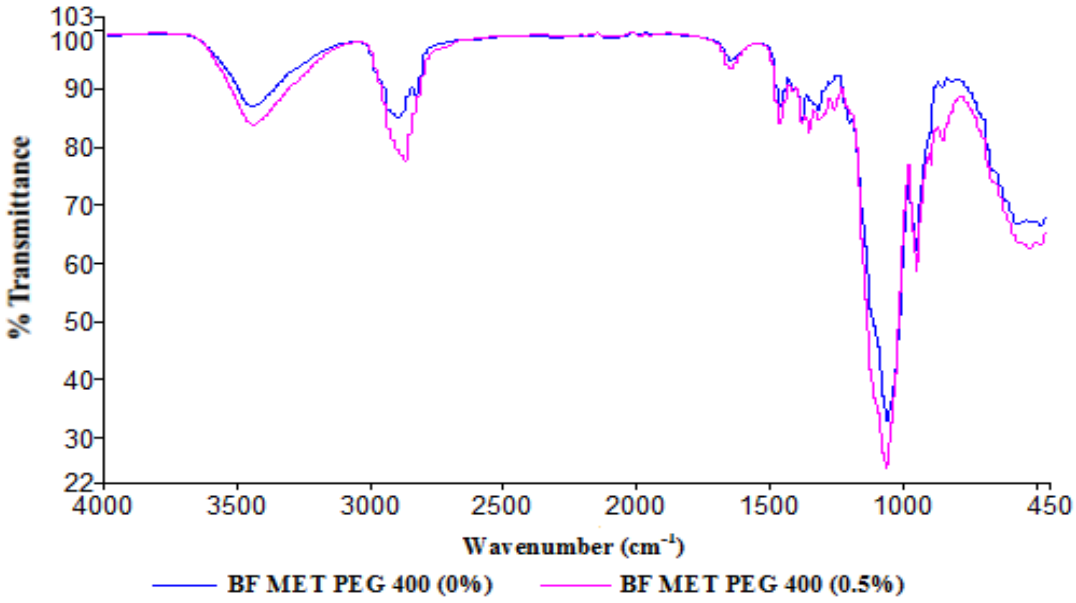

Figure 2.28 FT-IR spectra of films containing different concentrations of plasticiser (0.0% w/w PEG 400 or 0.5% w/w PEG 400), MET and prepared using 10% v/v EtOH as solvent

Table 2.12 Major FTIR peaks of interests for BLK MET films from 10% v/v EtOH gels

Peak No.	(cm^{-1})	(%T)	Peak No.	(cm^{-1})	(%T)	Peak No.	(cm^{-1})	(%T)
Unplasticised								
1	3452.94	87.66	2	2900.76	85.68	3	1454.50	87.58
4	1373.94	84.84	5	1051.87	32.84	6	945.05	62.53
Plasticised								
1	3446.58	84.26	2	2874.60	77.79	3	1454.92	84.44
4	1349.01	82.66	5	1058.60	24.31	6	944.88	58.86

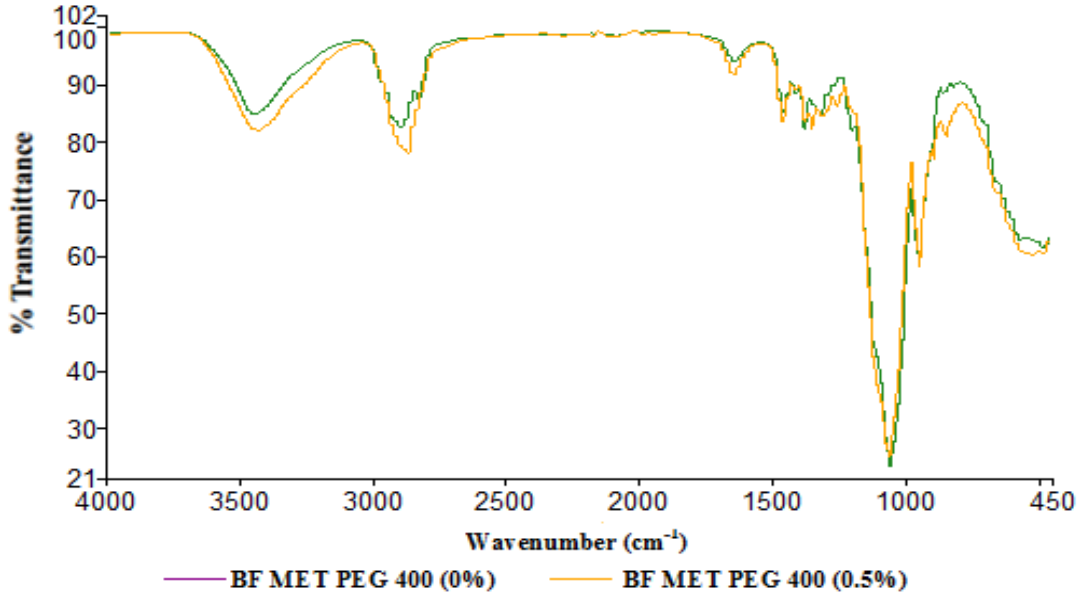

Figure 2.29 FT-IR spectra of films containing different concentrations of plasticiser (0.0% w/w PEG 400 or 0.5% w/w PEG 400), MET and prepared using 20% v/v EtOH as solvent.

Table 2.13 Major FTIR peaks of interests for BLK MET films from 20% v/v EtOH gels

Peak No.	**(cm^{-1})**	**(%T)**	**Peak No.**	**(cm^{-1})**	**(%T)**	**Peak No.**	**(cm^{-1})**	**(%T)**
				Unplasticised				
1	3453.16	85.64	2	2900.69	83.32	3	1454.38	85.73
4	1373.94	82.75	5	1052.01	23.22	6	945.17	58.21
				Plasticised				
1	3436.89	82.77	2	2876.04	78.65	3	1454.96	84.38
4	1349.02	82.95	5	1057.7	24.61	6	944.92	58.75

FT-IR results for SA

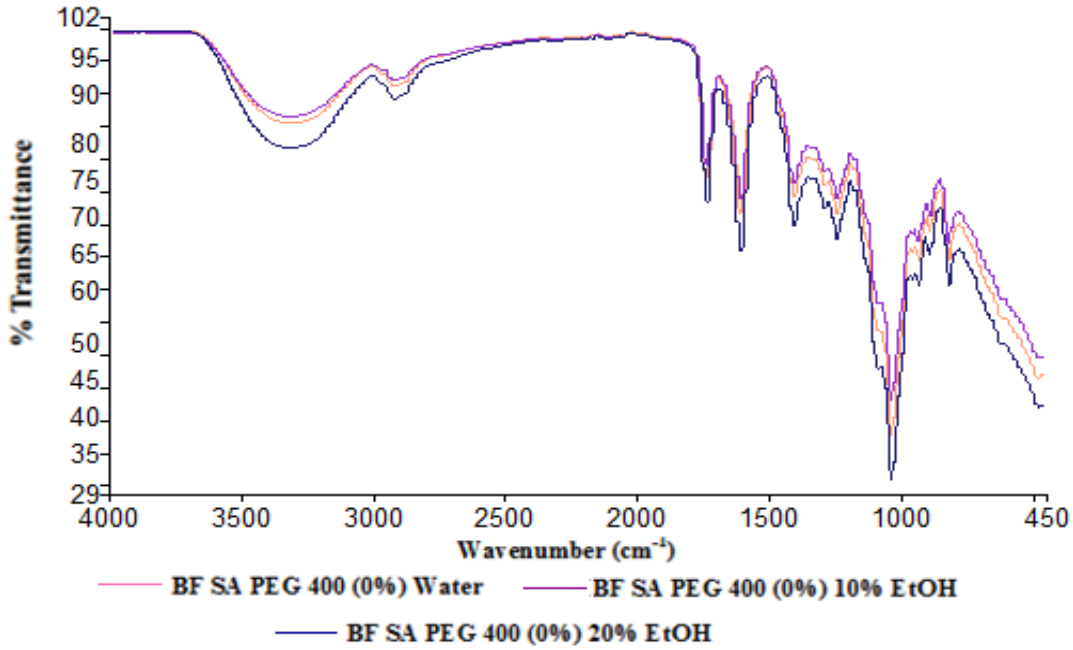

Figure 2.30 FT-IR spectra of unplasticised SA films (0.0% w/w PEG 400) cast from gels using three different solvents (water, 10% v/v EtOH, 20% v/v EtOH)

Table 2.14 Major FTIR peaks of interests for BLK unplasticised SA films

Peak No.	(cm^{-1})	(%T)	Peak No.	(cm^{-1})	(%T)	Peak No.	(cm^{-1})	(%T)
				Aqueous gels				
1	3334.96	85.88	2	1733.78	77.28	3	1605.91	71.81
4	1403.00	74.39	5	1236.15	71.72	6	1028.26	37.34
7	813.45	64.64						
				10% EtOH gels				
1	3324.04	87.15	2	1733.27	79.35	3	1605.88	74.12
4	1403.17	76.63	5	1236.06	74.27	6	1028.20	43.01
7	813.30	67.32						
				20% EtOH gels				
1	3325.11	82.08	2	1733.39	73.35	3	1605.42	65.91
4	1403.32	69.82	5	1236.23	67.86	6	1028.22	30.52
7	812.98	60.73						

2.4 SUMMARY

Oral films are intended for application in the oral cavity and they are an innovative and promising dosage form especially for use in paediatrics. On the European market, no licensed drug product (films) is available yet, and one aspect of this chapter focused on development of such a dosage form for paediatric use with an appropriate active substance. Another objective was to develop adequate analytical methods for their functional characterization and subsequent selection and drug loading of optimised film that will deliver therapeutically relevant drug concentrations via buccal mucosa route for paediatric patients.

Drug-free (BLK) films were prepared starting with pre-evaluation of different polymers, HPMC, MC, SA, CA and MET and polyethylene glycol (PEG 400 as plasticiser. MET and SA (0.0% and 0.5% w/w PEG 400) films were chosen for drug loadeding and based on tensile properties (tensile strength (toughness), elongation at break/elastic modulus (flexibility)). This was important becaue sustained release films should possess moderate tensile strength, high percent elongation (%), low elastic modulus and shorter time for disintegration with respect to their high percent of drug release (Dixit R, Puthli S., 2009)(Garsuch V. 2009).

Based on these preliminary evaluations, three polymeric films (HPMC, MC and CA) were discontinued. The reason HPMC films were poor was because the molecular structure of HPMC is predicated upon a base celluloid compound that is highly water soluble (Gosal et al., 2011). MC on the other hand is the most resistant to water and it is the lowest hydrophilic cellulose derivative. However cellulose derivatives based films generally have poor water vapour barriers because of the inherent hydrophilic nature of polysaccharides and therefore they process poor mechanical properties (Pathare et al., 2013) compared to other commonly used polymers such as alginate. CA is also a water-soluble polymer with a linear chain of partially sulphated galactans. The film formation in CA includes a gelation mechanism during moderate drying, leading to a three dimensional network formed by the polysaccharides double helices leading to formation of a solid film after solvent evaporation. As a result,the films tend to become brittle and rigid, especially without plasticiser which is what was observed in this study (Pathare et al., 2013).

On the other hand the mechanical properties also showed that the addition of PEG 400 decreased the tensile strength, increasing % elongation and decreased elastic modulus. As

Morales et al., (2011) stated "soft and weak polymers have low tensile strength, low elastic modulus and low elongation at break. In contrast a soft and strong polymer displays a reasonable tensile strength, low elastic modulus and a high elongation at break". The tensile properties (strength, elongation combined with elastic modulus) are important as they specify the toughness of the film under stress due to stretching and have an effect on paediatric patients acceptance of a given film. In addition, the flexibility of the films offer better patient compliance as they are less probable to cause contact irritation whilst very elastic films can cause problems with handling such as folding and stickiness (Boateng et al., 2009).

DSC results showed that the selected optimised films (MET and SA) from the preliminary studies, can be characterized as amorphous because there is not melting peak (sharp endothermic peak) observed in thermograms for any of the films, as only the broad endothermic peak can be observed between 50 - 75°C, which is attributed to water loss. The glass transition temperatures (*Tg*) of the pure materials and BLK films were not observed due to the large water peak interfering with the *Tg* and to overcome this a first heating stage is required which will remove the water, then cooled back to the starting temperature and heated back to the maximum temperature to observe the *Tg* peak which is normally a small step change in gradient of the thermogram.

Further, the XRD data confirmed the amorphous results observed from the DSC analyses. In the XRD diffractograms of MET and SA BLK films there were no sharp peaks which demonstrated possible amorphous nature. Generally, an amorphous film is advantageous in terms of better solubility. The swelling capacity is also affected by amorphous nature, as it absorbs more liquid and thus the release of the drug is accelerated. Though amorphous forms are known to be more soluble, they do present stability challenges owing to their tendency to convert back to the crystalline form (Tusi, 2004; Hancock & Parks., 2000) and will therefore require further investigation in a long term polymorphic stability study. XRD has application throughout the formulation development process, usually in combination with other experimental techniques such as thermal analysis. Effectiveness of XRD is more apparent when one considers the direct relationship that exists between the measured XRD pattern and the molecular structure of the drug incorporated in the films. This is because it also provides information about the structure of the excipient material, (whether it exhibits long range order as in crystalline materials, or short – range order as in glassy or amorphous materials) and unique to each individual material Ivanisevic et al., 2010).

Polymers contain some water molecules bonded to the monomer parts and impact directly on the glass transition temperature and other physico-chemical characteristics such as elastic modulus. In addition, their degradation points decreased in comparison to the original compounds, showing the effect of formulation process in changing the physico-chemical properties of the starting materials due to interactions between the various components (Stephenson et al., 2001). PEG 400 caused an increase in amount of residual water in the MET BLK films. This is because PEG 400 is a known as hydrophilic agent with high water affinity owing to PEGs water soluble monomers of oxyethylene and having general structure of H-[-O-CH_2-CX-] $_n$-OH (Craig., 1995).

Films prepared from aqueous gels showed considerably rougher surfaces than films prepared using 10% v/v EtOH, which in turn showed uneven surfaces than films prepared using 20% v/v EtOH. This could be related to the more rapid drying of ethanolic gels during film formation. The surface of films is important as it could affect the subsequent functional performance of different formulations with respect to hydration/ swelling capacity/ mucoadhesion and drug release characteristics (Boateng et al., 2010).

2.5 CONCLUSIONS

The main objective for the preliminary study was the formulation design, development and optimization of stable solvent cast films as potential platforms for buccal drug delivery in paediatric patients. Initially five different polymers (HPMC, MC, CA, SA and MET) with different ratios of plasticiser (PEG 400) were used to formulate films and characterised by TA, DSC, TGA, HSM, SEM, XRD and FT-IR. The two most important parameters which determines if a film is fit for purpose are (a) the the tensile strength (flexibility) and elongation at break/elastic modulus (toughness), and (b) the residual water which can affect the flexibility of the film by acting as a plasticizer and reducing the elastic modulus by lowering of glass transition temperature.

The results suggested that out of the different formulations, only MET with 0.0% w/w and 0.5% w/w PEG 400 and SA with 0.0% plasticiser (aqueous and ethanolic (10 and 20% v/v EtOH gels) films showed desired characteristics on the basis of an ideal balance between flexibility and toughness. These were therefore selected for drug loading and further testing.

CHAPTER THREE: FORMULATION DEVELOPMENT AND OPTIMIZATION OF OMEPRAZOLE LOADED SOLVENT CAST FILMS AND DRUG STABILISATION USING L-ARGININE

3.1 INTRODUCTION

Gastro oesophageal reflux (GER) is mainly the result of complications including oesophagus stricture and pulmonary disease are diseases that are well recognised in children. Up to date histamine H_2-receptor antagonists (H_2RAs) are often effective, however, in the cases where these are not as effective as required, proton pump inhibitors (PPIs) have been shown to be superior to H_2RAs for the treatment of more severe cases of GER. Larson and co-workers described omeprazole (OME) as the selective PPI in gastric mucosa, which is a substitution of benzimidazole (Larson et al., 1985).

OME can be found in oral dosage form such as capsules, delayed –release capsules or suspension, tablets and powder suspension. Frequently it is marketed in the form of enteric –coated beads (resistance against stomach acid/environment) containing the active ingredient but also filled into capsules (Pilbrant and Cedeberg, 1985). OME infusion is available in vials containing 40 mg of drugs as the sodium salt; it can also be present in formulations such as such disodium edentate. OME is also available in injection form of 40mg of drug as the sodium salt with an accompanying 10 mL of special solvent (distilled water and saline).

Each of these forms suffer from limitations, such as hepatic first pass metabolism, hence OME demonstrates poor bioavailability. Buccal mucosa is an alternative route for the oral administration of drugs which undergo degradation in the GIT and metabolism in the liver and offers other great advantage such excellent accessibility, which therefore allow direct access to systemic circulation through the internal jugular vein which bypasses the drugs from hepatic first pass metabolism (Riedel et al., 2005). Buccal drug formulations offer a safer mode of drug delivery and the dosage form is easily removed in the case of toxicity.

OME is a lipophilic, weak base with pKa 1 = 4.2 and pKa 2 = 9 that may be degraded unless protected against acid conditions. When present in solid state OME is degraded in the presence of high temperature, light and humidity. It contains a re-coordinated sulphur atom in a pyramidal structure and therefore can exist in two different optically active forms, (S) - and

(R)-OME. The number of decomposed products of OME in different conditions has been identified and characterized by Brändström and co-workers using derivative spectrophotometry and HPLC method (Brändström et al., 1989). L-arginine (L-arg) plays an important role in the increase of drug solubility and stability of free OME molecules. This is attributed to the amino acids, by establishing hydrogen bonds with drug molecules, forcing a significant desolvation of the OME molecules.

The aim of this chapter is to develop drug loaded solvent cast films for buccal delivery in paediatric patients using MET and SA as polymers, PEG 400 as plasticiser, OME as model drug and L-arg (to stabilise OME). The films characterised for tensile properties, physical form and surface topography as part of further development and optimisation prior to functional characterisation.

3.2 MATERIALS AND METHODS

3.2.1 Materials

Table 3.1 List of materials used

Name	Batch Number	Purity	Company	Location
Ethanol	1405343	-	Fisher Scientific	Loughborough, UK
Metolose (MET)	311615	-	Shin Etsu	Stevenage, Hertfordshire
Sodium alginate (SA)	LSL001301	-	FMC Bio-Polymers	Cork, Ireland
PEG 400	A0210931	-	Sigma Aldrich	Gillingham, UK
Omeprazole (OME)	PWAMM-HK00359	98%	TCI	Tokyo, Japan
L-arginine (L-arg)	MKBN277V	98%	Sigma Aldrich	Gillingham, UK

3.2.2 Consumables

Table 3.2 List of consumables

Consumable	Company	Location
Blue, white and yellow micropipette tips	Fisher Scientific	Loughborough, UK
100 mL beakers	Fisher Scientific	Loughborough, UK
Magnet stirrer	Fisher Scientific	Loughborough, UK
Tzero hermetic pans and lids	TA Instruments	Crawley, UK
SEM stubs	Agar Scientific	Essex, UK

3.2.3 Instruments

Table 3.3 List of instruments used

Instruments	Suppliers
Texture Analyser TA HD plus	Stable Micro Systems, Surrey, UK
DSC Q2000	TA Instruments, Crawley, UK
Q5000-IR Thermogravimetric Analyser	TA Instruments, Crawley, UK
Mettler Toledo FP82HT	Greifensee, Switzerland
SEM. Hitachi SU 8030	Hitachi High-Technologies, Tokyo, Japan
D8 Advantage X-ray diffractometer	Bruker, Coventry, UK
Perkin Elmer spectrophotometer	Spectrum Two, Perkin Elmer, US
Tzero sample encapsulation press	TA Instruments, Crawley, UK

3.2.4 METHODS

3.2.4.1 Formulation development and optimization of OME loaded films

Solvent cast films were formulated by using the two polymers (MET and SA) selected from previous chapter and loaded with drug (OME). The OME-loaded films were prepared by preparing MET and SA gels as previously described in chapter 2 section 2.2.4.1. However, the drug was added to the appropriate volume of water / ethanol (3 hrs at room temperature) to form an OME solution (but also refer to section 3.2.4.2 and 3.3.1 for drug stability implications) as can be shown in table 3.4. The polymer powder was then added slowly to the

vigorously stirred drug solution at room temperature to obtain the DL gels. The resulting gels were covered with para film, and left to stand to allow air bubbles to escape and then 20g was poured into Petri dishes and dried at 40 °C as shown in figure 3.1 (Morales et al., 2011).

3.2.4.2 Stabilization of OME in DL MET and SA films using L-arg

Due to the breakdown of OME following gel formation, L-arg was used as a stabilising agent to prevent drug degradation. Table 3.5 shows the details for the different ratios of OME and L-arg in the gel formulations which were investigated with different amounts of L-arg within the gel whilst keeping the original OME concentration (0.10% w/w) constant. The procedure for making these films was the same as non-DL films. The major difference was that, the OME and L-arg; were added to the solvent before adding MET, SA and PEG 400.

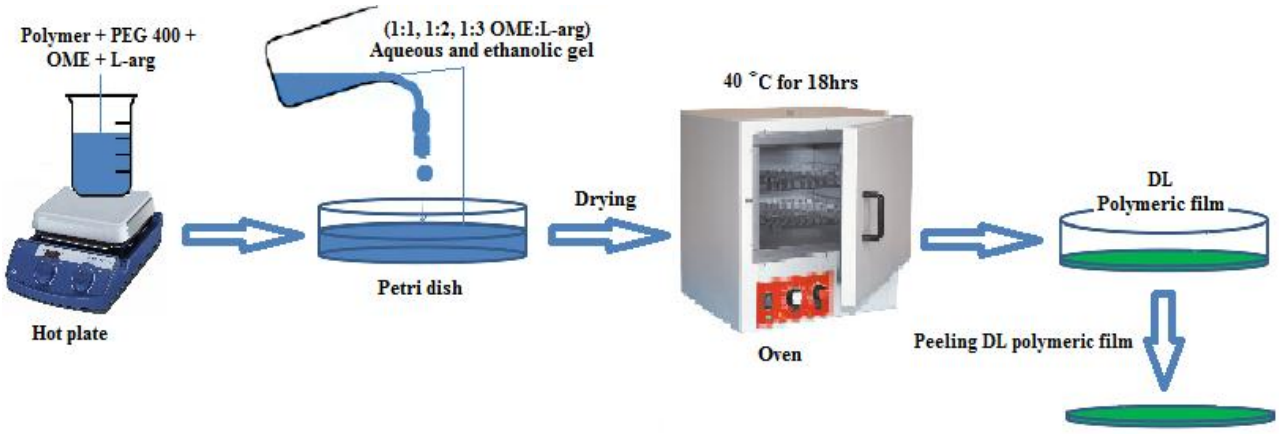

Figure 3.1 Schematic diagram showing preparation of DL films using different polymers (MET and SA), PEG 400 (0.5% w/w) and different ratios of OME: L-arg (1:1, 1:2, 1:3).

Table 3.4 Amount of OME in the gel without L-arg (Andrews, et al., 2009)

Solvent system	Water: EtOH (mL)	Polymer (MET & SA) (g)	Drug (OME) (g)	Plasticizer (PEG 400) (g)	
				0% w/w	0.5 w/w
Water	50:0 (1:0)	0.5	0.1	0.0	0.5
10% (v/v) EtOH	45:5 (9:1)	0.5	0.1	0.0	0.5
20% (v/v) EtOH	40:10 (4:1)	0.5	0.1	0.0	0.5

Table 3.5 Ratios of OME: L-arg in the gel formulation

Solvent system	Water: EtOH (mL)	Polymer (MET & SA) (g)	Drug (OME) (g)	L-arg (g)			Plasticizer (PEG 400) (g)	
				1:1	1:2	1:3	0% w/w	0.5% w/w
Water	50:0 (1:0)	0.5	0.1	0.1	0.2	0.3	0.0	0.5
10% (v/v) EtOH	45:5 (9:1)	0.5	0.1	0.1	0.2	0.3	0.0	0.5
20% (v/v) EtOH	40:10 (4:1)	0.5	0.1	0.1	0.2	0.3	0.0	0.5

3.2.4.3 Texture analysis (TA)

Texture analysis was used to characterise the tensile properties of the MET DL films (films plasticized with 0-0.5 % PEG 400, 20% EtOH, L-arg 1:1, 1:2 and 1:3 and OME). A texture analyser TA HD plus (Stable Micro System, Surrey, UK) equipped with 5 kg load cell was used to perform the experiment. Data evaluation was performed by texture exponent-32 software program. The films free from any physical imperfection with the average thickness of (0.07 - 0.1 mm) were selected for testing (Boateng et al., 2013). The dumb-bell shaped films were fixed between two tensile grips positioned 30 mm apart and stretched to break point. The peak force and elongation at break, elastic modulus of the films prepared with different polymers (MET) and PEG 400 as plasticiser (0-0.5 % w/w) based on polymer's weight and L-arg 1:1, 1:2 and 1:3) were determined when films broke. Three replicates were carried out for each type of film. The instrument settings used in the analyses are given in table 3.6.

Table 3.6 Texture analyser settings

Test parameter	Value	Description
Pre-test speed	0.1 mm/sec	Speed of probe before stretching
Test speed	1.0 mm/sec	Stretching speed during testing
Post-test speed	0.1 mm/sec	Speed at which probe returns to the starting position
Distance	50.0 mm	Distance to which grips separate from their starting position after stretching
Trigger type	Auto (Force N)	Force achieved before profile is plotted
Product length	30.0 mm	Length of film between clamps
Product width	10.0 mm	Width of the film
Contact area	300.0 mm^2	Total area of films between tow clumps

3.2.4.4 Hot Stage Microscopy (HSM)

The hot stage microscopy experiments were conducted on a Mettler Toledo FP82HT (Greifensee, Switzerland) with a Nikon Microphot. DL MET films were placed on a glass slide, covered with a coverslip, and heated from ambient temperature to 200 °C at a rate of 10 °C per minute. Changes in morphological behaviour were collected as a video recording by using PixeLINK PL-A662 camera (PixeLINK, Ontario, Canada).

3.2.4.5 Differential scanning calorimetry (DSC)

DSC was used to characterise the thermal behaviour of MET, OME and L-arg (pure materials and DL MET films (prepared from gels plasticized (0.5% w/w PEG 400) and unplasticised ethanolic (20% v/v) gels, containing L-arg: OME 1:1, 1:2 and 1:3 and OME and changes in their properties with introduction of PEG and drug within the films. About 2.5 mg of each sample was placed into hermetically sealed Tzero aluminium pans with a pin hole in the lid and heated a Q2000 (TA Instruments) calorimeter from -40 °C to 180 °C at a heating rate of 10 °C/min under constant purge of nitrogen (N_2) (100 mL/min) to evaluate the glass transition, melting, crystallisation and interaction between polymers and plasticisers (Boateng, et al., 2013).

3.2.4.6 Thermogravimetric analysis (TGA)

TGA studies were performed using a Q5000 (TA instrument) thermogravimetric analyser. About 1-2.5 mg of DL films and starting materials (MET, OME and L-arg) as in DSC were as placed into hermetically sealed Tzero aluminium pans with a pin hole in the lid. Samples were heated under nitrogen (N_2) gas at a flow rate of 25 mL/min, and heated from ambient temperature (20 °C) to 200 °C at a rate of 10 °C/min to evaluate the water content of the pure materials and DL films.

3.2.4.7 Scanning electron microscopy (SEM)

SEM was used to investigate the surface morphology of the DL MET films from plasticized unplasticised ethanolic (20% v/v EtOH) gels containing L-arg:OME 1:1, 1:2 and 1:3. The films were analysed using a Hitachi Triple detector CFE-SEM SU8030, (Hitachi High-

Technologies, Japan) scanning electron microscope. Films were mounted onto Agar Scientific G301 aluminium pin-type stubs (12 mm diameter) with Agar scientific G3347N double-sided adhesive carbon tapes and chrome coated (Sputter Coater S150B, 15 nm thickness). The coated films were analysed at 2 kV accelerating voltage (Engel et al., 1993; Frank et al., 2011).

3.2.4.8 X-ray diffraction (XRD)

D8 Advantage X-ray diffractometer was used to investigate the physical nature (crystalline or amorphous) of the MET DL films prepared from plasticised and unplasticised ethanolic (20% v/v EtOH) gels containing L-arg: OME 1:1, 1:2 and 1:3 and starting materials (MET, PEG 400, OME and L-arg). XRD patterns were obtained with a DIFFRAC plus instrument (Bruker Coventry, UK) with an XRD commander programme. A Goebel mirror was used as monochromator which produced a focused monochromatic $CuK\alpha_{1\&2}$ primary beam (λ=1.54184 Å) with exit slits of 0.6 mm and a Lynx eye detector for performing the experiment. The operating conditions during the experiment were 40 kV and 40 mA. Samples were prepared by cutting $2cm^2$ of films to fit the square tiles of the holder., mounted on the sample cell and scanned between 2 theta of 0° to 70° counting time (0.1 second step size) (Brügemann et al., 2004; Dittrich et al., 2009).

3.2.4.9 Fourier transform infrared (FT-IR) spectroscopy

FT-IR spectra were obtained using a Perkin Elmer spectrophotometer (Spectrum Two, Perkin Elmer, US) equipped with a crystal diamond universal ATR sampling accessory (UATR).
Before each measurement, the ATR crystal was carefully cleaned with ethanol. During the measurement, the sample was in contact with the universal diamond ATR top-plate. For each sample, the spectrum represented an average of 4 scans was recorded in the range of 4000-400 cm-1.

3.2.4.10 Assay/drug content of OME in films

The films (n=3) prepared were assayed for content of OME by dissolving each film in PBS (10 mL) pH 6.8 at 37° C and stirred until homogenous solution was formed, 1mL was withdrawn and examined by HPLC.

3.3 RESULTS AND DISCUSSION

3.3.1 Formulation development and optimisation of OME loaded films

MET and SA were used for formulation DL gels and subsequent DL films based on the results of preliminary formulation study as described in chapter 2.

Physical evaluation of DL films

When OME is added to water, it dissolves quickly to produce a clear solution. After adding polymer and desirable amount of plasticiser in solution for gel formation, the stability of OME plays a vital role in the overall stability of the gel (Wang et al., 2004). However, OME was degraded within 20 minutes and changed the colour of the gel into red as can be seen in figure 3.2 OME can only be stable in alkaline solution above pH 6.5. The stability of OME can be achieved in two ways; (i) introducing cyclo-dextrin (β and γ) and L-arg to the DL gel or (ii) adding only L-arg and the latter was the one chosen in this chapter. L-arg is suitable for paediatric patients and works at the molecular level by binding with drug to prevent its degradation. The difference in the final appearance of the films can be observed in figure 3.3 and 3.4

Figure 3.2 Degradation of OME in gel and change in colour to red.

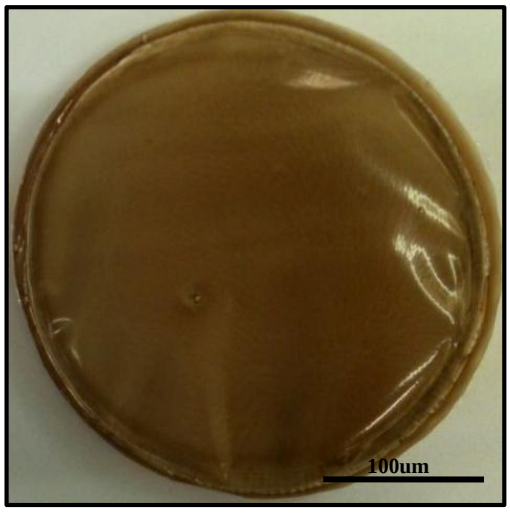

Figure 3.3 OME film without L-arg

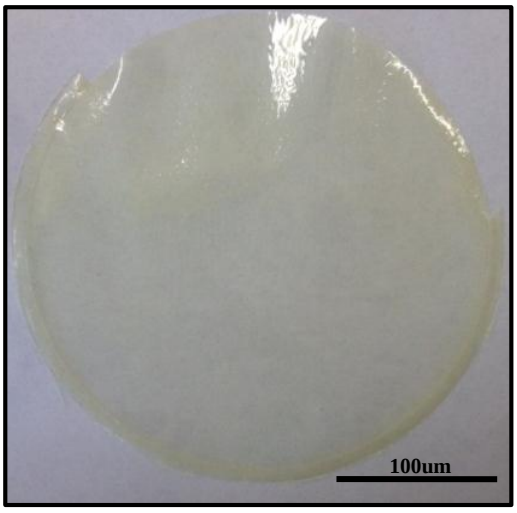

Figure 3.4 OME film with L-arg (stabilizer)

The preliminary observation of the physical characteristics of the formulated films, with and without drug (OME) + L-arg showed a slight difference in the colour of the films. BLK films showed complete transparency (chapter 2, figure 2.4) whereas DL films were slightly yellow (MET) and cream (SA) in colour as shown in figure 3.3 due to the added L-arg. It was also obvious that the addition of L-arg helped to stabilise the drug within the films (Figures 3.4), showing the desired homogeneity, transparency and uniform drug distribution. Figueiras and co-workers suggested that at a ratio of 1:1 OME: L-arg the H atom of the L-arg was observed to be in closer proximity to the nitrogen atom of OME. They also observed that the distance between the H (L-arg) and the N (OME) is relatively small which increases the chances of formation of hydrogen bonds between the two compounds (Figueiras et al., 2010).

MET and SA films with different concentrations of L-arg

DL MET films

Generally, plasicised DL films containing OME and different amounts of L-arg (1:1; 1:2 and 1:3) showed a significant difference in their visual appearance compared to unplasticised films with the former showing better transparency and uniformity. Another difference obeserved was that the films prepared from aqueous only gels, were hard to peel off from the Petri dish due to their thin nature. Further, the distribution of OME and L-arg was more uniform in the films prepared from the ethanolic gels (10% and 20% v/v EtOH).

The images shown in figure 3.5 are of unplasticised films prepared from gels loaded with 0.1 g OME and 0.1 g L-arg (ratio of 1:1). These films showed good peeling properties with acceptable strength. Films obtained from gels prepared with aqueuos are illustrated below in figure 3.5 (a-c) which shows the MET films (aqueous gel) were not transperant due to recrystallisation on the film surface which could be both the model drug (OME) and L-arg. Films prepared from ethanolic gels (10% v/v EtOH) showed the drug more uniformly dispersed compared to the aqueous equivalent. Films obtained from ethanolic gels (20% v/v EtOH) were the most transparent and uniform due possibly to complete molecular dispersion of both OME and L-arg within the polymeric matrix.

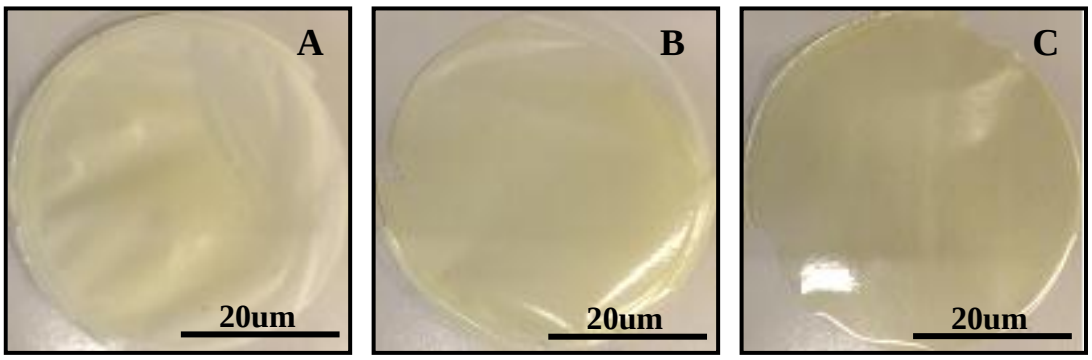

Figure 3.5 The digital photos of unplasticised solvent cast MET films containing 0.1 g OME + 0.1 g L-arg, (a) Films prepared from gels formed with only aqueous (b) films prepared from gels with 10% v/v EtOH (c) films prepared from 20% v/v EtOH gels

Plasicised MET films containing 0.1 g OME and 0.1g L-arg (ratio of 1:1) showed a significant difference (transparency) (figure 3.6) compared to films without plasticiser (figure 3.5). All the plasticised films showed better transparency compared to non-plasticised films. Films obtained from aqueous plasticised gels are illustrated below in figure 3.10. The films were transperant with model drug (OME) and L-arg uniformly distributed within the film matrix. Films prepared from ethanolic gels (with 10% and 20% v/v EtOH) showed higher drug loading compared to aqueous film and better drug dispersion and film uniformity. It was therefore concluded that films prepared from ethanolic gels (20% v/v EtOH) were the most transparent and uniform which could be due to complete molecular dispersion of drug (OME) and L-arg within the polymeric matrix.

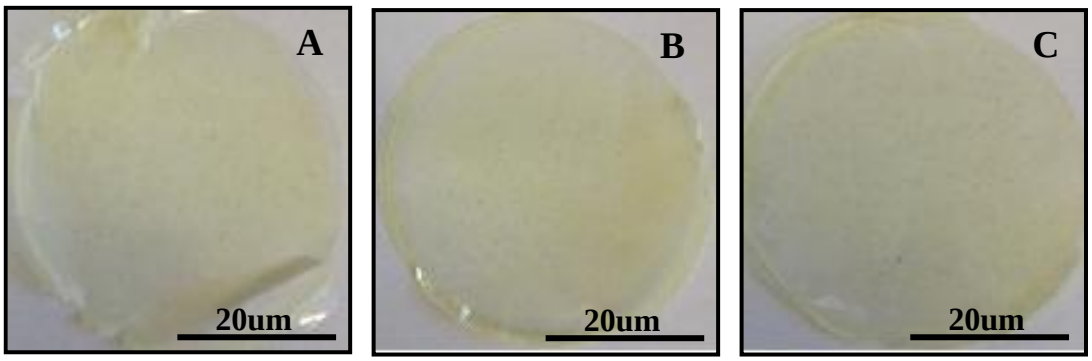

Figure 3.6 The digital photos of plasticised solvent cast MET films with 0.1 g OME + 0.1 g L-arg + PEG 400, with (a) water (b) EtOH 10% v/v (c) EtOH 20% v/v as casting solvents.

Figure 3.7 shows digital images of unplasticised MET films prepared from gels containing 0.1 g OME and 0.2 g L-arg (ratio of 1:2) in 10% v/v EtOH as solvent. All films showed better transperancy compared to films with a ratio of 1:1 (figure 3.5). The drug within films was stable because of the addition of L-arg and all stabilised films (figure 3.6) showed desired homogeneity, transparency and uniform drug distribution. No other significant difference observed between these films.

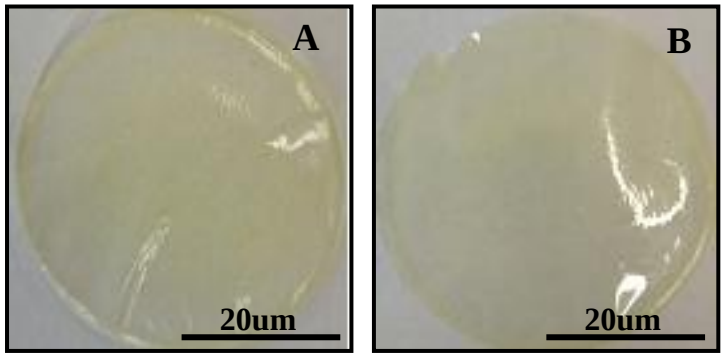

Figure 3.7 The digital photos of unplasticisedsolvent cast MET films prepared from gels with 0.1 g OME + 0.2 g L-arg, with (a) 10% v/v EtOH (b) 20% v/v EtOH as casting solvents.

When PEG 400 was present in the films with ratio of 1:2 of drug to L-arg, it also showed acceptable uniformity as can be seen in figure 3.8. Films prepared from aqueous gels were hard to peel off from the Petri dish without damaging them, due to stickiness as L-arg made it more plasticised. Films prepared from gels with 10% and 20% v/v EtOH and containing ratio of 1:2 of drug and stabiliser appeared to be the most suitable formulations.

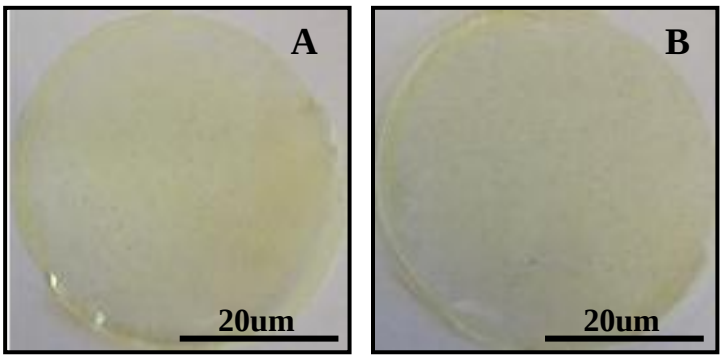

Figure 3.8 The digital photos of plasticised solvent cast MET films prepared from gels containing 0.1 g OME, 0.2 g L-arg, 0.5% w/w PEG 400 using (a) 10% v/v EtOH and (b) 20% v/v EtOH as casting solvents.

MET films containing a ratio of 1:3 (OME: L-arg), with and without PEG 400 prepared from aqueous and ethanolic (10% and 20% v/v EtOH) gels were hard to peel off from Petri-dish due to the distribution of OME and L-arg and stickness on the surface of the film. Based on the above observations, MET films containing OME:L-arg in a ratio of 1:2 was the formulation of choice to compare with the SA films before further development.

DL SA films

To determine the optimum concentration of L-arg required to stabilize the drug and determine its effect on SA film properties, drug was added to the original gels before drying. The images shown in figure 3.9 are of SA films prepared from gels loaded with 0.1 g OME and 0.2 g L-arg (1:2). These films showed good peeling properties but the films were brittle. Films obtained from gels prepared with only water are illustrated below in figure 3.9 (a-c).

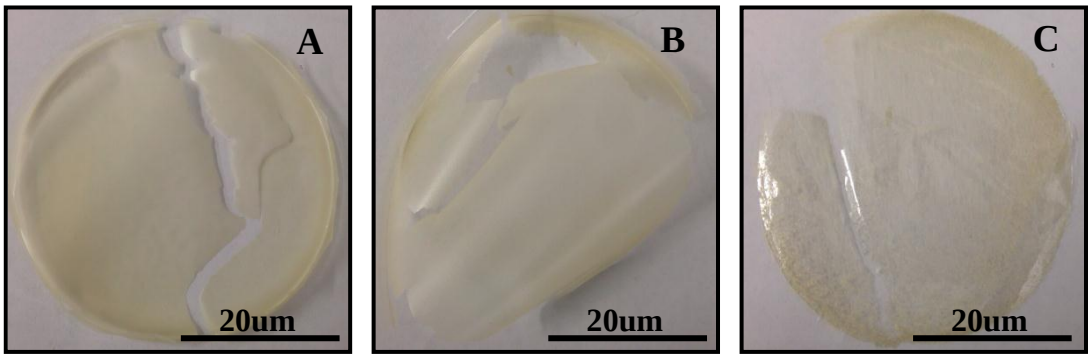

Figure 3.9 The digital photos of solvent cast SA films with 0.1 g OME + 0.2 g L-arg, cast from gels with (a) only water (b) 10% v/v EtOH (c) 20% v/v EtOH as casting solvent.

Table 3.7 Ideal characteristics of DL films of MET and SA

Solvent/gel	PEG (% w/w)	OME (g)	L-arg (g)	Peel off	Film characteristics	Thickness (rounded to two decimal places) (mm)
MET aqueous	0.00	0.10	0.10	YES	Not transparent/ slightly brittle	0.07
	0.00	0.10	0.20	NO	--------	0.06
	0.00	0.10	0.30	NO	--------	0.07
MET aqueous	0.50	0.10	0.10	YES	Not transparent/ slightly brittle	0.07
	0.50	0.10	0.20	NO	--------	0.07
	0.50	0.10	0.30	NO	--------	0.07
MET	0.00	0.10	0.10	YES	Transparent/flexible	0.07
10% v/v	0.00	0.10	0.20	YES	Transparent/flexible	0.07
EtOH	0.00	0.10	0.30	NO	--------	0.07
MET	0.50	0.10	0.10	YES	Transparent/flexible	0.07
10% v/v	0.50	0.10	0.20	YES	Transparent/flexible	0.07
EtOH	0.50	0.10	0.30	NO	--------	0.07
MET	0.00	0.10	0.10	YES	Transparent/flexible	0.07
20% v/v	0.00	0.10	0.20	YES	Transparent/flexible	0.07
EtOH	0.00	0.10	0.30	NO	--------	0.07
MET	0.50	0.10	0.10	YES	Transparent/flexible	0.07
20% v/v	0.50	0.10	0.20	YES	Transparent/flexible	0.07
EtOH	0.50	0.10	0.30	NO	--------	0.07
SA aqueous	0.00	0.10	0.20	YES	Brittle	0.07
10% v/v EtOH	0.00	0.10	0.20	YES	Brittle	0.07
20% v/v EtOH	0.00	0.10	0.20	YES	Brittle	0.07

The description of the physical appearance of the films based on most ideal characteristics (transparency, ease of peeling and flexibility) are summarised in table 3.7. Overall, based on the visual observation after determining different amounts of OME and L-arg within the different formulations, (MET and SA), it was concluded that DL MET films were most optimum as shown in table 3.7 and were therefore selected for physical and mechanical characterisation and future studies.

3.3.2 Texture analysis (TA)

Texture analysis was employed to determine the effect of OME and L-arg along with PEG 400 (0.0 and 0.5 % w/w) on the tensile properties of the MET films and the resulting data used to select the most appropriate formulations for further development including swelling, drug release, permeation and cyto toxicity studies.

The films showed significant differences in the tensile strength (brittleness) based on the PEG concentration and the results are shown in figures 3.10 and 3.11 respectively.

It has been suggested that the average % elongation at break point should ideally be between 30-60% (Boateng et al., 2009) which indicates a good balance between flexibility and elasticity. MET films prepared with OME and L-arg (1:1 and 1:2) from gels containing 0.5 % w/w of PEG satisfied this required criteria. The % elongation at break point of DL MET films gradually increased with increased concentration of PEG. Plasticised MET films prepared from ethanolic (10 and 20% v/v EtOH) gels containing 0.5% w/w PEG and L-arg (1:1 and 1:2), showed % elongation of break values between 35-45%. However, unplasticised films prepared using aqueous gel, 0.0% w/w PEG and L-arg (1:1 and 1:2) gave a very low % elongation at break as shown in figures 3.12 whilst films obtained from EtOH (10 and 20% v/v) gels showed a steady increase in % elongation from 1:2 ratio of OME:L-arg to a ratio of 1:1.

Based on these results and on the visual observation and the expected characteristics for an ideal film in terms of flexibility, uniformity and transparency, films prepared from ethanolic gels (20% v/v EtOH) containing 1:2 ratio of OME: Larg and 0.5% w/w PEG400 was confirmed as the most appropriate for further investigations.

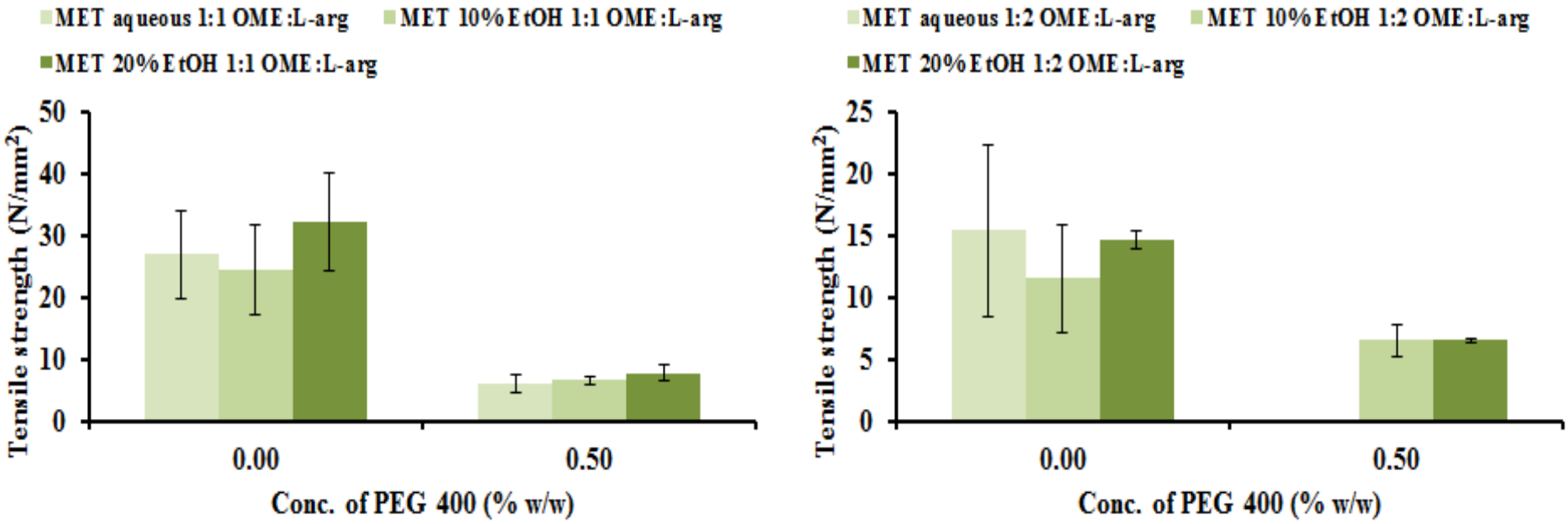

Figure 3.10 Mechanical (tensile) strength of DL MET films cast from aqueous and ethanolic (10% and 20% v/v EtOH) polymeric gels containing different amounts of plasticiser (0.0% and 0.5% w/w PEG 400) and OME: L-arg (1:1 and 1:2) (mean ± SD, (n=3))

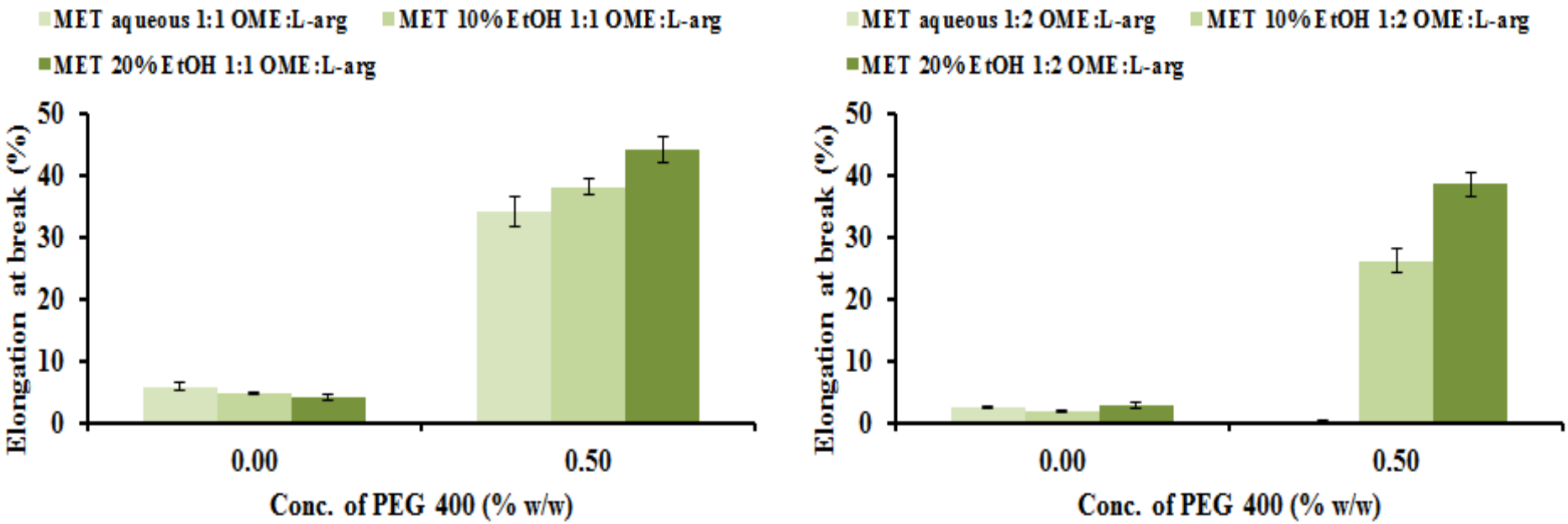

Figure 3.11 Mechanical (tensile) properties (% elongation at break) of DL MET films cast from aqueous and ethanolic (10% and 20% v/v EtOH) polymeric gels containing different amounts of plasticiser (0.0% and 0.5% w/w PEG 400) and OME: L-arg (1:1 and 1:2) (mean ± SD, (n=3))

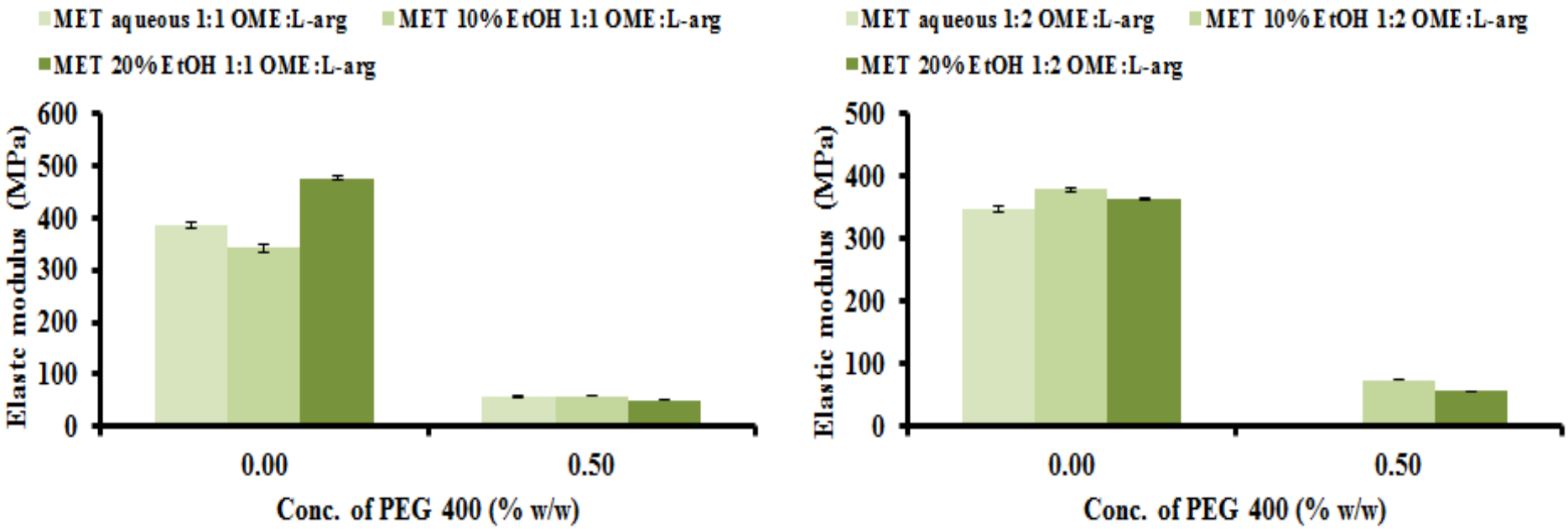

Figure 3.12 Mechanical (tensile) properties (elastic modulus) of DL MET films cast from aqueous and ethanolic (10% and 20% v/v EtOH) polymeric gels containing different amounts of plasticiser (0.0% and 0.5% w/w PEG 400) and OME: L-arg (1:1 and 1:2) (mean ± SD, (n=3))

3.3.3 Hot Stage Microscopy (HSM)

The main characteristics analysed by the HSM is the melting point range which is entirely dependent on the purity of the film, which enables the study materials as a function of temperature and time.

For the DL films (with/without any plasticizer) the results showed that as the temperature increased with time, the surface of the film went from rough to clear due to loss of water content in the film as seen in figure 3.13. As was the case for BLK, the HSM results obtained helped in developing suitable methods for TGA and DSC analysis and determined the maximum temperature to which samples could be heated before degradation.

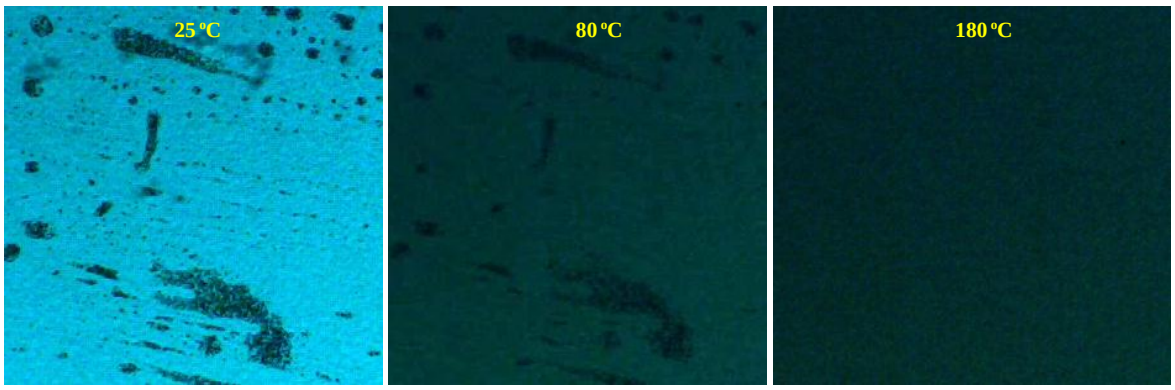

Figure 3.13 HSM results showing DL MET film during heating

3.3.4 Differential scanning calorimetry (DSC)

DSC was used to determine the interactions between the components of the film within the film matrix, MET, PEG 400, L-arg and model drug (OME). MET showed a broad endothermic peak at 67.07 °C which can be attributed to evaporation of water with no definite melt or glass transition peaks. OME showed sharp endothermic peak at around 159 °C, indicating the melting point of the drug, followed by an exothermic effect at 171°C, due to its thermal decomposition. L-arg showed a sharp endothermic peak at 100 °C due to melting as shown in figure 3.14. The thermograms (figure 3.15) of unplasticised MET DL films [aqueous and ethanolic (10% and 20% v/v EtOH) gels] containing OME: L-arg (1:1), showed a broad endothermic transition between 65 – 68 °C, followed by another endothermic peak at around 156-157 °C, indicating the melting of recrystallized OME. Plasticised films (PEG 400 (0.5% w/w) with OME: L-arg (1:1)) also showed broad endothermic transition between 61 – 68 °C, followed by a another small broad endothermic peak at 115 – 123 °C (figure 3.16) representing a possible shift of the recrystallized melt peak of OME though this is difficult to tell. This indicates that some OME may be present crystalline form after film formation or during heating for the particular ratio of OME: L-arg. A possible reason of the melting could also be due to formation of co-crystals between the L-arg and OME.. The reason why crystal may be present is that plasticisation by the PEG will cause molecular rearrangements in the film freeing up molecules that would have otherwise been molecularly dispersed (and trapped) to interact and crystallize.

The thermograms of MET DL films [aqueous and ethanolic (10% and 20% v/v EtOH)] containing PEG 400 (0.0 and 0.5% w/w) OME: L-arg (1:2), showed similar results to OME: L-arg (1:1) films with broad endothermic transition between 66 - 83°C, followed by a smaller broad endothermic peak between 135 – 160 °C indicating a possible recrystallization peak of OME which occurs during heating as shown in figures 3.17, 3.18 and table 3.8.

Generally, all the DL MET films can be characterized as amorphous. It can be said that the crystalline content in the films are generally very low due to the low enthalpies observed for the melting transition (Table 3.8).

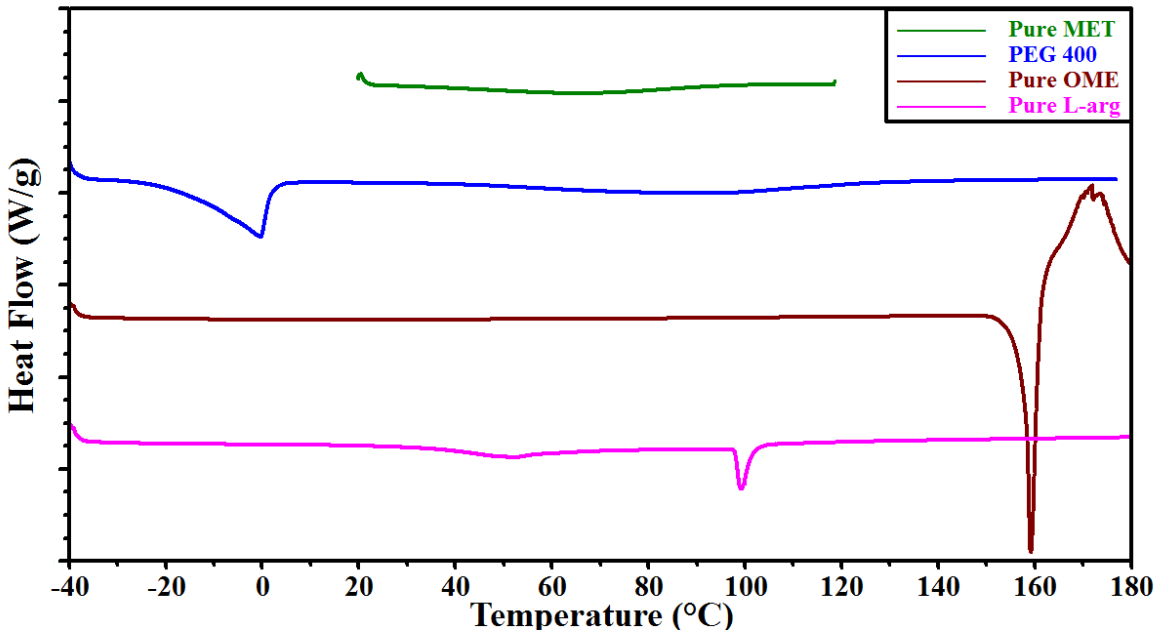

Figure 3.14 DSC thermograms for the pure MET, pure OME, pure L-arg and PEG 400 (plasticiser) (W/g (Watts/gram))

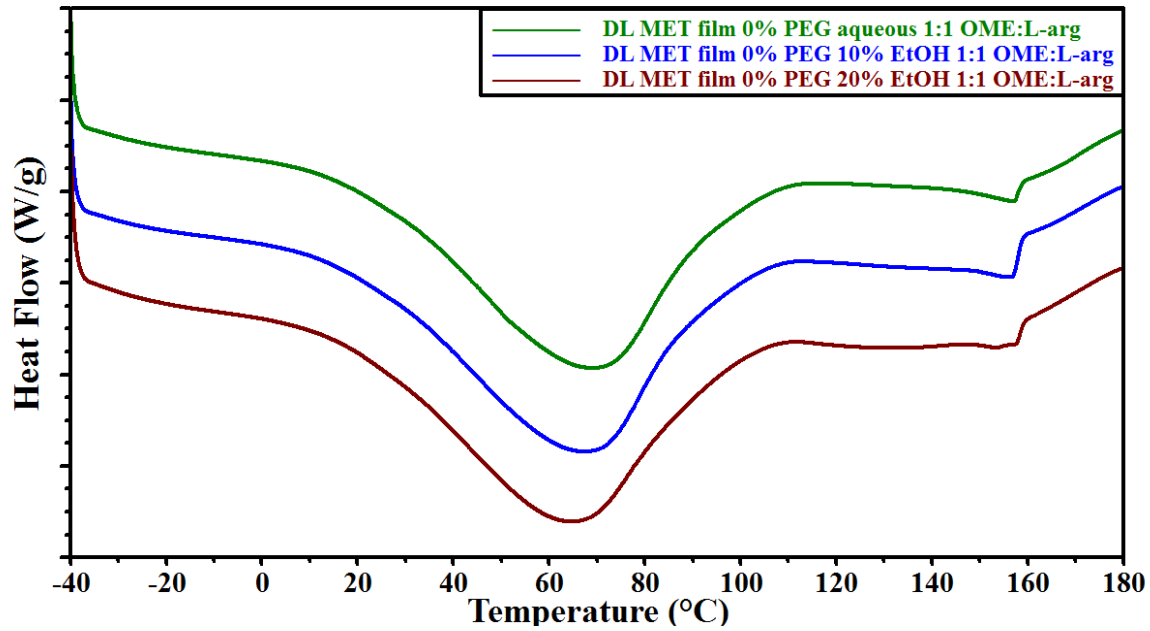

Figure 3.15 DSC thermograms of unplasticised DL MET films cast from aqueous and ethanolic (10% and 20% v/v EtOH) polymeric gels containing OME: L-arg (1:1) (W/g (Watts/gram))

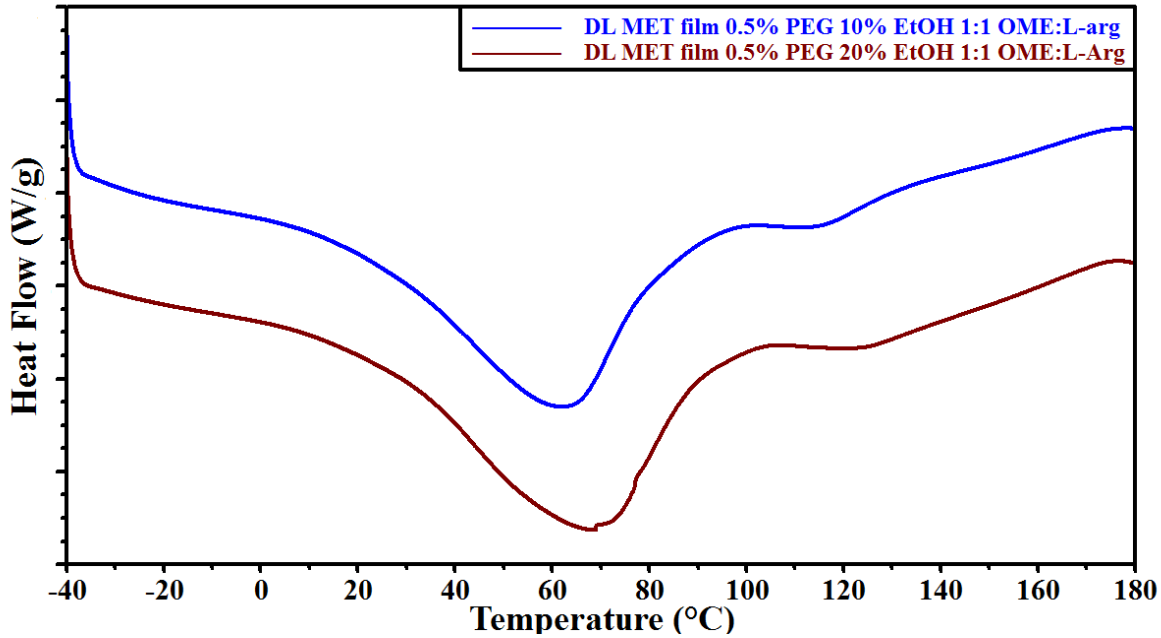

Figure 3.16 DSC thermograms of plasticised DL MET films cast from ethanolic (10% and 20% v/v EtOH) polymeric gels containing 0.5% w/w PEG 400 and OME: L-arg (1:1) (W/g (Watts/gram))

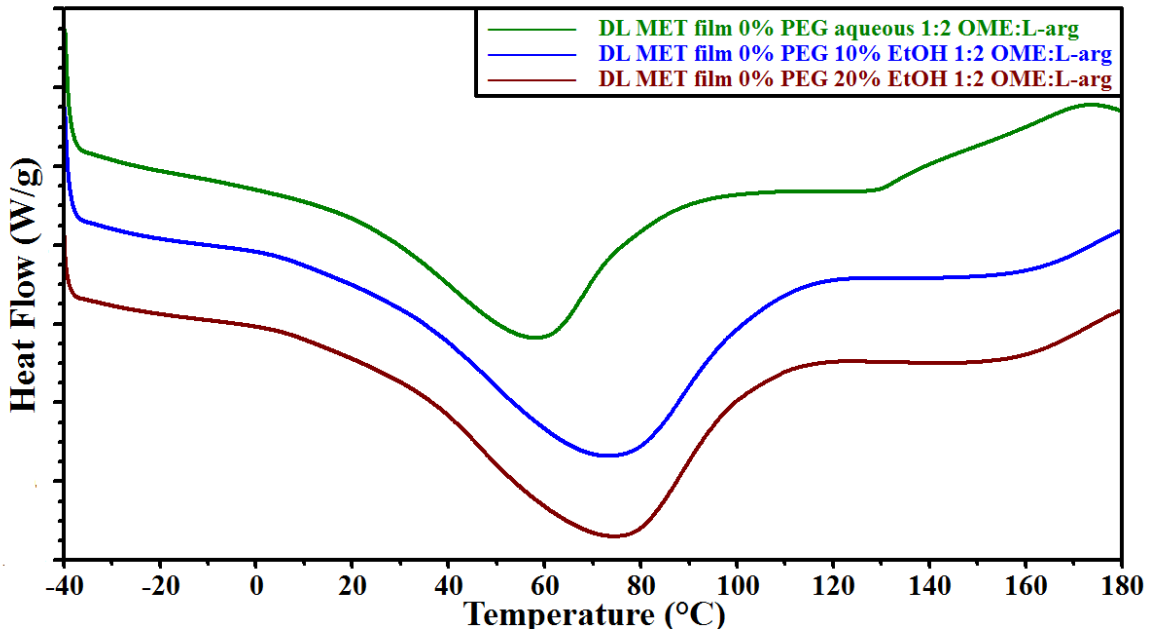

Figure 3.17 DSC thermogram of unplasticised DL MET films cast from aqueous and ethanolic (10% and 20% v/v EtOH) polymeric gels containing OME: L-arg (1:2) (W/g (Watts/gram))

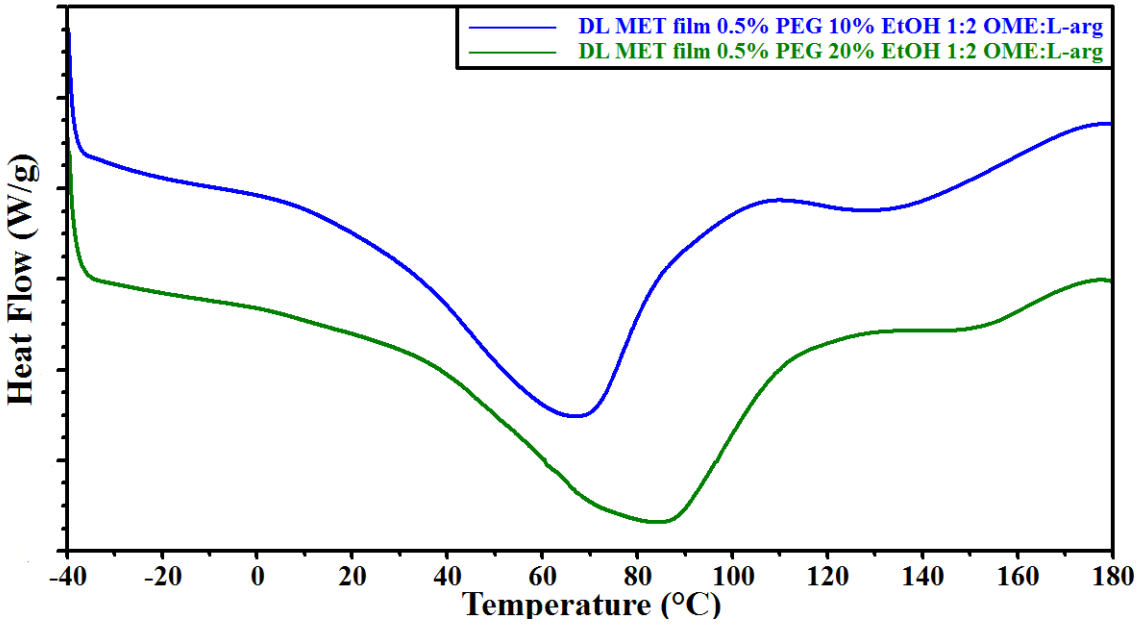

Figure 3.18 DSC thermograms of plasticised DL MET films cast from ethanolic (10% and 20% v/v EtOH) polymeric gels containing OME: L-arg (1:2) (W/g (Watts/gram))

As seen above from figure 3.15 to 3.18 there was no glass transition observed, this was due to the broad endothermic water peaks. However if a glass transition was to be observed a heat-cool-heat cycle can be used, heating the sample to its highest temperature without degrading, cooling it down and then re-heating it to observe a glass transition peak without any interfering water peaks.

Table 3.8 Temperature and heat changes observed for the endothermic transitions observed (pure materials and films (MET)).

	1st TRANSITION			2nd TRANSITION		
Pure materials/ gels	**Onset °C**	**Peak °C**	**ΔH (J/g)**	**Onset °C**	**Peak °C**	**ΔH (J/g)**
Pure MET	25.89	67.07	71.05	-	-	-
Pure OME	157.91	159.23	135.90	167.27	171.90	85.04
Pure L-arg	34.29	52.08	26.26	98.01	99.13	12.97
PEG 400	-	0	-	-	-	-
			PEG 400 (0% w/w)			
Aqueous 1:1	21.84	68.46	124.10	139.64	157.04	4.19
10% v/v EtOH 1:1	19.06	67.07	123.60	137.10	156.43	7.83
20% v/v EtOH 1:1	19.01	64.30	118.40	148.36	157.45	1.80
Aqueous 1:2	16.11	57.83	100.80	115.41	129.02	2.51
10% v/v EtOH 1:2	21.84	72.62	160.20	139.32	160.48	5.13
20% v/v EtOH 1:2	24.06	73.54	153.20	135.89	158.27	7.23
			PEG 400 (0.5% w/w)			
10% v/v EtOH 1:1	18.87	61.95	101.70	104.31	115.84	2.98
20% v/v EtOH 1:1	22.58	68.08	109.00	106.86	123.66	2.58
10% v/v EtOH 1:2	20.25	66.85	134.30	111.55	135.82	16.08
20% v/v EtOH 1:2	30.48	83.41	141.00	130.68	151.82	5.77

3.3.5 Thermogravimetric analysis (TGA)

The TGA results of starting materials (MET, OME, L-arg and PEG 400) are shown in table 3.9, the weight loss of MET, OME, L-arg and PEG 400 from ambient temperature (20 °C) to 100°C with a total weight loss of 0.87 %, 0.23 %, 5.96 % and 2.79 % respectively. The TGA results of MET DL films (aqueous and ethanolic) containing different ratios of OME: L-arg (1:1 and 1:2) are shown in table 3.9 indicating the percentage loss with heating, attributed to residual water present within the film matrix.

Table 3.9 Thermal transition with weight loss observed for MET films from aqueous and ethanolic (10% and 20 % v/v EtOH) gels containing different concentrations of PEG 400 (0.0, 0.5 % w/w) and ratios of OME: L-arg (1:1 and 1:2) analysed by TGA.

Sample	Weight loss (%)
Unplasticised films - PEG 400 (0% w/w)	
Aqueous 1:1	5.32
10% v/v EtOH 1:1	5.15
20% v/v EtOH 1:1	4.86
10%v/v EtOH 1:2	6.10
20% v/v EtOH 1:2	6.01
Plasticised films - PEG 400 (0.5% w/w)	
Aqueous 1:1	4.55
10% v/v EtOH 1:1	4.47
20% v/v EtOH 1:1	4.76
10% v/v EtOH 1:2	5.80
20% v/v EtOH 1:2	5.14
Pure materials	
Pure MET	0.87
PEG 400	2.79
Pure OME	0.23
Pure L-arg	5.95

It was hypothesized that the addition of PEG 400 will cause an increase in water loss content due to the hydrophilic characteristics of PEG400. However, this was not observed except at higher concentrations (0.5 % w/w of PEG). It also appears that the residual water was generally lower for films prepared using aqueous and ethanolic (10 and 20 % v/v) gels containing OME: L-arg (1:2) compared to gels that contained OME: L-arg (1:1) as shown in table 3.9.

3.3.6 Scanning electron microscopy (SEM)

Figure 3.19 shows microscopic appearance of pure OME and L-arg. The surface topography of unplasticised DL MET films containing OME: L-arg (1:1) in figure 3.20 showed rough surfaces with some lumps and holes. The surface topography of the unplasticised MET films containing OME: L-arg (1:2) prepared from aqueous gels showed considerably rougher surface with few crystals visible compared to the films cast from ethanolic gels (10% v/v EtOH), which in turn showed uneven surfaces with holes than films prepared from ethanolic gels (20% v/v EtOH) showing smooth and homogenous as seen in figure 3.22. This could be due to drug and stabilizer loading which meant uniformity could not be achieved in these films. However, the corresponding plasticised films showed continuous sheets with relatively smooth and homogeneous surfaces and suggest that all the components were uniformly mixed during gel formation as shown in figure 3.21. As seen in figure 3.23 increasing amount of L-arg (OME: L-arg 1:2) in plasticised films (PEG 0.5% w/w), prepared from 10% v/v ethanolic gels caused the films to loose smoothness and homogeneity whilst those obtained from 20% v/v ethanolic gels showed a smoother and homogenous uniform surface.

As previously noted, such differences in surface topography could influence uniformity of the films, because any pores or lumps in the film could affect the subsequent functional performance of different formulations with respect to hydration capacity/swelling studies, mucoadhesion and drug release characteristics. Based on these results, films prepared from ethanolic gels (20% v/v EtOH) containing 1:2 ratio of OME: Larg and 0.5% w/w PEG400 was confirmed as the most appropriate for further investigations.

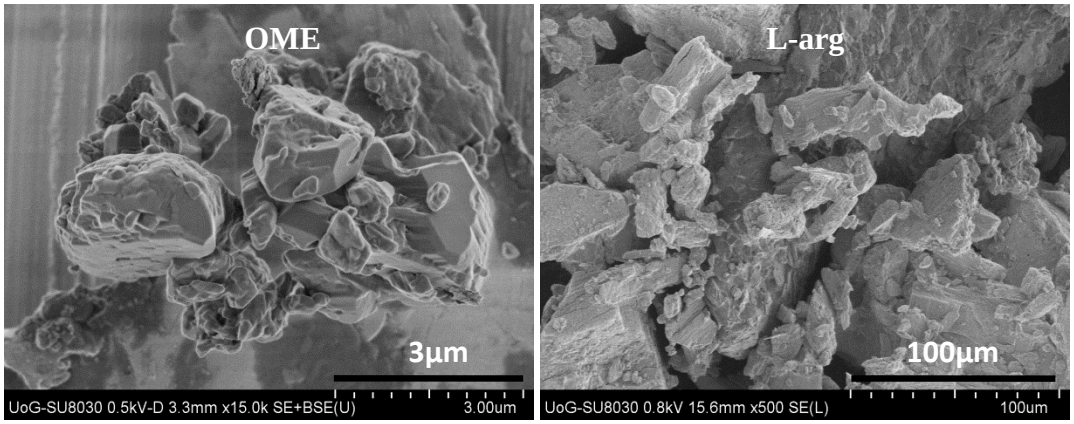

Figure 3.19 SEM micrograph of pure materials (OME (drug) and L-arg (stabilizer))

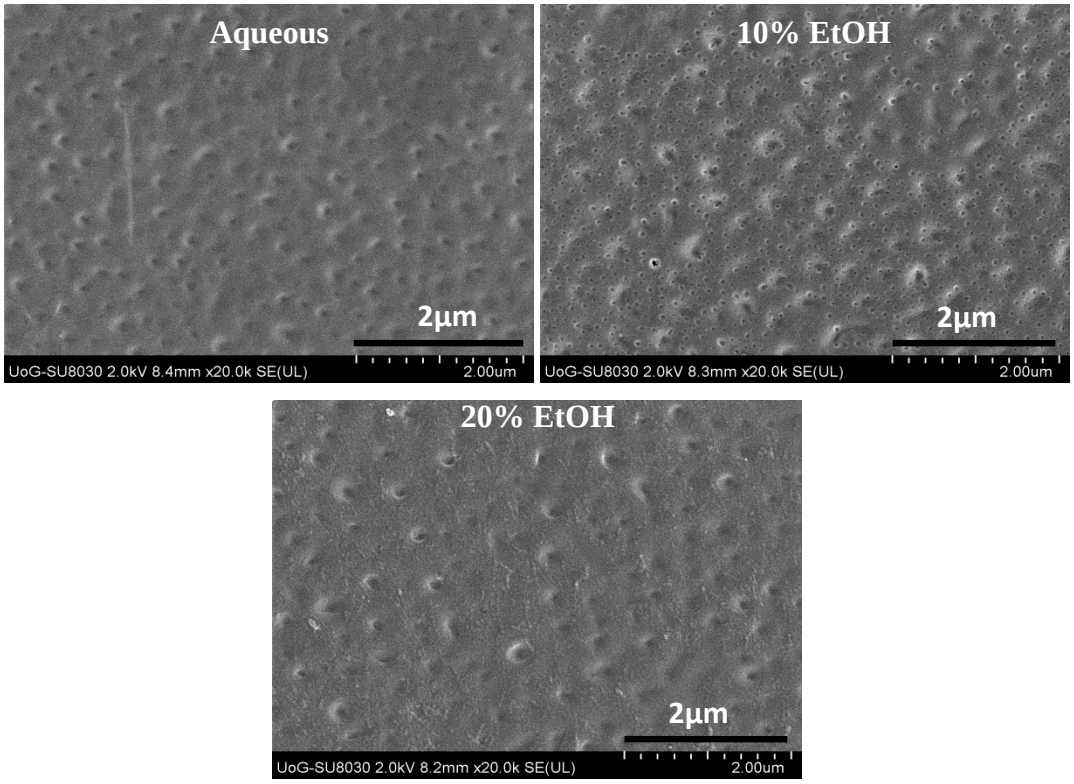

Figure 3.20 SEM micrographs of unplasticised DL MET films cast from aqueous and ethanolic (10% and 20% v/v EtOH) polymeric gels containing OME: L-arg (1:1)

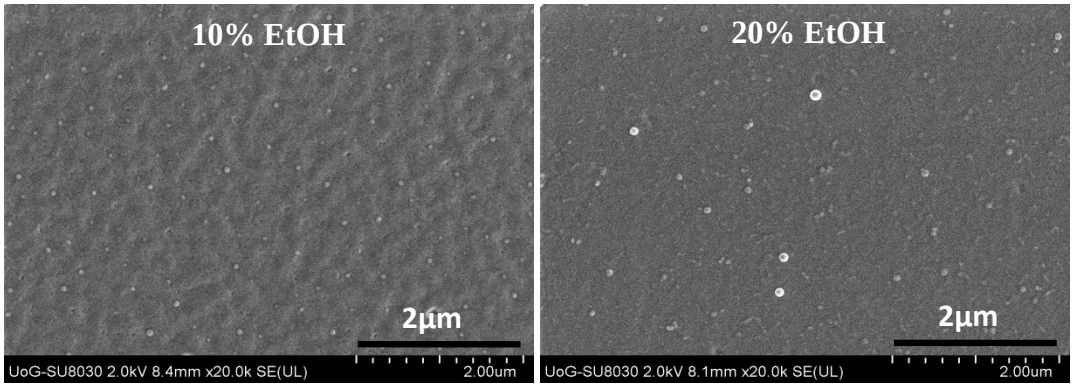

Figure 3.21 SEM micrograph of plasticised DL MET films cast from ethanolic (10% and 20% v/v EtOH) polymeric gels containing OME: L-arg (1:1)

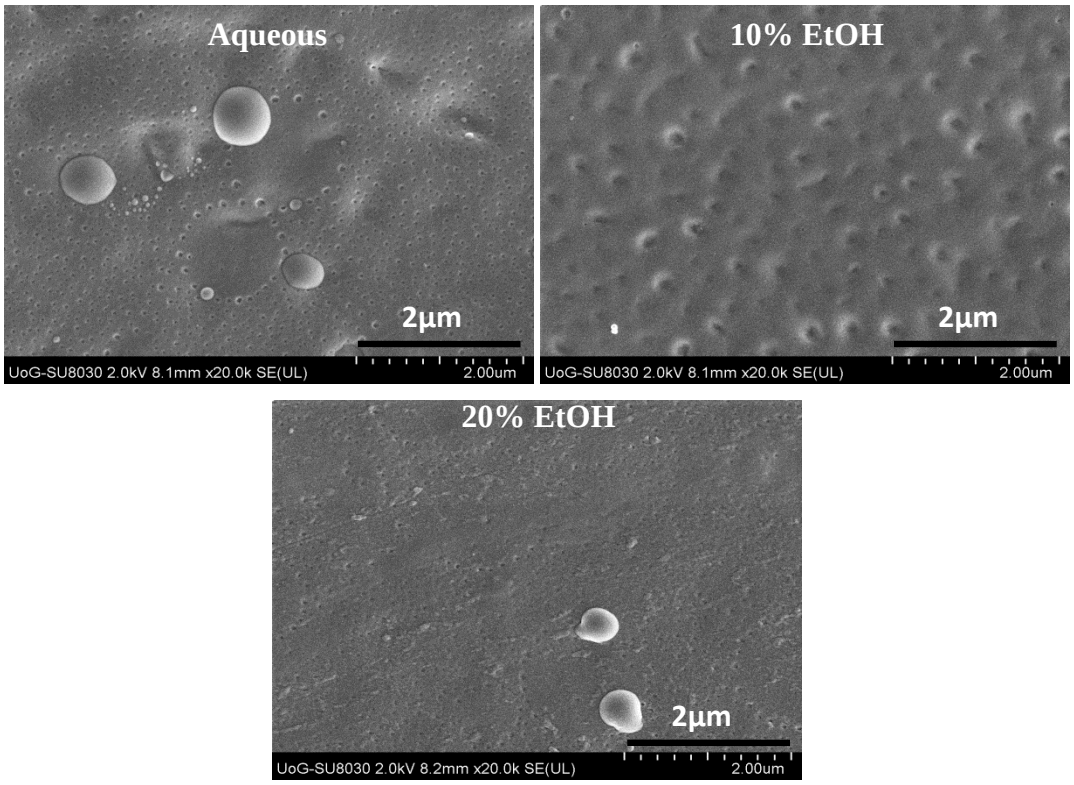

Figure 3.22 SEM micrograph of unplasticised DL MET films cast from aqueous and ethanolic (10% and 20% v/v EtOH) polymeric gels containing OME: L-arg (1:2)

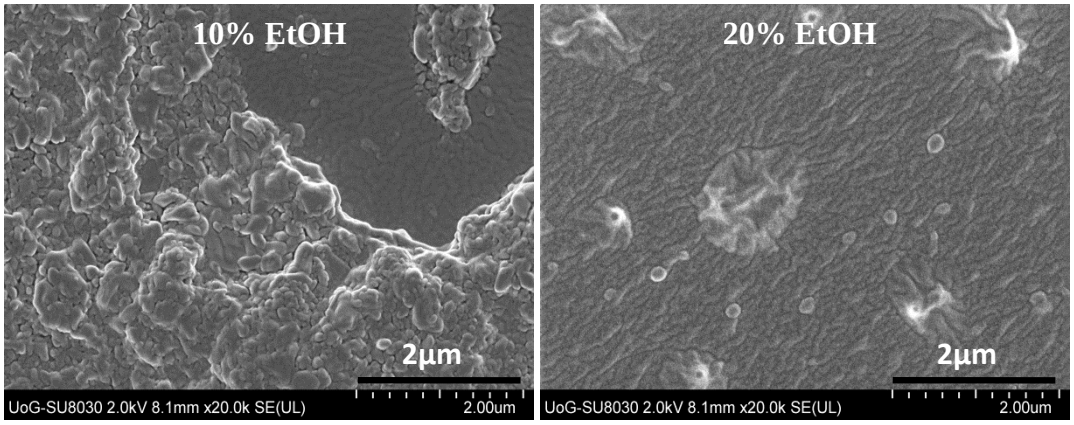

Figure 3.23 SEM micrograph of plasticised DL MET films cast from ethanolic (10% and 20% v/v EtOH) polymeric gels containing OME: L-arg (1:2)

3.3.7 X-ray diffraction (XRD)

XRD analysis was performed to check the crystalline- amorphous ratio and confirm the physical form of the various components within the films. Figure 3.24 shows the XRD diffractograms of the pure materials contained in the DL MET films. The results demonstrate that pure OME and L-arg showed crystalline nature whilst MET and PEG 400 were amorphous in nature.

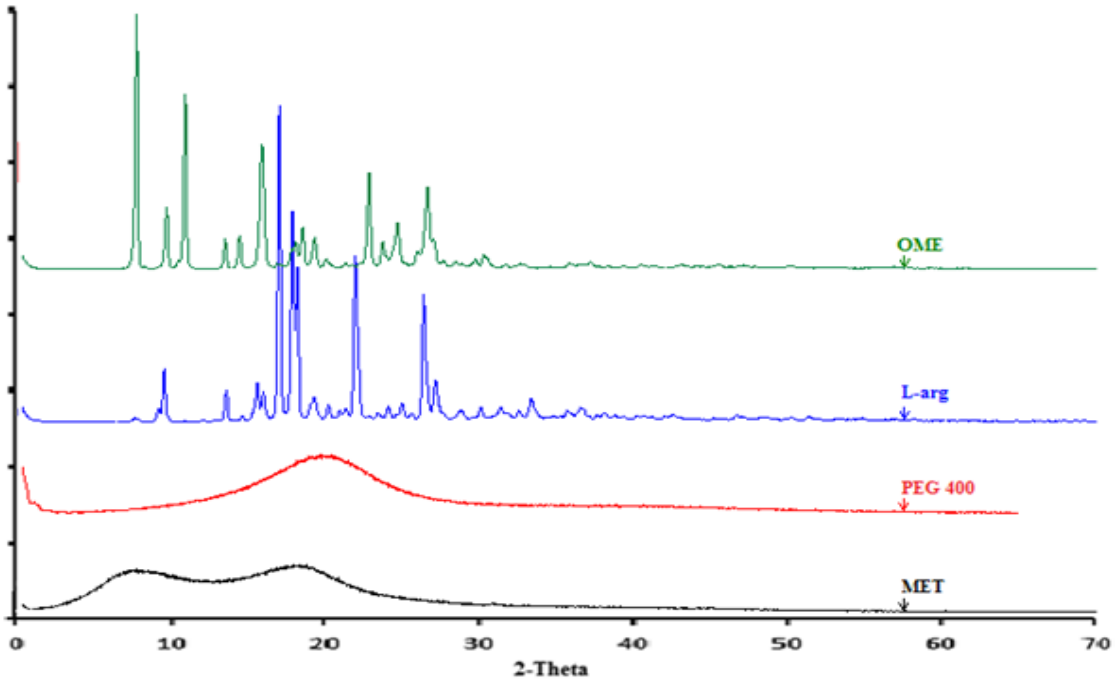

Figure 3.24 XRD diffractograms for the pure MET, OME, L-arg and PEG 400.

Figures 3.25 – 3.28 show the diffractograms of DL MET films cast from gels prepared with the three solvents [aqueous and ethanolic (10% and 20% v/v EtOH)] containing OME: L-arg (1:1 and 1:2) with and without PEG 400. Though the results show some peaks (corresponding to pure OME results) which indicated a small amount of crystallinity for the unplasticised films, they were in general largely amorphous. The crystalline: amorphous ratio was calculated at 1.99% which suggests there were small amounts of OME present in these films.

Figures 3.26 and 3.28 show the diffractograms DL MET films containing OME: L-arg (1:2) all showing broad peaks indicating amorphous nature of the film matrix. The results demonstrate that the DL films containing OME: L-arg 1: 2 had both the drug and L-arg originally added in crystalline form converted to amorphous form suggesting possible molecular dispersion of the drug within the film matrix. This is interesting as it confirms the DSC results previously discussed and also the fact the MET together with L-arg were able to successfully maintain the stability of OME in amorphous form within the film matrix during gel and film formulation and storage prior to analysis. It also appears, that the plasticiser (PEG 400) plays a role in maintaining this amorphous form.

These results are interesting, however, it is well known that the amorphous forms are generally unstable and have the tendency to convert back to the more stable crystalline forms. Therefore further physical and chemical stability studies under controlled conditions of temperature and humidity (both normal and accelerated) was required over a longer period of time (over 1 month) for confirmation of its long term stability in the current physical state. This is described in subsequent chapters.

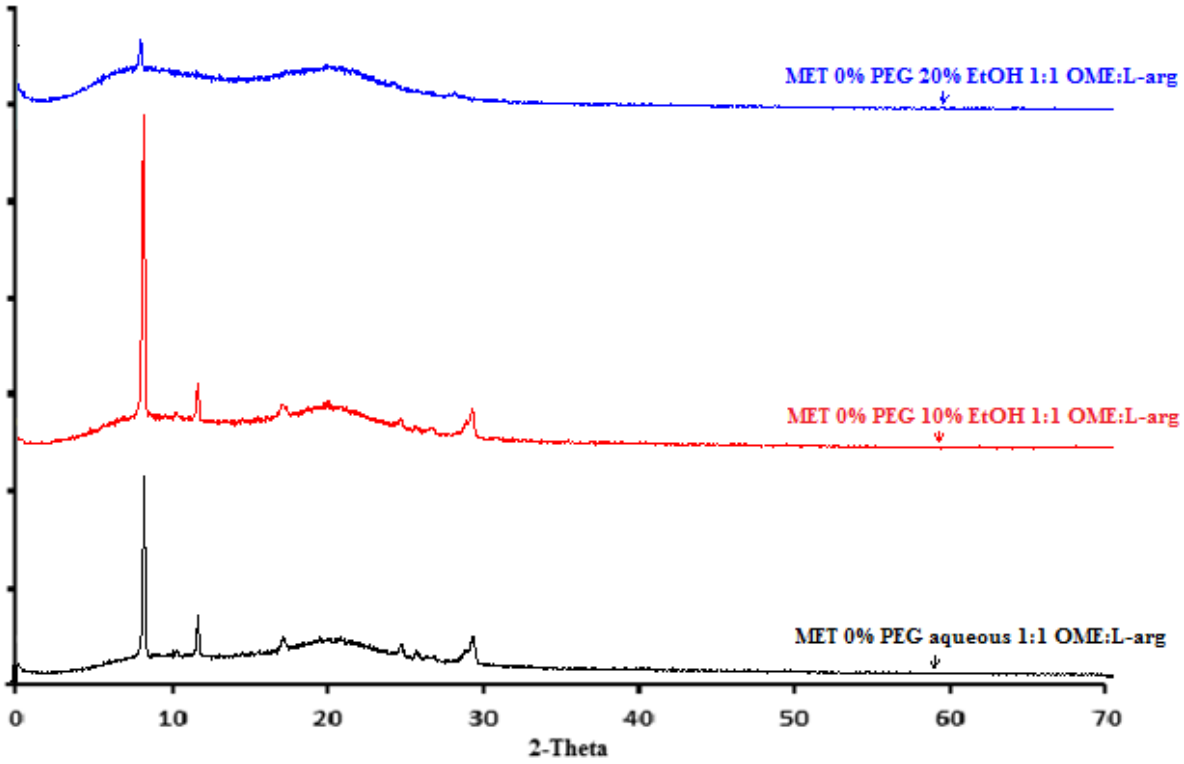

Figure 3.25 XRD diffractograms for unplasticised DL MET films cast from aqueous and ethanolic (10% and 20% v/v EtOH) gels containing OME: L-arg (1:1)

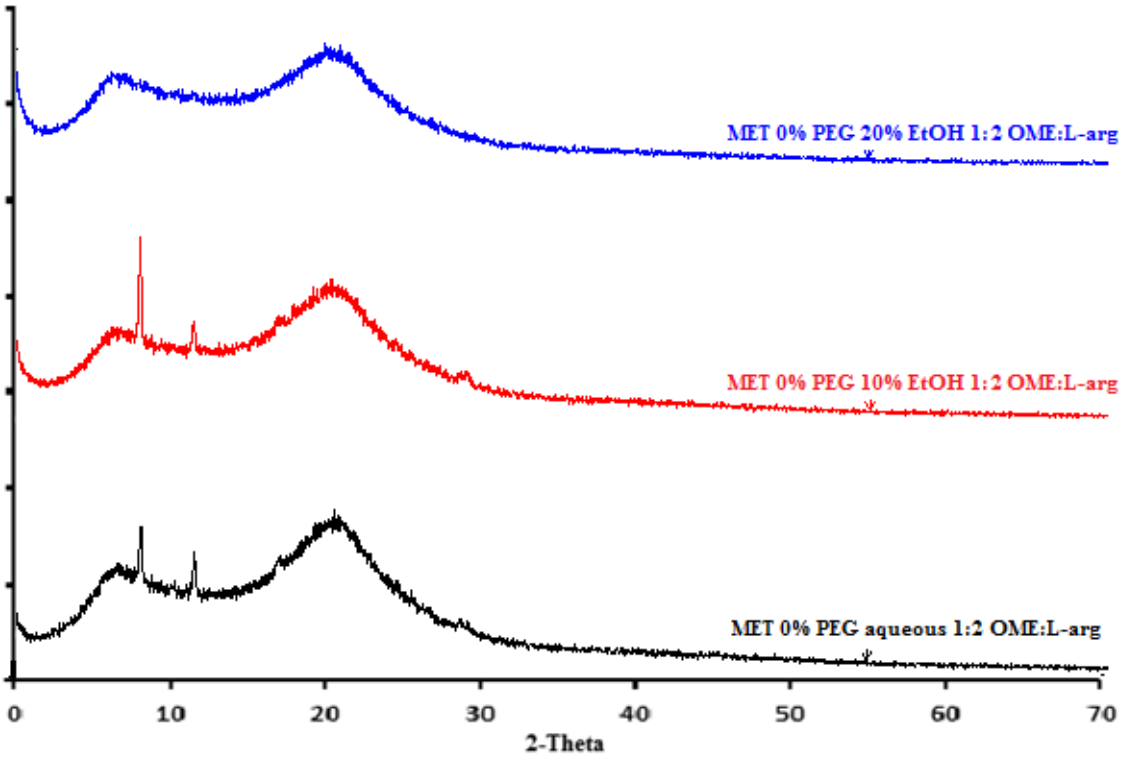

Figure 3.26 XRD diffractograms for unplasticised DL MET films cast from aqueous and ethanolic (10% and 20% v/v EtOH) gels containing OME: L-arg (1:2)

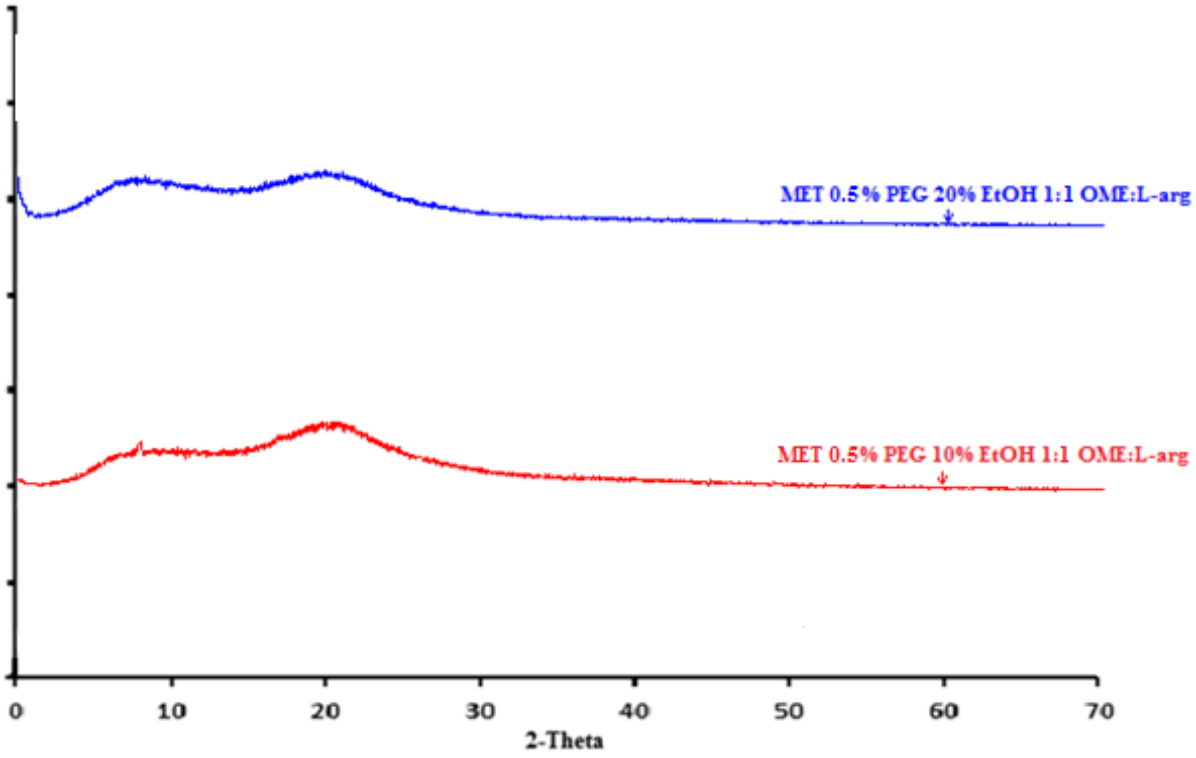

Figure 3.27 XRD diffractograms for plasticised DL MET films cast from ethanolic (10% and 20% v/v EtOH) gels containing 0.5% w/w PEG 400 and OME: L-arg (1:1)

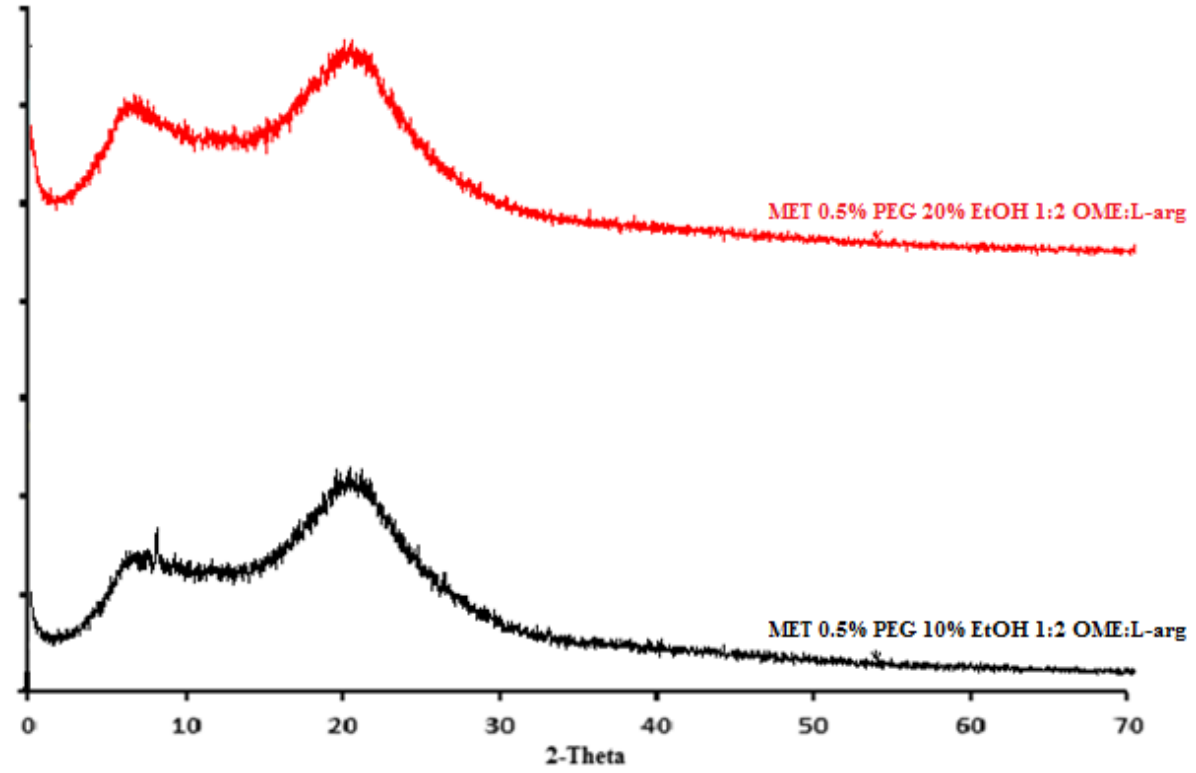

Figure 3.28 XRD diffractograms for plasticised DL MET films cast from ethanolic (10% and 20% v/v EtOH) gels containing 0.5% w/w PEG 400 and OME: L-arg (1:2)

3.3.8 Fourier transform infrared spectroscopy (FT-IR)

FTIR investigations are mainly carried out to examine a molecular change in the drug due to its interaction with other excipients.

The FT-IR absorption bands of OME and L-arg are summarised in table 3.10 (results for MET, PEG 400 and EtOH are already summarised in table 2.10 chapter 2 section 2.4.8, which shows similar corresponding characteristics bands between 3447.40cm^{-1} to 821 cm^{-1} (aromatic and aliphatic). Detailed FT-IR results of DL MET films with or without plasticiser (PEG) and OME: L-arg (1:1 and 1:2) are shown in figures 3.29 – 3.32. FT-IR of the changes in the wavenumbers of the spectral bands describes the different interaction occurring in a specific region.

The first band of the region of interest (3447 cm^{-1}) in figure 3.29 – 3.32 is generally classified as OH stretching. The presence of the hydrogen bonds permit the shift of absorption, to lower frequencies and it is recorded at 3100 cm^{-1}. The FTIR spectra of DL MET films containing the stabiliser (L-arg) with ratio 1:1, 1:2 and with/without plasticiser, shows that the characteristic bands of the drug may be decreased in intensity and may be attributed to the dilution factor of the mixture by the carrier. There were no new bands observed in the spectra, which confirms that no new chemical bonds were formed between the drug and the excipients as seen in figure 3.29-3.32.

Table 3.10 The observed FTIR bands (n=3) for pure materials with their characteristic band

Pure materials	**Absorption bands (cm^{-1})**	**Bands assignment**
OME	966, 885 and 821	C-H bending
	1070	-S=O stretching
	1157	C=O stretching
	1402 and 1309	C-H stretching
	1510	-C=C stretching
	1587	-C=C stretching
	1627	-C=C stretching
	2943 and 2904	C-H stretching
	3058	Aromatic C-H stretching
	3431	N-H stretching
L-arg	848 and 896	CC stretching, NH_2 bending
	1174	Symmetric stretching, CCC bond
	1325 and1356	OH bending, CH3 bending
	1410 and 1464	CH_3 symmetric, asymmetric bending
	1536 and 1574	OH bending, CO stretching
	1680	NH_2 bending
	2928	CH_3 stretching
	3150	NH stretching

The presence of C=N and N-H stretching band at 3431 and 1587 cm^{-1} confirms the presence of OME in DL films prepared from ethanolic (10 % and 20 % v/v) gels containing OME: L-arg (1:1 and 1:2) with and without PEG 400. In summary, the blend of polymer (MET) in DL film is responsible for the high molecular interaction between the functional groups and the formation of new H-bonds which could be due to change in physical stability of L-arg ratio (1:1 and 1:2), with or without PEG 400. It was observed that after the blending of polymer (MET), these interactions did not have effect of deterioration of the chemical constituents of the individual polymer entity and can support stability the added drug (OME).

DL MET films

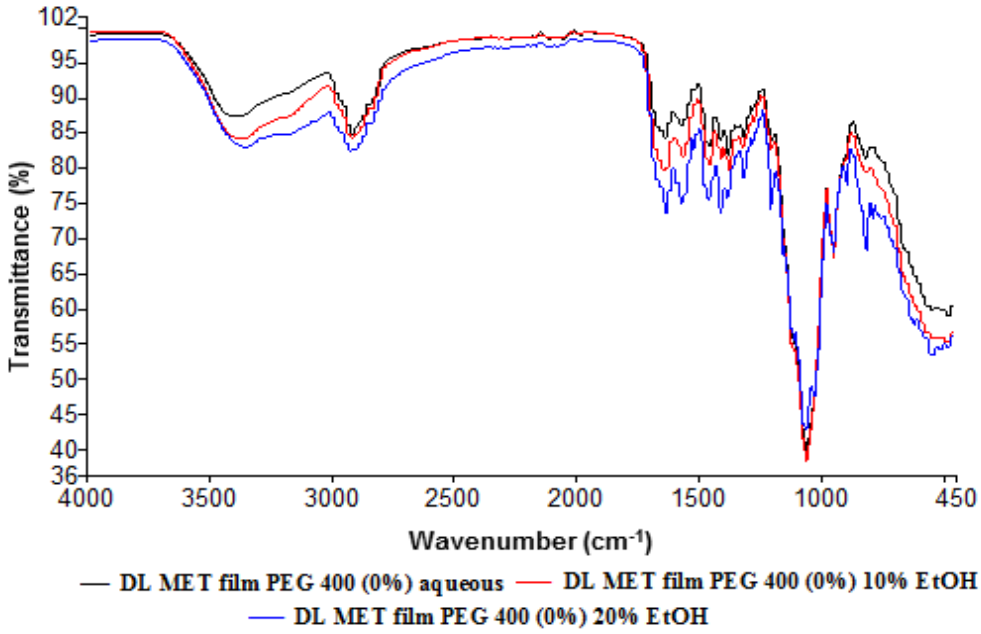

Figure 3.29 FT-IR spectra of DL MET films cast from aqueous and ethanolic (10% and 20% v/v EtOH) polymeric gels containing 0.0% w/w PEG 400 and OME: L-arg (1:1)

Table 3.11 Major FTIR peaks of interests for DL MET films unplasticised from (OME: L-arg 1:1)

Peak No.	(cm-1)	(%T)	Peak No.	(cm-1)	(%T)	Peak No.	(cm-1)	(%T)
				Aqueous				
1	3392.33	87.94	2	2917.97	85.43	3	1633.56	84.81
4	1453.45	83.50	5	1374.65	82.49	6	1054.36	39.39
7	945.48	67.48						
				10% EtOH				
1	3375.78	84.49	2	2920.08	84.49	3	1633.99	79.80
4	1454.17	80.60	5	1374.83	79.89	6	1054.54	37.91
7	945.62	67.30						
				20% EtOH				
1	3355.64	83.25	2	2932.86	82.75	3	1627.19	73.78
4	1454.69	75.59	5	1310.65	78.79	6	1058.84	42.37
7	946.16	68.13						

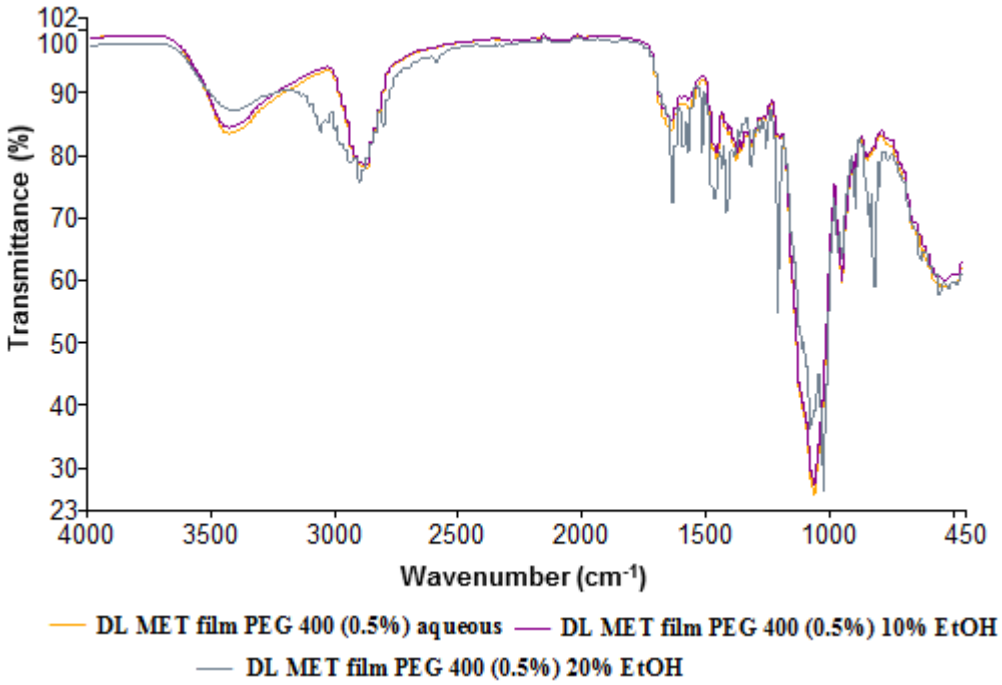

Figure 3.30 FT-IR spectra of DL MET films cast from aqueous and ethanolic (10% and 20% v/v EtOH) polymeric gels containing 0.5% w/w PEG 400 and OME: L-arg (1:1)

Table 3.12 Major FTIR peaks of interests for DL MET films plasticised from (OME: L-arg 1:1)

Peak No.	(cm-1)	(%T)	Peak No.	(cm-1)	(%T)	Peak No.	(cm-1)	(%T)
				Aqueous				
1	3435.63	84.12	2	2877.39	78.23	3	1639.18	84.73
4	1453.97	80.01	5	1373.16	79.64	6	1056.79	25.2
7	945.23	59.54						
				10% EtOH				
1	3437.24	85.09	2	2876.75	78.87	3	1634.45	86.12
4	1454.38	80.9	5	1373.22	80.67	6	1057.39	26.94
7	945.31	60.42						
				20% EtOH				
1	3437.24	85.09	2	2904.58	75.9	3	1627.85	72.54
4	1460.74	73.13	5	1311.49	78.45	6	1012.41	26.1
7	944.62	63.51						

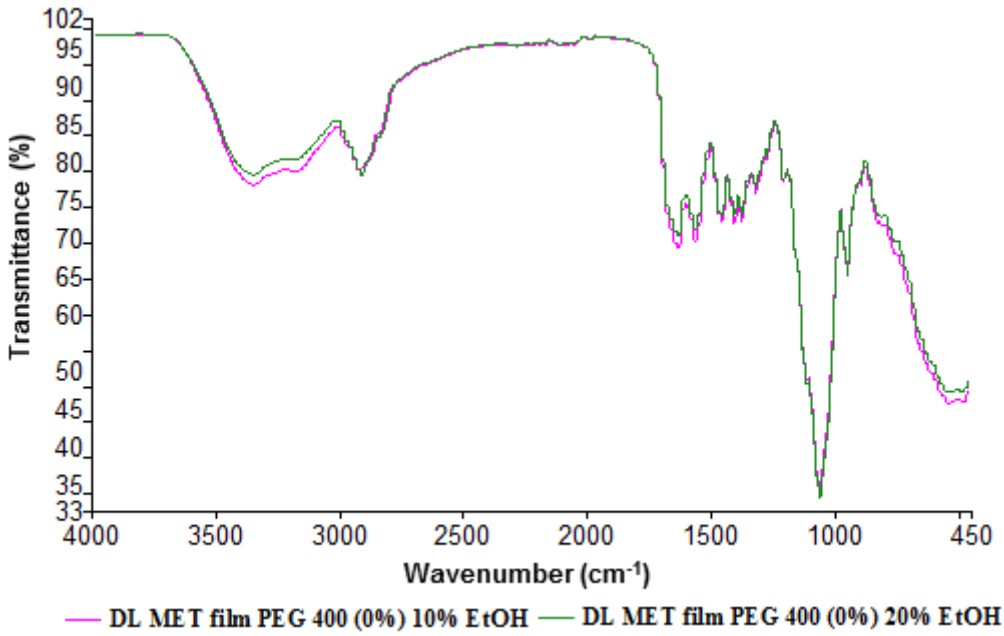

Figure 3.31 FT-IR spectra of DL MET films cast from ethanolic (10% and 20% v/v EtOH) gels containing 0.0% w/w PEG 400 and OME: L-arg (1:2)

Table 3.13 Major FTIR peaks of interests for unplasticised DL MET films containing (OME: L-arg 1:2)

Peak No.	**(cm-1)**	**(%T)**	**Peak No.**	**(cm-1)**	**(%T)**	**Peak No.**	**(cm-1)**	**(%T)**
				10% EtOH				
1	3356.36	78.42	2	2932.39	80.64	3	1633.41	69.56
4	1557.58	70.49	5	1453.94	73.39	6	1404.66	73.08
7	1055.69	35.17	8	945.97	66.13			
				20% EtOH				
1	3356.07	79.86	2	2917.84	79.80	3	1633.70	71.16
4	1557.76	72.18	5	1454.41	74.11	6	1375.29	74.11
7	1055.14	34.32	8	945.95	65.61			

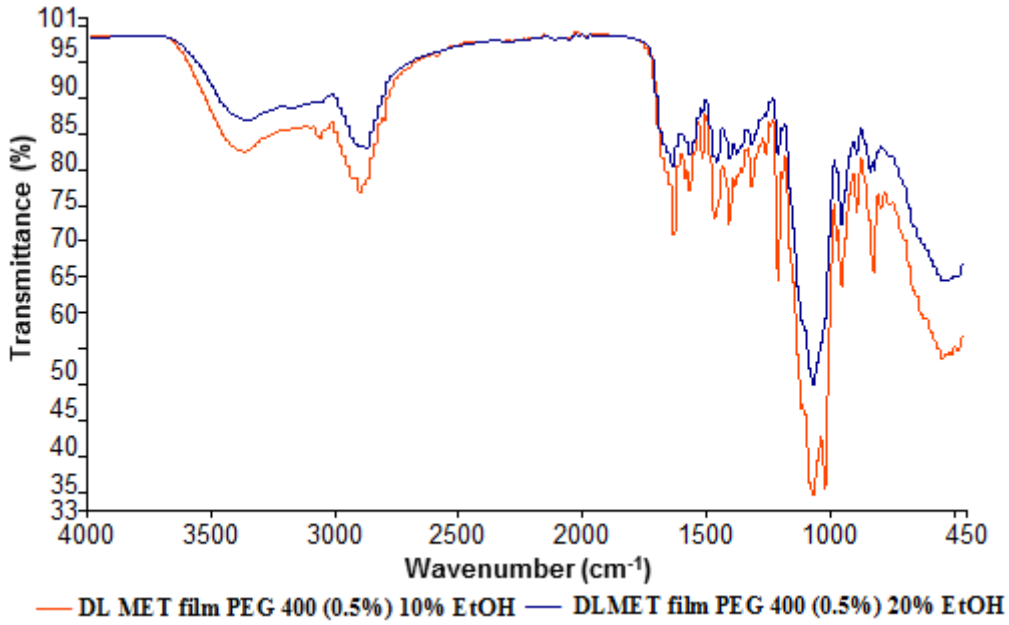

Figure 3.32 FT-IR spectra of DL MET films cast from ethanolic (10% and 20% v/v EtOH) gels containing 0.5% w/w PEG 400 and OME: L-arg (1:2)

Table 3.14 Major FTIR peaks of interests for plasticised DL MET films (OME: L-arg 1:2)

Peak No.	**(cm-1)**	**(%T)**	**Peak No.**	**(cm-1)**	**(%T)**	**Peak No.**	**(cm-1)**	**(%T)**
				10% EtOH				
1	3432.23	83.20	2	2904.61	76.72	3	1627.92	70.97
4	1566.93	76.99	5	1408.98	72.24	6	1204.06	64.53
7	1060.49	34.25	8	945.11	63.70			
				20% EtOH				
1	3436.11	87.32	2	2877.31	83.30	3	1628.42	80.65
4	1554.01	81.28	5	1406.59	81.93	6	1204.25	82.33
7	1059.40	49.64	8	945.33	72.55			

3.3.9 Assay/drug content of OME in films

Table 3.15: Assayed drug content in OME films

Drug loaded films (MET)	% Drug content
Aqueous 1:1 0.0% w/w PEG	51±0.5
10% EtOH 1:1 0.0% w/w PEG	83±1.2
20% EtOH 1:1 0.0% w/w PEG	92±1.1
10% EtOH 1:1 0.5% w/w PEG	71±0.4
20% EtOH 1:1 0.5% w/w PEG	77±1.1
Aqueous 1:2 0.0% w/w PEG	67±0.3
10% EtOH 1:2 0.0% w/w PEG	87±0.5
20% EtOH 1:2 0.0% w/w PEG	86±2.0
10% EtOH 1:2 0.5% w/w PEG	90±0.5
20% EtOH 1:2 0.5% w/w PEG	92 ±0.4

3.4 SUMMARY

OME is a common antiulcerative drug that has been extensively used to control acid disorders by inhibiting the acid gastric secretion by blocking the H^+/K^+ ATPase pump. OME formulations present pharmaceutical drawbacks related to the physico-chemical instability to heat, light, moisture and acidic conditions. Mathew (1995) reported that the degradation of OME is acid catalyzed and is very stable at high (alkaline) pH. Other investigators have observed a degradation of OME when exposed to various salts (phosphate buffer, calcium carbonate, sodium bicarbonate and sodium chloride) and metal ions (Zn(II), Cu(II) and Co(II)) (El-Badry et al., 2009). In addition, the low aqueous solubility of OME is responsible for low dissolution rates and poor bioavailability (Toledo et al., 2006).

The main goal of the complexation procedure with L-arg was to improve the biopharmaceutical properties of OME due to its well known poor water solubility and stability as outlined above. In this study L-arg was incorporated as a second component in the formation of inclusion complexes because L-arg plays an important role in the increase of the solubility and stability of free OME molecules. This is mainly attributed to the L-arg, which forms hydrogen bonds with drug (H atom of L-arg to the N atom of OME), resulting in a

significant desolvation of OME molecules. Furthermore, it is reported that two of the most important preformulation parameters in drug formulation development are solubility and stability, to ensure better bioavailability. The combination of L-arg was observed to help achieve this purpose purpose (Figueiras et al., 2010) and this was confirmed in the current study.

SA films were rejected due to poor transparency, difficulty of peeling and low flexibility. MET DL film (OME: L-arg 1:2, 20% EtOH, 0.5% w/w PEG 400) were chosen for further characterisation based on tensile properties (tensile strength (toughness), elongation at break/elastic modulus (flexibility)) (Dixit & Puthli, 2009) (Garsuch, 2009). Also SA DL films were brittle which may be due to the presence of high guluronic acid side chains which could not dissipate stresses generated during the formation of the solvent cast film after drug loading, resulting in small volumes between polymeric chains which resulted in brittleness (Boateng et al., 2009).

DSC, SEM and XRD all confirmed the amorphous nature of MET DL film (OME: L-arg 1:2). As noted in the previous chapter, an amorphous DL film is expected to be advantageous in terms of better solubility; however, it is associated with stability challenges, which needs to be further, investigated. Further, XRD can be employed to monitor re-crystallization of amorphous material and this technique would be to characterize the extent of crystallinity during storage over the intended shelf life of the drug product to certify safety and efficacy (Ivanisevic et al., 2010). In addition, the other functional characteristics such as swelling capacity is also affected by amorphous nature, as it absorbs more dissolution medium and thus the diffusion and eventual release of the drug can be accelerated.

The results shown in table 3.9 demonstrated the different DL MET films (Different OME:L-arg ratio) have similar water content as L-arg. Further, their degradation points decreased in comparison to the original compounds demonstrating the effect of the formulation process in changing the physico-chemical properties of the starting materials due to interactions between the various components (Stephenson et al., 2001). L-arg shows high water content due to hydrogen bond formation allowing it to attracts more water via these weak bonds

Co-crystals formation has not been reported in previous literature for L-arg and OME. The reason co-crystal method is important is because most new drugs that are discovered are extremely difficult to develop into viable dosage forms due to their inherently poor physico-chemical properties. Many of these drugs are poorly soluble and therefore the active

ingredient is difficult to dissolve, for example in the gastrointestinal fluids which limits its ability to be transferred into the body by absorption and eventually bioavailability. A co-crystal is a new crystalline structure produced from two materials, which is a solid at room temperature. One of the methods that could be used to form co-crystal is by dissolving the two co-formers (in this case OME and L-arg) in a solvent and precipting out the co-crystals, or grinding the two together with a small amount of solvent to form a physical mixture of the two co-formers (OME and L-arg)(Paradkar et al., 2015). This will be an interesting study to undertake and will be considered as future work.

3.5 CONCLUSION

Based on the visual observations and the expected characteristics for an ideal film in terms of flexibility, uniformity and transparency, films prepared from ethanolic gels (20% v/v EtOH) containing 1:2 ratio of OME: L-arg and 0.5% w/w PEG400 was the most appropriate for further investigations. These were confirmed by the analytical characterisation studies which also showed that the OME originally added in crystalline form was molecularly dispersed within the film matrix and therefore amorphous in nature. It was also obvious that the addition of L-arg helped to stabilise the drug within the films, which showed desired homogeneity, transparency and uniform drug distribution.

CHAPTER FOUR: HYDRATION, *IN-VITRO* MUCOADHESION AND DRUG STABILITY STUDIES OF OME LOADED MET FILMS

4.1 INTRODUCTION

An effective buccal dosage form is required to possess certain functional properties including bioadhesion. Recent studies have shown that there are three known mechanisms responsible in for bioadhesion bio adhesive bonds are not fully known. The process involves wetting and swelling of polymer, interpenetration between the polymer chains and the mucosal membrane and formation of the chemical bonds between the entangled chains and mucin (Palacio et al,, 2012). Hydration which is commonly referred to as swelling, is the process that occur mainly when polymers such as (MET) spreads over the surface of a mucosal membrane in order to produce direct contact with the membrane. Bio adhesives have the capacities to adhere /bond to the mucous membrane and this process occurs due to the help of the surface tension and forces that exist at the site of contact. Swelling of polymers occurs because the intracellular component situated within the polymers has an affinity for water.

The term "mucoadhesive" is defined as the ability of materials that bind to mucous layer of a biological membrane (Tiloo et al, 2011). Shikaret al (2012) "stated that since the early 1980s the concept of mucoadhesion has already gained great deals of interest in pharmaceutical technology". Mucoadhesion has gained such interest because of the various well established advantages associated with this concept. For example it prolongs the residence time of the dosage form at the site of applications. This concept provides a tightly controlled release of drugs which will therefore improve the therapeutic outcome in many cases such vesiculo bullous disease. It has been proven it this article that mucoadhesive concept is of great advantages of accessibility and it has been well accepted for the administration of drugs in chronic disease. The concept of this drug deliver gives facility to include a permeation enhancer in the formation in designing multidirectional or unidirectional release system for local and systemic action (Roy et al, 2009).

There are several approaches used to assess the mucoadhesive performance of polymers and polymeric dosage forms (Ayensu et al., 2012). These include texture analyser and rheometric measurements. The texture analyser technique (TA) assesses the stickiness, the total work of adhesion (TWA) and the cohesiveness of the dosage forms. Stickiness is described as the

maximum force required to separate the probe attached to films from the mucosal substrate whereas, the total amount of work or energy implicated in the probe withdrawal from the substrate is calculated from the area under the forces versus distance curve and cohesiveness is defined as the intermolecular attraction between the substrate and formulation, this is determined by the travel distance in mm on the force against distance profile (Thirawong et al., 2007).

Although drug content is a crucial stability indicating parameter, the method of determination must also be able to identify and quantify possible degradation products in order to assure safety and efficacy. According to the International Committee for Harmonisation (ICH) (2003) QA1, recommendations, "stability studies must include testing of those attributes of the drug substance that are likely to change during storage and are likely to affect quality, safety and efficacy. These may include physical, chemical, biological and microbiological attributes, using validated stability indicating analytical procedures".

In this chapter, the functional characteristics (swelling and mucoadhesion) of different optimised films prepared previously using MET have been investigated as well as stability of DL films. The effect of different formulation variables on the hydration and mucoadhesive properties were determined as part of further optimization to select the best formulation to be taken forward for *in vitro* drug dissolution and permeation studies.

4.2 MATERIALS AND METHODS

4.2.1 Materials

Table 4.1 List of materials used

Materials	**Batch number**	**Purity**	**Suppliers**
Potassium dihydrogen phosphate	073346	100%	Fisher Scientific (Leicester, UK)
Sodium hydroxide	1152687	98%	Fisher Scientific (Leicester, UK)
Sodium Chloride	7647-14-5	-	Fisher Scientific (Leicester, UK)
Sodium phosphate dibasic	1204925	99%	Fisher Scientific (Leicester, UK)
Gelatine	1411655	-	Sigma-Aldrich (Gillingham, UK)

4.2.2 Instruments

Table 4.2 List of instruments

Instruments	Suppliers
TA HD plus texture analyser	Stable Micro System Ltd, Surry, UK

4.2.3 Methods

4.2.3.1 Hydration capacities

The hydration (swelling) capacities of the formulated (BLK and DL films with drug (OME) and stabiliser (L-arg) were determined by incubating the samples in 10 mL of 0.01M PBS solution (pH 6.8 ± 0.1 simulating salivary pH) and simulated saliva (SS) (pH 6.8 ± 0.1) and both set at 37 ± 0.1°C. The buffer solution was prepared by dissolving 6.8 g of potassium dihydrogen phosphate in 1L of deionised water and adjusting the pH to 6.8 using sodium hydroxide (NaOH). SS solution was prepared by dissolving potassium dihydrogen phosphate (0.19 g), sodium chloride (8.0 g) and sodium phosphate dibasic (2.382 g) in 1L of deionised water and adjusting the pH to 6.8 using phosphoric acid. The films were cut into 2 × 2 cm. The films were placed into small Petri-dish containing10 mL of the media (PBS or SS) and initially weighed. At predetermined time intervals of 5 minutes the liquid media was removed using a syringe and weighed again. Before the films were weighed excess buffer solution was blotted off with tissue. After a weight had been recorded, 10 mL of fresh buffer solution was placed back in the Petri dish using a syringe. These studies were performed in triplicate (n = 3) for each set of formulated samples and average values were calculated for data analyses. The % swelling capacity index was calculated using the equation below:

$$Swelling\ Index(\%) = \frac{Ws - W}{W} \times 100 \quad \text{Equation 4.1}$$

Where *W*s is the weight of the film before hydration and *W*is the initial weight of the film after hydration.

4.2.3.2 Mucoadhesion

The *in vitro* mucoadhesion experiments were performed BLK and DL films with a TA HD plus Texture Analyser (Stable Micro Systems, Surrey, UK) fitted with a 5 kg load cell. The film was attached to an adhesive rig probe (75 mm diameter) with double sided adhesive tape. An 88 mm diameter Petri dish was used containing 20 g of gelatine solution (6.67% w/w) allowed to set as a solid gel and the surface of the gel was equilibrated with 0.5 mL of SS (pH 6.8) and PBS (pH 6.8) to represent the buccal mucosal and saliva conditions (Boateng et al., 2013). The film was positioned in contact with the gelatine gel for 60 seconds to provide optimal contact. The probe was set to approach the model buccal mucosal surface with set parameters for adhesivity as shown in table 4.3, allowing 60s for complete contact and hydration before being detached.

Texture Exponent 32 software was used to record and process the data. The peak adhesive force (PAF) required to separate the film from the mucosal surface was determined by the maximum force. The area under the curve (AUC) representing the total work of adhesion (TWA) was estimated from the force-distance plot whiles the cohesiveness of the sample was determined by the distance of travel as shown in figure 4.1b

Table 4.3 Texture analyser settings for determining the peak adhesive force (PAF), total work of adhesion (TWA) and cohesiveness of formulation.

Parameters	TA settings
Pre-test speed	0.5 mm/sec
Test speed	0.5 mm/sec
Post-test speed	1.0 mm/sec
Applied force	1.00 N
Return distance	10.0 mm
Contact time	60.0 sec
Trigger type	Auto
Trigger force	0.05 N

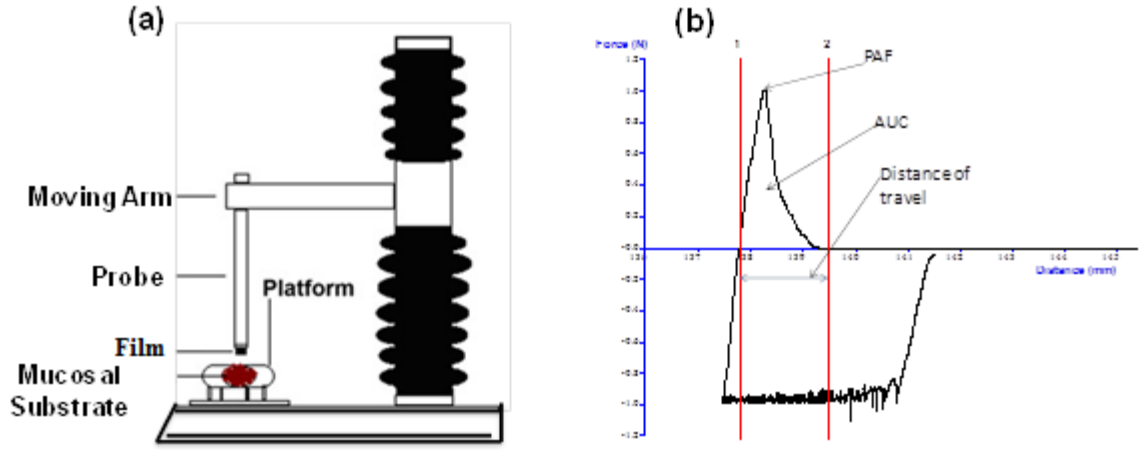

Figure 4.1 (a) Displays schematic of texture analyser with xerogel attached to the probe and the mucosal substrate on the platform (b) Typical texture analysis force-distance plot.

4.2.3.3 Drug stability

Drug stability of MET DL films with OME and stabiliser (L-arg) were determined by high performance liquid chromatography (HPLC). An Agilent1200 HPLC equipped with auto sampler (Agilent Technology, Cheshire, UK) with Chemstation® software program was used to determine the amount of drug present in the films after storing under two sets of conditions. Samples were placed in humidity controlled desiccators and placed in an oven (40°C) and the other at room temperature (ambient). The stability was studied for 3 months (Appendix C shows the HPLC stability chromatograms).

MET DL film (OME: L-arg 1:2, PEG 400 (0.5% w/w), 20% v/v EtOH) was placed in the desiccators and wrapped with aluminium foil due to its light sensitivity. The films were also wrapped in paraffin film to prevent moisture absorption by MET.

For HPLC analysis, the samples were weighed (5mg) and dissolved using 0.01M PBS solution (pH 6.8 ± 0.1 simulating salivary pH) in volumetric flasks (10 mL). 1 mL of the sample from each flask was taken and placed in HPLC vials to be measured. The column used for analysis was Hypersil™ ODS C18 HPLC columns, 5µm particle size (250 x 4.6 mm) (Thermo Scientific, Hampshire UK). The mobile phase consisted of a mixture of ammonium acetate and acetonitrile in the ratio of 60:40 v/v. The flow rate of the mobile

phase was maintained at 2 mL/min and diode array UV detector wavelength for OME was set at 302 nm; 20 µl volumes were injected during each run, respectively.

4.2.3.4 Statistical data analysis

Statistical data analysis was performed to compare hydration and mucoadhesion results using two tailed student t-test with 95 % confidence interval (p-value < 0.05) as the minimal level of significance. All the results were performed in triplicates for all experiments with mean and standard deviation. The pairs of data evaluated included the following;

- Unplasticised *vs* plasticised
- BLK *vs* DL films
- PBS *vs* SS hydration of films.

4.3 RESULTS AND DISCUSION

4.3.1 Hydration capacity

The hydration (swelling) capacity of mucosal formulations such as solvent cast films plays an important role for functional properties such as uniform and prolonged release of the drug and effective mucoadhesion via buccal route of administration which could be achieved by using a delivery system where swelling is the controlling mechanism for drug release. Two media were used (PBS and SS) in both plasticised and unplasticised films. Figures 4.2 to 4.5 show the data from the swelling index test for the films cast from aqueous and ethanolic (10% and 20% v/v EtOH) gels with and without PEG 400, L-arg and OME in different ratios of drug and stabiliser. By observing all data/profile from the data it is very clear that film percentage swelling index increased with time.

All the prepared films using different solvent as mention above films were able to maintain their structural integrity at the beginning of the experiment, but after 20 min they started losing their integrity, which is because of excessive absorption of water molecules. Significant differences were observed between unplasticised films and plasticised films (0.5% w/w PEG), drug and stabiliser. DL films dissolved in the buffer solution (pH 6.8) within the first 5 minutes whereas plasticised films with were not dissolved but instead absorbed water. From figures 4.2 to 4.5, it can be observed that plasticised MET DL films have higher swelling index when compared to unplasticised MET DL films. Comparing the swelling index together the films prepared from aqueous gels is not as good due to brittleness as ethanolic (10% and 20% v/v EtOH) films with different ratios of 1:1 and 1:2. With EtOH gels, the resulting films showed faster hydration in the first five minutes, after which they showed steady hydration at constant rate until they lost their integrity.

The initial contact of the films with buffer causes a gel like structure to form in films without PEG 400, and this mechanism was not observed in plasticised films. Plasticiser increases the space between the molecules/polymeric chain which allows more water to occupy the area between those spaces (Roy et al, 2009). There were differences in the hydration capacities between films cast from aqueous, ethanolic 10% and 20% v/v EtOH gels, whilst films containing OME and L-arg with ratios of 1:1 and 1:2 of aqueous films showed lower swelling

index 1542 – 1841 % and 1444 – 1981 % statistically significant (p = 0.0025). On other hand, swelling index for ethanolic films with 10% and 20% is almost similar for both 1:1 and 1:2 of OME: L-arg.

Data observed from figure 4.6, which demonstrates MET DL film containing 0.5% w/w PEG 400, OME, L-Arg 1:2 ratios in ethanolic (20% EtOH) and SS pH 6.8 showed lower swelling index compared to PBS pH 6.8 extremely statistically significant (p = 0.0001). This may be due to the difference in ionic strength of the media which plays an important role in affecting the swelling of MET films. The effect of ionic strength and pH on the swelling polymer has been described by Park and Robinson (Peh and Wong, 1999). The results recorded from SS showed similarities to the results discussed by Park and Robinson.

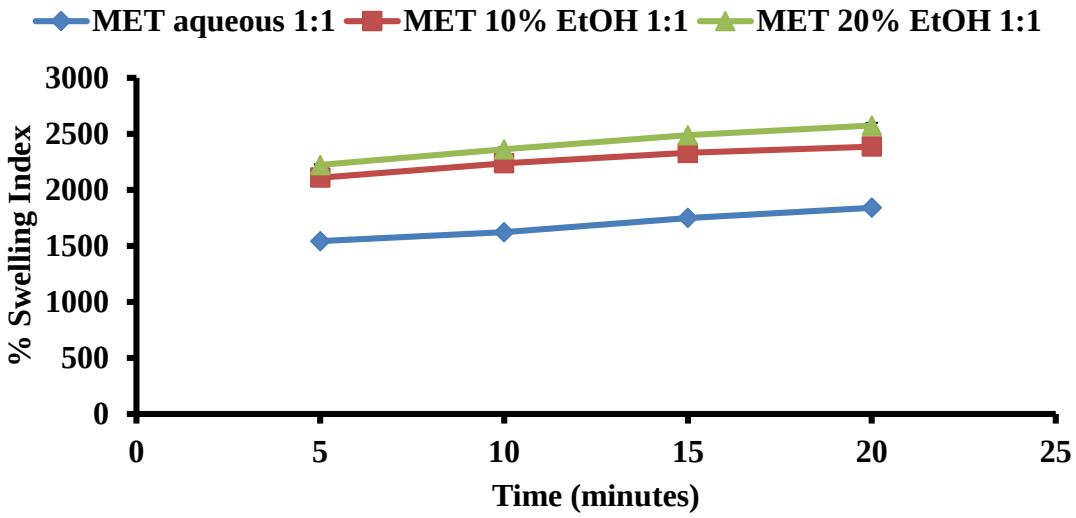

Figure 4.2 Swelling profiles of unplasticised MET DL films cast from aqueous and ethanolic (10% and 20% v/v EtOH) gels containing OME:L-Arg 1:1 in PBS pH 6.8 (mean ± SD,(n=3))

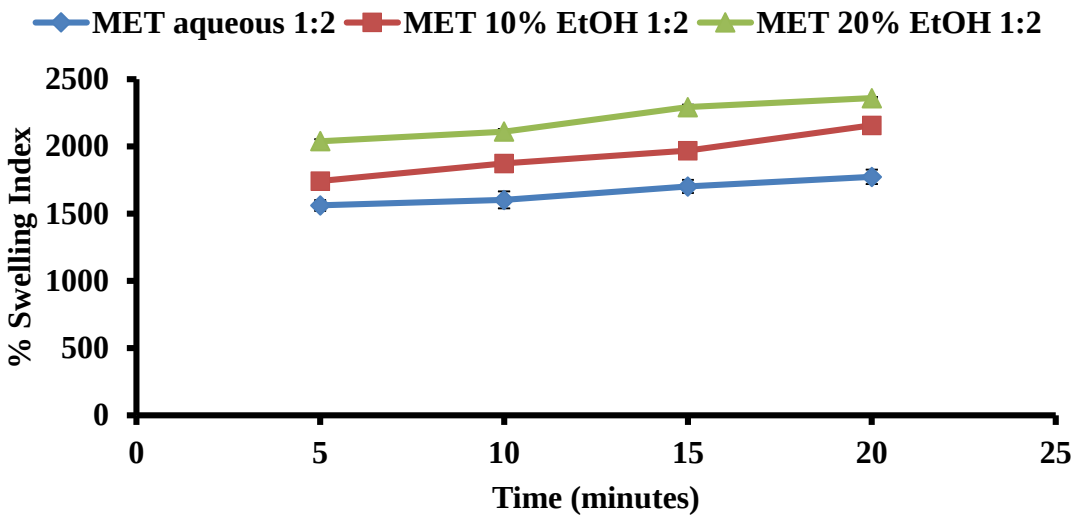

Figure 4.3 Swelling profiles of unplasticised MET DL films from aqueous and ethanolic (10% and 20% v/v EtOH) gels containing OME: L-Arg 1:2 in PB pH 6.8 (mean ± SD, (n=3))

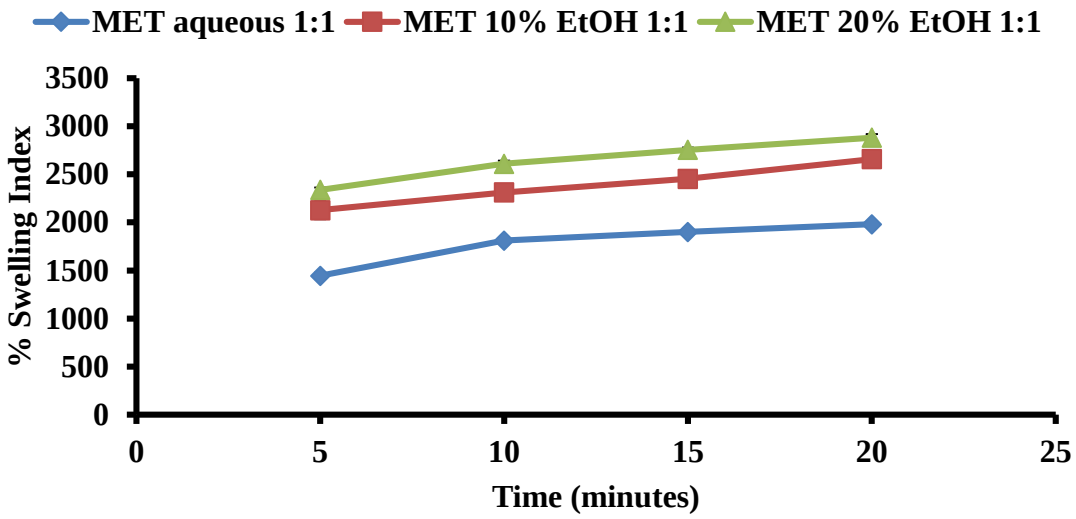

Figure 4.4 Swelling profiles of plasticised MET DL films from aqueous and ethanolic (10% and 20% EtOH) gels containing 0.5% w/w PEG 400 and OME: L-Arg 1:1 in PBS pH 6.8 (mean ± SD, (n=3))

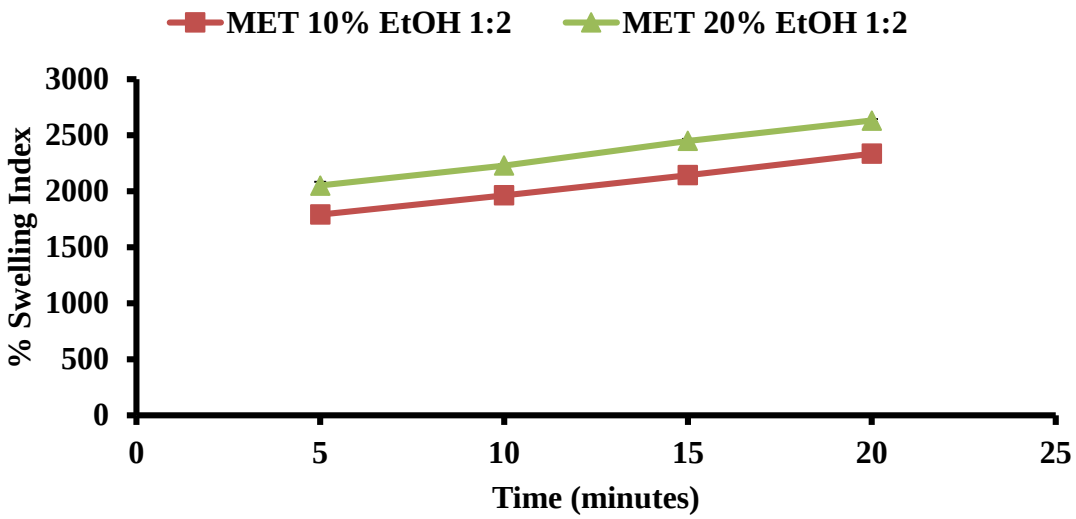

Figure 4.5 Swelling profiles of plasticised MET DL films cast from ethanolic (10% and 20% EtOH) gels containing 0.5% w/w PEG 400 and OME: L-Arg 1:2 in PBS pH 6.8 (mean ± SD, (n=3))

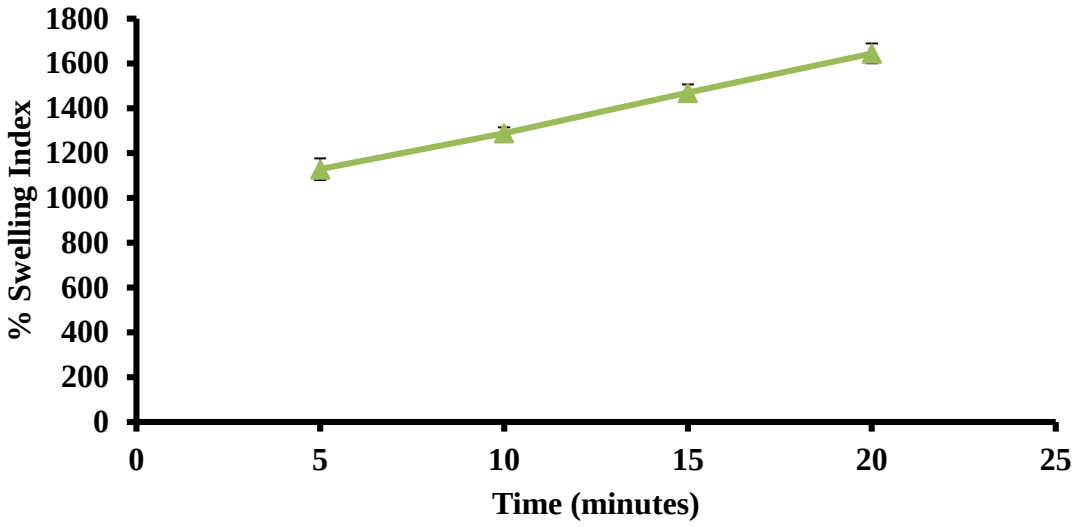

Figure 4.6 Swelling profiles of plasticised MET DL films cast from ethanolic (20% EtOH) gel containing 0.5% w/w PEG 400 and OME: L-Arg 1:2 in SS pH 6.8 (mean ± SD,(n=3))

4.3.2 Mucoadhesion

In-vitro mucoadhesion studies were performed to predict the stickiness and attraction between the films and mucosal substrate which was represented by gelatine. Unplasticised BLK MET films showed higher values in comparison to the plasticised BLK MET films from

aqueous and ethanolic (10% and 20% v/v) gels as shown in figures 4.7 and 4.8. BLK films containing unplasticised in aqueous gels showed low significant difference (P = 0.88) for all three mucoadhesive parameters PAF, TWA and cohesiveness compared to EtOH 10%, were PAF and TWA was not significant difference (P = 0.83) and for cohesiveness it was not significant difference (P = 0.55). However, films cast from ethanolic 20% gels showed no significant difference for all the data points (p = 1.00).

Figures 4.9 to 4.13 shows the mucoadhesive profiles of the various formulations tested in this chapter. The data showed a slight increase in PAF for unplasticised films containing OME: L-arg 1:1 compared to the corresponding plasticised formulations obtained from gels prepared using the three different solvents (water, 10% v/v EtOH, 20% v/v EtOH) with p values of 0.0612, 0.4671 and 0.4210 respectively between the three solvents for each film being compared. In addition, the TWA values for the above formulations compared were not significantly different (p = 0.8185, 0.4971, 0.4942 respectively) as well as cohesiveness values (p = 0.5951, 0.0642, 0.5628 respectively).

Figure 4.12 shows that there was no difference between plasticised films obtained from aqueous gels compared to figure 4.11 unplasticised films. The data showed slight increase in PAF for plasticised films containing OME: L-arg 1:2 compared to the corresponding unplasticised formulations obtained from gels prepared using the three different solvents (10% v/v EtOH, 20% v/v EtOH) with p values of 0.2923, 0.2203 respectively for the different solvents used to prepare each film being compared. In addition, the TWA values for the above formulations compared were not significantly different (p = 0.2117, 0.1700 respectively) and as well as cohesiveness values (p = 0.5479, 0.0456 respectively).

The mucoadhesive data obtained from equilibrating gelatine with SS pH 6.8 (figure 4.13) for plasticised MET DL film (OME: L-Arg 1:2) prepared from ethanolic (20% v/v EtOH) gels showed low PAF, TWA and cohesiveness compared to when gelatine was equilibrated with PBS pH 6.8. Once again this may be due to the difference in ionic strength of the media as observed during the hydration (swelling) study.

The films prepared from 20% v/v EtOH gel provided more stable mucoadhesion properties (PAF, TWA and cohesiveness) in all experiments carried out and demonstrate a high detachment force leading to the strong interaction between polymeric chains and the mucosa

surface. A slight difference was observed between its mean compared to TWA of films prepared from 10 % v/v ethanolic gels. Analysing the data a close trend was observed in PAF but slight increase in the cohesiveness. The addition of L-arg is a possible factor that could have created larger pores spaces within the polymers which facilitate the process of water ingress and therefore enhanced the initial hydration which plays a role in the mechanism of mucoadhesion as discussion in chapter 1.

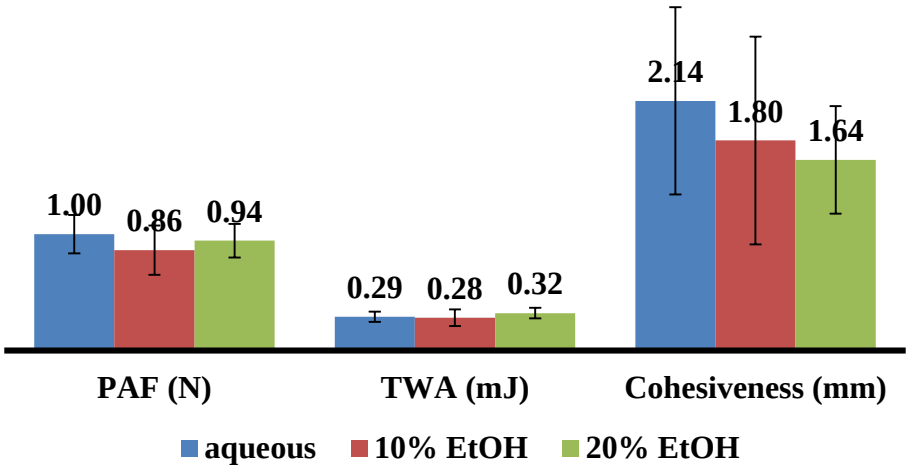

Figure 4.7 *In-vitro* mucoadhesion measurements (PAF, TWA and cohesiveness) of unplasticised BLK MET film cast from different gels (aqueous and ethanolic (10% and 20% v/v EtOH)) using mucosal substrate equilibrated with PBS (pH 6.8) of (mean ± SD, (n=3))

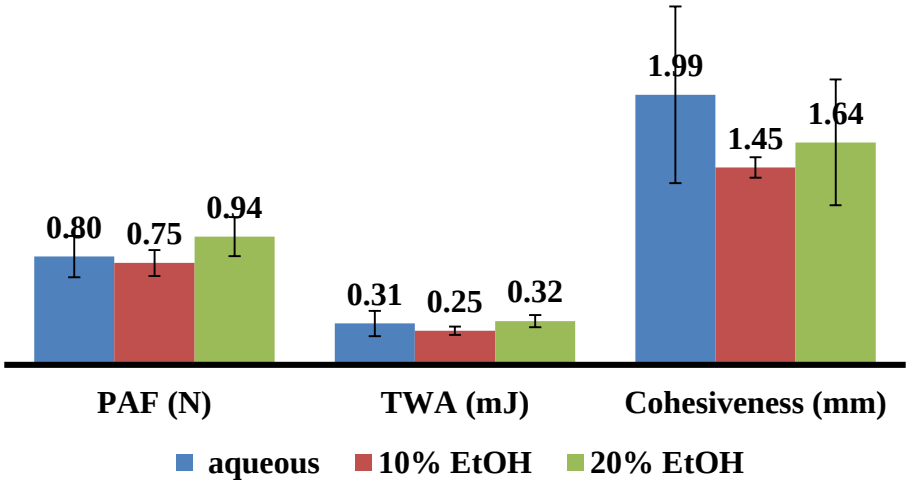

Figure 4.8 *In-vitro* mucoadhesion measurements (PAF, TWA and cohesiveness) of plasticised BLK MET film cast from different gels (aqueous and ethanolic (10% and 20% v/v EtOH)) using mucosal substrate equilibrated with PBS (pH 6.8) of (mean ± SD, (n=3))

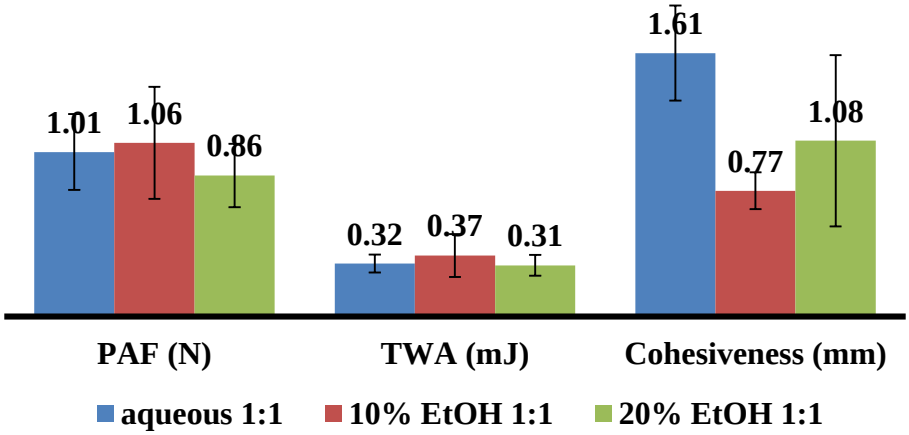

Figure 4.9 *In-vitro* mucoadhesion measurements (PAF, TWA and cohesiveness) of unplasticised DL MET film cast from different gels (aqueous and ethanolic (10% and 20% v/v EtOH)) containing OME:L-arg 1:1 using mucosal substrate equilibrated with PBS (pH 6.8) of (mean ± SD, (n=3))

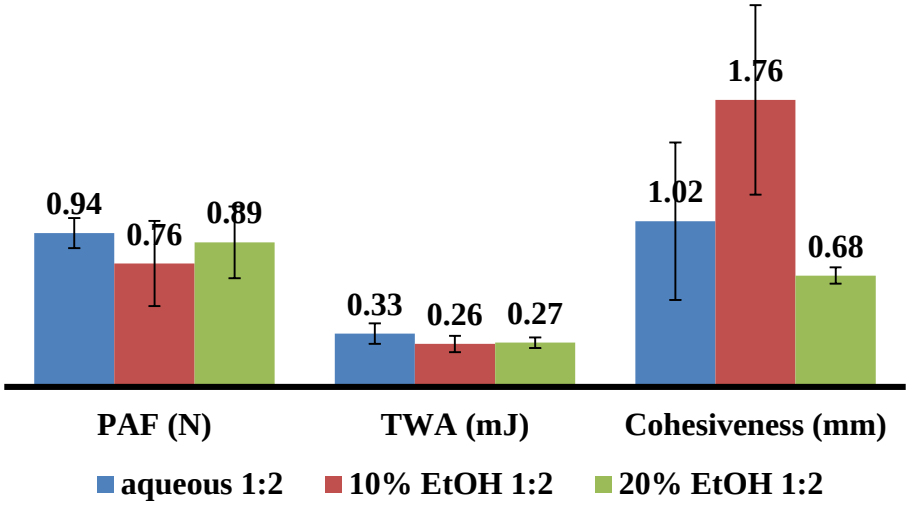

Figure 4.10 *In-vitro* mucoadhesion measurements (PAF, TWA and cohesiveness) of unplasticised DL MET film cast from different gels (aqueous and ethanolic (10% and 20% v/v EtOH)) containing OME:L-arg 1:2 using mucosal substrate equilibrated with PBS (pH 6.8) of (mean ± SD, (n=3))

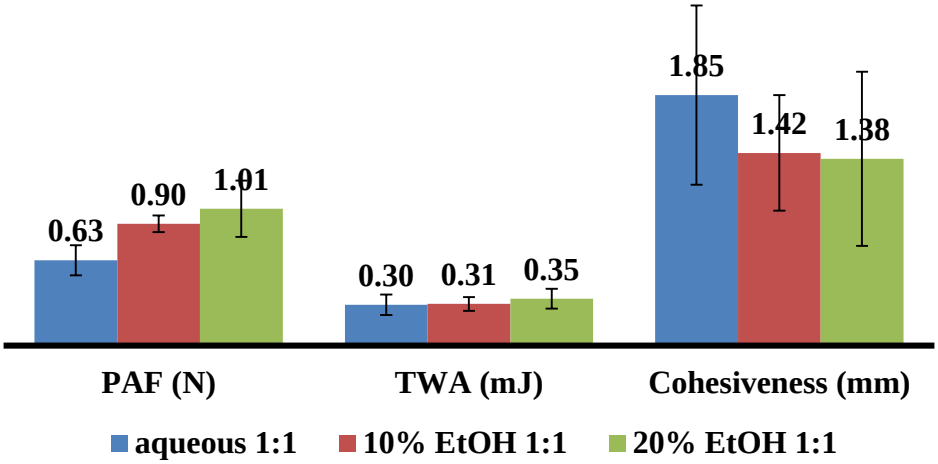

Figure 4.11 *In-vitro* mucoadhesion profiles (PAF, TWA and cohesiveness) of plasticised DL MET film cast from gels (aqueous and ethanolic (10% and 20% v/v EtOH)) containing OME: L-arg 1:1 on gelatine equilibrated with PBS (pH 6.8) of (mean ± SD, (n=3))

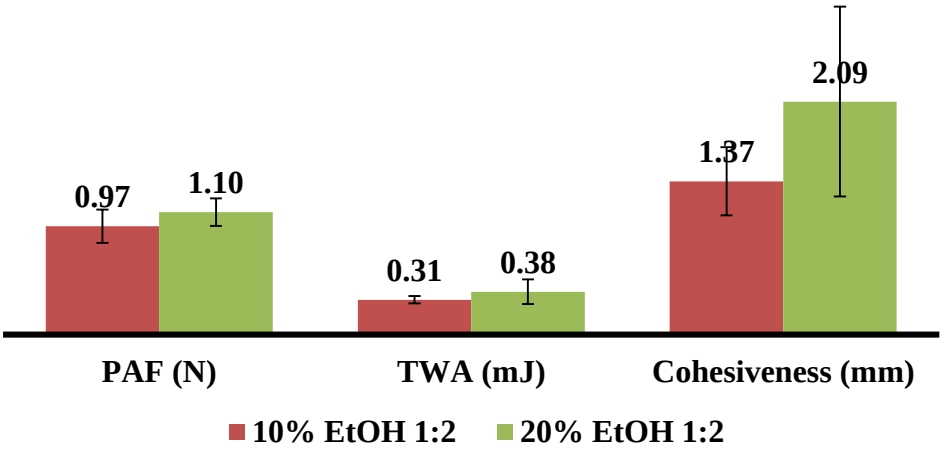

Figure 4.12 *In-vitro* mucoadhesion profiles (PAF, TWA and cohesiveness) of plasticised DL MET film cast from gels (10% and 20% v/v EtOH) containing OME: L-arg 1:2 on gelatine equilibrated with PBS (pH 6.8) of (mean ± SD, (n=3)

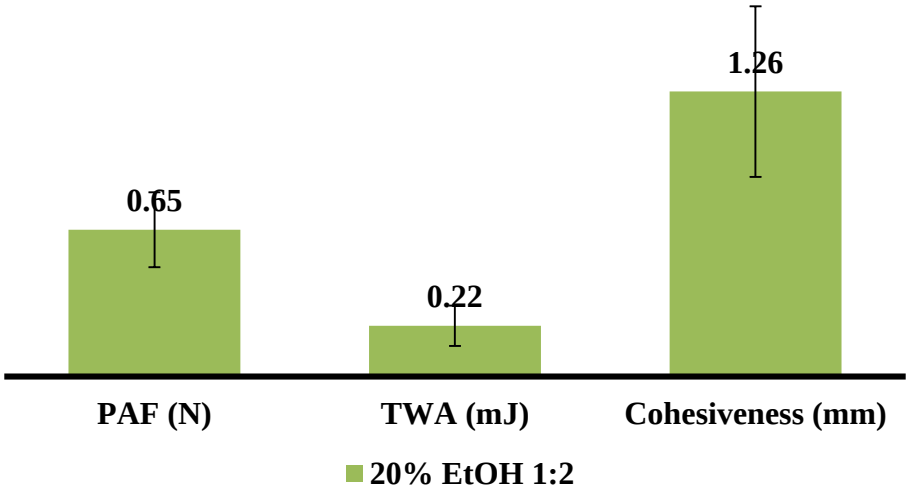

Figure 4.13 *In-vitro* mucoadhesion measurements (PAF, TWA and cohesiveness) of plasticised DL MET film cast from ethanolic (20% v/v EtOH) gel containing OME:L-arg 1:2 using mucosal substrate equilibrated with SS (pH 6.8) of (mean ± SD, (n=3))

4.3.3 Statistical data analysis

- BLK vs DL

  BLK film recorded higher values (PAF, TWA and cohesiveness) compared to DL films.

- Aqueous vs EtOH 10 % v/v and 20% v/v

  Films prepared with aqueous gels showed higher values (PAF, TWA and cohesiveness) compared to 10% and 20% EtOH gels.

- Plasticised vs unplasticised

  Plasticised film overall showed higher values than unplasticised films.

- OME:L-arg 1:1 VS OME:L-arg 1:2

  Films containing OME:L-arg 1:1 and OME:L-arg 1:2 did not show much difference in the mucoadhesive values (PAF, TWA and cohesiveness).

4.3.4 Drug stability

Short-term stability studies were performed for MET DL film (OME: L-arg 1:2, PEG 400 (0.5% w/w), 20% v/v EtOH) and exposed to two conditions 40ºC (± 0.5 ºC) and 20ºC ± 0.5ºC) (ICH guidelines) for a period of three months and the results are shown in figure 4.14 . The results of the stability study reveal that there was statistically significant (p = 0.0853) difference in the drug loss (%) between the films kept in the oven and ambient conditions. In the first 14 days the percentage of OME remaining at 40ºC was 87% compared to 80% at room temperature and after 28 days the % drug content was 82% 28% at 40 ºC and 62% at room temperature which was quite unexpected. However, the % drug content after 84 days remained constant at room temperature whilst the % content decreased to 47% at 40 ºC. These finding suggest that films are relatively more stable in room temperature (ambient ± 0.5 ºC) conditions though the % loss after 3 months was still quite high in terms of long term storage (Appendix C showing the HPLC stability chromatograms).

The experiments were validated as follows:

- Each sample was analysed in triplicate (n=3)
- Calibration curve and repeatability linear
- No degradation measurements undertaken because the samples were analysed as soon as aliquots were withdrawn from dissolution media

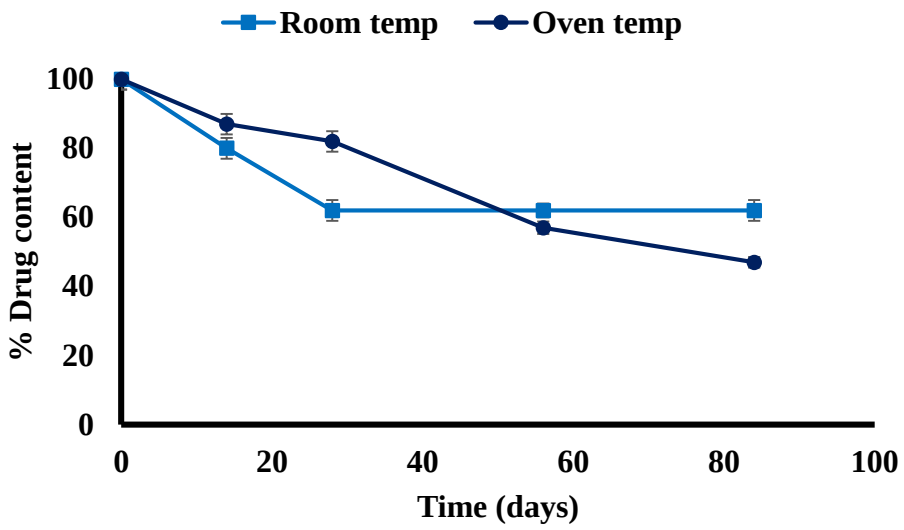

Figure 4.14 Plot showing the % OME content for MET DL film during storage at oven temperature 40ºC (± 0.5 ºC) and room temperature (ambient ± 0.5 ºC) 3% RH up to three months (mean ± SD, (n=3))

4.4 SUMMARY

The main goal in drug delivery is to develop a useful system which delivers therapeutic agents at a controlled rate over an extended period. This can be achieved by using release systems in which swelling is the controlling mechanism for the drug release (Lowman, et al., 2004). The critical factors that must be considered in a dosage form for buccal mucosa drug administration include stability, solubility, bioadhesion and bioavailability (Dixit et al., 2009). Further, adequate hydration is an essential property for uniform and prolonged release of the drug and for effective mucoadhesion (Peppas & Buri, 1985). Therefore, the mechanical, bioadhesive and swelling properties of buccal film are critical and essential to be evaluated (Kok et al., 1999). The swelling state of the polymer was reported to be crucial for bioadhesive behaviour (Huntsberger, 1971). Adhesion occurs shortly after the beginning of swelling but the bond formed is not very strong (Chen and Cyr., 1970). Subsequently, the adhesion will increase with the degree of hydration until a point where over hydration leads to a rapid drop in adhesive strength due to disentanglement at the polymer/tissue interface and in some cases, formation of slippery mucilage which just slips across the mucosal surface (Ayensu et al., 2012). PBS had higher swelling index compared to SS and implies that ionic strength and pH play an important role in affecting the swelling of MET films. The effect of ionic strength and pH on swelling of the polymer matrix has been described by Park and

Robinson (1985). They observed that the strength of mucoadhesion attraction at the mucosal membrane of polymers possessing carboxyl groups is much stronger than that those with neutral (non polar) functional groups. The pH of saliva as a dissolution medium affects the behaviour of the polymer depending on the salivary flow rate and method used to determine it. The pH range has been estimated between 6.5 and 7.5. The pH of the surrounding medium to which mucoadesive polymers come in contact can alter the ionization state and subsequently the adhesion properties of the polymer. The rate of swelling of MET films in PBS was higher than MET films in SS solution/media, indicating that MET films in PBS exhibited faster rate of water uptake and hydration than MET films in SS.

In vitro mucoadhesion were performed to predict the stickness and ability of MET films to adhere to buccal surface. Ruiz and Ghaly (2006) have confirmed that MET films have the ability to adhere to gelatine and therefore using gelatine surface equilibriated with SS was a suitable model. Bioadhesivity involves the process whereby polymer (synthetic or bio materials adhere to biological tissues and if the attachment occurs with mucus or a mucosal membrane, this phenomenon is referred to as mucodhesion (Smart., 2005). The adhesive force depends on several factors such as hydrophilicity, stage of hydration and rate of polymer erosion after being contact with the hydrating mucosal surface (Patel et al., 2009). Smart (2005) noted that mucoadhesion bond formation depends on the nature of the mucous membrane and mucoadhesive materials, formulation type, the attachment procedure and the environment of the bond. These forces include ionic, covalent and hydrogen bonds (Laidler et al., 2003) and these are discussed in more detail in chapter 1 section 1.11. Smart (2005) also confirmed that in addition to hydrogen bonds, mucoadhesion can be generated due to van der Waals bonds or interaction between the polymer matrix and gelatine surface depending on the media. pH affects the mucoadhesive interface owing to generation of ionizible groups (these are some of the weakest forms of interation that arise from dipole-dipole and dipole-induced dipole attractions in polar molecules and dispersion forces with non-polar substance) which overcomes the attraction force between the surface of the film and the surface of the gelatine. The strength of the bonds formed between the polymeric matrix during the contact time with the gelatine also affects the mucoadhesive properties (Bansal et al., 2009).

Bioadhesive systems for controlled drug release over extended period in paediatrics which have potential to be used to meet the desirable characteristics of ideal effective drug delivery which are risk of chewing and physiological conditions (age of the child and gastric pH).

Also the strong interaction between the polymer and mucosal lining of the tissue helps increase the contact time.

4.5 CONCLUSION

PEG 400 was found to increase the softness elasticity (as discussed in chapter 2 and 3) and bioadhesive strength of the MET films. Plasticised MET films appeared to be tougher, more elastic (discussed in chapter 2 and 3), more bioadhesive *in vitro* and swelled at a more steady rate, this suggest that MET films may be preferred as drug vehicle for buccal delivery. BLK films showed higher swelling index compared to DL films one possible reason is due to the formation of sodium chloride and sulphate in the latter which affect their swelling capacity. The stability studies suggested that films remained more stable at room temperature (ambient ± 0.5 ºC) conditions when compared to 40 ºC.

CHAPTER FIVE: *IN VITRO* DRUG DISSOLUTION CHARACTERISTICS AND RELEASE MECHANISMS OF OME LOADED MET FILMS

5.1 INTRODUCTION

Drug dissolution refers to the process by which drug solute migrates from the initial site in a polymeric system to the polymers outré surface and then into dissolution medium. Drug release is affected by several factors such as physiochemical properties of the drug solutes, dissolution condition and environment, structural characteristics of the polymeric system and the possible interactions between these factors as described by Fu and Kao, (2010). Polymer dissolution controlled drug release system is made of a drug molecularly dispersed in a polymeric matrix. The penetration of water in the polymer causes swelling and a thin layer in the rubbery state (gel layer) is formed surrounding a dry core. Drug diffusion through the gel layer formed is relatively fast. Initially the gel layer thickness is increased due to swelling and then remains constant due to synchronisation of swelling, which results in drug diffusion and finally decreases as dissolution takes over (Narasimhan et al., 1997).

Diffusion, swelling and erosion are the most important mechanisms that control drug release from the polymeric system (Langer et al., 1984). Diffusion can be described by using Fick's first and second laws. Release kinetics are mathematical models that are used to study and evaluate the kinetic and overall mechanism of drug release from polymeric dosage forms such as films. The different models are then compared to the experimental dissolution data in order to obtain the model that best fits the release data. Such model is then selected based on the correlation coefficient (R^2) value and model that produces the highest R^2 value is then considered as the most appropriate to study and evaluate the release data (Dash et al., 2010). As previously noted, the main mathematical models include

- Zero order release/kinetic model
- First order release/kinetic model
- Higuchi release/kinetic model
- Korsmeyer-Peppas release/kinetic model

The main aim of this chapter was to evaluate the dissolution properties of the OME loaded films described in the previous chapters. The mechanisms of drug release were evaluated by fitting the drug release data to different kinetic models named above to identify the best model fitting the release of OME from the film.

5.2 MATERIALS AND METHODS

5.2.1 Materials

Table 5.1 List of materials

Materials	**Batch numbers**	**Purity**	**Suppliers**
Potassium dihydrogen phosphate	073346	100%	Fisher Scientific (Leicester, UK)
Sodium hydroxide	1152687	97%	Fisher Scientific (Leicester, UK)
Sodium Chloride	7647-14-5		Fisher Scientific (Leicester, UK)
Sodium phosphate dibasic	1204925	99%	Fisher Scientific (Leicester, UK)
Mucin from bovine submaxillary gland, Type I-S	M 3895-1G	-	Sigma-Aldrich (Gillingham, UK)

5.2.2 Instruments

Table 5.2 List of instruments

Instrument	**Supplier**
Agilent 1200 HPLC	Agilent Technologies, Cheshire, UK,)

5.2.3 METHODS

5.2.3.1 *In vitro* release of OME using Franz-type diffusion cell

Before the dissolution studies, drug assay and uniformity of OME within the film was determined. This was measured by weighing the film accurately to 5mg (n=3) and hydrated in 8 mL of drug dissolution media (0.01M PBS pH 6.8 and SS pH 6.8 at 37°C). Film was stirred at 37 ± 0.5°C until completely dissolved. The concentration of OME was analysed using HPLC.

In vitro drug dissolution studies were carried out using Franz-type diffusion cells. 5 mg of optimised MET DL film were placed in the donor compartment (chamber) on stainless steel wire mesh (0.5 mm x 0.5 mm) which separated the donor and receiver compartments, with the mucoadhesive surface in contact with the wire mesh and facing the receiver compartment of the Franz diffusion cell (Cui et al., 2008). The receiver chamber was filled with 8 mL of 0.01 M PBS pH 6.8 and SS pH 6.8 [(potassium dihydrogen phosphate (0.19 g), sodium chloride (8.0 g) and sodium phosphate dibasic (2.382 g)] in 1L of deionised water and adjusting the pH to 6.8 using phosphoric acid) at 37 °C with magnetic stirring at a speed of 250 rev/min. The chambers were held together by a cell clamp and sealed with parafilm, in order to limit evaporation and the temperature of the diffusion cell was maintained at 37 ± 0.5 °C and stirred throughout the experiment as shown in Figure 5.1

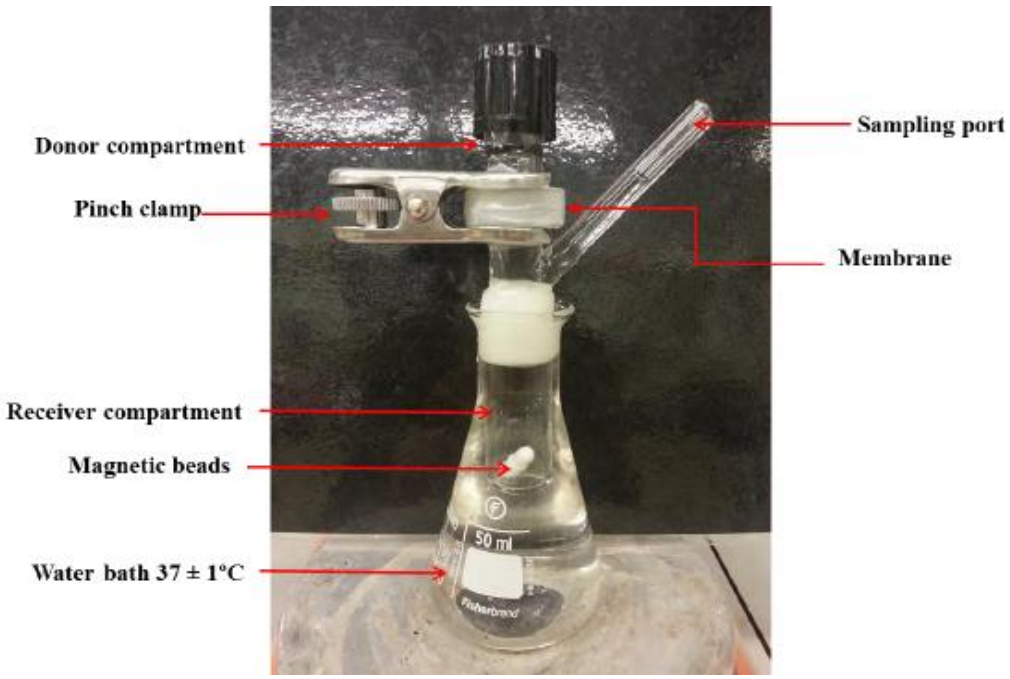

Figure 5.1 Digital photograph of modified Franz-type diffusion cell as set up for drug release experiment.

1 mL of the dissolution medium was sampled at predetermined time intervals and replaced with the same amount of fresh medium to maintain a constant volume for 2 hrs. The sampled dissolution medium was measured at 302 nm using HPLC.

The concentration of OME released from the film was determined by interpolation from the linearized calibration curve (R^2 > 0.99) and cumulative percentage drug release profiles

plotted. The release profiles of drug from film prepared from gels containing 20% EtOH, 0.5% w/w PEG 400 and OME:L-arg 1:2 were determined.

5.2.3.2 HPLC analysis

Concentration of DL films as well as drug release in dissolution studies were analysed using an Agilent 1200 HPLC equipped with an auto sampler (Agilent Technologies, Cheshire, UK,) with a Chemstation® software program. The stationary phase used for analysis was a Hypersil™ ODS C18 HPLC column, 5 µm particle size (250 x 4.6 mm) (Thermo Scientific, Hampshire UK). The mobile phase consisted of a mixture of ammonium acetate and acetonitrile in the ratio of 60:40v/v. The flow rate of the mobile phase was maintained at 2 mL/min and detector wavelength for OME was set at 302 nm respectively. 20 µl volumes were injected during each run. Standards from 10-50 µg/mL were used to plot calibration curves for OME (R2> 0.99).

5.2.3.3 Evaluation of drug release mechanisms

Model dependent release mechanisms:

Based on the drug dissolution results, the following kinetic models with their corresponding relationships in Table 5.3 were constructed by fitting the drug release data to equations [1.1 – 1.4] (chapter 1 section 1.13.4 above).

Table 5.3 Various plots with corresponding kinetic /mechanism model (buccal)

Plot parameters	Kinetic/mechanism model
Cumulative % drug release against time	Zero order kinetic model
Log cumulative of % drug remaining against time	First order kinetic model
Cumulative % drug release against square root of time	Higuchi model
Log cumulative % drug release against log of time	Korsmeyer-Peppas model

5.2.3.4 Comparison of release profiles

Release parameters from the dissolution profiles for the various formulations and variables under investigation were used to characterise the drug release data and compare the various drug loaded formulations. The parameters used were $t_{x\%}$, and sampling time. The $t_{x\%}$ corresponds to the time necessary for the release of a determined percentage of drug (e.g., $t_{20\%}$, $t_{50\%}$, $t_{80\%}$). Sampling time corresponds to the amount of drug dissolved in that time (e.g., $t_{20min,}$). In this study, the time to release 20% of the drug originally loaded ($t_{20\%}$) and the percentage cumulative release at 60 minutes (t_{60min}) were used to compare the drug loaded formulations (Costa et al., 2001).

5.2.3.5 Assay/drug content of OME in films

The films (n=3) prepared were assayed for content of OME by dissolving each film in PBS (10mL) pH 6.8 at 37° C and stirred until homogenous solution was formed, 1 mL was withdrawn and examined by HPLC.

5.3 RESULTS AND DISSCUSION

5.3.1 *In vitro* release of OME using Franz-type diffusion cell

Drugs can be released from the matrix by diffusion through the swollen polymer and subsequent erosion of the matrix. The drug release may be controlled by diffusion, or by a combination of diffusion and erosion or only by erosion of the delivery system (Turvinen et al, 2003). By comparing polymer dissolution and drug release, it is hoped to gain insight into what processes control release.

5.3.1.1 *In vitro* drug dissolution studies (calibration curves)

The standard calibration curves using the two dissolution media (PBS and SS) are shown in figures 5.2 and 5.3 which shows that a linear relationship between concentration and peak area were observed, was maintained for both drugs at wavelength of 302nm respectively (Boateng et al., 2009).

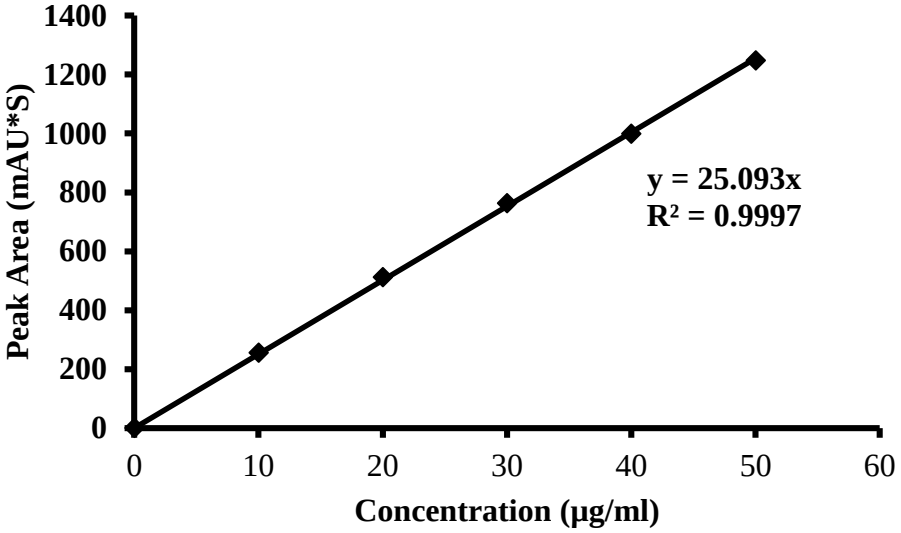

Figure 5.2 Standard HPLC calibration curve using PBS for determining the release of OME during drug dissolution study for MET DL film.

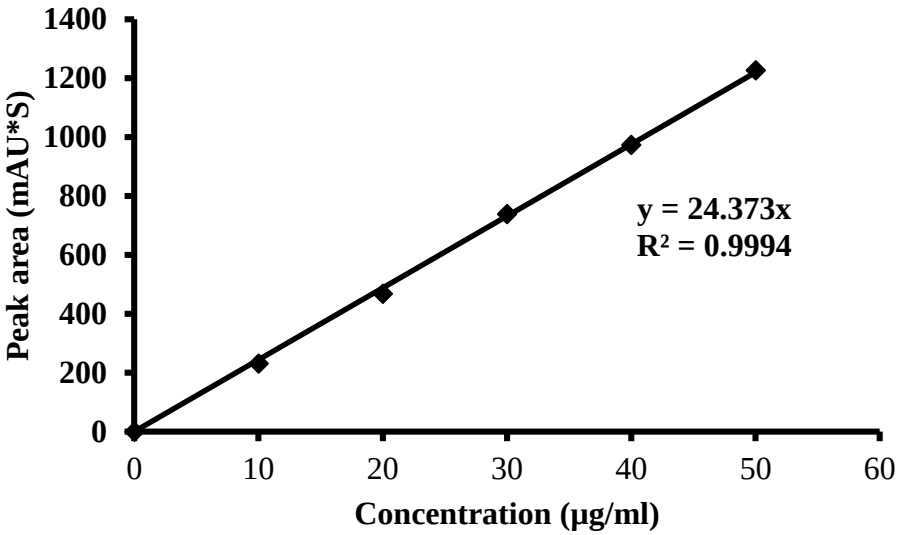

Figure 5.3 Standard HPLC calibration curve using SS for determining the release of OME during drug dissolution study for MET DL film.

5.3.1.2 Drug dissolution studies

Prior to drug dissolution studies, the drug loading in each film sample was determined using the two different media employed. Based on the results the drug loading was higher in PBS compared to SS. This can be due to the matrix of the polymeric film and the interaction with the two media as a result of the differences in ionic strength.

Table 5.4 The % DL capacity (OME) and content uniformity of MET DL films in PBS and SS

OME Loaded films	**% Drug loading, content uniformity (mean ± SD, n=3)**
MET DL film (PBS)	75.6 ± 0.2
MET DL film (SS)	61.1 ± 0.2

5.3.1.2.1 0.01M PBS solution (pH 6.8 ± 0.1)

The dissolution profile for MET DL films (PEG 400 (0.5% w/w), 20% v/v EtOH, OME:L-arg 1:2) in PBS solution (pH 6.8 ± 0.1) is shown in figure 5.4. During the early stage of dissolution of percentage cumulative release vs time showed an almost linear fit was

observed. with 55.8 % release within the first 15 minutes and 10.35 % after 30 minutes, after which the % release was fairly constant between 1 – 3%. The release studies show that the complexity of drug OME with L-arginine has the ability to enhance drug solubility; therefore, this facilitates the process of hydration (Figueiras et al, 2010). This hydration occurs via water penetration through the process of diffusion and dissolution mechanism. After 60 minutes the release was 69% and after 2 hrs it decreased to 62%. After 60 minutes the release was observed to be sustained.

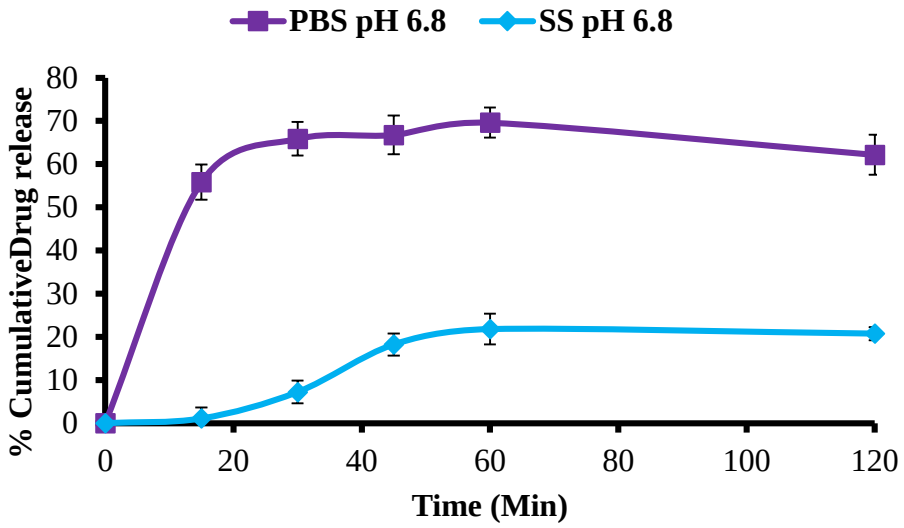

Figure 5.4 Drug dissolution profile of MET DL films prepared from ethanolic (20% v/v EtOH) gel containing 0.5% w/w PEG 400 and OME: L-Arg 1:2 ratio in PBS at pH 6.8 and SS pH 6.8 (mean ± SD, (n=3))

5.3.1.2.2 SS (pH 6.8 ± 0.1)

The dissolution profile for MET DL films (PEG 400 (0.5% w/w), EtOH 20%, L-arg) containing OME were also determined using SS at pH 6.8 ± 0.1, to more accurately mimic the environment within the oral cavity in terms of both pH and ionic strength as seen in figure 5.4. The dissolution characteristic of OME was observed over a period of two as was the case in PBS During the early stage of dissolution, the % release was observed to be low with 1.08% released in the first 15 minutes after which it gradually increased to 18.21% and 21.77% at 45 and 60 minutes respectively, and then the release remained largely steady till 120 minutes.

All the films appeared to show good controlled release in the two dissolution media. However PBS at pH 6.8 showed higher cumulative release (69%) than in SS (21%) at 60 minutes. The controlled release of the OME from the MET films could be attributed to the swelling of the polymeric network, releasing the drug progressively into the dissolution medium. The results show that drug release rates were faster in PBS due to difference in osmotic pressure and ionic strength as SS contains more salts (sodium chloride and sulphate) than PBS.

5.3.2 Evaluation of drug release mechanisms

Data of the *in-vitro* release were fitted to different equations and kinetic models to explain the release kinetics of OME from buccal films as shown in sections 5.3.2.1.2 and 5.3.1.2.2 The release parameters obtained from fitting experimental dissolution release data to the different kinetic equation evaluated has been summarised in table 5.5 (Shoaib et al., 2006). Interpretation of the data was based on the value of the resulting regression coefficient. The release kinetics of OME in PBS (pH 6.8) and in SS both followed Korsmeyer-Peppas model as the R^2 values were the highest compared to other models as shown in table 5.5. The 'n' values from the Korsmeyer-Peppas equation, describe the diffusion state or release exponent used for elucidation of the drug release mechanism. The 'n' is estimated from linear regression of Log (M_T/M) versus log t plot. Analysis of the experimental data using kinetic equations and interpretations of the release exponents (n) gives a better understanding of the controlling release mechanism. OME in PBS of pH 6.8 recorded a value 0.2 which is less than 0.45 which indicate that the drugs follow release mechanism of non-Fickian diffusion. This suggests that the OME was released through the hydrated polymer via diffusion combined with and erosion controlled drug release. However, SS recorded an n value of 2.2 which is greater than 0.89 therefore follows the super case II transport mechanism of drug release. This indicates controlled drug release with zero-order kinetics attributed to the erosion of the polymeric chain matrix.

Over a period of 15-45 minutes, the drug release in PBS medium was observed to be almost linear. The visual observation of the dissolution process reveals that OME loaded films in SS shows the lowest extent of swelling in the medium. Talukdar (1998) reported similar drug release profile with lower release rate at the beginning and increasing rates subsequently.

5.3.2.1 Kinetic mechanism of 0.01M PBS solution (pH 6.8 ± 0.1)

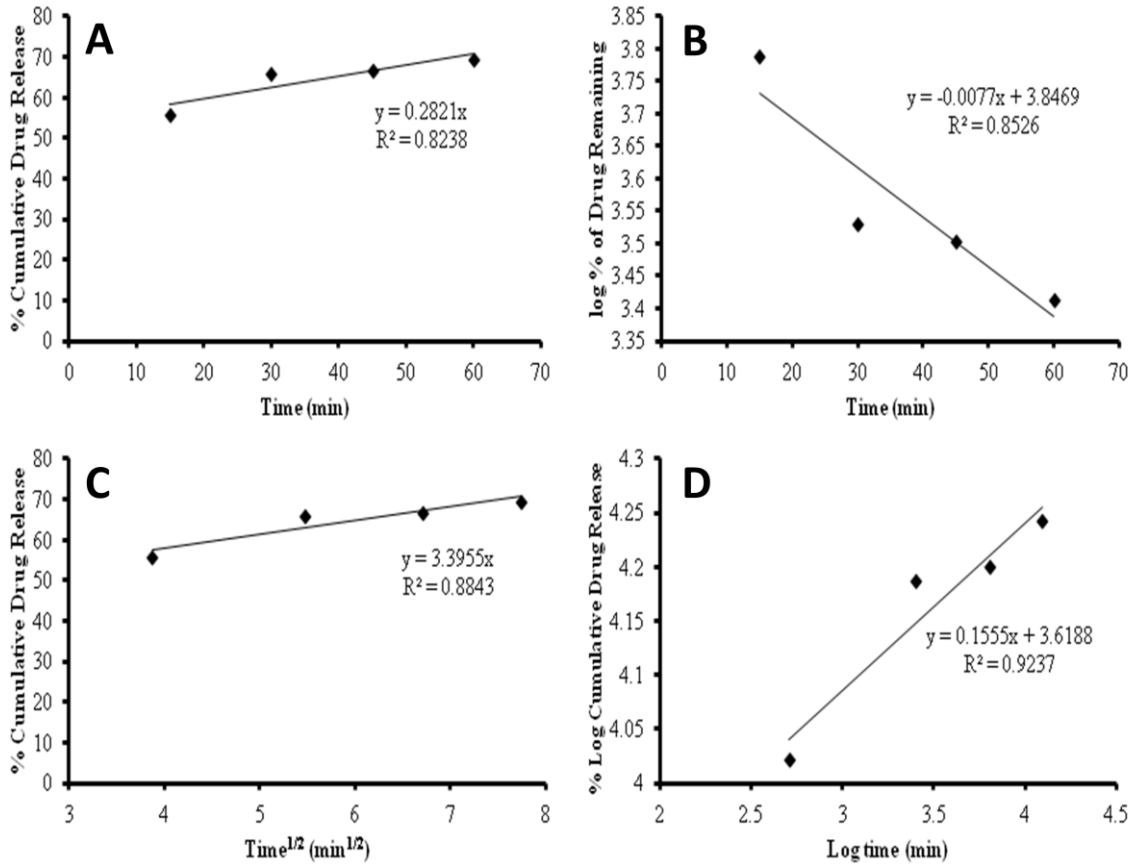

Figure 5.5 Representative release plots obtained by fitting experimental release data of OME from DL MET films (OME:L-arg 1:2) to (A) zero order kinetic, (B) first order kinetic, (C) Higuchi kinetic, (D) Korsmeyer-Peppas kinetic models/equation.

Table 5.5 Release parameters obtained from fitting experimental drug dissolution (release) data to different kinetic equations for films containing OME in PBS and SS pH 6.8.

OME	Zero order		First order		Higuchi		Korsmeyer-Peppas		
	K_0 (% min^{-1})	R^2	K_1 (min^{-1})	R^2	K_H (% $min^{-1/2}$)	R^2	K_P (% min^{-n})	n	R^2
DL PBS (pH 6.8)	0.2821	0.8238	-0.0077	0.8526	3.3955	0.8843	3.6188	0.2	0.9237
DL SS (pH 6.8)	0.3781	0.9687	-0.0055	0.9682	4.3919	0.9685	5.8754	2.2	0.9703

K_o, K_1, K_H, K_p are the release rate constant for zero order, first order, Higuchi and Korsmeyer-Peppas models, R^2 is the correlation coefficient and n is the release exponent.

5.3.3 Comparison of release profiles

To compare the dissolution profiles, release parameters (tx% as discussed in section 5.2.3.4) was used rather than a modified Moore and Flanner, (1996) equation for calculating the difference (f_1) and similarity (f_2) factors. The f1 value measures the percent error between two curves over all time points, while the f_2 value is a logarithmic transformation of the sum-squared error of differences between the test Tj and reference products Rj over all time points. Difference (f_1) and similarity (f_2) factors, equations shown below (Moore and Flanner., 1996) (Boateng et al., 2009).

$$f_1 = \frac{\sum_{j=1}^{n} |Rj - Tj|}{\sum_{j=1}^{n} Rj} \times 100 \qquad \text{equation 5.1}$$

$$f_2 = 50 \times \log \{ \left[\frac{1}{N}\sum_{j=1}^{n} |Rj - Tj|^2\right]^{-0.5} \times 100\} \qquad \text{equation 5.2}$$

The equations are used based on the following parameters:

- Minimum of three dissolution time points are measured.
- Number of samples tested for dissolution is 12 for both test and reference.
- Not more than one mean value of > 85% dissolved for each product. No more data points to be taken into consideration if more than 85%.
- Standard deviation should not be more than 10% from the second to last dissolution time points.

In this study, the f_1 and f_2 values were not employed to compare the dissolution profiles because there were only two formulations being compared and therefore no reference available to compare to either profiles. Pure OME could not be used as the reference due to the obvious instability in aqueous media, as discussed in chapter 3.

The time to 20% release ($t_{20\%}$) of initial amount of OME present, for each media can be seen in table 5.6. The results showed that in SS media 20% of drug was released in 50 minutes whereas in PBS media 20% was released in 5.5 minutes indicating extremely statistically significant (p = 0.0001). The t_{60min} in PBS and SS was 70% and 22% respectively indicating statistically significant (p = 0.0001) differences in rate of release between PBS and SS. These

results could be related to the swelling of the DL films within the two media due to difference in osmotic pressure and ionic strength as SS contains more salts (sodium chloride and sulphate) than PBS as noted previously.

Table 5.6 Comparison of the effect of OME on the time to release 20% ($t_{20\%}$) of drug from each DL films and comparison of the effect of mean cumulative percentage of OME released at 60 minutes ($t_{60\ min}$) in PBS and SS.

DL MET films media	Time to release 20% of drug (t_{20})	Mean % release at 60 min (t_{60min})
	Films	
PBS	5.5	70.0
SS	50.0	22.0

5.4 SUMMARY

A key goal in drug delivery is to develop systems that deliver therapeutic agents at a controlled rate over an extended period. This can be achieved by using systems in which polymer swelling and subsequent drug diffusion are the controlling mechanism of drug release (Lowman et al., 2004). Drug release rates can increase or decrease, and is theoretically subject to the type of polymer and type of drug delivery system. Drug delivery systems are categorized according to their structural design (physical-mechanical properties) or their rate-controlling release mechanism such as diffusion, erosion/chemical reactions and swelling (Frenning, 2011). The timely and reproducible release of active pharmaceutical ingredients (API) from delivery vehicles of various kinds is of paramount significance for safe and efficient treatment of disease (Frenning, 2011). Drug release, from a polymeric system initially involvess the uptake of water by a glassy polymer and subsequent swelling to form a gel layer which controls drug release by viscous resistance to drug diffusion (Boateng et al., 2009). Control of the drug release from a dosage form such as film depend on the type of drug(s), the dose, type and amount of the polymers and excipients, preparation method and environmental circumstances during drug release as well as geometry of the drug delivery system.

Various kinetic models were established to define the relationships that exist between drug dissolution and geometry on drug release patterns mathematically. It is evident from the pharmaceutical literature that no single approach is widely accepted to determine if dissolution profiles are similar or different. The application and evaluation of model dependent methods and statistical methods are more complicated, whereas the model dependent methods represent an acceptable model approach to the true relationship that exist between the dependent and independent variables of the dissolution date (Dash et al., 2010).

The total cumulative percentage of released and permeating was observed to be higher for PBS than SS due to its higher rate of hydration and possibly enhanced cohesiveness. The cohesion and stability of a drug delivery system over the intended duration of drug release is often a requirement for controlled release (Peppas & Bury., 1985). The difference between PBS and SS was (p = 0.0001) was statistically significant with PBS formulation exhibiting sustained release profile and this difference could possibly be attributed to two different release mechanisms; (1) diffusion of molecules based on the concentration of OME and (b) degradation of polymer matrix.

The control of drug release consists of a series of interrelated molecular events, such as polymer surface wetting, hydration, hydrogel formation and erosion/dissolution. For hydrophilic drugs, the swelling behavior of hydrophilic polymers (MET) is thought to be controlled by factors such as temperature and pH because this is mainly achieved by the drug molecules diffusing through the hydrated gel layer to reach the delivery site. Swelling studies can give information about the drug release and hydration/ erosion behavior in the presence of PBS and SS, therefore it is important to understand the underlying mechanisms (Fan et al., 2001). At the molecular level, Siepmann and Siepmann (2008) summarised the phenomena controlling release of drug, which involved wetting by water and its diffusion into the system, phase transition (e.g glassy to rubbery) of the polymer, excipients and drugs. This is further affected by changes in the microenviromental pH due to variation in the rate of drug or excipient degradation, physical drug-drug or polymer-drug or exciepents interaction, changes in drug or exciepnts solubility, diffusion of drug oe exciepent out of the dosage form.

Regardh et al (1985) studied the pharmacokinetics of OME in four species (mouse, rat, dog, and man). From theirdata it was shown that the drug is rapidly absorbed in all species. The systemic bioavailability was observed to be relatively high in dog, and high in man provided

that the drug is protected from acidic degradation in stomach. In man the fraction of the oral dose reaching the systemic circulation was found to increase from an average of 40.3–58.2% when the dose was raised from 10 to 40 mg, which suggests that absorption and subsequent bioavailability was dose dependent. Further, OME distributes rapidly to extravascular sites and is also 95% bound to proteins in human plasma. The drug is eliminated almost completely by metabolism and no unchanged drug has been recovered in the urine in the species studied. Two metabolites, the sulfone and sulfide of OME, have been identified and quantified in human plasma.

5.5 CONCLUSION

It can be concluded that on the basis of experimental data analysis, OME release into PBS is much faster than in SS. Maximum concentration of drug released in PBS was obtained within 1 hr, and in SS the release was obtained to be slower. The rate of drug release from films was dependent on their physical structure and the amounts of OME present (Boateng et al, 2009). The model dependent mathematical functions used for describing the release profiles of OME showed that the Korsmeyer-Peppas equations fit the dissolution data for PBS and SS, on the basis of drug concentration, dissolution and polymer characteristics. The drug release in PBS followed zero order release kinetics via non-Fickian diffusion whilst release in SS followed super case II transport, attributed to both drug diffusion and polymer erosion.

CHAPTER SIX: *EX VIVO*, PERMEATION AND MUCOADHESION USING PIG BUCCAL TISSUE, AND CELL TOXICITY OF OMEPRAZOLE LOADED FILMS

6.1 INTRODUCTION

Drug permeation through buccal mucosa, from several animals such as hamster (Tsutsuni et al., 1999; Eggerth et al., 1987), rabbit (Nair & Chien, 1993; Dowty et al., 1992), dog (Galey et al., 1976) and pig (Chen et al., 1999; Artusi et al., 2003; Sandri et al., 2004) have been used. However the epithelium of the rodent (Hamster) buccal tissue is thick and keratinised, and the surface area is small (Shojaei 1998). Though dog buccal mucosa is non keratinised and similar to human buccal epithelium, it is expensive for routine use in *in vitro* permeation experiments (Shojaei.,1998). Pig buccal mucosa is non-keratinised and closest to human tissue in terms of structure and permeability (Shojaei., 1998). In addition, its low cost makes it an ideal model for drug penetration studies. The disadvantages of using the porcine buccal mucosa are small cheek surface, damaged by mastication and firmly attached to the underlying muscular tissue. To overcome these drawbacks, some investigators have used pig oesophageal mucosa to replace the buccal mucosa.

The porcine oesophageal mucosa tissue is smooth and intact. It consists of stratified, squamous, non-keratinised epithelium supported on a connective-tissue layer (Squier & Kremer., 2001). Furthermore, membrane coating granules (MCGs), which extrude lipids to form the permeability barrier in the buccal mucosa (Shojaei., 1998), have also been found in oesophageal epithelium (Hopwood et al., 1978). The appearance and localization of the MCGs in oesophageal mucosa are similar to those in the buccal mucosa, and it has been proved that the secreted material has been correlated to the performance of the permeability barrier (Hill et al., 1982; Hopwood et al., 1991). Buccal and oesophageal mucosae have a very similar structure comprising stratified non-keratinised epithelium, supported on a loose connective tissue layer, which contains the microcirculation (lamina propria). The basal lamina separates the epithelium from lamina propria. One major difference between the mucosae is the presence of a smooth muscle cell layer arranged longitudinally in the oesophagus (Squier & Kremer., 2001).

The permeability of fentanyl citrate through pig oesophageal mucosa and buccal tissue have been compared by Del Consuelo and his colleagues (del Consuelo et al., 2005). The results

from their studies showed that the permeability of pig oesophageal mucosa and buccal mucosa was very similar for fentanyl. The permeability barrier of oesophageal mucosa and buccal mucosa are both located in the epithelium and their results showed that separation of epithelia did not disturb the integrity of the barrier function. Moreover, freezing the tissue did not affect fentanyl transport through the mucosae (del Constuelo et al., 2005).

Cell viability and cytotoxicity assays are used for drug screening and cytotoxicity test for chemicals and several reagents are used for cell viability detection. Cell culture can be used to screen for toxicity both by estimation of the basal function of the cell. General toxicity is aimed mainly at detection of the biological activity of the test substance. Cytotoxicity test using specialised cells have proven most useful when the *in vivo* toxicity of a chemical is already well established and where *in vitro* investigations using specialised cell cultures have been used to clarify the mechanism of toxic action on the target (Ekwall et al,.1990).

The aim of this chapter was to investigate the permeation of OME released from MET films across pig buccal tissue, *in vitro* bio-adhesion of the films on the buccal membrane and cell toxicity using MTT assay to assure the safety of the starting materials (MET, L-arg, OME) and the optimised films (BLK (0.0% - 0.5% w/w PEG 400) 20% v/v EtOH) and DL (0.5% w/w PEG 400, 20% v/v EtOH, OME:L-arg 1:2).

6.2 MATERIALS AND METHODS

6.2.1 Materials

Table 6.1 List of materials used

Materials	Batch number	Purity	Suppliers
Potassium dihydrogen phosphate	073346	100%	Fisher Scientific (Leicester, UK)
Sodium hydroxide	1152687	97%	Fisher Scientific (Leicester, UK)
Sodium chloride	7647-14-5		Fisher Scientific (Leicester, UK)
Sodium phosphate dibasic	1204925	99%	Fisher Scientific (Leicester, UK)
Krebs-Ringer bicarbonate buffer	K4002-10X1L	-	Sigma-Aldrich (Gillingham, UK)
Thiazolyl blue tetrazolium bromide	08797HJ	-	Sigma-Aldrich (Dorset, UK)
MTT reagent [(3-(4,5-dimethylthiazol-2-yl)-2,5-diphenyltetrazolium bromide]	08797HJ, M2128-10G	-	Sigma-Aldrich (Dorset, UK)
Dulbecco's-Minimal Essential Medium (D-MEM)	21969-035, 500 mL	-	Gibco (Paisley, UK)
Dimethyl sulfoxide (DMSO)	0600100	-	Sigma-Aldrich (Dorset, UK)

6.2.2 Instruments

Table 6.2 List of instruments

Instruments	Suppliers
TA HD plus texture analyser	Stable Micro System Ltd, Surry, UK
Agilent 1200 HPLC	Agilent Technologies, Cheshire, UK,)

6.2.3 Method

6.2.3.1 Tissue preparation

A buccal tissue (cheek) from pigs was obtained from a local slaughterhouse (Powder Mill Lane, Southborough, Tunbridge Wells, Kent. TN4 9EG). After removal, the tissue was immediately transferred into cold Krebs buffer (pH 6.8) modified with sodium carbonate, placed in sealed ice box filled with dry ice cubes and immediately transported to the laboratory. The buccal mucosa, with part of sub mucosa, was carefully separated from the fat and muscles using a scalpel and the epithelium were isolated from the underlying tissue. The thickness of the sample was approximately 500 µm using microscope and the buccal epithelium was used within 2 hrs upon removal (Patel et al., 2007).

6.2.3.2 *Ex vivo* buccal permeation studies

The mucosal membrane prepared above was washed with physiological PBS (pH 6.8) and SS (pH 6.8) at 37 °C. The obtained buccal mucosa membrane was mounted between the donor and receiver compartments of the Franz-type diffusion cell, with the epithelial side facing the donor compartment (Attia et al., 2004). The receiver chamber was filled with 8 mL of SS (pH 6.8) at 37 °C and uniform mixing was provided by magnetic stirring at 250 rev/min. After an equilibration period of 30 minutes, 0.5 mL of SS (pH 6.8) was placed in the donor compartment and 5 mg of the OME loaded film was placed in the donor chamber with the mucoadhesion layer in contact with the epithelial surface. The chambers were held together by cell clamp and sealed with parafilm to limit evaporation. At predetermined time intervals, samples (1 mL) were withdrawn from the sampling port of the receiver compartment and replaced with the same amount of SS to maintain a constant volume for 2 hrs. The sampled medium were analysed using HPLC (n=3) for permeation parameters.

6.2.3.3 *Ex-vivo* mucoadhesion evaluation using porcine buccal tissue

The *ex vivo* mucoadhesion experiments were performed on DL MET films (x 3) to estimate the effect of PBS and SS on adhesion of the films on porcine buccal tissue. The samples were tested using a TA HD plus Texture Analyser (Stable Micro Systems, Surrey, UK) fitted with

a 5 kg load cell. The film was attached to an adhesive probe (75 mm diameter) with double sided adhesive tape. An 88 mm diameter Petri dish was used containing epithelium (porcine) to mimic the buccal mucosa. The film was positioned in contact with the epithelium for 60 seconds to provide optimal contact before being detached. Texture Exponent 32 software was used to record and process the data. The peak adhesive force (PAF) required to separate the film from the porcine mucosa epithelium surface was determined by the maximum force. The area under the curve (AUC) representing the total work of adhesion (TWA) was estimated from the force-distance plot whiles the cohesiveness of the sample was determined by the distance of travel as shown in chapter 4, section 4.2.3, figure 4.1.

6.2.3.4 Cell toxicity studies (MTT assay)

MTT assay was used to evaluate the cytotoxicity of pure MET, pure L-arg, pure OME, optimised BLK [(MET, PEG 400 (0.5% w/w), 20% v/v EtOH)] and DL films (MET, OME, L-arg, PEG 400 (0.5% w/w), 20% v/v EtOH). Vero cells (ATCC®CCL-81™) are adherent cells derived from the kidney of the African Green monkey (Cercopithecus aethiops) and are one of the commonly used mammalian cell lines in cell, micro and molecular biology (Ammerman et al., 2008). These cells were obtained from cell and tissue culture labs within the Faculty of Engineering and Science, (Richardson Lab, University of Greenwich, Medway) and stored at -80°C. The cells (Vero, $1x10^4$cells/well) were used to seed a sterile, flat-bottomed 96 well tissue culture plate with DMEM,FBS 10% (v/v), penicillin (100units/mL), streptomycin (100 µg/mL), glutamine 0.292 mg/mL (all from Gibco, Paisley, UK). Two cultures (treated and control) were kept under sterile conditions in a laminar hood) and incubated at 37°C in 5 % (v/v) CO_2 for 24 hrs.

After 24 hrs, the cells (except the cells in the control wells) were exposed to either pure MET, pure L-arg, pure OME, BLK film [(MET, PEG 400 (0.5% w/w), 20% EtOH) and DL film (MET, OME: L-arg 1:2, PEG 400 (0.5% w/w), 20% v/v EtOH)] which was prepared at different concentrations (0-2mg/mL) in cell culture medium and incubated for 68 hrs. This was used to replace the existing media covering the cells after the designated incubation period. After this time, 10 µL (equivalent to 50 µg) of MTT from stock solution (5 mg/mL) prepared by dissolving 250 mg of MTT reagent in 50 mL of PBS (1x) buffer, was sterilized by passing it through a 0.22 µm filter (Corning®, Germany). This was added to each well and

the plate incubated for a further 4 hrs using the same incubator conditions as above bringing the total incubation time to 72 hrs. The contents of the plate were decanted and 100 µl of DMSO was added to each well, incubated at room temperature for 30 minutes and the absorbance read on a Multi-scan EX Micro-plate photometer (Thermo Scientific, Essex, UK) at optical density (OD) 540 nm. Data obtained was expressed as percentage cell viability (mean ± standard error of the mean) for all the samples tested above.

6.3 RESULTS AND DISCUSSION

Porcine buccal mucosa resembles human buccal mucosa in structure and permeability (Werts, .1991) and therefore a suitable model to investigate drug permeability. .Maintaining buccal tissue integrity and viability during isolation and storage before experimental testing is crucial to obtaining reliable permeation results (Patel et al., 2012). For example, the storage of porcine buccal mucosa in Krebs bicarbonate Ringer solution helped to retain its integrity whiles storage in other solutions such as PBS at 4 °C for 24 h led to loss of epithelial integrity (Kulkarni et al., 2010). This study investigated the permeation study of OME model drug release using a pig buccal tissue and mucoadhesion studies of the film. Average percentage cell viability was plotted for the different test a set conditions using five different samples as seen below. The cell viability was measured over a period of time to measure the toxicity of drugs.

6.3.1 *Ex vivo* buccal permeation studies

Before a buccal drug delivery system can be optimised, the permeation characteristics must be investigated to determine the feasibility of this route of administration for the delivery of the drug (OME) of interest. The permeability profile of OME from PEG plasticised MET films in the presence of L-arg is shown in figure 6.1.There was a lag period of about 20 minutes and then near linearity was observed up to 60 minutes of permeation which followed a first order kinetic mechanism. The total cumulative amount of OME permeating over 2 hrs was 275 ug/cm^2. This suggests that porcine buccal membrane is generally quite permeable and also confirms that the OME is released from the MET films. Another barrier to OME permeability in SS is the enzymatic degradation. SS contains moderate level of esterases, phosphatises and carbohydrases and due to biological variation. Due to poor physical contact with the pig buccal epithelial surface and/or possibly absence or very minimal volume of mucosal fluid (mucin) on the membrane, no significant covalent could be established. This is possible as the membrane was initially washed in a physiological fluid during preparation before mounting on the donor compartment of the Franz-type diffusion cell.

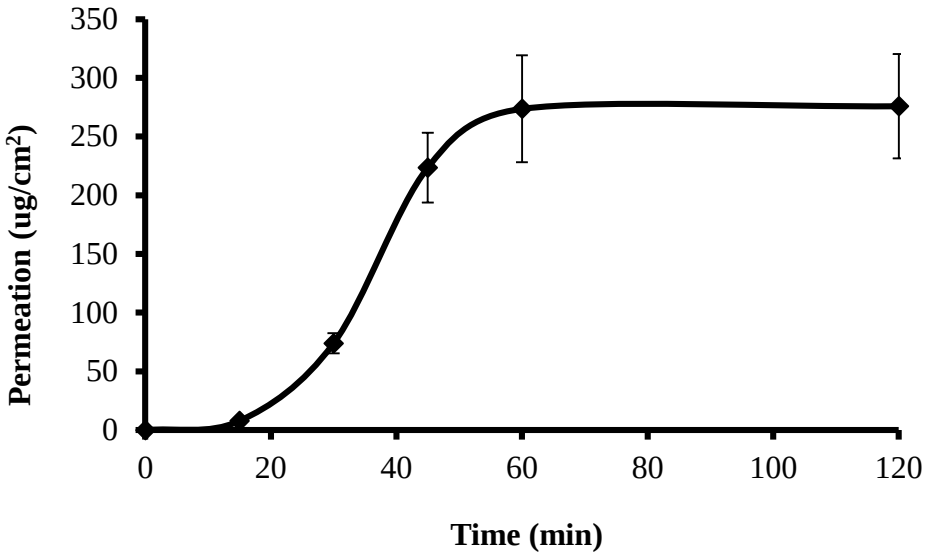

Figure 6.1 Cumulative permeation curve of OME released from MET film through pig buccal tissue (mean ± SD, (n=3))

6.3.2 *Ex-vivo* mucoadhesion evaluation using porcine buccal tissue

Films are considered one of the most suitable dosage forms for buccal administration (Nunn and Williams, 2005). The data collected suggest that the MET films can circumvent the short residence time of oral gels on the mucosa, which are easily washed away and removed by saliva.

Figure 6.2 illustrates the adhesive properties of the films compared for the three mucosal surfaces i.e. gelatine surface with PBS and SS and porcine epithelium. SS showed the lowest adhesive values compared to PBS equilibrated gelatine and porcine epithelium. In porcine buccal tissue the backing layer helps retard the diffusion of saliva into the hydrated film layer, thus prolong the adhesion time. Because the mucous was washed with Krebs buffer, the polymer adheres directly to the tissue surface rather than to mucous by means of covalent bonding (Miller et al., 2005).

The results (Figure 6.2) show that the MET DL film (PBS) had the highest cohesiveness which indicates the long distance (mm) travelled for the film. Porcine buccal tissue had the highest TWA which indicates the strong hydrogen bond interaction between the entangled polymer chains due to the presence of hydrogen bond forming groups such as OH and COOH. Also polymers that are hydrophilic in nature are able to form strong adhesive bonds

with mucosal membranes because the mucus layer contains large amount of water. Films on PBS equilibrated gelatine surface had a higher PAF (stickiness) values compared to SS equilibrated gelatine surface and porcine buccal tissue.

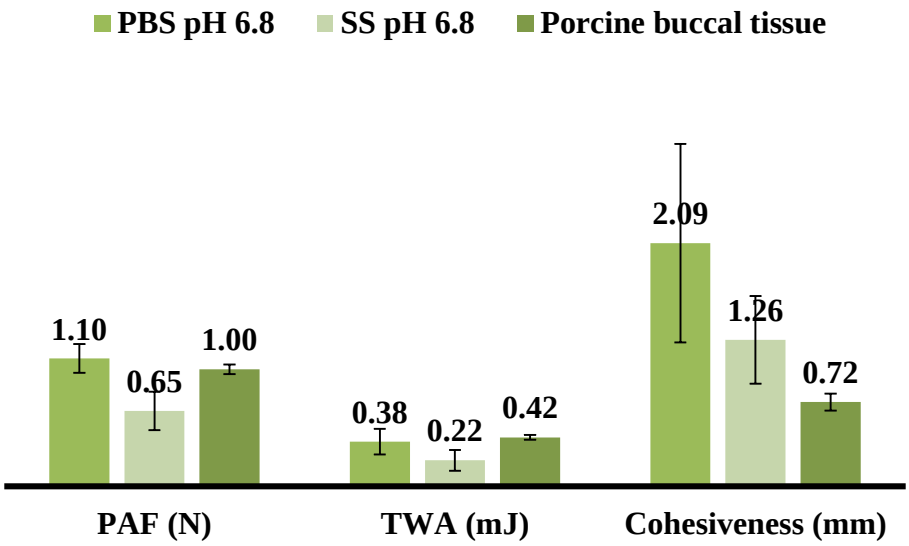

Figure 6.2: In-vitro mucoadhesion measurements of MET DL film containing 0.5% w/w PEG 400, OME: L-Arg 1:2 ratio and 20% v/v EtOH in PBS pH 6.8, SS pH 6.8 (gelatine surface) and epithelium of porcine buccal of PAF, TWA and cohesiveness (mean ± SD, (n=3))

6.3.3 Cell toxicity studies (MTT assay)

Tissue viability was assessed using 3-[4,5-dimethylthiazol-2-yl]-2,5 diphenyl tetrazolium bromide) (MTT) cytotoxicity study for pure OME, L-arg , BLK film (MET, PEG 400 (0.5% w/w, EtOH 20%) and DL film (MET, PEG 400 (0.5% w/w, EtOH 20%, and OME: L-arg 1:2). This is a reduction assay where yellow MTT was reduced to purple formazzan primarily by the action of enzymes which are located inside the mitochondria of the viable cells (Koschier et al., 2011). Figure 6.3 displays the respective cell viability data for the samples described above exposed to buccal tissue construct as measured by MTT assay. Cell death is typically assayed by quantifying plasma membrane damage.

The results as seen in figure 6.3 show a clear profile of the cytotoxity of the pure materials and DL films on adherent mammalian cells (Vero cells) with almost 100% cell viability confirming that the pure drug (OME), starting materials and the drug released from the DL films were non-toxic and can be employed for paediatric drug delivery. Data accumulated on

the level of cytotoxicity will help to prevent damage to cells and tissue during administration of drugs.

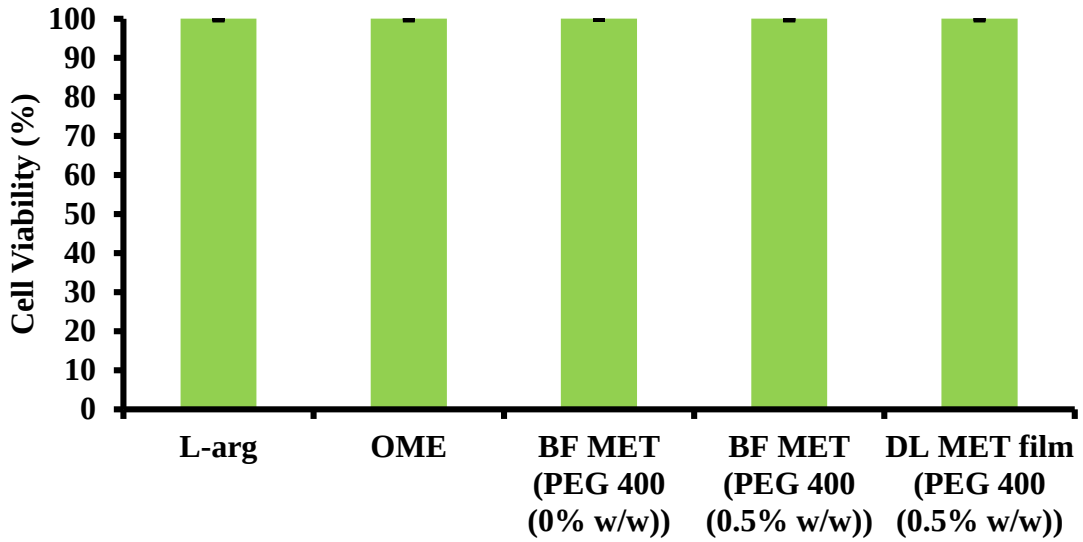

Figure 6.3 MTT assay results, showing cell viability showing pure OME, L-arg, BLK and DL films (mean ± SD, (n=3))

6.4 SUMMARY

There are several factors involved in determining the successful and safe application of polymers as drugs carriers in humans, with toxicity being a major and important factor. Kendall (2003) revealed that OME is generally regarded as a non-toxic drug. However, none of those literature have shown a clear profile on the complete absence of toxicity of OME on endothelial cells. Therefore this study was carried out for accuracy and confirmation purposes to be certain that OME posed no physical threats to endothelial cells when used as a drug carrier for potential application in paediatrics (Kendall, 2003).

The buccal mucosa, along with other mucosal has been under investigation as a potential site for controlled delivery of small molecules (butyric acid and butanol (Siegel et al., 1985)) therapeutic agents such as acyclovir (Shojaei et al., 1997), propranolol (Manganaro et al., 1996) and salicyclic acid (Gandhi et al., 1996)because of its accessibility and low enzymatic activity when compared to the gastro-intestinal tract. Another interesting advantage is its tolerance to potential sensitizers when compared to nasal mucosa and skin.

The porcine buccal membrane serves as an attractive site for systemic delivery in administration and testing of horseradish peroxidise and lanthum nitrate (Squier, 1984 and Hill, 1979). This is because of its inherent permeability similar to the human buccal mucosa. Therefore, porcine buccal mucosa was chosen as it resembles the human buccal mucosa more closely with regards to permeability, barrier lipid composition, histology and ultrastructure and organisation (Junginger et al., 1999).

The permeability of a tissue is related to its structure and highly permeable membranes such as that lining the guts, where absorption is an important function, tend to be single-layered epithelia. At the other extreme, one of the most important barriers against external environment, the skin tissues, are stratified and keratinised. The oral mucosa is intermediate between that of the epidermis and intestinal mucosa in terms of permeability. It is estimated that the permeability of the mucosa is 4-4000 times greater than that of the skin. There are considerable differences in permeability between different regions of the oral cavity because of the diverse structures and functions of the different parts of the oral mucosa. To ensure complete absorption of APIs in the oral mucosa region, permeation enhancers play an important role. Water soluble polymers achieve rapid disintegration which is an excellent property of the films in terms of convenience. The disintegration rate of the polymer is decreased by increasing the molecular weight of polymer film bases. (Siddiqui et al,.2011).

The active molecules administered through the buccal mucosa pass directly into the systemic circulation thereby minimising the first hepatic pass and other adverse gastro –intestinal effects. However, other significant advantages include lower enzymatic activity when compared with the GI tract, suitability for drugs such as OME which mildly and reversibly damage or irritate the mucosa, the possiblility to include permeation enhancers/ enzyme inhibitors or pH modifiers in the formulation (Figueiras et al., 2009) for the purpose of improving drug absorption and eventually bioavailability.

The MTT assay was used for quantitative colorimetric measurement of mammalian cell survival and proliferation. The original assay was modified to assess the viability of the tissue specimens. MTT is converted in viable cells to formazan by enzymes in active mitochondria. It was observed that the cell viability of the buccal mucosa after incubation remained 100% in all samples (Figueiras et al., 2008) implying the optimised OME loaded film formulations were safe and therefore suitable for use in children. Satishbabu (2008) reported that this

aspect can be further confirmed by measurement time, which is described as the most important characteristics of different mucoadhesive films.

Kulkarni and co-workers have studied the effect of experimental conditions (tissue storage condition and method of epithelium separation) on the performance of porcine buccal mucosa in assessing in vitro permeability. The permeability of model diffusants (antipyrine, buspirone, bupivacaine and caffeine) was significantly higher in the region behind the lip when compared to the cheek region because the latter has a thicker epithelium. Porcine buccal mucosa retained its integrity in Kreb's bicarbonate Ringer solution at 4 °C for 24 h while many other storage conditions such as storing tissues either in phosphate buffer saline pH 7.4 (4 °C), dry wrapped in aluminum (−20 °C) or cryoprotected in 20% glycerol solution (−20 °C) for either 6, 24 or 48 h resulted in loss of epithelial integrity (Patel et al 2012). This validates the treatment of the porcine buccal tissue obtained from the slaughter house in this study, which was immediately transferred into Kreb's bicarbonate Ringer solution as a valid approach to handling this type of tissue.

Further, Nicolazzo (2008) suggested that the most widely used *in vitro* methodology to study oral mucosal permeability is by testing drug permeation across isolated mucosal tissue mounted in permeability chambers. The use of diffusion cells makes it possible to determine the actual amount of drug that diffuses across the mucosal barrier as well as the rate of drug diffusion. Most commonly two types of permeability cells have been used: vertical (Franz diffusion cell) and side-by-side horizontal (using chambers) (Patel et al, 2012) with the former being employed in the current study.

6.5 CONCLUSIONS

It can be concluded that the OME buccal adhesive MET film could potentially be attached to human cheek without collapse based on the porcine buccal model employed in this study. The films stabilzed the drug and showed relatively fast drug permeability after release of OME. This is expected to ensure therapeutic bioavailability and therefore a useful alternative to oral administration via the GI tract as OME degrades rapidly in aqueous acidic medium. The adhesive properties suggest it will provide a long enough residence time in the cheek to allow high drug permeation and be relatively safe for continuous attachment in the cheek region.

CHAPTER SEVEN: FAST DISSOLVING FILM FROM SLOW RELEASE MET FILM USING SUPERCRITICAL FLUID (CO_2) TECHNIQUE

7.1 INTRODUCTION

The supercritical state was first reported in 1822 by Baron Gagniard de la Tour and in 1879 it was demonstrated that it also possessed solvating power (Sihvonen et al., 1999), but the technique was not used immediately. The process is achieved when the temperature and pressure of a substance is raised over its critical point, where distinct liquid and gas phases do not exist. Supercritical fluids (SCFs) are therefore defined as substances which are above their critical pressure (P_c) and temperature (T_c). It exists as a single phase which possesses properties of both liquid and gas. A number of different SCFs have been used in various applications such as organic synthesis, cleaning and materials processing. Technical and economic grounds is the unique combination of properties and attributes of SCFs most advantageously applied in developing improved processes and products:

- Where environmental compliance pressures will soon require a change in the process
- Where regulatory pressures will soon require a change in product purity
- Where increased product performance will soon be required
- Where an improved product can create a new market position and where none of these can be achieved by industry's more traditional industrial processes.

However carbon dioxide (CO_2) remains the most widely used in the application of SCFS because of the advantages such as being environmentally benign, non-toxic, non-flammable, non-corrosive and compared to the others CO_2 is readily available, affordable and it can be easily be removed from the reaction systems in comparison with organic solvents. Overall, supercritical CO_2 is an excellent solvent for many non-polar and some polar low molecular weight compounds and selected polymers for example the amorphous fluoropolymers and silicones as demonstrated in figure 7.1. CO_2 possesses a low T_c of (304.3 K or 31.15 ^oC) and P_c (7.38 MPa or 73.8 bar). The relationship between temperatures, pressure and the formation of a supercritical fluid for CO_2 can be understood by phase diagram in figure 7.2 (Ginty et al, 2005).

The technology of SCFs has been involved in the advancement of several pharmaceutical industry operations such as in crystallization, particle size reduction, preparation of drug delivery systems, coating and product sterilisation. It has been observed to be a practicable option in the formulation of particulate drug delivery systems such as microparticles, nanoparticles and polymer/drug dissolved in films which control drug delivery (Falk et al,. 1997).

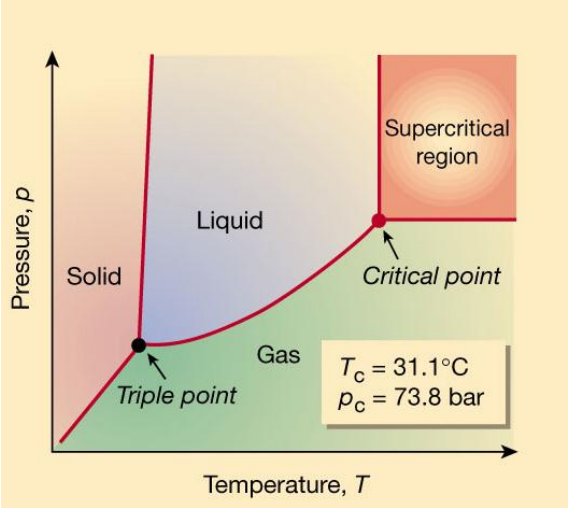

Figure 7.1 Phase diagram for CO_2, showing the critical point and the supercritical region.

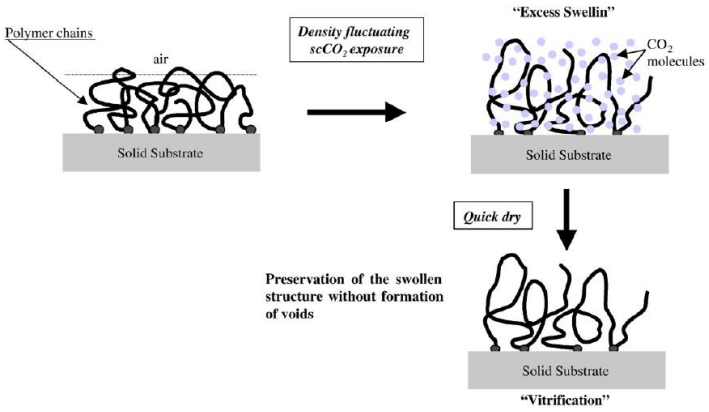

Figure 7.2 Schematic concept of the supercritical carbon dioxide ($scCO_2$) –based processing for achieving low-density polymer thin films

The aim of this chapter was to investigate the effect of supercritical CO_2 ($scCO_2$) on BLK and DL MET films and comparing their properties with the non-treated optimised films described in previous chapters by using various analytical techniques as described in chapters two and three. The scCO2 treated and non-treated films have been characterised for their hydration and adhesive properties and OME dissolution as well as release kinetics.

7.2 MATERIALS AND METHODS

7.2.1 Materials

Table 7.1 List of materials used

Name	Batch Number	Purity	Company	Location
Ethanol	1405343	-	Fisher Scientific	Loughborough, UK
Metolose (MET)	311615		Shin Etsu	Stevenage, Hertfordshire, UK
PEG 400	A0210931	-	Sigma Aldrich	Gillingham, UK
Omeprazole (OME)	PWAMM-HK00359	98%	TCI	Tokyo, Japan
L-Arginine (L-arg)	MKBN277V	98%	Sigma Aldrich	Gillingham, UK
Potassium dihydrogen phosphate	073346	100%	Fisher Scientific	Leicester, UK
Gelatine	1411655	-	Sigma-Aldrich	Gillingham, UK

7.2.2 Consumables

Table 7.2 List of consumables

Consumable	Company	Location
Blue, white and yellow micropipette tips	Fisher Scientific	Loughborough, UK
Magnetic stirrer	Fisher Scientific	Loughborough, UK
Tzero hermetic pans and lids	TA Instruments	Crawley, UK
SEM stubs	Agar Scientific	Essex, UK

7.2.3 Instruments

Table 7.3 List of instruments used

Instruments	Suppliers
Supercritical fluid (SCF) instrument	Thar Technologies Inc.
TA HD Plus texture analyser	Stable Micro System Ltd, Surry, UK
DSC Q2000	TA Instruments, Crawley, UK
Q5000-IR Thermogravimetric Analyser	TA Instruments, Crawley, UK
Hitachi SU 8030 SEM	Hitachi High-Technologies, Tokyo, Japan
D8 Advantage X-ray diffractometer	Bruker, Coventry, UK
Perkin Elmer spectrophotometer	Spectrum Two, Perkin Elmer, US
Tzero sample encapsulation press	TA Instruments, Crawley, UK

7.2.4 METHODS

7.2.4.1 Preparation of BLK and DL solvent cast films

Methods used for this experiment are described in chapters two and three, sections 2.2.4.1 and 3.2.4.1.

7.2.4.2 Supercritical fluid (CO_2) treated films

All the experiments were performed with a Thar Technology Inc instrument. BLK and DL films were cut (2cm x 2cm) and were placed in a glass vial (so the film stays in its place when CO_2 enters the vessel), the glass vial placed in the reaction vessel. The reaction vessel was heated to 40 °C after which the CO_2 was pumped into the reaction vessel until the required pressure (100 bars) was achieved. The CO_2 was allowed to flow continuously at 100 g/min for 2 hrs and the CO_2 pump was stopped and the remaining CO_2 in the reaction vessel depressurized by the control of Automated Back Pressure Regulator (ABPR). After all the CO_2 escaped, the reaction vessel was opened, the sample taken out, digitally photographed and kept for further investigations.

7.2.4.3 Differential scanning calorimetry (DSC)

Methods used for this experiment was to measure melting point (T_m) and glass transition (T_g) for BLK and DL films are as discussed in chapters two and three, sections 2.2.3.4 and 3.2.4.5 and respectively.

7.2.4.4 Thermogravimetric analysis (TGA)

Methods used for this experiment was to measure water content of BLK and DL films as discussed in chapters two and three, sections 2.2.3.5 and 3.2.4.6 respectively.

7.2.4.5 Scanning electron microscopy (SEM)

Methods used for this experiment to measure surface morphology, check for film uniformity and the presence of any cracks of the BLK and DL films were as discussed in chapters two and three, sections 2.2.3.6 and 3.2.4.7.

7.2.4.6 X-ray diffraction (XRD)

Methods used for this experiment was to measure physical nature (crystalline or amorphous) of the BLK and DL films as discussed in chapters two and three, sections 2.2.4.7 and 3.2.4.8.

7.2.4.7 Fourier transform infrared (FT-IR) spectroscopy

Methods used for this experiment was to measure the interaction of polymer and drug in BLK and DL films as discussed in chapter two and three, section 2.2.4.8 and 3.2.4.9.

7.2.4.8 Hydration capacities

Methods used for this experiment was to measure drug release capacity as discussed in chapter four, section 4.2.3.1.

7.2.4.9 Mucoadhesion

Methods used for this experiment was to measure the mucoadhesive strength of BLK and DL films (peak adhesive force (PAF) required to separate the film from the mucosal surface was determined by the maximum force. The area under the curve (AUC) representing the total work of adhesion (TWA) was estimated from the force-distance plot whiles the cohesiveness of the sample was determined) as discussed in chapter four section 4.2.3.2.

7.2.4.10 *In vitro* release of OME using Franz-type diffusion cell

Methods used for this experiment was to investigate the drug dissolution profiles of the $scCO_2$ treated DL films compared to the non-treated DL films of the drug as discussed in chapter five, section 5.2.3.1.

7.3 RESULTS AND DISCUSSION

7.3.1 Supercritical fluid (CO_2) treated films

The preliminary observation of the physical characteristics of the formulated films treated in $scCO_2$, showed a slight difference in the colour and apparent physical strength of the films (BLK and DL). BLK films showed rough surface whereas DL films were slightly yellow in colour but both films remained tough as shown in figure 7.3 and 7.4.

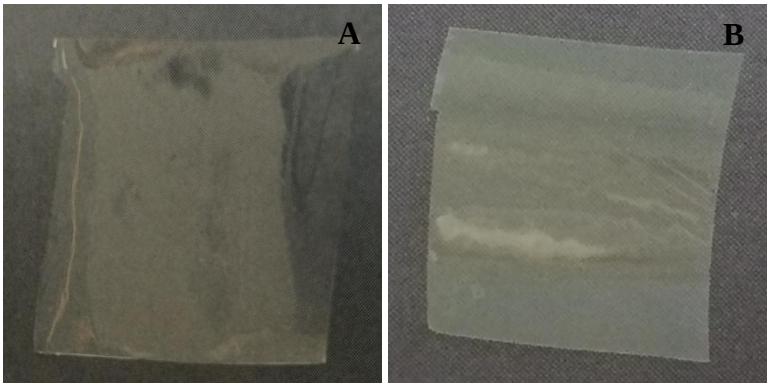

Figure 7.3 Non treated BLK (A) and DL MET (B) films

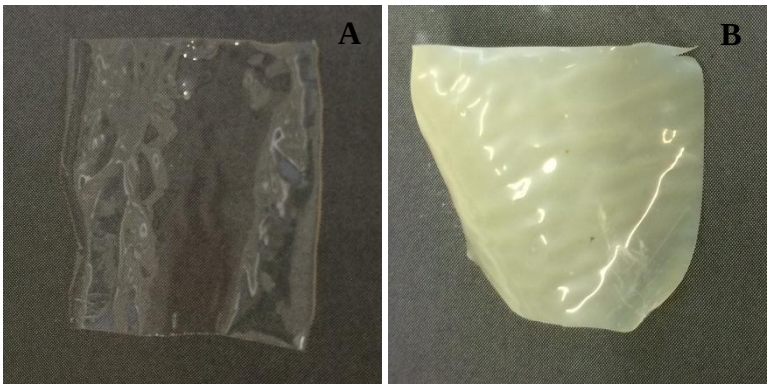

Figure 7.4 BLK (A) and DL MET (B) films treated in $scCO_2$

7.3.2 Differential scanning calorimetry (DSC)

Figure 7.5 and 7.6 respectively show the thermograms of BLK and DL MET films treated in SCF compared with non SCF treated original films previously discussed in chapter two and three, section 2.3.4 and3.3.4.

In figure 7.5 the thermogram of BLK film treated in $scCO_2$ was characterised by broader endothermic peak at 56.57 °C, which can be attributed to evaporation or loss of water and no definite melt or glass transition peaks was obtained and was similar to that of non-treated BLK film which showed a peak at 56.67 °C as shown in table 7.4. It is possible that the water for the scCO2 treated film may have been picked up during sample preparation for DSC analysis. In figure 7.6 the thermograms of DL film treated in $scCO_2$ also showed a broad endothermic peak at 63.31°C which can be attributed to evaporation or loss of water and no definite melt or glass transition peaks, followed by another endothermic peak at 133.49 °C, indicating the melting of potentially recrystallized OME. This is different from the non-treated DL film which showed a broad peak at 83.41 °C, followed by another endothermic peak at 151.82 °C as shown in table 7.4.

The $scCO_2$ treatment seems to have enhanced the ease at which water molecules are removed (hence lower dehydration temperature) and also seems to have resulted in crystals with lower melting points. The presence of the crystals were subsequently confirmed with SEM and XRD (see below). The lower enthalpy points observed for the melting process for the films generated by $scCO_2$ compared to the non-treated film suggest the presence of a different crystalline form. The SCF process generates a film matrix that allows quick evaporation of moisture, through the preservation of the swollen structures (Gin et al., 2009).

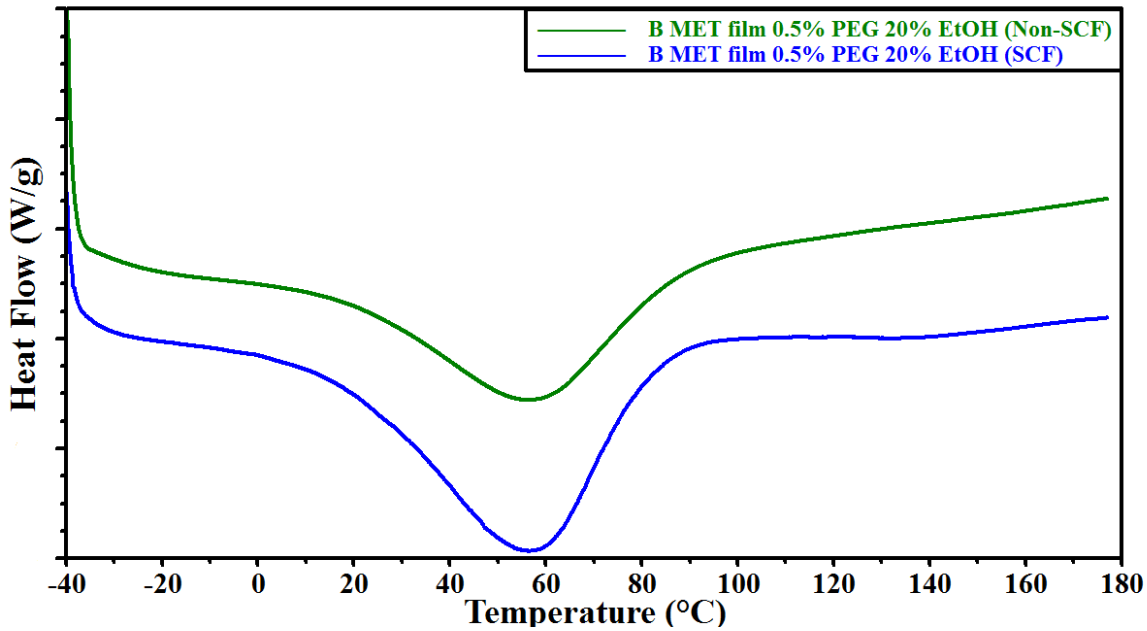

Figure 7.5 DSC thermogram of BLK MET films prepared from ethanolic gel (20% of EtOH) and PEG 400 (0.5% w/w) treated with and without $scCO_2$ (W/g (Watts/gram))

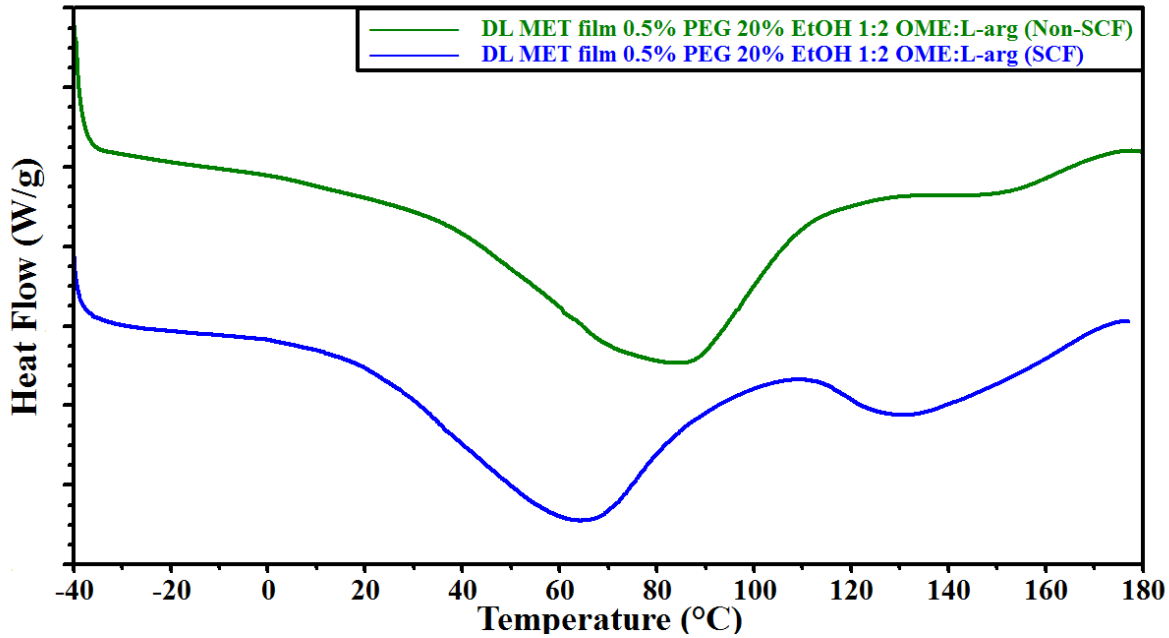

Figure 7.6 DSC thermogram of DL MET films prepared from ethanolic gel (20% of EtOH), PEG 400 (0.5% w/w) and OME: L-arg (1:2) treated with and without SCF (W/g (Watts/gram))

Table 7.4 Temperature and heat changes observed for the endothermic transitions observed (MET films treated with and without SCF).

	1st TRANSITION			2nd TRANSITION		
Gels	**Onset °C**	**Peak °C**	**ΔH (J/g)**	**Onset °C**	**Peak °C**	**ΔH (J/g)**
BLK, MET, 0.5% w/w PEG, 10% v/v EtOH, Non-SCF	6.32	56.67	106.40	-	-	-
BLK, MET, 0.5% w/w PEG, 10% v/v EtOH, SCF	16.65	56.57	97.92	-	-	-
DL, MET, 0.5% w/w PEG, 20% v/v EtOH, Non-SCF	30.48	83.41	141.00	130.68	151.82	5.77
DL, MET, 0.5% w/w PEG, 20% v/v EtOH, SCF	19.29	63.31	110.00	113.03	133.49	30.18

7.3.3 Thermogravimetric analysis (TGA)

As discussed in chapter two and three, TGA was used to determine the residual moisture content (%), dynamic weight loss and degradation temperature of the BLK and DL MET films treated with and without SCF.

As seen in table 7.5 the greater percentages of weight loss were observed in SCF treated DL MET film at 5.91 % which was 0.77% (p = 0.0054 very statistically significant) greater than non SCF treated DL MET film. In the SCF treated BLK MET film, the residual moisture was 3.16 % which was greater by 1.17 % than the non-SCF treated. This indicates that the BLK and DL films goes through quick evaporation which permit the weight loss percentage, whereas when treated with SCF this result in higher residual water. This could be due to the generation of relatively higher free volume in the films when using SCF.

Table 7.5 Thermal transition with weight loss observed for DL MET films from ethanolic (20 % v/v EtOH), PEG 400 (0.5 % w/w) gels containing OME: L-arg (1:2) treated with and without SCF.

Gels	**Weight loss (%)**
BLK MET, 0.5% w/w PEG, 20% v/v EtOH (Non-SCF)	1.99
BLK MET, 0.5% w/w PEG, 20% v/v EtOH (SCF)	3.16
DL MET, 0.5% w/w PEG, 20% v/v EtOH, OME: L-arg (1:2) (Non-SCF)	5.14
DL MET, 0.5% w/w PEG, 20% v/v EtOH, OME: L-arg (1:2) (SCF)	5.91

7.3.4 Scanning electron microscopy (SEM)

The surface morphology and topographic characteristics of BLK and DL MET films cast from gels prepared with ethanolic solvent (20% v/v EtOH), PEG (0.5% w/w) containing, drug (OME) and stabilizer (L-arg) ratio (OME:L-arg 1:2), were evaluated using SEM. Figure 7.7 shows microscopic appearance of pure OME and L-arg. Figure 7.8 showed rough surfaces with some lumps for BLK film treated in SCF compared to BLK film not treated with SCF. Microscopic appearance of BLK showed continuous sheets with relatively smooth and homogeneous surfaces and confirmed that all the components were uniformly mixed during gel formation as discussed in chapter 2 section 2.3.6 ((image 2.20) (0.5 % w/w PEG)). This indicates that $scCO_2$ had effect on the film matrix between the polymers network (MET)

and plasticizer (PEG 400). Figure 7.9 showed rougher surface with a lot of crystals visible on the surface in the DL film treated in SCF compared to the DL film that wasn't treated in SCF, which in turn showed a smoother and homogenous uniform surface shown in chapter 3 section 3.5.5 (image 3.30 (20% v/v EtOH)). Such differences in surface topography could be attributed to CO_2 entering the film matrix and drying the film which causes the drug to recrystallize in solid state (Lan et al., 2011).

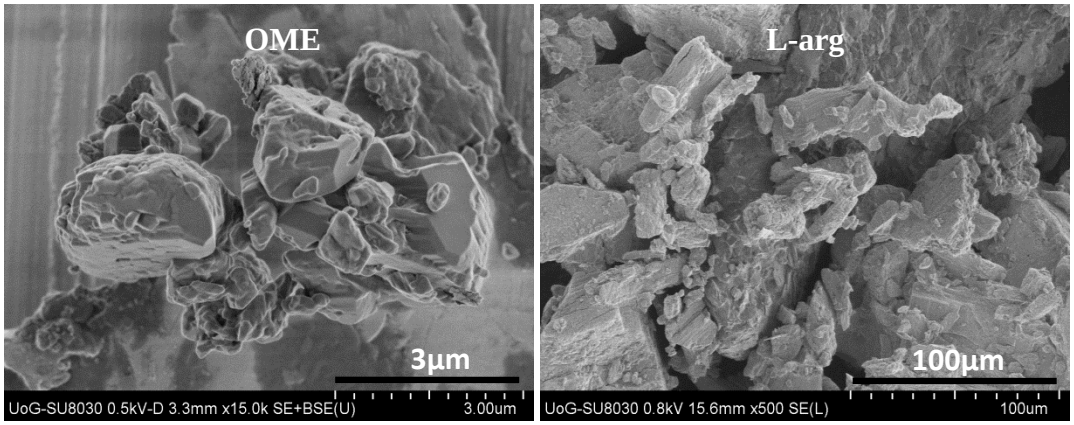

Figure 7.7 SEM micrograph of pure materials (OME (drug) x15.0 and L-arg (stabilizer) x500)

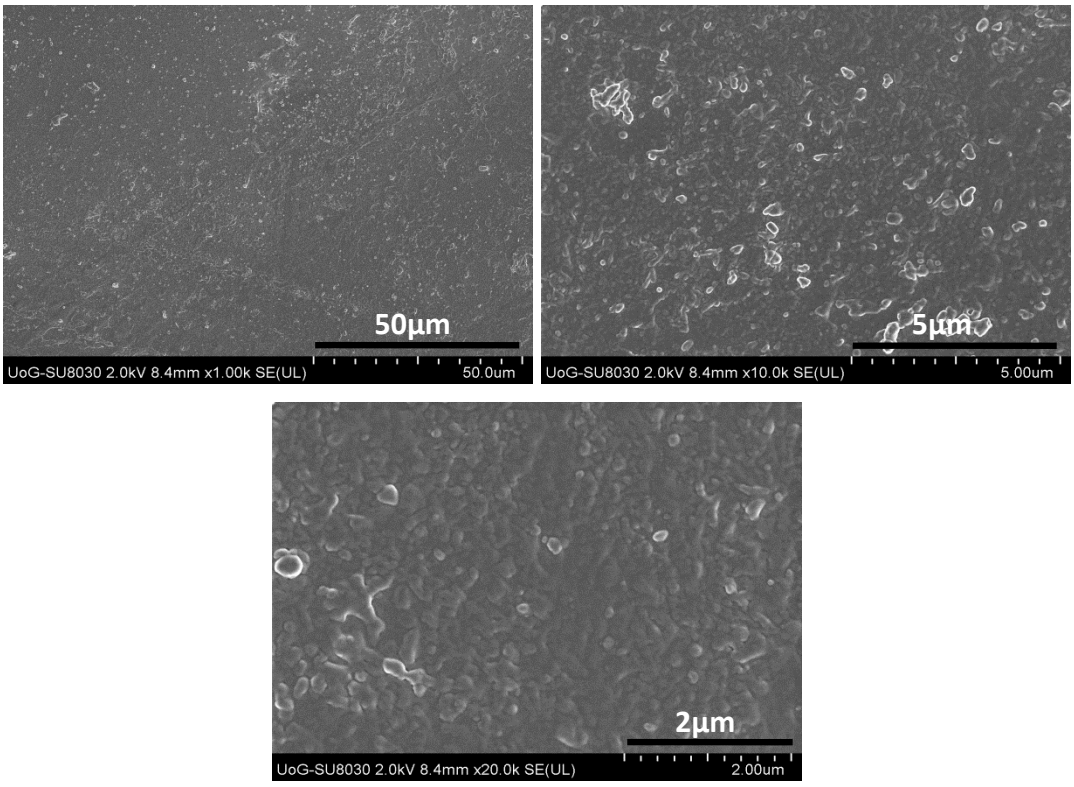

Figure 7.8 SEM micrograph (x20.0) of $scCO_2$ treated BLK MET films cast from ethanolic (20% v/v EtOH) gels containing 0.5% w/w PEG 400.

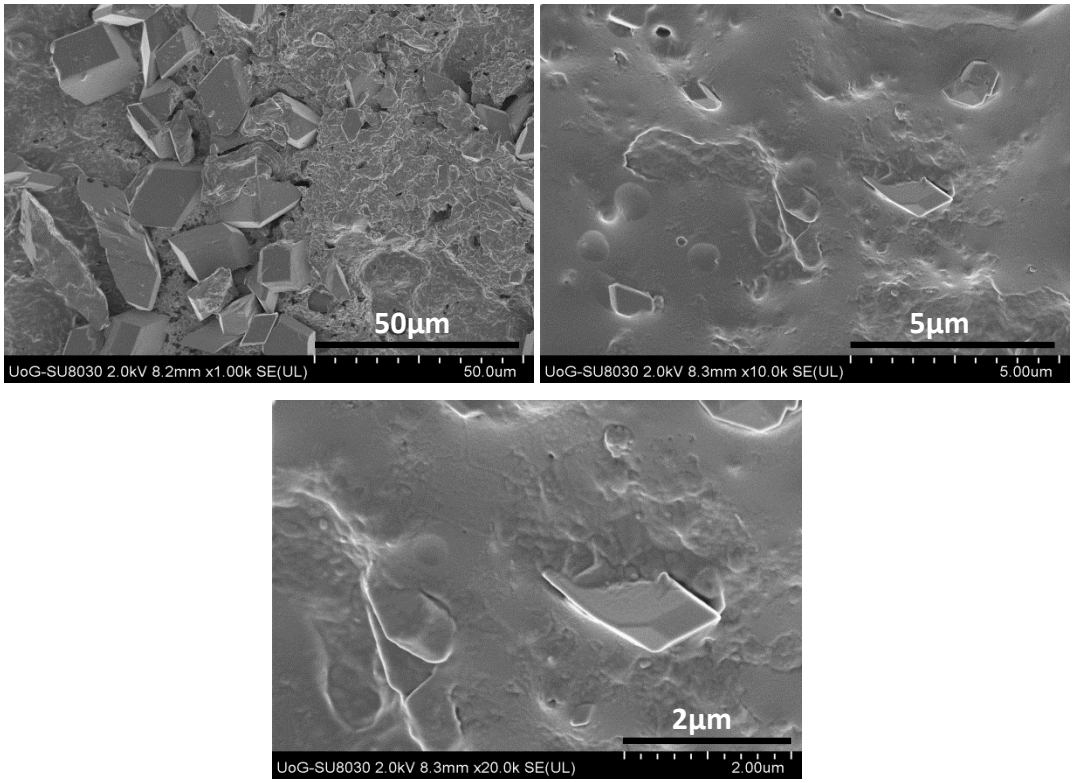

Figure 7.9 SEM micrograph (x20.0) of $scCO_2$ treated DL MET films cast from ethanolic (20% v/v EtOH) gels containing 0.5% w/w PEG 400 and OME: L-arg (1:2).

7.3.5 X-ray diffraction (XRD)

XRD analysis was performed to determine the crystalline - amorphous ratio and confirm the physical form of the various components within the films.

Figures 7.10 and 7.11, shows the XRD diffractograms of MET BLK and DL films with and without SCF treatment. The results demonstrate that in BLK film there was no difference observed between the film treated with SCF and non-treated equivalent, whereas DL MET film treated with SCF indicated 5% of crystallinity compared to non-treated SCF which showed complete amorphous nature as explained in chapter three section3.3.7. The crystallinity of DL MET film treated in SCF in figure 7.11 (2-theta peak 9˚ and 24˚) confirms the DSC and SEM results.

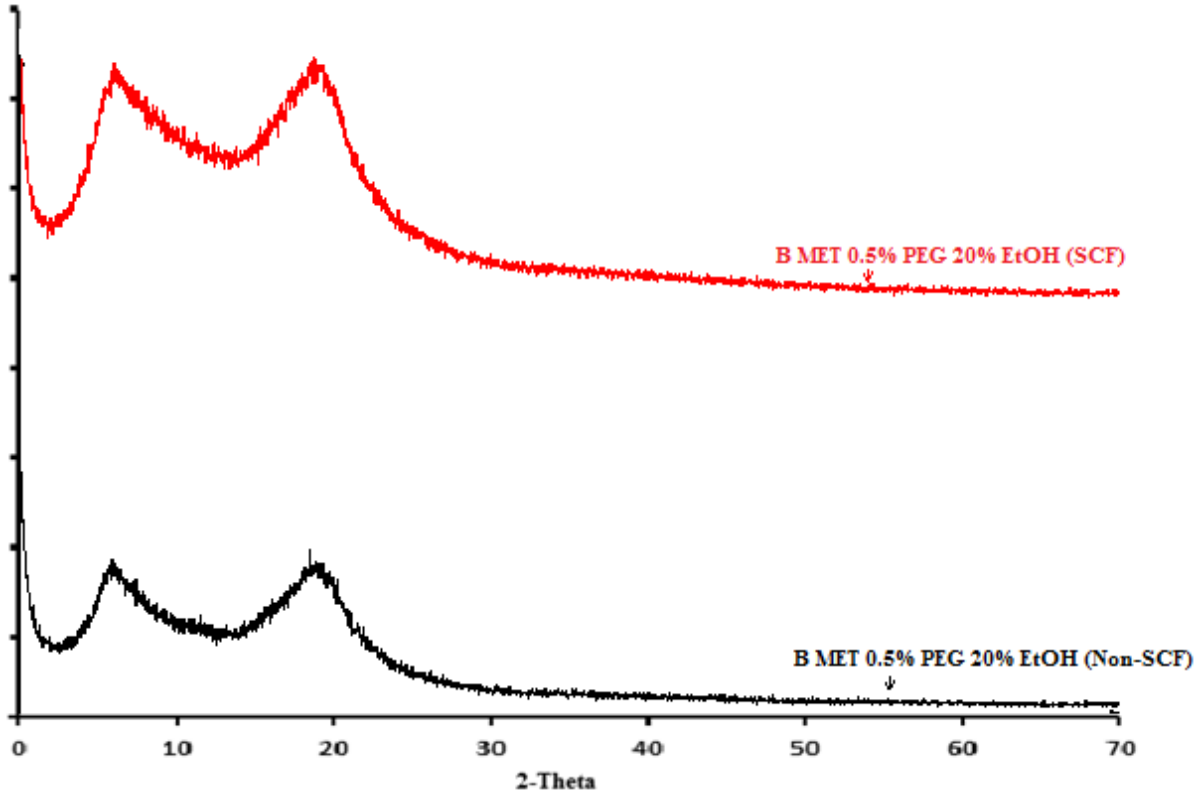

Figure 7.10 XRD diffractogram for BLK MET films cast from ethanolic gels (20% v/v EtOH) containing 0.5% w/w PEG 400 with and without SCF treatment.

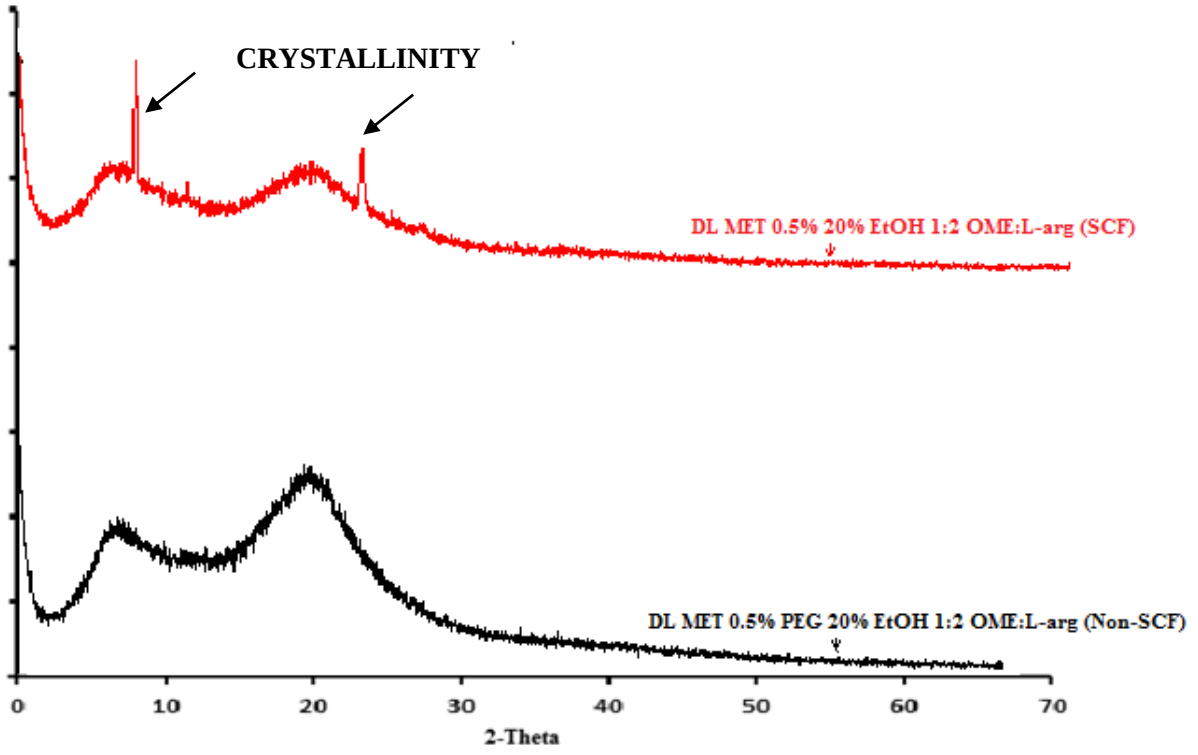

Figure 7.11 XRD diffractogram for DL MET films cast from ethanolic gels (20% v/v EtOH) containing 0.5% w/w PEG 400 treated with and without SCF.

7.3.6 Fourier transform infrared (FT-IR) spectroscopy

The principles and mechanism of (FT-IR) was discussed previously in chapter 1. The FT-IR spectra of MET, OME, L-arg, PEG 400 and EtOH are already shown in tables 2.10 and 3.10, figure 3.36 in chapters two and three respectively.

Figures 7.12 and 7.13 show the FT-IR spectra for BLK and DL MET films treated with and without SCF. There were slight changes observed in SCF films compared to non-SCF films as shown in the summarised major peaks in tables 7.6 and 7.7. This indicated that the physical property of OME did change and the hydrogen bonds between the polymer and PEG as well as with the drug did change.

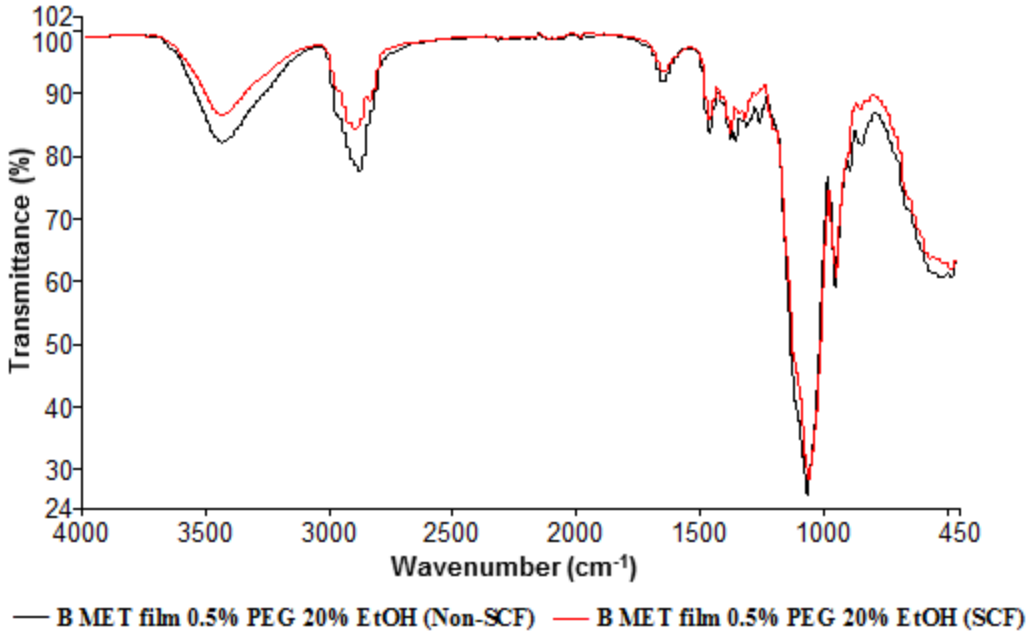

Figure 7.12 FT-IR spectra of BLK MET films cast from ethanolic (20% v/v EtOH) gel containing 0.5% w/w PEG 400 with and without SCF treatment.

Table 7.6 Major FTIR peaks of interests for BLK MET films plasticised from 20% EtOH

Peak No.	(cm^{-1})	(%T)	Peak No.	(cm^{-1})	(%T)	Peak No.	(cm^{-1})	(%T)
Non-SCF treated								
1	3436.89	82.77	2	2876.04	78.65	3	1454.96	84.38
4	1349.02	82.95	5	1057.70	24.61	6	944.92	58.75
SCF treated								
1	3445.31	86.97	2	2899.32	84.70	3	1642.42	93.99
4	1454.86	86.28	5	1374.15	83.93	6	1314.06	86.33
7	1053.56	27.98	8	944.97	60.73			

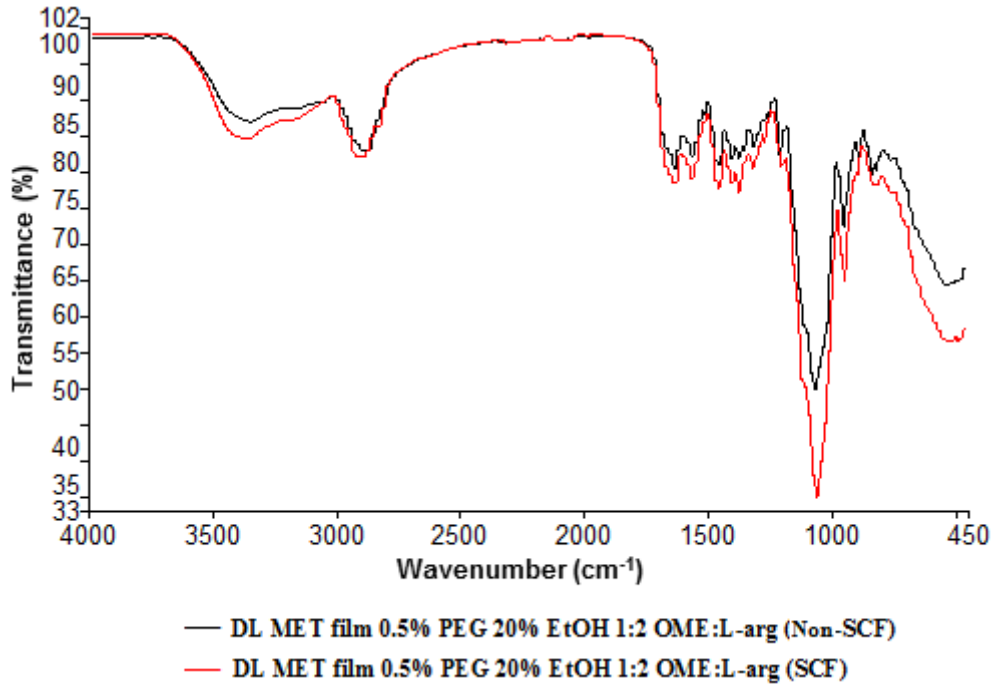

Figure 7.13 FT-IR spectra of DL MET films cast from ethanolic (20% v/v EtOH) polymeric gel containing 0.5% w/w PEG 400 and OME: L-arg (1:2) with and without SCF treatment.

Table 7.7 Major FTIR peaks of interests for DL MET films plasticised from 20% EtOH (OME: L-arg 1:2)

Peak No.	(cm-1)	(%T)	Peak No.	(cm^{-1})	(%T)	Peak No.	(cm^{-1})	(%T)
Non-SCF treated								
1	3436.11	87.32	2	2877.31	83.30	3	1628.42	80.65
4	1554.01	81.28	5	1406.59	81.93	6	1204.25	82.33
7	1059.40	49.64	8	945.33	72.55			
SCF treated								
1	3374.27	85.32	2	2926.33	82.47	3	1630.45	78.84
4	1561.06	79.46	5	1453.21	78.15	6	1404.00	78.84
7	1375.02	77.62	8	1310.40	80.89	9	1055.37	34.88
10	945.78	65.01						

7.3.7 Hydration capacities

In chapter 4 section 4.3.1 the concept and mechanism of hydration capacities was discussed in detail. BLK and DL MET films cast from gels prepared with solvent (20% v/v EtOH) with PEG (0.5% w/w) containing, drug (OME) and stabilizer (L-arg) ratio (OME: L-arg 1:2), showed swelling index of 1841 % for BLK film and 2630% for DL film in 20 minutes. After 20 minutes the DL films start losing its swelling capacity.

From the result obtained in table 7.8, MET BLK and DL film treated in SCF showed swelling index 24.8 and 36.5 seconds. The reason why swelling profile was recorded in seconds (sec) and not in percentage (%) was because as soon as the film got in contact with the PBS (pH 6.8) it started to disintegrate and eventually dissolved and no swelling % could be accurately recorded. This indicates that drug release in the mucosa will be more rapidly achieved. The main step of SCF consists of the anomalous swelling of polymer thin films due to the density fluctuation in $scCO_2$ within the film matrix. Good miscibility between the SCF and polymer enhances swelling effect and "CO_2-philic" polymers are known to have favourable free energies of mixing with CO_2 (Li et al, 2007) (Pham et al, 2003).

Table 7.8 Swelling profiles of SCF treated BLK and DL MET films cast from ethanolic (20% EtOH) gels containing 0.5% w/w PEG 400 and OME: L-arg (1:2) (mean ± SD, n=3))

Film	Time (sec)			
	1	2	3	Ave
BLK	25.0	24.0	25.5	24.8
DL	37.5	35.0	37.0	36.5

7.3.8 Mucoadhesion

The results (figures 7.14 and 7.15) show that in all cases, the non-treated BLK and DL films recorded higher adhesive values (cohesiveness, PAF and TWA).

Figure 7.14 shows results for BLK film treated with and without SCF showing that PAF (stickiness) not quite statistically significant ($p = 0.0808$). However no statistically significant difference was observed in TWA ($p = 0.2541$) and cohesiveness ($p = 0.3084$).

Figure 7.15 shows results for DL film treated with and without SCF recorded that PAF (stickiness) was statistically significant ($p = 0.0042$). However no statistically significant difference was observed in TWA ($p = 0.111$) and in cohesiveness ($p = 0.6023$).

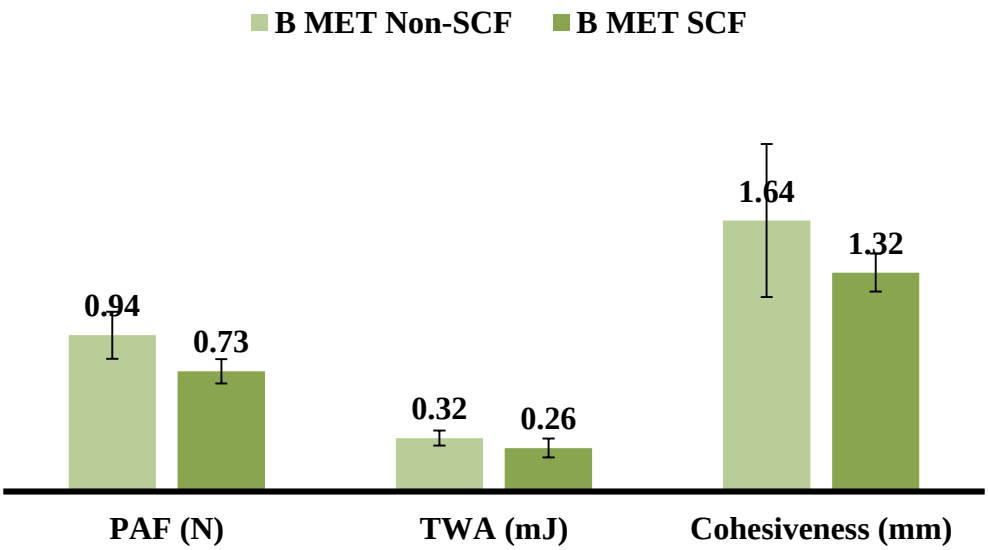

Figure 7.14 *In-vitro* mucoadhesion measurements of BLK MET film prepared from gels containing 0.5% w/w PEG 400, OME: L-Arg 1:2 ratio, using 20% v/v EtOH with and without SCF treatment (mean ± SD, n=3))

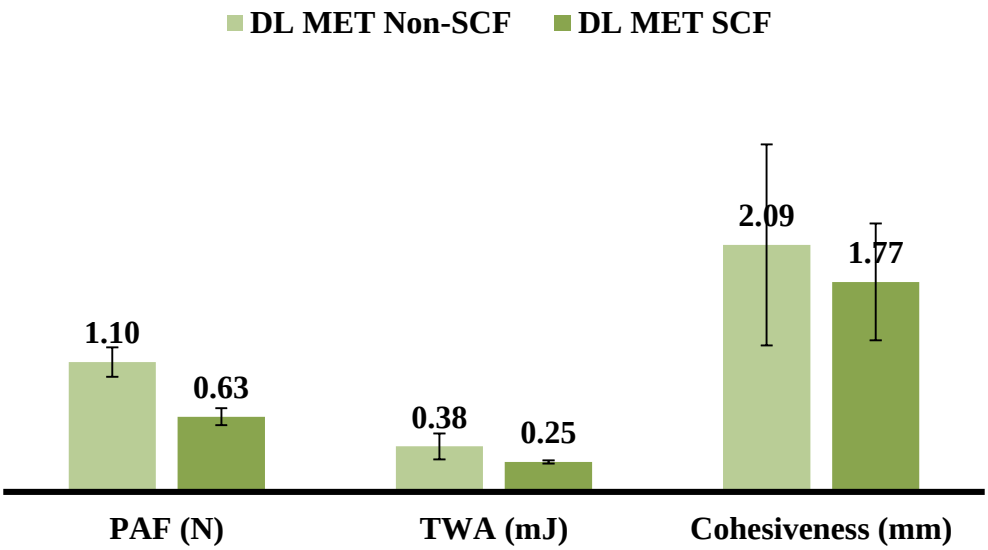

Figure 7.15 *In-vitro* mucoadhesion measurements of DL MET film prepared from gels containing 0.5% w/w PEG 400, OME: L-Arg 1:2 ratio, 20% v/v EtOH with and without SCF treatment (mean ± SD, n=3))

This is due to strong interaction (hydrogen bonding) between the polymer (MET) and the PBS (pH 6.8 mimicking simulated saliva conditions), also less free hydrogen bonding sites leading to higher hydration for TWA and PAF. Li and co-workers noted that "the low cohesive energy density of CO_2 would account for excess CO_2 in the interfacial region of the

polymer at CO_2/polymer interface between the film and the mucoadhesive surface" (Li et al, 2007).

7.3.9 *In vitro* release of OME using Franz-type diffusion cell

Figure 7.16 shows the dissolution profile of DL MET film treated in SCF in PBS (pH 6.8). SCF treated DL showed higher cumulative release (94%) over 10 minutes than DL non SCF treated (70%) over 60 minutes. The high cumulative release in SCFDL film is related to rapid disintegration of the film, the comparative difference in solubility of the OME as well as the interaction between the polymers and PEG 400. The control release of OME from the non-treated film could be attributed to the initial swelling of the polymeric network of MET which controls the diffusion of drug into the dissolution medium.

The rapid disintegration of the DL films treated with SCF could be explained by the swelling and hydration compared with the non-treated films which swelled over a long period. This implies that SCF treated films hydrate very rapidly and eventually disintegrating (10 minutes) to release the drug more rapidly than the non-treated films.

However it is clearly evident that graph 7.16 demonstrates three phases of release. The first phase up to 1 minute released 30% of the drug, the second phase from 1 to 10 minutes released total of 90% before it plateaus. The different phases suggests different mechanisms may be at play during dissolution most likely hydration followed by drug diffusion and eventually erosion/disintegration which 'dumps' most of the drug into the medium during the second phase as shown from the Korsmeyer kinetics results below.

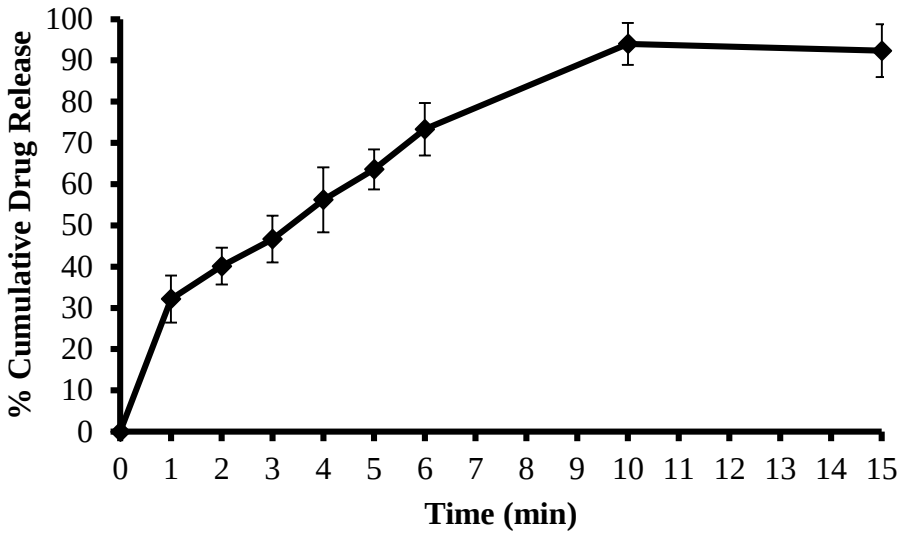

Figure 7.16 Drug dissolution profile showing cumulative percent release against time of OME from DL MET films prepared from ethanolic (20% EtOH) gel containing 0.5% w/w PEG 400, OME: L-Arg (1:2) and treated in SCF (mean ± SD, n=3))

7.3.10 Kinetic release mechanisms

The mass transport mechanism which determines the drug release characteristics is provided by mathematical models of release kinetics. In polymeric matrix such as solvent cast films swelling, solute diffusion and matrix degradation are proposed as the main forces responsible for drug release (Fu and Kao 2010). OME release from the film was assessed by determining the best fit of percentage cumulative release versus time data to zero order, first order, Higuchi and Korsmeyer-Peppas equations (coefficient, R^2 values) as shown in figures 7.17 and table 7.9.

The release kinetics of OME in PBS (pH 6.8) treated in SCF followed Higuchi model as the R^2 value (0.9932) was the highest compared to other models. This suggests drug release from a monolithic system whereby drug particles are dispersed uniformly throughout the matrix which is dependent upon the diffusion. The 'n' values from the Korsmeyer-Peppas equation, describe the diffusion state or release exponent used for elucidation of the drug release mechanism and outlined in table 7.9. Analysis of the experimental data using kinetic equations and interpretations of the release exponents (n) gives a better understanding of the controlling release mechanism. OME release data from DL MET film treated in SCF gave an n value of 0.4 which is less than 0.45 and indicates that the drug release follows non-Fickian

diffusion mechanism. This suggests that the OME was released through the hydrated polymer via diffusion combined with and erosion controlled drug release.

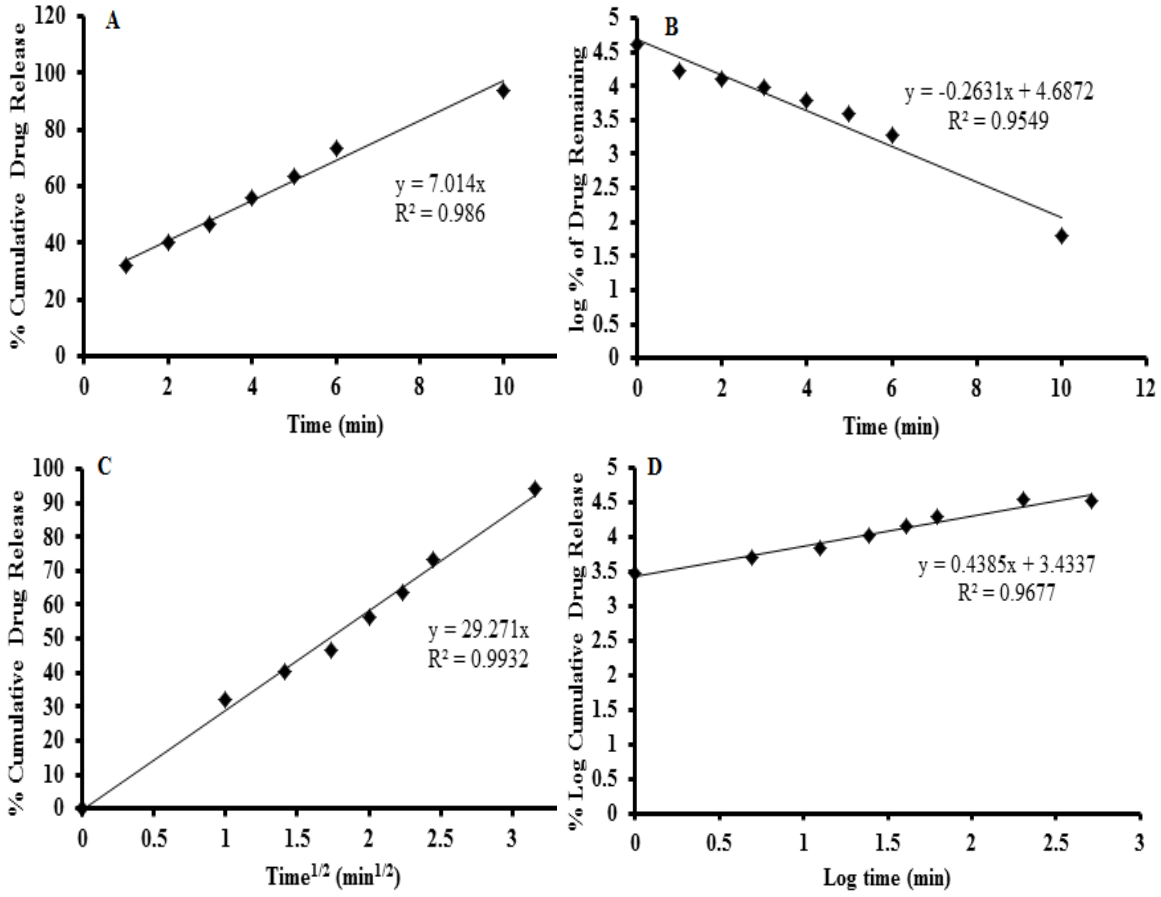

Figure 7.17 Representative release plots obtained by fitting experimental release data of OME from DL MET films treated in SCF to (A) zero order kinetic, (B) first order kinetic, (C) Higuchi kinetic, (D) Korsmeyer-Peppas kinetic models/equation.

Table 7.9 Release parameters obtained from fitting experimental drug dissolution (release) data to different kinetic equations for SCF treated films containing OME in PBS.

	Zero order		First order		Higuchi		Korsmeyer-Peppas		
OME	K_0 (% min^{-1})	R^2	K_1 (min^{-1})	R^2	K_H (% $min^{-1/2}$)	R^2	K_P (% min^{-n})	n	R^2
DL PBS (pH 6.8)	7.014	0.986	-0.2631	0.9549	29.271	0.9932	3.4337	0.4	0.9677

K_o, K_1, K_H, K_p are the release rate constant for zero order, first order, Higuchi and Korsmeyer-Peppas models, R^2 is the correlation coefficient and n is the release exponent.

In summary, supercritical fluid technology have established application in the production and processing of fast oral dissolving film and is now considered to be an innovative and promising way to design and modify pharmaceutical drug delivery. Carbon dioxide (CO_2) use as a supercritical solvent enabled the achievement of the supercritical region at moderate conditions of pressure and temperature to permit maximum dryness of the film. Supercritical applications are being developed for pharmaceuticals and biopharmaceuticals.

7.3.11 Comparison of release profiles

In this study, the time to release 20% of the drug original loaded ($t_{20\%}$) and the percentage cumulative release at 15 minutes (t_{15min}) were used to compare the treated and non-treated formulations (Costa et al, 2001). The time to 20% release $t_{20\%}$ of initial amount of OME present various for each media as seen in table 7.10. The results showed that SCF treated DL film released 20% of OME within 0.6 minutes whereas non-treated SCF DL film took 5.5 minutes to release the same percentage of the drug. However within the 15 minutes, non-treated DL film released up to 55% and whilst treated SCF DL film released 92% of drug within 15 minutes which is a significant difference and goes to confirm the conversion of a relatively slow release formulation to rapid disintegration film after treatment with SCF.

Table 7.10 A comparison of the effect of OME on the time to release 20% ($t_{20\%}$) of drug from each DL films and the effect of mean cumulative percentage of OME released at 60 minutes ($t_{60\ min}$) in PBS and SS films

DL MET films media	Time to release 20% of drug ($t_{20\%}$)	Mean % release at 15 min (t_{15min})
	Films	
PBS (non-treated SCF DL film)	5.5	55
PBS (treated SCF DL film)	0.6	92

7.4 SUMMARY

There are several important issues to take into account when $scCO_2$ is used as a polymerization solvent because CO_2 is an ambient gas with drying, solubilizingy and polymer plasticization effects. Simple depressurization technique is applied when isolating polymer films which results in a dryer polymeric end product. This feature eliminates the need for energy-intensive and environmentally unfriendly drying procedures in order to to remove solvent (Kendall et al., 1999).

Zhai (2007) argued that it has been reported from previous studies that $scCO_2$, with non-toxic, nonflammable and environmentally benign characteristics have the ability to swell and plasticize glassy polymers, which can lead to a depression in their glass transition temperature (*Tg*) to almost the same extent as affected by vapours or liquids. The plasticization effect of $scCO_2$ causes an increase in the mobility of polymer chains, reduces the energy-barrier for crystallization, and hence induces crystallization under moderate conditions. Wang (1982) and Chiou (1985) have confirmed that an important feature of $scCO_2$ in polymerisation is plasticisation, which results in the lowering of the polymers glass transition temperature (*Tg*). This plasticicsation imparts important effects such as the removal of residual monomer from the polymer, incorporation of additives and formation of foams. Beckman (1987) demonstrated that the exposure of thin films in CO_2 at a temperature range of 50 °C to 87 °C and up to 600 bar for 12 hrs, results in a crystalline polymer. In DSC the crystalline sample was observed as an endothermic peak at about 210 – 230 °C of the heating cycle and DeSimone (1997) obtained similar CO_2-induce crystallisation result.

In general, there is a pressure threshold required for the induction of crystallization in $scCO_2$, because of the weak solvent strength of CO_2 which has no polarity. It has been established that a small amount of a polar co-solvent such as water/ethanol can significantly increase the interaction between supercritical fluids and polar low molar mass solutes, based on the molecular simulation (Zhai et al., 2007). In polymeric materials, particularly those containing a regular chain structure, crystallization is a general phenomenon and a very important process because it controls the polymers structural formation and thereby strongly influences the functional properties of the final product (Zhai et al., 2009). In the case of high-molecular weight polymers, the related increase in the molecular interaction has also been observed with the addition of small amount of polar co-solvent in supercritical CO_2. As a result the

increase of plasticizing strength of $scCO_2$ it tends to impart much higher mobility for polymer chains, which therefore affects the crystallization behavior of the polymers. This hypothesis has been verified by Liao et al (2003). The addition of ethanol during gel formulation in this study, could have promoted OME crystallization in $scCO_2$ due to drying of ethanol in the film matrix, thought this will need to be verified. In other studies that was carried out in the presence of co-solvent it was deduced that there was a change in the melting behavior and crystal form transformation of the polymers in the presence of $scCO_2$ (Ma et al., 2005).

In this chapter, the $scCO_2$ treatments improved the ease at which the water molecules were removed and resulted in crystals with lower melting point. The presence of crystals was subsequently confirmd with SEM and XRD. This is because the process of $scCO_2$ on film matrix allows quick evaporation of residual water (Gin et al., 2009). Toledo (2006) noted that $scCO_2$ seems to be a promising medium to develop inclusion complexes of very sensitive drugs such as OME by the formation of complexes, which lead to improvements in the physico-chemical properties such as solubility and bioavailability of the molecule (OME). In addition, the data from release profiles of OME suggested that 99% was released within 30min due to the enhancement of OME solubility and change in the physical properties of the polymeric matrix and transforming from a sustained release system (chapter 3) to a rapid disintegration system in the presence of $scCO_2$.

Regardh et al (1986) observed that about 54% of an oral dose of OME, administered in young healthy subjects, is available in the systemic circulation. The distribution of the drug after an intravenous dose was consistent with localization of a major fraction of the drug in the extracellular water, with about 25% restricted to the blood. In their study, OME was rapidly cleared and possessed the characteristics of a high clearance drug; with insignificant amounts of carbon 14 labelled OME excreted by the kidneys, though metabolites were excreted very rapidly. They also reported that six different metabolites were detected with the major one being hydroxyomeprazole.

Drugs released from buccal films have a direct access to the systermic circulation through the internal jugular vein, which bypasses the hepatic first pass metabolism leading to high bioavailability. The film can be defined as a dosage form that employs a water dissolving polymer (MET), which allows the dosage form to quickly hydrate, adhere and dissolve when placed in the oral cavity. However there is no record of any work done from previous researchers showing that a fast dissolving film from slow release MET film using $scCO_2$

technique has been performed. Therefore the results from this chapter are very interesting and other functional characteristics and advanced characterisation needs to be investigated further.

7.5 CONCLUSION

The results show that SCF caused significant changes to the functional and physical properties of the MET films and clearly converted the original DL MET films from a sustained release formulation (2 hrs to maximum release) to a rapid release system, releasing > 90% of OME within 15 minutes. Therefore, the processes of SCF offers real opportunities for the formulation of fast dissolving thin films and the films have potential for paediatric buccal administration.

CHAPTER EIGHT: FORMULATION DEVELOPMENT AND OPTIMIZATION OF OMEPRAZOLE LOADED SOLVENT CAST FILMS AND DRUG STABILISATION USING L-ARGININE AND CD (β AND γ)

8.1 INTRODUCTION

Cyclodextrins (CDs) are cyclic oligosaccharides which are useful excipients used in different fields such as to prepare inclusion complexes utilised in pharmaceutical formulations. It can form water-soluble complexes with lipophilic guests that fit (completely or partially) in the cavity of CDs (Kumar et al., 2013). There are three main types of CDs designated as α, β and γ. The α, β and γ CDs are cyclic oligosaccharides consisting of 6, 7 and 8 D-glucose units, respectively. Furthermore there are also CDs built of 9 and more glucose residues. In CDs glucose (more precisely, glucopyranose) units in 4C1- chair conformation is linked through α (1→4) bonds. The glucoses are syn-oriented i.e. their O-6 hydroxyls are on one side of the ring and their O-2, O-3 hydroxyls on the other side. The round conformation of the CD macrocycle is stabilized through the intermolecular inter-glucose O2 (n) O3 (n-1) hydrogen bonds.

OME is poorly soluble and it also shows low physicochemical stability under neutral and acidic conditions (Markovic et al., 2006). This drawback gives rise to difficulty in obtaining oral pharmaceutical formulation with an acceptable bioavailability due to its rapid degradation in the stomach (Stroyer, 2006).

The internal hydrophobic cavity of CD facilitates the inclusion; CDS have also been successful as a drug carrier to improve drug solubility, chemical stability, dissolution and bioavailability or to decrease unfavourable side effects.

The molecular simulation of L-arg and OME forming an inclusion complex with CD has been reported (Figuerias et al., 2010).

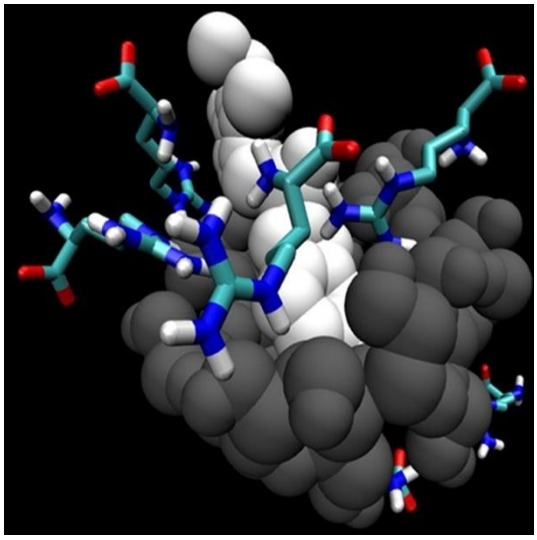

Figure 8.1 Snapshot from the molecular dynamics simulation of the multicomponent inclusion complex formed between OME (*light grey*) and βCD (*dark grey*) in the presence of ARG (*coloured: blue (light and dark) and red*). (Figueiras et al., 2010)

As seen in figure 8.1 above "the presence of ARG is in the system, the difference between the average distance from the e and f atoms of the OME to the centre of mass of the O4 atoms of the CD that can be considered as a reference to the centre of the CD inner cavity of the two complexes is not significant. This can explain to a large extent the large difference observed for the Δδ in the OME: βCD and the small difference in the Δδ for OME: βCD upon the addition of ARG, leading to overall similar Δδ results when the ARG is present. Upon the OME: ARG interaction in aqueous solution, to highlight this interaction, the system is studied in the absence of CD" (Figueiras et al., 2010). The original stability study in chapter 5 showed that L-arg was only able to stabilize OME at room temperature for only 28 days. Therefore CD could represent a suitable addition to the optimised MET DL film containing L-arg as discussed in chapter 3 section 3.3.1 (Badry et al., 2009)

The aim of this chapter therefore, was to investigate the stabilizing effect of βCD and γCD on DL films and comparing their physic-chemical properties with the original MET DL film (OME:L-arg 1:2) without any βCD and γCD by using various techniques as described in chapters two and three. The DL films have been characterised for their hydration, adhesive properties, OME dissolution with release kinetics and as well as stability studies.

8.2 MATERIALS AND METHODS

8.2.1 Materials

Table 8.1 List of materials used

Name	Company	Batch Number	Purity	Location
Ethanol	Fisher Scientific	1405343	-	Loughborough, UK
Metolose (MET)	Shin Etsu	311615		Stevenage, Hertfordshire
PEG 400	Sigma Aldrich	A0210931	-	Gillingham, UK
Omeprazole (OME)	TCI	PWAMM-HK00359	98%	Tokyo, Japan
L-Arginine (L-arg)	Sigma Aldrich		-	Gillingham, UK
βCD	Sigma Aldrich	065K0197	98%	Gillingham, UK
γCD	TCI	UUUXL-0B	98%	Tokyo, Japan

8.2.2 Consumables

Table 8.2 List of consumables

Consumable	Company	Location
Blue, white and yellow micropipette tips	Fisher Scientific	Loughborough, UK
100 mL beakers	Fisher Scientific	Loughborough, UK
Magnet stirrer	Fisher Scientific	Loughborough, UK
Tzero hermetic pans and lids	TA Instruments	Crawley, UK
SEM stubs	Agar Scientific	Essex, UK

8.2.3 Instruments

Table 8.3 List of instruments used

Instruments	Suppliers
Texture Analyser TA HD plus	Stable Micro Systems, Surrey, UK
DSC Q2000	TA Instruments, Crawley, UK
Q5000-IR Thermogravimetric Analyser	TA Instruments, Crawley, UK
Mettler Toledo FP82HT	Greifensee, Switzerland
Hitachi SU 8030 SEM	Hitachi High-Technologies, Tokyo, Japan
D8 Advantage X-ray diffractometer	Bruker, Coventry, UK
Perkin Elmer spectrophotometer	Spectrum Two, Perkin Elmer, US
Tzero sample encapsulation press	TA Instruments, Crawley, UK
Agilent 1200 HPLC	Agilent Technologies, Cheshire, UK,)

8.2.4 METHODS

8.2.4.1 Preparation of DL solvent cast films

The DL films were prepared as previously described in chapter 3 section 3.3.1

8.2.4.2 Formulation development and optimization of OME, β and γ CD loaded films

The main purpose for the development and optimization was to stabilise OME films using βCD and γCD in the presence of L-arg. The OME-loaded films were prepared by preparing MET gel as previously described in chapter 2 section2.2.4.1. However, the drug was first added to the appropriate volume of solvent (20% v/v ETOH) along with βCD and γCD at different ratios with OME (OME: CD 1:1, 1:2 and 1:3) to form an OME solution as can be shown in table 8.4(a). The polymer (MET) powder was then added slowly to the vigorously stirred drug solution at room temperature as previously described to obtain the DL gel. The resulting gel were covered with para film, and left to stand to allow air bubbles to escape and then 20g was poured in Petri dishes and dried at 40 °C (Morales *et al*., 2011).

8.2.4.3 Stabilization of OME in DL MET films using L-arg

Due to the breakdown of OME in the presence of either βCD or γCD following gel formation, L-arg was used as a stabilising agent to prevent drug degradation. Table 8.4 (b) shows the details for the different ratios of OME, L-arg, βCD and γCD in the gel formulations which were investigated. This step was performed by using L-arg (0.10% w/w) within the gel whilst keeping the original OME concentration (0.10% w/w) βCD (0.10% w/w) and γCD (0.10% w/w) constant. The procedure for making these films was the same as DL films described in chapter 3 section 3.3.1. The major difference was that, the OME, L-arg, β and γCD; were added to the solvent before adding MET and PEG 400.

Table 8.4 Amount of OME in the solution with β and γCD using ethanolic (20% v/v EtOH) gels containing (a) 0.50% w/w PEG 400) and (b) containing 0.50% w/w PEG 400 as well as L-arg (Andrews, et al., 2009)**.**

(a)

MET (%w/w)	**OME (%w/w)**	**βCD (%w/w)**			**PEG 400 (% w/w)**
0.5	0.1	0.1	0.2	0.3	0.5
γCD (%w/w)					
0.5	0.1	0.1	0.2	0.3	0.5

(b)

MET (%w/w)	**OME (%w/w)**	**L-arg (%w/w)**	**βCD (%w/w)**	**PEG 400 (% w/w)**
0.5	0.1	0.1	0.1	0.5
γCD (%w/w)				
0.5	0.1	0.1	0.1	0.5

8.2.4.4 Texture analysis (TA)

Texture analysis was used to characterise the tensile properties of the MET DL films (films plasticized with 0.5 % PEG 400, 20% EtOH, OME:L-arg: βCD 1:1:1 and OME:L-arg: γCD

1:1:1). A texture analyser TA HD plus (Stable Micro System, Surrey, UK) equipped with 5 kg load cell was used to perform the experiment. Data evaluation was performed by texture exponent-32 software program. The films free from any physical imperfection with the average thickness of (0.07 + 0.1 mm) were selected for testing (Boateng, et al., 2013). The dumb-bell shaped films were fixed between two tensile grips positioned 30 mm apart and stretched to break point. The peak force and elongation at break, elastic modulus of the films prepared with different polymers (MET) and PEG 400 as plasticiser (0.5 % w/w based on polymer's weight and L-arg 1:1, 1:2 and 1:3) (Ayensu, et al., 2012) were determined when films broke. Three replicates were carried out for each type of film. The instrument settings used in the analyses are shown in chapter 3 section 3.2.4.3.

8.2.4.5 Hot Stage Microscopy (HSM)

The hot stage microscopy experiments were conducted on a Mettler Toledo FP82HT (Greifensee, Switzerland) with a Nikon Microphot. MET DL films (films plasticized with 0.5 % PEG 400, 20% EtOH, OME:L-arg: βCD 1:1:1 were placed on a glass slide, covered with a coverslip, and heated from ambient temperature to 200 °C at a rate of 10 °C per minute. Changes in morphological behaviour were collected as a video recording by using PixeLINK PL-A662 camera (PixeLINK, Ontario, US).

8.2.4.6 Differential scanning calorimetry (DSC)

Methods used for this experiment was to measure melting point (T_m) and glass transition (T_g) for MET DL films (films plasticized with 0.5 % PEG 400, 20% EtOH, OME:L-arg: βCD 1:1:1 are as discussed in chapters two and three, sections 2.2.3.4 and 3.2.4.5.

8.2.4.7 Thermogravimetric analysis (TGA)

Methods used for this experiment was to measure water content of MET DL films (films plasticized with 0.5 % PEG 400, 20% EtOH, OME:L-arg: βCD 1:1:1 are as discussed in chapters two and three, sections 2.2.3.5 and 3.2.4.6.

8.2.4.8 Scanning electron microscopy (SEM)

Methods used for this experiment to measure surface morphology, check for film uniformity and the presence of any cracks of the MET DL films (films plasticized with 0.5 % PEG 400, 20% EtOH, OME:L-arg: βCD 1:1:1 are as discussed chapters two and three, sections 2.2.3.6 and 3.2.4.7.

8.2.4.9 X-ray diffraction (XRD)

Methods used for this experiment was to measure physical nature (crystalline or amorphous) of the MET DL films (films plasticized with 0.5 % PEG 400, 20% EtOH, OME:L-arg: βCD 1:1:1 are as discussed in chapters two and three, sections 2.2.4.7 and 3.2.4.8.

8.2.4.9 Fourier transform infrared (FT-IR) spectroscopy

Methods used for this experiment was to measure the interaction of polymer and drug in MET DL films (films plasticized with 0.5 % PEG 400, 20% EtOH, OME:L-arg: βCD 1:1:1 films are as discussed in chapters two and three, sections 2.2.4.8 and 3.2.4.9.

8.2.4.10 Hydration capacities

Methods used for this experiment was to measure drug release capacity for MET DL films (films plasticized with 0.5 % PEG 400, 20% EtOH, OME:L-arg: βCD 1:1:1 are as discussed in chapter four, section 4.2.3.1.

8.2.4.11 Mucoadhesion

Methods used for this experiment was to measure the mucoadhesive properties of MET DL films (plasticized with 0.5 % PEG 400, 20% EtOH, OME:L-arg: βCD 1:1:1 as discussed in chapter four, section 4.2.3.2.

8.2.4.12 *In vitro* release of OME using Franz-type diffusion cell

Methods used for this experiment was to measure the controlled and sustained release of the drug are as discussed in chapter five, section 5.2.3.1.

8.2.4.13 Drug stability

Drug stability of MET DL films with OME and stabiliser (L-arg) were determined by high performance liquid chromatography (HPLC). An Agilent1200 HPLC equipped with auto sampler (Agilent Technology, Cheshire, UK) with Chemstation® software program was used to determine the amount of drug present in the films after storing in two sets of conditions. Samples were placed in humidity controlled desiccators and placed in oven (40°C) and the other at room temperature (ambient) over a period of one month (4 weeks). MET DL film (OME: βCD: L-arg 1:1:1, PEG 400 (0.5% w/w), 20% v/v EtOH) was placed in the desiccators and wrapped with aluminium foil due to its light sensitivity and to prevent moisture absorption by MET.

For HPLC analysis, the samples were weighed (5mg) and dissolved using 0.01M PBS solution (pH 6.8 ± 0.1 simulating salivary pH) in volumetric flasks (10 mL). 1 mL of the sample from each flask was taken and placed in HPLC vials to be measured. The column used for analysis was Hypersil™ ODS C18 HPLC columns, 5µm particle size (250 x 4.6 mm) (Thermo Scientific, Hampshire UK). The mobile phase consisted of a mixture of ammonium acetate and acetonitrile in the ratio of 60:40 v/v. The flow rate of the mobile phase was maintained at 2 mL/min and diode array UV detector wavelength for OME was set at 302 nm; 20 µl volumes were injected during each run, respectively.

8.3 RESULTS AND DISCUSSION

8.3.1 Formulation development and optimisation

MET were used for formulation DL gels and subsequent DL films based on the preliminary formulation study as described in chapter 2 section 2.3.1 and chapter 3 section 3.3.1.

Physical evaluation of DL films

When OME is added to water, it dissolves quickly to produce a clear solution as described in chapter 3 section 3.4.1. OME can only be stable in alkaline solution above pH 6.5. The stability of OME can be achieved by introducing CD (β and γ) DL gel. When βCD and γCD was added to OME in three different ratios as seen in table 8.4 and 8.5, it changed the colour of the gel into red. The difference in the final appearance of the films can be observed in figures 8.2 and 8.3.

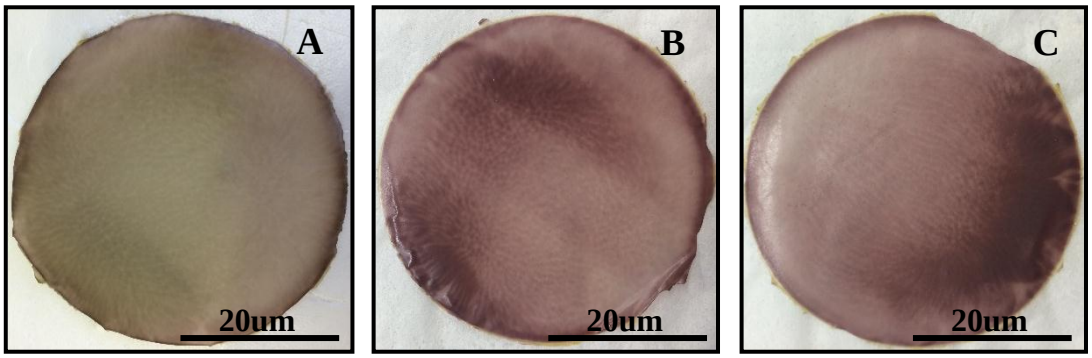

Figure 8.2 Digital photographic images of OME and βCD DL MET fims in different OME: βCD ratios (A) 1:1, (B) 1:2 and (C) 1:3 without L-arg

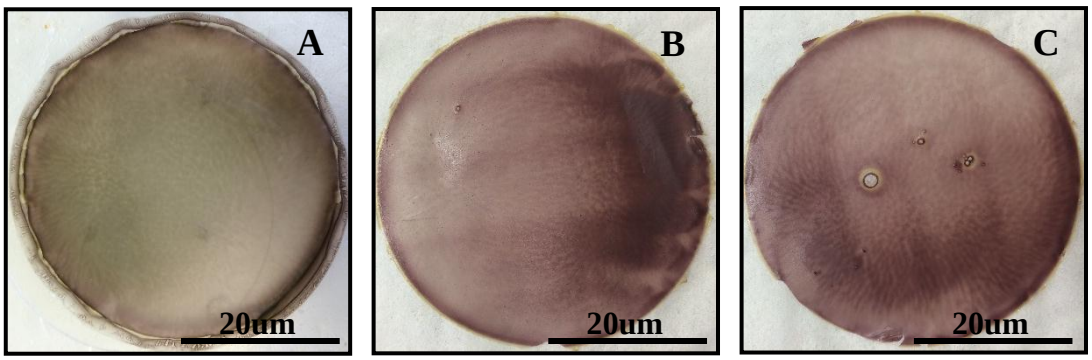

Figure 8.3 Digital photographic images of OME and γCD DL MET fims in different OME: γCD ratios (A) 1:1, (B) 1:2 and (C) 1:3 without L-arg

It was also obvious that the addition of L-arg helped to stabilise the drug and CD within the films as seen in figure 8.4, showing the desired homogeneity, transparency and uniform drug distribution. Figueiras and co-workers suggested that from ratio of 1:1 OME: L-arg the H atom of the L-arg was observed to be in closer proximity to the nitrogen atom of OME (Figueiras et al., 2010). They also observed that the distance between the H (L-arg) and the N (OME) is relatively small which increases the chances of formation of hydrogen bonds between the two compounds.

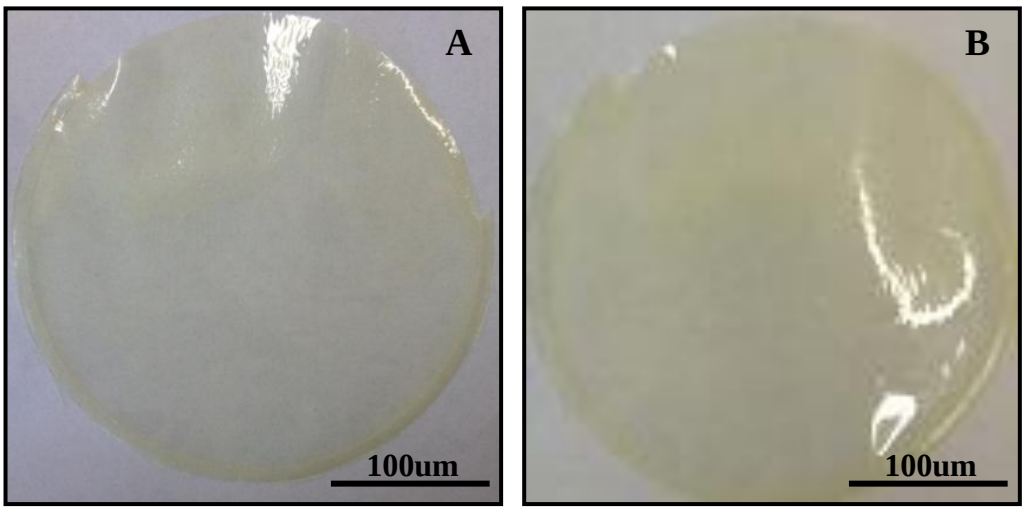

Figure 8.4 Digital photographic images of OME and CD DL fims (A) βCD and (B) γCD with L-arg ratio (1:1:1)

The description of the physical appearance of the films based on most ideal characteristics (transparency, ease of peeling and flexibility) are summarised in table 8.5. Overall, based on the visual observation after determining that DL MET films containing L-arg and βCD and γCD were most optimum and were therefore selected for physical and mechanical characterisation and future studies.

Table 8.5 Ideal characteristics of DL films of βCD and γCD

Polymers	Solvent/gel	PEG (%w/w)	OME (g)	βCD (g)	L-arg (g)	Peel off	Film Characteristics
MET	**20% EtOH**	0.5	0.1	0.1	0.1	YES	Transparent/flexible

Polymers	**Solvent/gel**	**PEG (% w/w)**	**OME (g)**	**γCD (g)**	**L-arg (g)**	**Peel off**	**Film Characteristics**
MET	**20% EtOH**	0.5	0.1	0.1	0.1	YES	Transparent/flexible

8.3.2 Texture analysis (TA)

Texture analysis was employed to measure the tensile properties of the films including tensile strenghth (brittleness), elastic modulus (rigidity) and % elongtion at break (flexibility and elasticity) of the DL films. This technique was used to determine the effect of OME, βCD, γCD and L-arg on the tensile properties of the plasticised MET films prepared from gels containing 0.5% w/w PEG 400 and the resulting data used to select the most appropriate formulations for further development including drug release.

The films (βCD and γCD) showed significant differences in the tensile strength (brittleness) based on the PEG (0.5% w/w). The effects of CD on the tensile strength values of the films produced with MET (ethanolic (20% EtOH)), OME and L-arg (1:1) are shown in figures 8.5 respectively. It has been suggested that the average % elongation at break point should ideally be between 30-60% (Boateng et al 2009) which indicates a good balance between flexibility and elasticity. βCD loaded film containing OME and L-arg (1:1) from gels containing 0.5 % w/w of PEG satisfied this required criteria. However, γCD film prepared with OME and L-arg (1:1) from gels containing 0.5 % w/w of PEG gave low % elongation at break as shown in figure 8.5. Based on these results and on the visual observation and the expected characteristics for an ideal film in terms of flexibility, uniformity and transparency, films prepared from ethanolic (20% v/v EtOH) gels containing 1:1:1 ratio of OME: βCD:

Larg and 0.5% w/w PEG400 was confirmed as the most appropriate for further investigations.

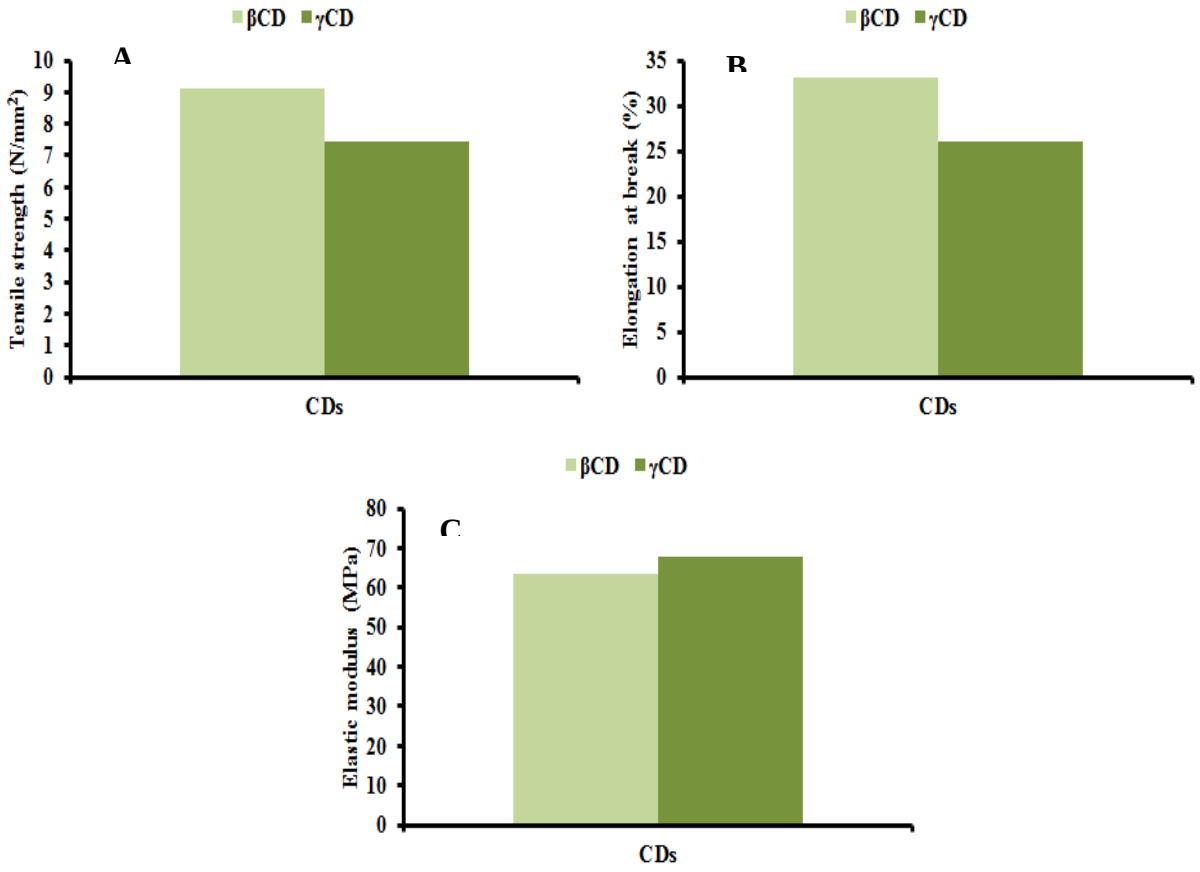

Figure 8.5 Mechanical properties (A) tensile strength, (B) elongation at break and (C) elastic modulus of DL MET films cast from ethanolic (20% v/v EtOH) polymeric gels containing plasticiser (0.5% w/w PEG 400), OME: βCD: L-arg (1:1:1) and OME: γCD: L-arg (1:1:1) (mean ± SD, (n=3))

8.3.3 Hot Stage Microscopy (HSM)

For the plasticised DL films containing βCD the results showed that as the temperature increased with time, the surface of the film went from rough to clear due to loss of water content in the film as seen in figure 8.6. The literature (Cui et al., 2012) suggests that βCD does not undergo a melt transition, however, figure 8.6 appears to show melting after 260°C, which is followed immediately by decomposition. The HSM results obtained helped in

developing suitable methods for TGA and DSC analysis and determined the maximum temperature to which samples could be heated.

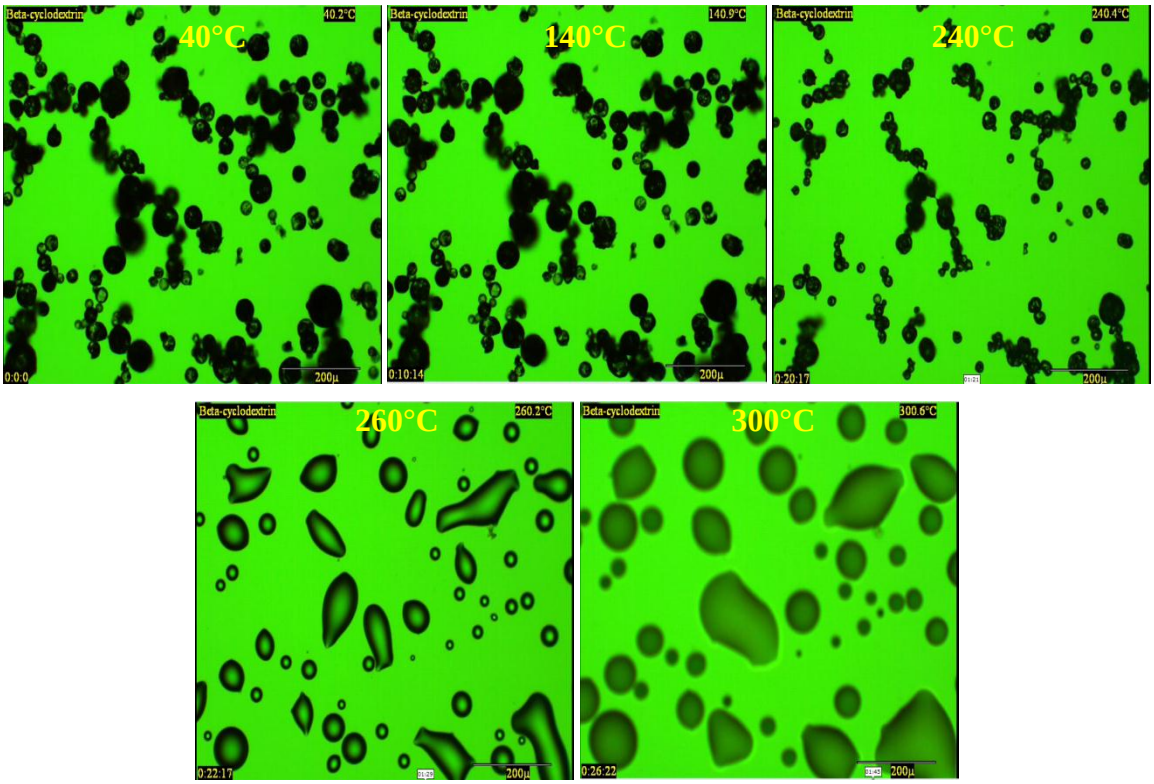

Figure 8.6 HSM results showing DL MET containing βCD film during heating

8.3.4 Differential scanning calorimetry (DSC)

DSC was used to determine the interactions between the components of the film within the film matrix, MET, PEG 400, L-arg and model drug (OME) as seen in chapter 2 section 2.3.4 and chapter 3 section 3.3.4. βCD showed broad but relatively sharp endothermic peak at 100°C. βCD peak can be attributed to water loss with no definite melt or glass transition peaks as shown in figure 8.7. This was further confirmed with TGA.

The thermograms (figure 8.8) of MET DL plasticised films [ethanolic (20% v/v EtOH)] containing OME:L-arg (1:1), showed a broad endothermic transition between 62 °C, Generally, DL MET films can be characterized as amorphous but to confirm this SEM and XRD were carried out.

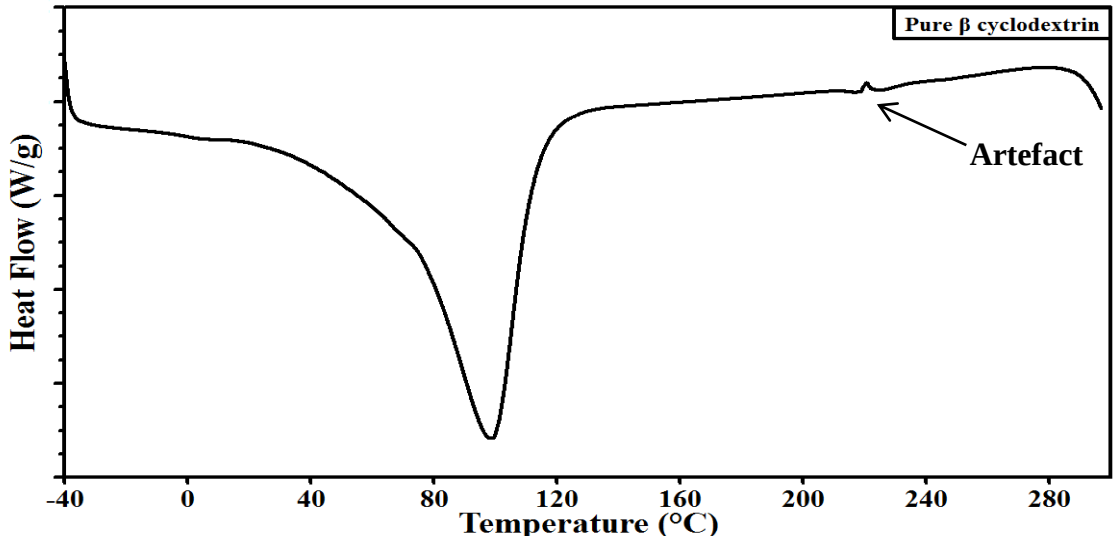

Figure 8.7 DSC thermogram of pure βCD (W/g (Watts/gram))

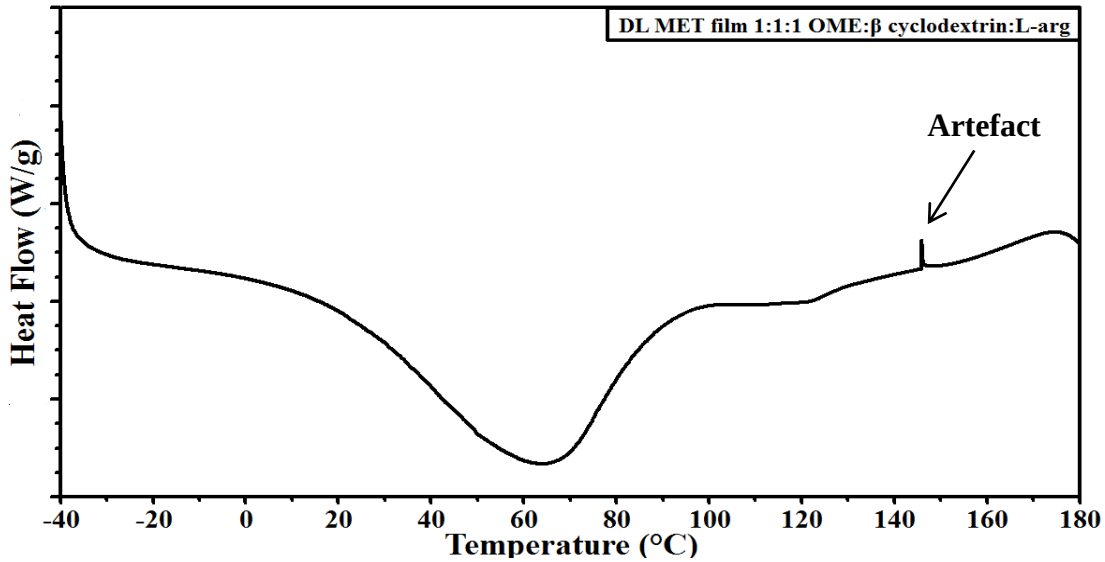

Figure 8.8 DSC thermograms of plasticised DL MET films cast from ethanolic (20% v/v EtOH) polymeric gels containing 0.5% w/w PEG 400 and OME: βCD: L-arg (1:1:1) (W/g (Watts/gram))

Table 8.6 Temperature and heat changes observed for the endothermic transitions observed (pure βCD and film (DL MET) containing 0.5% w/w PEG 400 and OME: βCD: L-arg (1:1:1) .

	1st TRANSITION			2nd TRANSITION		
Pure materials/ gels	**Onset °C**	**Peak °C**	**ΔH (J/g)**	**Onset °C**	**Peak °C**	**ΔH (J/g)**
Pure βCD	65.83	100.00	371.15	-	-	-
PEG 400 (0.50% w/w)						
Film	18.72	63.19	95.60	145.85	145.96	0.15

8.3.5 Thermogravimetric analysis (TGA)

TGA was used to determine the residual moisture content (%), dynamic weight loss of the starting materials (MET, OME, L-arg and PEG 400) and DL films as discussed in chapter 3 section 3.3.5.

The TGA result of starting material βCD is shown in table 8.11 the weight loss for βCD after heating from ambient temperature (20°C) to 100°C was 13.09 %.

The TGA results of MET DL films (ethanolic) containing OME: βCD: L-arg (1:1:1) showed percentage loss with heating of 4.04 %, attributed to residual water present within the film matrix. It appears that the residual water was generally lower for films prepared using ethanolic (20 % v/v) gels containing OME: L-arg (1:2) without any βCD. This is due to EtOH speeds up water evaporation during drying of the films.

8.3.6 Scanning electron microscopy (SEM)

The surface morphology and topographic characteristics of DL MET films cast from gels prepared with solvent (20% v/v EtOH) with PEG (0.5% w/w) containing, drug (OME) and stabilizer (L-arg) and βCD ratio of (OME: βCD: L-arg 1:1:1), were evaluated using SEM.

Figure 8.9 shows microscopic appearance of pure βCD. The surface topography of pure βCD appears as irregular particles without any well-defined shapes.

The surface topography of the plasticised MET films containing OME: βCD: L-arg (1:1:1) prepared from ethanolic gels (20% EtOH) showed continuous sheets with relatively smooth and homogeneous surfaces suggesting that all the components were uniformly mixed during gel and film formation as shown in figure 8.10. This could be due to drug and stabilizer loading. However, small circular shaped structures were observed which could be OME or βCD due to the increasing rapid drying of ethanolic gels during film formation. This will however, require further investigation.

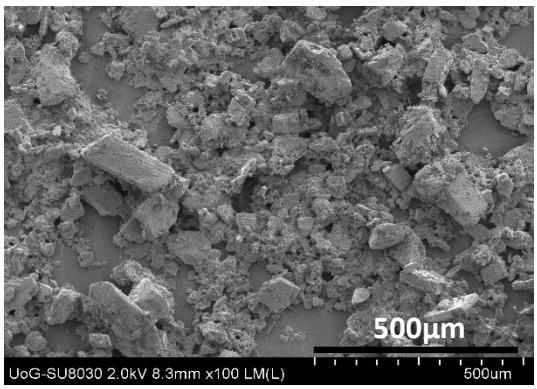

Figure 8.9 SEM micrograph of pure βCD

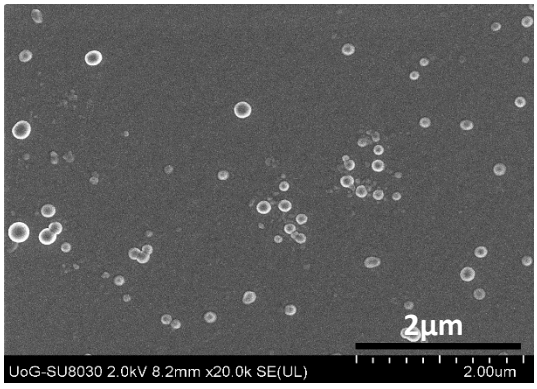

Figure 8.10 SEM micrograph of plasticised DL MET films cast from ethanolic (20% v/v EtOH) gels containing 0.5% w/w PEG 400 and OME: βCD: L-arg (1:1:1)

3.3.7 X-ray diffraction (XRD)

XRD analysis was performed to check the crystalline- amorphous ratio and confirm the physical form of the various components within the films. Figure 8.11 shows the XRD diffractograms of the pure βCD and DL MET films cast from gels prepared with ethanolic (20% v/v EtOH) gels containing OME: βCD: L-arg (1:1:1) with 0.5% w/w PEG 400. The

results demonstrate that pure βCD was crystalline in nature. Figures 8.11 also shows some peaks (corresponding to pure OME and βCD) which indicated a small amount of crystallinity for the plasticised film, however, the films were largely amorphous. The crystalline: amorphous ratio was calculated at 2% which suggests there could be small amounts of OME and/or βCD present in these films compared to the lower amounts in films described in chapter 3 section 3.3.7.

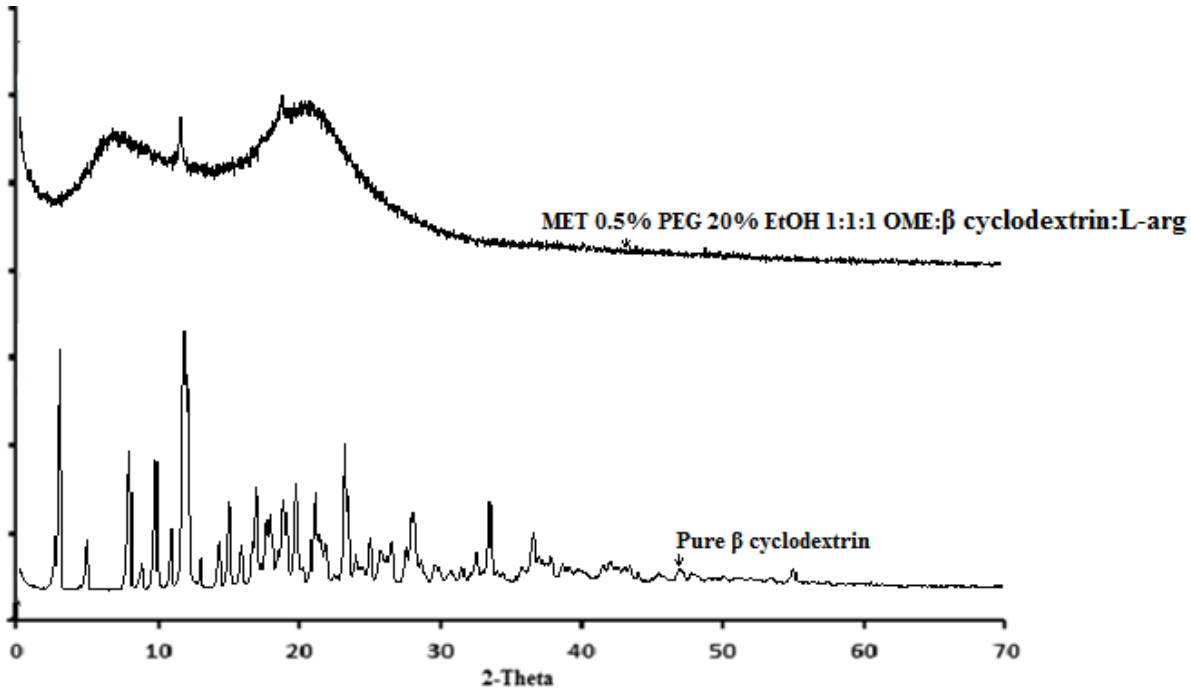

Figure 8.11 XRD diffractograms for pure βCD and DL MET films cast from ethanolic (20% v/v EtOH) polymeric gels containing 0.5% w/w PEG 400 and OME: βCD: L-arg (1:1:1)

8.3.8 Fourier transform infrared (FT-IR) spectroscopy

FTIR investigations are mainly carried out to examine a molecular changes in the drug due to its interaction with other excipients. The FT-IR absorption bands of βCD are summarised in table 8.7 (results for MET, PEG 400, OME, L-arg and EtOH are summarised in table 2.10 chapter 2 section 2.3.8 and table 3.10 chapter 3 section 3.3.8, which shows similar corresponding characteristic bands between 3447.40cm^{-1} to 821 cm^{-1} (aromatic and aliphatic). Detailed FT-IR results of DL MET films with plasticiser (PEG) and OME: βCD: L-arg (1:1:1) as shown in figure 8.12 and table 8.8. FT-IR of the changes in the wavenumbers of the spectral bands describes the different interaction occurring in a specific region.

Table 8.7 The observed FTIR bands (n=3) for pure material with their characteristic band

Pure materials	Absorption bands (cm^{-1})	Bands assignment
βCD	998.00	C-H bending
	1077.00	-S=O stretching
	1152.00	C=O stretching
	1415.00	C-H stretching
	1644.00	-C=C stretching
	2925.00	C-H stretching
	3295.00	N-H stretching

The FTIR spectra of DL MET films containing the drug (OME), stabiliser (L-arg) and (βCD) 1:1:1 and with plasticiser, shows that the characteristic bands of the drug was decreased in intensity and may be attributed to the dilution factor of the mixture by the βCD. There were no new bands observed in the spectrum, which confirms that no new chemical bonds were formed between the drug and the excipients as seen in figure 8.12.

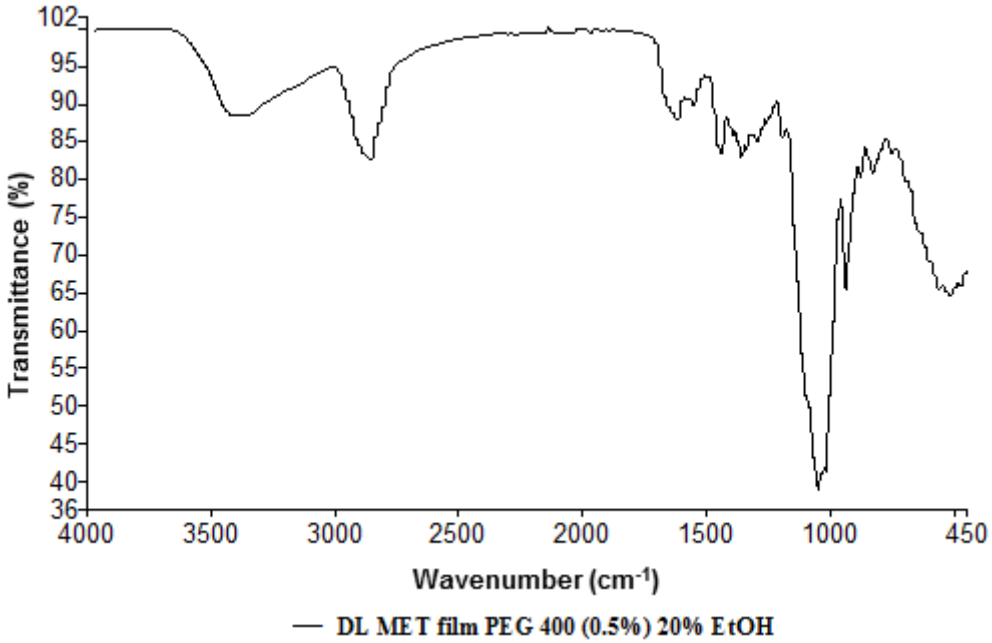

Figure 8.12 FT-IR spectra of DL MET films cast from ethanolic (20% v/v EtOH) polymeric gels containing 0.5% w/w PEG 400 and OME: βCD: L-arg (1:1:1)

Table 8.8 Major FTIR peaks of interests for DL MET films plasticised from (OME: βCD: L-arg 1:1:1)

Peak No.	X (cm^{-1})	Y (%T)	Peak No.	X (cm^{-1})	Y (%T)	Peak No.	X (cm^{-1})	Y (%T)
1	3401.81	86.89	2	2877.01	80.33	3	1631.46	86.28
4	1567.80	88.37	5	1453.81	81.16	6	1201.03	83.46
7	1056.11	31.13	8	1029.79	33.56	9	945.27	60.88

8.3.9 Hydration capacities

In chapter 4 section 4.3.1 the concept and mechanism of hydration capacities was discussed in detail. DL MET films cast from gels prepared with 20% v/v EtOH containing PEG (0.5% w/w), drug (OME) and stabilizer (L-arg) ratio (1:2), showed swelling index of 2630% in 20 minutes. After 20 minutes the DL films the swelling stayed flat or decreased due to a loss of structural integrity. From the result obtained in figure 8.13, DL film containing βCD showed swelling index 1197 % after 20 minutes compared to the above DL film containing no βCD. This could be due to the interaction between polymer and βCD complex within the film matrix which competes with water for bonding interactions with the polymer chains to absorb water with a consequent decrease in swelling rate and capacity. This is interesting given the fact that CDs are generally hydrophilic because of large number of OH groups.

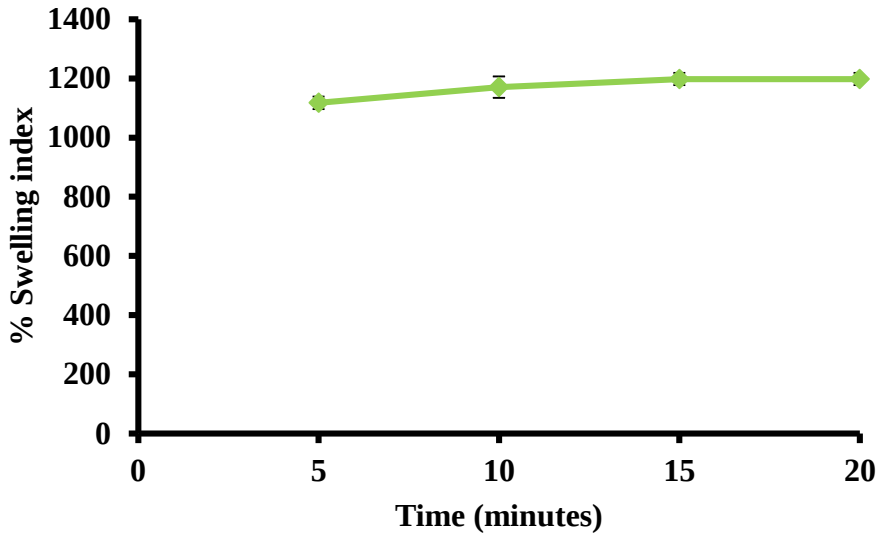

Figure 8.13 Swelling profiles of MET DL films cast from ethanolic (20% EtOH) gel containing 0.5% w/w PEG 400 and OME: βCD: L-Arg 1:1:1 ratio in PBS pH 6.8 (mean ± SD, (n=3))

8.3.10 Mucoadhesion

Figure 8.14 shows results for DL MET film treated with and without βCD showed statistically significant differences in PAF (stickiness) (p = 0.0284) and TWA (P =0.0522). However no statistically significant difference was observed in cohesiveness (p = 0.2136). This is due to strong interaction (hydrogen bonding) between the polymer (MET) and the βCD which contains a high number of OH groups.

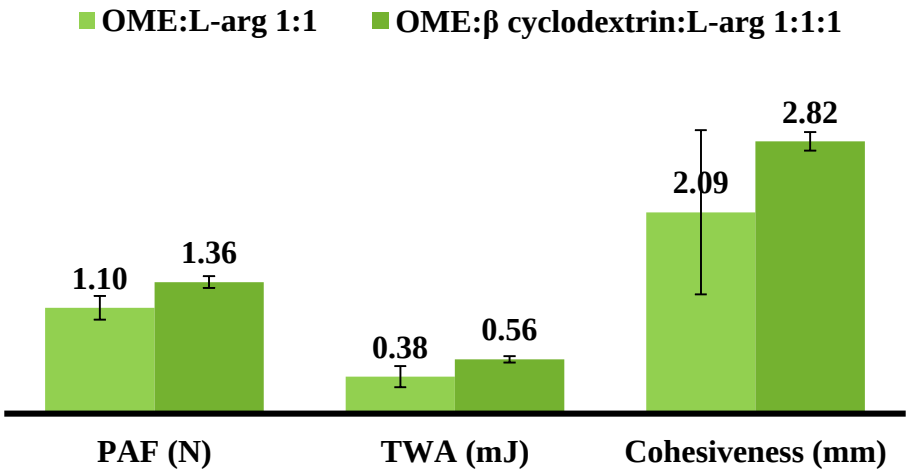

Figure 8.14 *In-vitro* mucoadhesion measurements (PAF, TWA and cohesiveness) of plasticised DL MET film cast from ethanolic (20% v/v EtOH) gel containing OME:βCD:L-arg (1:1:1) using mucosal substrate equilibrated with PBS (pH 6.8) of (mean ± SD,(n=3)).

8.3.11 *In vitro* release of OME using Franz-type diffusion cell

The drug release may be controlled by diffusion, or by a combination of diffusion and erosion or only by erosion of the delivery system (Tuovinen et al., 2003). By comparing polymer dissolution and drug release, it is hoped to gain insight into what processes control release.

8.3.11.1 Calibration curves

The standard calibration curve for PBS is shown in figure 8.15 (Boateng et al., 2009).

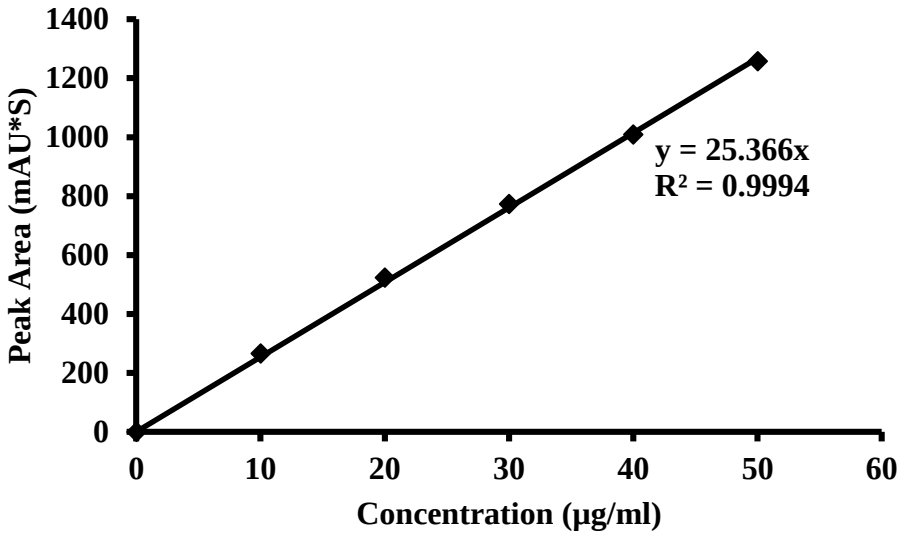

Figure 8.15 Standard HPLC calibration curve for PBS for determining the release of OME during drug dissolution study for MET DL film.

8.3.11.2 Drug loading capacity and content uniformity

Based on the results MET DL films in PBS with βCD had the higher % drug loading capacity (86.7 ± 0.2) compared to MET DL film without βCD in PBS (refer to chapter 5 section 5.3.1.2). This can be due to the matrix of the polymeric film and the interaction between the βCD and the drug (OME).

8.3.11.3 Using 0.01M PBS solution

The dissolution profiles of OME were observed over a period of two consecutive hrs because after 60 minutes the percentage of OME release decreased due to no more drug release in the media. Figure 8.16 shows the dissolution profile of DL MET film containing βCD in PBS (pH 6.8), mimicking the saliva pH. βCD DL film showed similar cumulative release (71%) over 60 minutes compared to DL without βCD (70%) over 60 minutes. This indicates a sustained release.

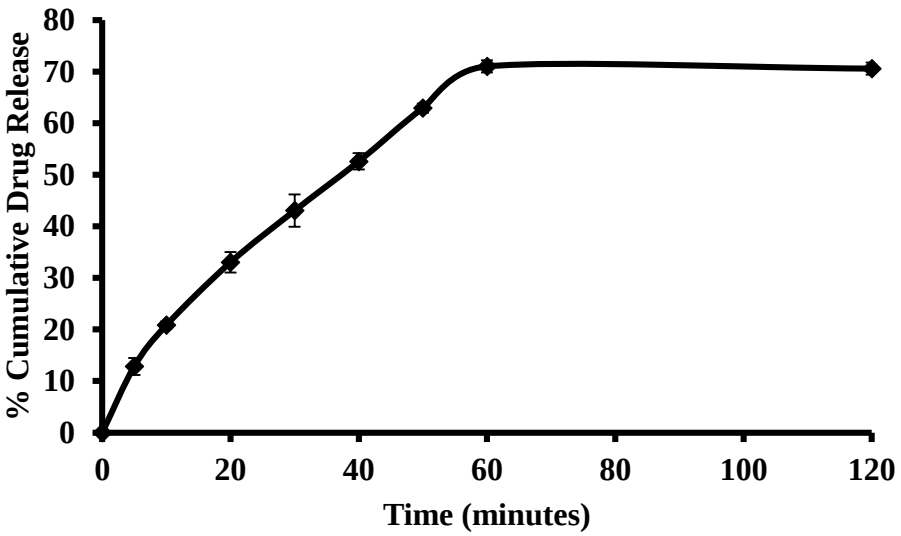

Figure 8.16 Drug dissolution profile of MET DL films prepared from ethanolic (20% v/v EtOH) gel containing 0.5% w/w PEG 400 and OME: βCD: L-Arg 1:1:1 ratio in PBS at pH 6.8 (mean ± SD,(n=3)).

8.3.11.4 Evaluation of drug release kinetics from OME

OME released from the film was assessed by determining the best fit of percentage cumulative release versus time data to zero order, first order, Higuchi and Korsmeyer-Peppas equations (coefficient, R^2 values) (Korsmeyer et al., 1983) as shown in figures 8.17 and table 8.9. The release kinetics of OME in PBS (pH 6.8) containing βCD followed Korsmeyer-Peppas model as the R^2 value (0.9996) was the highest compared to other models. This suggests that the drug release through the matrix is dependent upon the Fickian diffusion or non-Fickian diffusion which is combination of both diffusion and erosion controlled rate release. Analysis of the experimental data using kinetic equations and interpretations of the

release exponents (n) gives a better understanding of the controlling release mechanism. OME release data from DL MET film containing βCD gave an n value of 0.6 which is more than 0.45 which indicates that the drug release follows Fickian diffusion mechanism. This suggests that the OME was released through the hydrated polymer via diffusion combined with and erosion controlled drug release.

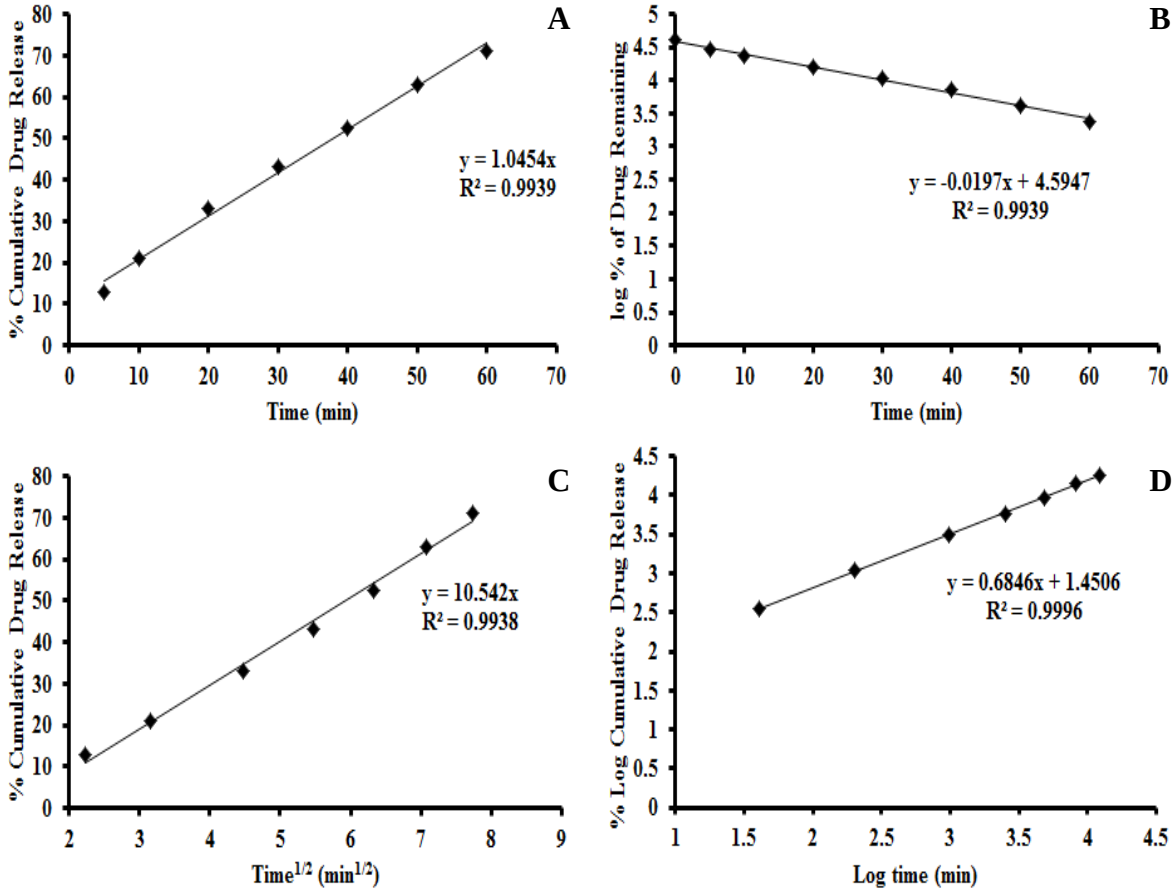

Figure 8.17 Representative release plots obtained by fitting experimental release data of OME from DL MET films to (A) zero order kinetic, (B) first order kinetic, (C) Higuchi kinetic, (D) Korsmeyer-Peppas kinetic models/equation.

Table 8.9 Release parameters obtained from fitting experimental drug dissolution (release) data to different kinetic equations for films containing OME in PBS.

OME	Zero order		First order		Higuchi		Korsmeyer-Peppas		
	K_0 (% min^{-1})	R^2	K_1 (min^{-1})	R^2	K_H (% $min^{-1/2}$)	R^2	K_P (% min^{-n})	n	R^2
DL PBS (pH 6.8) containing βCD	10.229	0.9939	-0.0197	0.9939	10.542	0.9938	1.4506	0.6	0.9996

K_o, K_1, K_H, K_p are the release rate constant for zero order, first order, Higuchi and Korsmeyer-Peppas models, R^2 is the correlation coefficient and n is the release exponent.

8.3.12 Drug stability

Short-term stability studies were performed for MET DL film (OME: βCD: L-arg 1:1:1, PEG 400 (0.5% w/w), 20% v/v EtOH) which was placed in the desiccators and wrapped with aluminium foil due to its light sensitivity. MET DL films were also wrapped in paraffin film to prevent moisture absorption by MET and exposed to oven (40 ± 0.5 ºC) and room temperature (ambient ± 0.5 ºC) (ICH guidelines) for a period of one month (4 weeks). The visual appearance of the films after the 4 weeks storage can be seen in figure 8.18. The results of the stability study shown in figure 8.19 reveal that there was extremely statistically significant difference (p = 0.0001) in the % drug remaining within the film kept in the oven at 40 ± 0.5ºC whilst the film kept under ambient conditions remained stable. In the first two weeks the drug content of OME in films kept at 40 ± 0.5ºC was 63% compared to room temperature of 99% and after four weeks the drug content was 59% at 40 ± 0.5ºC and 99% at room temperature. These findings suggest that when βCD is introduced into the film, the OME is stable at room temperature (ambient ± 0.5 ºC) conditions but not under accelerated conditions of 40 ± 0.5ºC.

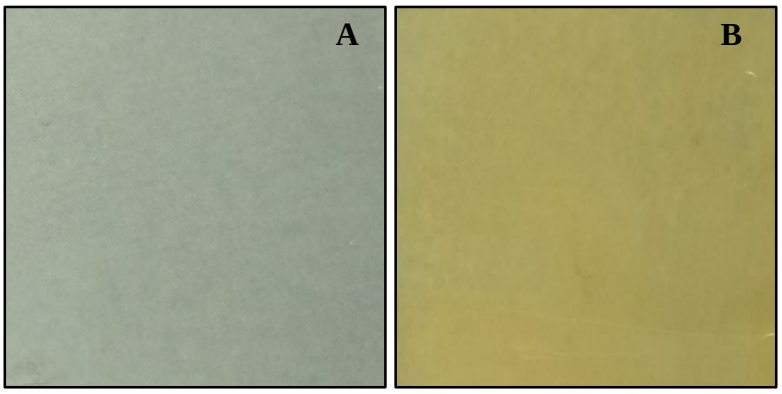

Figure 8.18 Digital photographic images of (A) MET DL film after 1 month of storage at room temperature (ambient ± 0.5ºC) showing clear transparent appearance as time zero; and (B) MET DL film after 1 month of storage in oven (40 ± 0.5ºC) showing discoloration due to drug degradation.

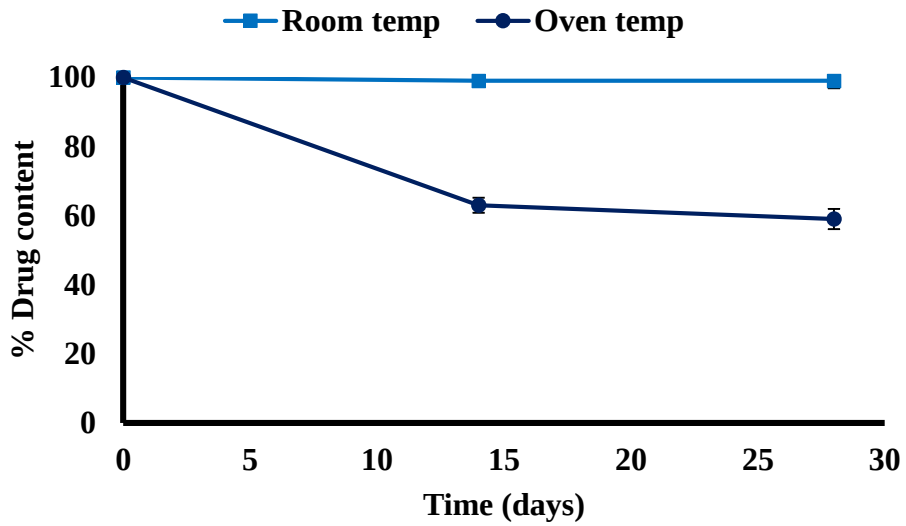

Figure 8.19 Plot showing the percentage of drug remaining within the film during storage at oven temperature (40 ± 0.5ºC) and room temperature (ambient ± 0.5ºC) 3% RH up to one month (mean ± SD, (n=3))

8.4 SUMMARY

Recently βCDs have been employed as a new class of penetration enhancers (Senel & Hincal., 2001). These molecules are cyclic oligosaccharides with a hydrophilic outer surface and a hydrophobic central cavity. The hydrophilic exterior of the βCD molecules make them water-soluble while the hydrophobic cavity provides a microenvironment which is ideal for variously sized non-polar molecules. βCDs are able to form dynamic molecular inclusion

complexes with many drug by incorporating the drug molecules e.g. OME or commonly a lipophillic moiety into the central cavity.

The resulting non-covalent complexes offer a diversity of physicochemical advantages over the unmodified drugs such as possibility to increase their water solubility and stability. It is now recognised and acknowledged that βCD act as a carrier by keeping the hydrophobic drug molecules in solution and delivering them to the membrane. Furthermore βCD can enhance drug permeation by increasing drug availability and stability at the surface of the biological barrier, act as absorption enhancer by different pathways. These hydrophobic CD act as absorption enhancers by transiently changing membrane permeation ability to overcome the aqueous diffusion barrier and opening tight jucnctions (Figueiras et al., 2009).

Figueiras (2009) suggests that the inclusion of OME in the βCD cavity increased the OME stability. However, in the presence of L-arg the improvement on drug stability was more pronounced, especially when the drug was complexed with βCD as L-arg plays an active role in the multicomponent complex formation by having tendency to be located near the inner ring surface of the CD. Furthermore their result confirmed that in the presence of βCD, L-arg or degradation products do not interfere with the HPLC retention time corresponding to the OME peak due to the stability of OME (Figueiras et al., 2009).

Furthermore, Hirose (2001) and Liu (2002) demostarted that in aqueous solution, CDs are able to form inclusion complexes with many drugs by taking up the drug molecule or lipophilic moiety of the molecule, into the central cavity. However, no covalent bonds are formed or broken during complex formation. The drug (OME) molecules in complex are in rapid equilibrium with free molecules in the solution. The driving force for the complex formation includes release of enthalpy rich water molecules from the cavity, hydrogen bonding and van der Waals interaction. The formation of the inclusion complex between OME and βCD has been studied and the stoichiometry of the complexes was found to be 1:1 mol:mol OME:βCD (Rasheed et al., 2008).

However, βCDs on their own can sometimes have a destabilising effect on drugs through direct catalysis for example, aqueous drug suspensions. The catalytic effect is associated with deprotonisation of hydroxyl groups located at the rim of the CD cavity. The catalytic effect is manly observed under conditions with increasing pH (Rasheed et al., 2008). However βCDs are able to improve aqueous solubility of some large lipophilic molecules leading to

increased drug absorption at mucosal surface that will lead to increased oral bioavailability for drugs released dosage forms such as buccal formulations.

In the presence of L-arg, the mucoadhesion performance increased when complexed with βCD in the current study. In this particular case L-arg could possibly establish hydrogen bonds with the βCD's hydroxyl groups and the polymeric end chains therefore remained free for mucoadhesion interaction in the initial stages. βCD andthe presence of L-arg increased eventually increased the absorbance of water, hence excessive hydration of polymers and consequently reducing the mucoadhesion due to the possible formation of a slippery mucilage after the initial hydration and swelling phase of mucoadhesion (Figueiras et al., 2010).

Based on the fact that improvement in OME solubility and stability are two important parameters to address in the oral thin film with better bioavailablty, the combination of βCD and L-arg has been proven to be an appropriate approach for improving the stability of OME in the MET DL film whilst βCD on its own could not achieve this objective.

8.5 CONCLUSION

The results show that incorporation of βCD into the original optimised DL MET film did not significantly affect the DSC and FTIR profiles and drug release characteristics. However, there were changes observed in TGA, SEM, XRD, swelling and mucoadhesion properties. More importantly and interestingly, the OME present in βCD loaded films remained stable at room temperature over a 4 week period whilst the corresponding films with no βCD loaded showed OME degradation within 2 weeks of storage at room temperature.

CHAPTER NINE: SUMMARY COMMENTS, KEY FINDINGS AND FUTURE WORK

9.1 Summary comments

The main objective for the preliminary study was the formulation design, development and optimization of stable solvent cast films as potential platforms for buccal drug delivery in paediatric patients. Initially five different polymers (HPMC, MC, CA, SA and MET) with different ratios of plasticiser (PEG 400) were used to formulate films. The results suggested that out of the five formulations, only MET and SA with 0% and 50% PEG 400 showed desired characteristics required in the film on the basis of an ideal balance between flexibility and toughness.

OME in aqueous environment is known to have poor solubility; therefore L-arg was required in drug loaded films as a stabilizing agent. The most promising characteristics were showed with plasticised (50 % w/w PEG 400) MET films prepared from ethanolic (20% v/v) gels and containing OME: L-arg ratio of 1:2. Based on the visual observation and the expected characteristics for an ideal film in terms of flexibility, uniformity and transparency, films prepared from ethanolic gels (20% v/v EtOH) containing 1:2 ratio of OME: Larg and 0.5% w/w PEG400 was the most appropriate for further investigations. These were confirmed by the analytical characterisation studies which also showed that the OME originally added in crystalline form was molecularly dispersed within the film matrix and therefore amorphous in nature. It was also obvious that the addition of L-arg helped to stabilise the drug within the films, which showed desired homogeneity, transparency and uniform drug distribution.

The addition of PEG 400, was found to increase the softness, elasticity and bioadhesive strength of the MET films. MET films appeared to be tougher, more elastic, more bioadhesive *in vitro* and swelled at a more reasonable rate, this suggest that MET films may be preferred as drug vehicle for buccal delivery. The mucoadhesive performance is a critical assessment that is used to establish the residence time of buccal films in the buccal region to allow for continual drug release and eventual bioavailability. Although significant differences were observed in the mucoadhesive performances of the MET films the differences were not considerable.

Films containing were plasticiser observed to have higher swelling capacity when compared to non-plasticised films due to the effect of the PEG 400 which permit a higher rate of water ingress to its hydrophilic nature and hence the improved water absorption. BLK films showed higher swelling index compared to DL films possibly due to the formation of sodium chloride and phosphate dibasic in SS which affect their swelling capacity.

On the basis of experimental data analysis, OME was released into PBS much faster than into SS with maximum concentration of drug released in PBS obtained within 1 hr compared to SS where only 21% was released in 1 hr. The rate of drug release from films was dependent on their physical structure and the amount of OME present. By fitting of release profiles data of OME showed that the Korsmeyer-Peppas equations best fit the dissolution data for PBS and SS. The drug released in PBS best followed zero order release kinetics via non-Fickian diffusion whilst release in SS followed super case II transport, attributed to both drug diffusion and polymer erosion. OME buccal adhesive MET film could potentially be attached to human cheek without collapse. The films stabilzed the drug and showed relatively fast drug permeability after release of OME. This is expected to ensure therapeutic bioavailability and therefore a useful alternative to oral administration via the GI tract as OME degrades rapidly in aqueous acidic medium. The adhesive properties suggest it will provide a long enough residence time in the cheek to allow high drug permeation.

Overall the application of SCF caused significant changes to the functional and physical properties of the MET films and clearly converted the original DL films from a sustained release formulation (1hr) to a rapid release system, releasing > 90% of OME within 15 minutes. This suggests that the process of SCF offers real opportunities for the formulation of fast dissolving thin films and the films have potential for paediatric buccal administration. The release kinetics of OME treated with SCF in PBS (pH 6.8) followed Higuchi model. This suggests drug release from a monolithic system whereby drug particles are dispersed uniformly throughout the matrix which is dependent upon diffusion. OME release data from DL MET film treated in SCF gave an n value of 0.4 which is less than 0.45 which indicates that the drug release follows non-Fickian diffusion mechanism. This suggests that the OME was released through the hydrated polymer via diffusion combined with and erosion controlled drug release.

9.2 Key research findings

- A novel MET film has been developed with optimal hydration, bio-adhesive properties for buccal drug delivery.

- The model drug (OME) is unstable during gel and film formulation could not be stabilized by CDs but was stabilized by L-arg in ratio of 1:2 (OME: L-arg), the drug molecularly dispersed within film matrix. However, in the presence of βCD, only a 1:1 ratio of OME: L-arg was required.

- DL films not treated with SCF showed sustained drug release over two hrs but slower rate in simulated saliva compared to PBS due to the higher ionic strength in the SS media. However, treatment with SCF converted the sustained release films to rapid dissolving formulations which released most of the loaded drug within a few minutes.

- *Ex vivo* permeation and bioadhesion studies showed enough drug permeating the pig membrane as well as confirming good bioadhesion which will be ideal for ensuring long enough residence times to allow drug permeation.

- The overall implication of these findings is the potential application of the novel MET films for buccal delivery of OME in paediatric patients

9.3 Future work

1. Due to the constraints of time, the stability studies were only performed over 3 months and 1 month for MET DL (OME:L-arg 1:2) and MET DL (OME: βCD:L-arg 1:1:1) respectively. Stability studies of the drug-loaded films based on the International conference on harmonization (ICH) guidelines will be conducted for longer periods up to 6 months. These will cover drug and polymer stability with the help of HPLC and gel permeation chromatography (GPC) technique respectively. From this, the rate and mechanism of degradation could be estimated from which shelf life could be predicted.

2. Perform *in vitro* swelling, mucoadhesion and drug dissolution studies on SCF treated films and βCD loaded films using simulated saliva (SS) as the dissolution medium and comparing to SCF treated and βCD loaded films using PBS with OME: L-arg 1:2. Further drug permeation and bio-adhesion studies of the films will be carried out using *in vitro* human tissue culture models (EpiOral^{TM}).

3. The results from (2) above will be used to predict the *in vivo* performance of the drug released from the optimised films using chemometrics and bioinformatics approaches.

4. One of the major limitations of thin films is the low drug loading capacity due to the very small volume and therefore excess drug not molecularly dispersed, tend to precipitate on the surface. Therefore one key future work will be to investigate the possibility of increasing the amount of OME loading within the films using βCD by forming inclusion complexes with the drug.

5. Preliminary taste characterisation of DL loaded films will be undertaken using commercial taste sensors and human adult volunteers and where necessary include other additives to ensure suitable taste masking of the OME, which is essential for paediatric oral mucosa administration. It is expected that the CDs used towards the end of this study, which are natural sugars will be able to provide such taste masking.

CHAPTER TEN: REFERENCES

Abdulla, S. & Sagara, I., 2009. Dispersible formulation of artemether/lumefantrine: specifically developed for infants and young children. Malaria Journal, 8(1) 1475-2875.

Abruzzo, A. et al., 2012. Mucoadhesive chitosan/gelatin films for buccal delivery of propranolol hydrochloride. Carbohydrate Polymers, 87(1) 581-588.

Aggrawal, J., Gurpeet, S., Saini, S. & Rana, A., 2011. Fast dissolving films: A novel Approach to oral drug delivery. International Research Journal of Pharmacy, 2(12) 69-74.

Alexander, A., Swarna, A. & Tripathi, D., 2011. Polymers and Permeation Enhancers: Specialized Components of Mucoadhesives. Stamford Journal of Pharmaceutical Science, 4(1) 91-95.

Alvares, T., Junior, C., Silva, J. & Paschoalin, V., 2012. Acute L-Arginine supplementation does not increase nitric oxide production in healthy subjects. nutrition and metabolism, 54(9) 1-8.

Alvarez-Fuentes, J., Fernandez-Arevalo, M., Holgado, M. A.,Caraballo, I., Llera, J. M., Rabasco, A. M. 1994. Characterization of morphine polymeric co precipitates. Pharmazie.49: 834-839

Ameen, V., Pobiner, B., Giguere, G. & Carter, E., 2006. Ranitidine (Zantac) Syrup versus Ranitidine Effervescent Tablets (Zantac, EFFERdose) in children. Pediatr Drugs, 8(4) 265-270.

Andrews, G., Laverty, T. & Jones, D., 2009. Mucoadhesive polymeric platforms for controlled drug delivery. European Journal of Pharmaceutics and Biopharmaceutics, 71(3) 505-518.

Artusia M, S. P., (2003). Buccal delivery of thiocolchicoside: in vitro and in vivo permeation studies. Int J of Pharm., 203-213.

Arya, A., Chandra, A., Sharma, V. & Pathak, K., 2010. Fast Dissolving Oral Films: An

Innovative Drug Delivery System and Dosage Form. International Journal of ChemTech Research, 2(1) 576-583.

Attia MA1, El-Gibaly I, Shaltout SE, Fetih GN., 2004. Transbuccal permeation, anti-inflammatory activity and clinical efficacy of piroxicam formulated in different gels. Int J Pharm, 11-28.

Ayensu, I., 2012. Development of Novel Formulations for Mucosal Delivery of Protein Based Drugs. University of Greenwich. 45-46.

Ayensu, I., Mitchell, J. & Boateng, J., 2012. In vitro characterisation of chitosan based xerogels for potential buccal delivery of proteins. Carbohydrate Polymers, 89(3) 935-941.

Baker, K. C., Bellair, R., Manitiu, M., Kannan, R.M., 2009. Structure and mechanical properties of supercritical carbon dioxide processed porous resorbable polymer constructs. Journal of the Mechanical Behaviour of Biomedical Materials, 2(6) 620-626.

Bala, R., Pawar, P., Khanna, S., Arora, S., 2013. Orally dissolving strips: A new approach to oral drug delivery system. Int J Pharm Investig. 3(2) 67-76.

Balaji, N., Peppa, N., A., (1997) Molecular analysis of drug delivery system controlled by dissolution of the polymer carrier, Journal of Pharmaceutical Science. 86(3) 297-304.

Bansal, K., Rawat, M. K., Jain, A., Rajput, A., Chaturvedi, T.P., Singh, S. 2009. Development of Satranidazole Mucoadhesive gel for the treatment of periodontitis. AAPS PharmSciTech, 10 (3), 716-723.

Barton, A.F.M., Handbook of solubility parameters and Other cohesion parameters, 2nd ed, Boca Raton, CRC Press.

Bemkop, A., 2005. Thiomers: A new generation of mucoadhesive polymers. Advanced drug delivery reviews, 57(11) 1569-1582.

Boateng J, Stevens H, Eccleston G, Auffret A, Humphrey J, Matthews K., 2009.

Development and mechanical characterization of solvent-cast polymeric films as potential drug delivery systems to mucosal surfaces. Drug Development and Industrial Pharmacy, 35(8) 986-996.

Boateng, J., Pawar, H. & Tetteh, J., 2013. Polyox and carrageenan based composite film dressing containing anti-microbial and anti-inflammatory drugs for effective wound healing. International Journal of Pharmaceutics, 441(1-2) 181-191.

Boateng, J.S., Auffret, A.D., Matthews, K. H., Humphrey, M. J., Stevens, N.E., Eccleston, G. M., 2010. Characterisation of freeze-dried wafers and solvent evaporated films as potential drug delivery systems to mucosal surfaces. International Journal of Pharmaceutics, 389 (1-2) 24-31.

Boateng, J.S., Auffret, A.D., Matthews, K. H., Humphrey, M. J., Stevens, N.E., Eccleston, G. M., 2009. In vitro drug release studies of polymeric freeze-dried wafers and solvent-cast films using paracetamol as a model soluble drug. International Journal of Pharmaceutics, 378 (1-2) 66-72.

Bobade, N. et al., 2013. A Review on Buccal Drug Delivery System. International Journal of Pharmacy and Pharmaceutical Science Research, 3(1) 35-40.

Bowles, A., Keane, J., Ernest, T., Clapham, D., Tuleu, C., 2010. Review specific aspects of gastro-intestinal transit in children for drug delivery design. Int. J. Pharm. 395(1-2) 37-43.

Boyd, D., Marsh, T., 2008. CHED 30 - Thermal analysis in the undergraaduate chemistry laboratory: Thermogravimetric analysis and differential scanning calorimetry as an introduction to materials chemistry.. Abstracts of Papers of the American Chemical Society, (30) 236.

Brändstrom A., Lindberg P., Bergman N-K., Alminger T., Ankner K., Junggren U. et al.1989. Acta Chem. Scand. 43, 538–548.

Breuer, E., Chorchade, M., Fisher, J., Golomb, G. 2009. Glossary of terms related to pharmaceutics. IUPAC Publication, 81.

Brügemann, L., Gerndt, E., 2004. Detectors for X-ray diffraction and scattering: a user's overview. Nuclear Instruments and Methods in Physics Research , 531(1-2) 292-301.

Byun, Y., Ward, A., Whiteside, S., 2012. Formation and characterization of shellac-hydroxypropyl methylcellulose composite films. Food Hydrocolloids, 27(2), pp. 364-370.

Caykara, T., Demirci, S., Eroglu, M. S. and Guven, O., 2005. Poly (ethylene oxide) and its blends with sodium alginate, Polymer, 46(24), 10750-10757.

Chadha, R., Arora, P., Bhandari, S., Bala., 2012. Thermomicroscopy and its pharmaceutical applications. Formtex, 1013-1024.

Chapman, B., Rees, C., Lippert, D., Sataloff, R., 2011. Adverse Effects of Long-Term Proton Pump Inhibitor Use: A Review for the Otolaryngologist. Journal of Voice, 25(2) 236-240.

Chapman, L., 2004. Application of high temperature DSC technique to nickel based superalloys. International symposium in liquid metals, 39, 7229-7236.

Chen LL, C. D., 1999. A mechanistic analysis to characterize oramucosal permeation properties. Int J Pharm, 63-72.

Chen, J.L. and Chy, C.N. 1970. Composition producing adhesion through hydration, in Manlly, R.S (ed), Adhesion in biological systems. Academic Press,New York, 163 – 184.

Chin, L., 2000. FDA. [Online]
Available at: http://www.fda.gov/ohrms/dockets/ac/00/backgrd/3650b1b_tab_09.pdf
[Accessed february 2013].

Choi, H.-G.et al., 2000. Formulation and in vivo evaluation of omeprazole buccal adhesive tablet. Journal of Controlled Release, 68(3) 405-412.

Choonara, I., 1999. Essential Drugs for Infants and Children: European Perspective. American Academy of Pediatric, 104(3) 605-607.

Chul, J., Tordoff, J., Kennedy, J. & Relth, D., 2004. Trends in accessibility to medicines for children in New Zealand: 1998–2002. British Journal of Clinical Pharmacology, 57(3) 322-

327.

Cilurzo, F., Selmin, F., Minghetti, P. & Rimoldi, I., 2005. Fast-dissolving mucoadhesive microparticulate delivery system containing piroxicam. European Journal of Pharmaceutical Sciences,, 24(4) 355-361.

Cooper, A.I., 2001. Recent developments in materials synthesis and processing using supercritical CO2. Advanced Materials, 13(14) 1111-1114.

Cotsa, P., Lobo, J.M.S. 2001. Modelling and comparison of dissolution profiles. European Journal of Pharm Sci, 3(2)123-133.

Cui, F., He, C., He, M., Cui, T., Yin, L., Qian, F., Yin, C., 2008. Preparation and evaluation of chitosan-ethylenediaminetetraacetic acid hydrogel films for the mucoadhesive transbuccal delivery of insulin. Journal of Biomedical Materials Research part A, 1064-1071.

Cui, L., Zhang, Z. H., Sun, E., Jia, X. B., 2012. Effect of β-Cyclodextrin Complexation on Solubility and Enzymatic Conversion of Naringin. Int. J. Mol. Sci., 13, 14251-14261.

Dash, S., Murthy, N.P., Nath, L., Chowdhury, P. 2010. Kinetic modeling on drug release from controlled drug delivery systems. Acta Pol Pharma-Drug Res, 67(3), 217-223.

Das, K. S., Rajabalaya, R, David, S., Gani, N., Khanam, J., Nanda, A., 2013. Cyclodextrins-The Molecular Container. Research Journal of Pharmaceutical, Biological and Chemical Sciences. 2(4) 1694-1720.

Diaham, S., Locatelli, M., Lebey, T. & Malec, D., 2011. Thermal imidization optimization of polyimide thin films using Fourier transform infrared spectroscopy and electrical measurements. Thin Solid Films, 519(6) 1851-1856.

Diaz Del Consuelo l, F. F., 2005. Transport of fentanyl through pig buccal and esophageal epithelia in vitro: influence of concentration and vehicle pH. Pharm Res., 1525-1529.

Diaz Del Consuelo l, P. G., 2005. Evaluation of pig esophageal mucosa as a permeability barrier model for buccal tissue. J Pharm Sci., 2777-2888.

Dittrich, H. & Bieniok, A., 2009. Measurment methods | Structural Properties: X-Ray and Neutron Diffraction. Encyclopedia of Electrochemical Power Sources, 718-737.

Dixit, R., Puthli, S. 2009. Oral strip technology: Overview and future potential. J Control Release, 139 (38) 94-107.

Dodds, M., Johnson, D. & Yeh, C.-k., 2005. Health benefits of saliva: a review. Journal of Dentistry, 33(3) 223-233.

Dojo, M., Azuma, T., Saito, T. & Ohtani, M., 2001. Effects of CYP2C19 gene polymorphism on cure rates for Helicobacter pylori infection by triple therapy with proton pump inhibitor (omeprazole or rabeprazole), amoxycillin and clarithromycin in Japan. Digestive and Liver Disease, 33(8) 671-675.

Dowty ME, K. K., 1992. Transport og thyrotropin releasing hormone in rabbit buccal mucosa in vitro. Pharm Res, 1113-22.

Eggerth RM. Rashidbaigi ZA, M. M., 1987. Evaluation of hamster cheek pouch as a model for buccal absorption. Proceed Int Symp Control Rel Bioact Mater., 180-181.

Ekwall, B., Silano, V., Stammati, P., Zucco., 1990. Toxicity test with mammalian cell cultures. Short-term Toxicity test for non-genotoxic effects. 75-93

El-Badry, M., Taha, E. I., Alanazi, A K., Alsarra, I.A., 2009. Study of omeprazole stability in aqueous solution influence of cyclodextrins. J. Drug Del.Sci.Tech, 19(5) 347-351.

Engel, A., Colliex, C., 1993. Application of scanning transmission electron microscopy to the study of biological structure. Current Opinion in Biotechnology, 4(4) 403-411.

Estelle, P., Lanos, C., Melinge, Y., Servais, C., 2006. On the optimisation of a texture analyser in squeeze flow geometry. Measurment, 39(8) 771-777.

Falk R, Randolph TM, Meyer JD, Kelly RM., 1997. Controlled Release of ionic compound from poly (L-Lactide) microspheres produces by precipitation with a compressed anti-solvent. Journal of Controlled Release, 44 (1) 77.

Fan, L., Jiang, L., Xu, Y., Zhou, Y., Shen, Y., Xie, W., Long, Z., Zhou, J., 2011. Synthesis and anticoagulant activity of sodium alginate sulfates. Carbohydrate Polymers, 83(4) 1797-1803.

Fan, L., Wang, L., Gao, S., Wu, P., Li, M., Xie, W., Liu, S. and Wang, W. 2011. Synthesis, characterization and properties of carboxymethyl kappa carrageenan. Carbohydrate Polymers, 86(3), 1167-1174.

Fass, R.1., Fennerty, M.B., Ofman, J.J., Gralnek, I.M, Johnson, C., Camargo, E., Sampliner, R.E., 1998. The Clinical and Economic Value of a Short Course of Omeprazole in Patients With Noncardiac Chest Pain. Gastroenterology, 115(1) 42-49.

Favati, F., King, J.W., Friedrich, J.P., Eskins., K.,1988. Supercritical CO2 extraction of carotene and lutein from leaf protein-concentrates. Journal of Food Science, 53(5): p. 1532-1536.

Figueiras A, Hombach J, Veiga F , Bernkop-Schnurch A. 2009. In vitro evaluation of natural and methylated CDs as buccal permeation enhancing system for omeprazole delivery. European Journal of Pharmaceutics and Biopharmaceutics.71.339-345.

Figueiras A, Sarraguça J, Pais A, Carvalho R, and Veiga F., 2010. The Role of L-arginine in Inclusion Complexes of Omeprazole with cyclodextrins. AAPS Pharm Sci Tech.11(1) 233-240.

Figueiras, A., Paris, A. C. C., Veiga, F. J. B., 2010. A Comprehensive Development Strategy in Buccal Drug Delivery. AAPS Pharm Sci Tech, 11(4) 1703-1712.

Frank, L., Hovorka, M., Konvalina., Mikmekova, S., Mullerova, I., 2011. Very low energy scanning electron microscopy. Nuclear Instruments and Methods in Physics Research, 645(1) 46-54.

Frenning, G. 2011. Modelling drug release from inert matrix system: from moving-boundry to continuous-field description. Inter Jour of Pharm, 418 (1), 88-99.

Fu Y and Kao WJ., 2010. Drug release Kinetics and transport mechanisms of non-degradable polymeric delivery system .Expert Opinion on Drug Delivery 7(4): 429-444.

Funami, T. Fang, Y., Noda, S., Ishihara., Nakauma., Draget., 2009. Rheological properties of sodium alginate in an aqueous system during gelation in relation to supermolecular structures and Calcium binding. Food Hydrocolloids, 23(7) 1746-1755.

Gandhi, P., 2011. A review article on mucoadhesive buccal drug delivery system. International Journal of Pharmaceutical Research and Development, 3(5) 159-173.

Garsuch, V. 2009. Preparation and characterization of fast-dissolving oral films for pediatric use [Doctoral thesis]: Heinrich Heine University, Dusseldorf.

Geandier, G. Gautier, E.A., Settefrati, A., Dehmas, M., Appolaire,B., 2012. Study of diffusive transformations by high energy X-ray diffraction. Comptes Rendus Physique, 13(3) 257-267.

Ghosal, K., Chakrabarty, S., Nanda, A. 2011. Hydroxypropyl methylcellulose in drug delivery. Der Pharmacia Sinica. 2 (2)152-168.

Gin P., Asada M., Endoh M. K., Gedelian C., Lu T. M., Koga T., 2009. Introduction of molecular scale porosity into semicrystalline polymer thin films using supercritical carbon dioxide. Applied Physics Letters. 94, 121908.

Ginty P, Whittaker M, Shakesheff K, Howdle S., 2005. Drug Delivery goes supercritical. Nontoday, 42-48,

Giovino, C., Ayensu, I., Tetteh, J. & Boateng, J., 2012. Development and characterisation of chitosan films impregnated with insulin loaded PEG-b-PLA nanoparticles (NPs): A potential approach for buccal delivery of macromolecules. International Journal of Pharmaceutics,

428(1-2) 143-151.

Gomez, A.M. and E.M. de la Ossa., 2000. Quality of wheat germ oil extracted by liquid and supercritical carbon dioxide. Journal of the American Oil Chemists Society, 77(9) 969-974.

Gupta, S.K., Singhvi, I.J., Shirsat, M., Karwani, G., Agarwal, A., Agarwal, A., 2011. Buccal Adhesive Drug Delivery System: A Review. Asian Journal of Biochemical and Pharmaceutical Research, 2(1) 105-114.

Gury, R., Meyer, J.-M. & Peppa, N., 1984. Bioadhesive intraoral release systems: design, testing and analysis. Biomaterials, 5(6) 336-340.

Harrison, J., Ojeda, J. & Romero, M., 2012. The applicability of reflectance micro-Fourier-transform infrared spectroscopy for the detection of synthetic microplastics in marine sediments. Science of The Total Environment, 416(1) 455-463.

Hancock, B.C and Parks, M. 2000. What is the true solubility advantage for amorphous pharmaceuticals, Pharm Res, 17(4) 397-404.

Herrero, M., A. Cifuentes., E. Ibanez., 2006. Sub- and supercritical fluid extraction of functional ingredients from different natural sources: Plants, food-by-products, algae and microalgae - A review. Food Chemistry, 98(1) 136-148.

Herrero, M., Mendiola, J.A., Cifuentes., Ibanez, E., 2010. Supercritical fluid extraction: Recent advances and applications. Journal of Chromatography A, 1217(16) 2495-2511.

Hill MW, S. C., 1982. A histological method for the visualization of the intercellular permeability barrier in mammalian stratified squamous epithelia. Histochem J., 641-648.

Hopwood D, L. K., 1978. The electron microscopy of normal human oesophageal epithelium. Virchows Arch B Cell Pathol., 345-358.

Hopwood D, M. G.,1991. Uptake of horseradish peroxidase by human oesophageal explants over 24 h. Histochen J., 409-414.

http://polymer.ustc.edu.cn/xwxx_20/xw/201109/P020110906263097048536.pdfd

http://www.fda.gov/downloads/Drugs/GuidanceComplianceRegulatoryInformation/Guidances/ucm070237.pdf

https://www2.chemistry.msu.edu/faculty/reusch/virttxtjml/Spectrpy/InfraRed/irspec1.htm

Huntsberger, J.R. 1971. Surface energy, wetting and erosion. J Adhesion, 6:11-14.

Ivanisevic, I., McClurg, R.B and Schields, P.J. 2010. Usese of X-Ray Powder Diffraction in the Pharmaceutical Industry, New York: John Wiley & sons, Inc, 38-45.

Jackman, H., Krakhmalev, P., Svensson, K., 2013. Image formation mechanisms in scanning electron microscopy of carbon nanotubes, and retrieval of their intrinsic dimensions. Ultramicroscopy, 124, 35-39.

Jelesarov, I., Bosshard, H., 1999. Isothermal titration calorimetry and differential scanning calorimetry as complementary tools to investigate the energetics of biomolecular recognition. Journal of Molecular Recognition, 12, 3-18.

Jeng-Lin, H., 2010. Role of proton pump inhibitors in the management of peptic ulcer bleeding. World J Gastrointest Pharmacol Ther, 1(2) 51-53.

Jimenez, A., J. Zhang, M.A. Matthews., 2008. Evaluation of CO2-based cold sterilization of a model hydrogel. Biotechnology and Bioengineering, 101(6) 1344-1352.

Johnson, C., 2013. Differential scanning calorimetry as a tool for protein folding and stability. Archives of Biochemistry and Biophysics, 531(1-2) 100-109.

Junginger, H., Hoogstraate, J. & Verhoef, C., 1999. Recent advances in buccal drug delivery and absorption - in vitro and in vivo studies. Journal of Controlled Release, 62(1-2) 149-159.

Kairuz, T. et al., 2007. Extemporaneous compounding in a sample of New Zealand hospitals: a retrospective survey. The New Zealand Medical Journal, 120(1251) 11-19.

Kendall, M. J., 2003. Review article: esomeprazole the first proton pump inhibitor to be developed as an isomer. Alment Pharmacol Ther. 17, 1-4.

Kendall, J.L., Canelas, D.A., Young, J.L., DeSimone, J.M. 1999. Polymerization in supercritical Carbon dioxide. Chem Rev. 99, 543-563.

Kianfar, F., Antonijevic, M., Chowdhry, B. & Boateng, J., 2013. Lyophilized wafers comprising carrageenan and pluronic acid for buccal drug delivery using model soluble and insoluble drugs. Colloids and Surfaces B: Biointerfaces, 103, 99-106.

Kianfar, F., Chowdhry, B., Antonijevic, M. and Boateng, J., 2011. Carrageenan freeze-dried wafers incorporating paracetamol or indomethacin for mucosal delivery. The AAPS Journal, 13 (S2). ISSN 1550-7416.

Kianfar, F., Chowdhry, B. Z., Antonijevic, M. D., Boateng, J.S., 2012. Novel films for drug delivery via the buccal mucosa using model soluble and insoluble drugs. Drug Development and Industrial Pharmacy, 38 (10) 1207-1220.

Kok, K. P., Choy, F. W. 1999. Polymeric Films as Vehicle For Buccal Delivery: Swelling, Mechanical, and Bioadhesive Properties, J Pharm Pharmaceut Sci. 2, 2, 53-61.

Korsmeyer, RW, Gurny, R, Doelker, E, Buri, P and Peppas, N.A., 1983. Mechanisms of solute release from porous hydrophilic polymers. Int. J. Pharm., 15: 25-35.

Koschier F, K. V., 2011. In vitro effect of ethanol and mouthrinse on permeability in an oral buccal mucosal tissue contruct. Food Chem., 2524-2529.

Kristensen, H., 2012. WHO guideline development of paediatric medicines: Points to consider in pharmaceutical development. International Journal of Pharmaceutics, 435(2) 134-135.

Kulkarni U, M. R., 2010. Porcine buccal mucosa as in vitro model: effect of biological and experimental variables. J Pharm Sci, 1265-1277.

Kumar, A., Negi, Y., Bhardwaj, N. & Choudhary., 2012. V. Synthesis and characterization of methylcellulose/PVA based porous composite. Carbohydrate Polymers. 88(4) 1364-1372.

Kumar, P., Doddayya, H., Reddy, R., 2011. Design and evaluation studies on novel floating

tablets for peptic ulcer treatment. Journal of Advanced Pharmacy Education & Research, 2(1) 159-176.

Laidler, K.J., Meiser, J.H., Sanctuary, B.C. 2003. Physical Chemistry, 4th edition, Boston: Houghton Mifflin Company, 25-278.

Lan, Q., Yu, J., Zhang, J., He, J. 2011. Ehanced crystallization of Bisphenol a polycarbonate in thin and ultrathin films by supercritical carbon dioxide. ACS Publication. 44, 5743-5749.

Langer M, Robison J., 1986. Fundamental aspects of bioadhesion, Pharm.Int ,7,114-117
.

Larsson, H., Mattsson, H., Sundell, G., Carlsson, E. 1985. Animal phamacodynamics of omeprazole. A survey of the phamacological properties of omeprazole in animals. Scand.J. Gastroenterol. 20, 23-25

Le Brun, P., Fox, P., De Vries, M. & Bodde, H., 1989. In vitro penetration of some β-adrenoreceptor blocking drugs through porcine buccal mucosa. International Journal of Pharmaceutics, 49(2) 141-145.

Lehr, C., 2000. lectin-mediated drug delivery: the second generation of bioadhesives. Journal of control release, Volume 65, 19-29.

Lehrsch, G., Sojka, R., Koehn, A., 2012. Surfactant effects on soil aggregate tensile strength. Geoderma, Volume 189-190, 199-206.

Li, Y., Park, E. J., Lim, K. T., Johnston, K.P., Green, P. F., 2007. Role of interfacial interactions on the anomalous swelling of polymer thin films in supercritical carbon dioxide. Wily Inter Science. 45, 1313-1324.

Liao, X., Wang, J., Li, J.S, He, J. 2004. Polym. Sci Part B: Polym. Phys. 42, 280.

Lim, K., Kim, D., Paik, U. & Kim, S., 2003. Effect of the molecular weight of poly(ethylene glycol) on the plasticization of green sheets composed of ultrafine BaTiO3 particles and poly(vinyl butyral). Materials Research Bulletin, 38(1) 1021-1032.

Lind, T, Cederberg, C, Ekenved, G, et al., 1989. Effect of omeprazole-A gastric proton pump inhibitor-On pentagastrin stimulated acid secretion in man. 24,270-276.

Liu, F., Moreno, P. & Basit, A., 2010. A novel double-coating approach for improved pH-triggered delivery to the ileo-colonic region of the gastrointestinal tract. European Journal of Pharmaceutics and Biopharmaceutics, 74(2-3) 311-315.

Liu, F., Ranmal, S.,Batchelor, H.K., Orlu-Gul, M., Terry B., Thomas, E.W., Flanagan, T., Tuleu, T., 2014. Patient-Centred Pharmaceutical Design to Improve Acceptability of Medicines: Similarities and Differences in Paediatric and Geriatric Populations. Adis. DOI 10.1007/s40265-014-0297-2

Lousinian, S., Missopolinou, D. & Panayiotou, C., 2013. Fibrinogen adsorption on zinc oxide nanoparticles: A Micro-Differential Scanning Calorimetry analysis. Journal of Colloid and Interface Science, 395(1) 294-299.

Lowman, A. et al., 2004. Tructural and dynamic response of neutral and intelligent networks in biomedical environments.. Advances in Chemical Engineering, 29(01) 75-130.

Lowamn, A.M., Dziubla, T.D., Bures, P., Peppas, N.A. 2004. Structural and dynamic response of neutral and intelligent network in biomedical environment in Sefton, A. P.a.M.V. ed Adv in Chem Engineering, Acadamic Press, 75-130.

Ma, W.M., Yu, J., He, J.H. 2005. Macromal. Rapid Commun. 26. 112.

Madanick, R., 2011. Proton pump inhibitor side effects and drug interactions: Much ado about nothing?. Cleveland clinic journal of medicine, 78(1) 39-49.

Malviya, R., Bansal, V., Pal, O. P., Sharma, P. K., 2009. High performance liguid chromatography: A short review. J of Global Pharm Tech. 22-26.

Markovic N, Agotonovic-Kustrin S, Glass B, Prestidge CA., 2006. Physical and thermal characterisation of chiral omeprazole sodium salts. J Pharm and Biom Anal. 42:25–31.

Martel, R., Paquin, P., Buijs, H., 1991. Water Absorption in Fluid Milk Using Fourier

Transform Infrared Spectroscopy. Journal of Dairy Science, 74(7) 2073-2076.

Miller, N., Chittchang, M. & Johnson, T., 2005. The use of mucoadhesive polymers in buccal drug delivery. Advanced drug delivery, Volume 57, pp. 1666-1691.

Min DS, Um KA, Kim YS, Park PW., 1995. Method for preparing enteric-coated oral drugs containing acid-unstable compounds. U.S. Patent.

Mishra, R., Amin, A., 2011. Manufacturing Techniques of Orally Dissolving Films. Pharmaceutical Technology, 35(1) 70-73.

Missaghi, S., 2006. Formulation design and fabrication of acid-labile compaounds employing enteric coating technique using omeprazole as a model drug. s.l.:temple university graduate board.

Mitra, A. K., Alur, H. H., Johnston, T. P., 2002. Peptides and proteins—buccal absorption. Encyclopaedia of Pharmaceutical Technology, 2nd edn, Marcel Dekker, Inc., New York, 2081-2095.

Moore, J.W., Flanner, H.H., 1996. Mathematical comparison of curves with an emphasis on in vitro dissolution profile. Pharmaceutical Technology. 20 (6), 64-74.

Morales J, McConville J. 2011. Manufacture and characterization of mucoadhesive buccal films. European Journal of Pharmaceutics and Biopharmaceutics. 77(2):187-199.

Mukharya, A., Chaudhary, S., Bheda, A., Mulay, A., Mansuri, N., Laddha, N. 2011. Stable and bioequivalent formulation development of highly acid labile proton pump inhibitor: Rabeprazole. Inter Jour of Pharm Res & Inno. 2:1-8.

Nahata, M., 1999. pediatric drug formulations: A rate-Limiting step. Drug information journal, 33(1-2) 393-396.

Nair M, C. Y., 1993. buccal delivery of progestational steroids: l. Characterization of barrier properties and effect of penetrant hydrophilicity. Int J of Pharm., 41-49.

Nair, A.B.1., Kumria, R., Harsha, S., Attimarad, M., Al-Dhubiab, B.E., Alhaider, I.A., 2013.

In vitro techniques to evaluate buccal films. Journal of Controlled Release, 166(1) 10-21.

Neelagiri, R., Reddy, M., Rao, N., 2013. Buccal patch as drug delivery system: An overview. International Journal of Current Pharmaceutical Research, 5(2) 40-47.

Nibha, K., Pancholi, S., 2012. An Overview on: Sublingual Route for Systemic Drug Delivery. International Journal of Research in Pharmaceutical and Biomedical Sciences, 3(2) 913-923.

Nishioka, K., Nagao, T., Urushidani, T., 1999. Correlation between Acid Secretion and Proton Pump Activity during Inhibition by the Proton Pump Inhibitors Omeprazole and Pantoprazole. Biochemical Pharmacology, 58, 1349-1359.

Nono, M., Durand, D., Nicolai, T., 2012. Rheology and structure of mixtures of ι-carrageenan and sodium caseinate. Food Hydrocolloids, 27(1) 235-241.

Nunn, T., Williams, J., 2004. Formulation of medicines for children. British journal of clinical Pharmacology, 59(6) 674-676.

Palacio, M. L., Schricker, S. R., Bhushan, B., 2011. Bio-adhesion of various proteins on random, diblock and triblock copolymers surface and the effect of pH condition. J R Soc Interface, 8(58), 630-640.

Panda, B., Dey, N., Rao, M., 2012. Developmemt of Onnovative Orally fast Disintegrating film Dosage Forms: A Review. International journal of Pharmaceutical Science and Nanotechnology, 5(2) 1666-1674.

Papkov, M.S., Agashi, K., Olaye, A., Shakesheff, K., Domb, A.J., 2007. Polymer carriers for drug delivery in tissue engineering. Advanced Drug Delivery Reviews, 59(4-5) 187-206.

Pappas, C., Takidelli, C., Tsantili, E., Tarantilis, P.A., Polissiou, M.G., 2011. Quantitative determination of anthocyanins in three sweet cherry varieties using diffuse reflectance infrared Fourier transform spectroscopy. Journal of Food Composition and Analysis, 24(1) 17-21.

Park, H. and Robinson, J.R., 1985. Physico-chemical properties of water insoluble polymers important to mucin/epithelial adhesion. J Controlled Release, 2:47-57.

Paradkar, A., Kelly, A., Gough, T., Coates, D., Blagden, N. 2015. A novel continuous method for co-crystal formation. Process Environment & Sustain. EP/J003360/1.

Patel, R.S., Poddar, S.S. 2009. Development and Characterization of Mucoadhesive Buccal Patches of Salbutamol Sulphate. Curr Drugs Deliv, 6, 140-144.

Patel, V., Desai, T., Chavda, B., Katira, R., 2011. Extemporaneous dosage form for Oral liquids. Pharmacophore, 2(2) 86-103.

Patel, V., Liu, F., Brown, M., 2012. Modeling the oral cavity: In vitro and in vivo evaluations of buccal drug delivery systems. Journal of Controlled Release, 161(1) 746-756.

Pathera, V, Y., Hastak, S, V., Bajaj, N, B. 2013. Polymers used for fast disintegrating oral films: a review. Int. J. Pharm Sci, 21:1:169

Peh, K.K., Wong, C.F., 1999. Polymer films as vehicle for buccal delivery: Swelling, Mechanical, and Bio-adhesive properties. J Pharm Pharmaceut Sci, 2:53-61, 1999.

Peppas , N., Buri, P., 1985. Surface, interfacial and molecular aspects of polymer bioadhesion on soft tissues. Journal of Controlled Release , 10(1) 0168-3659.

Peppas, N.A., Bury, P.A. 1985. Surface interfacial and molecular aspects of polymer bioadhesion on soft tissues. Journal of cont Release. 2, 257-275.

Pham, V. Q., Rao, N., Ober, C. K., 2003. Swelling and dissolution rate measurement of polymers thin films in supercritical carbon dioxide. J. of supercritical fluids. 31, 323-328.

Pilbrant, A., Cederberg, C., 1985. Development of an oral formulation of omeprazole. Scand. J. Gastroenterol. 20:113-120.

Pintye-hodi, K., Regdon Jr, G., Eros, I., Suvegh, K., Marek, T., Kery, I., Zelko, R. 2006. Metolose-PEG interaction as seen by positron annihilation spectroscopy. Inter J Pharm. 313;66-71.

R.P. Dixit, S. P., 2009. Oral strip technology: Overview and future potential. Journal of

Controlled Release. 139(2):94-107.

Rajabi-Siahboomi, A.R., Bowtell, R.W., Mansfield, P., Davies, M.C., Melia, C.D., 1993. "NMR microscopy studies of swelling and water mobility in HPMC hydrophilic matrix systems undergoing hydration," Proc. Int. Symp. Contr. Rel. Bioact. Mater., 20, 292-3.

Rajgor N, P. M. V., 2011. Implantable drug delivery system:An overview. Sytematic Reviews in pahramcy, 91-95.

Reddy, A. K., Debnath, S., Babu, M. N. 2013. A review on diffusion and dissolution controlled drug delivery systems. Journal of Pharm Biology, 3(2), 58-62.

Reddy, C., Chaitanya, K. & Rao, M., 2011. A review on bioadhesive buccal drug delivery systems: current status of formulation and evaluation methods. A review on bioadhesive buccal drug delivery systems: current status of formulation, 19(6) 385-403.

Reidel, A., Leopold, C., 2005. Degradation of Omeprazole induced by enteric polymer solutions and aqueous dispersions; HPLC Investigations. Drug development and Industrial Pharmacy.2;151-160

Regardh, C.G., Gabrielsson, M., Hoffman, J.K., Lofberg, I., Skanberg, I., Gastroenterol, J. 1985. 108 (Suppl.) (1985) 79–94.

Rizvi, S.S.H., Benado, A.L., Zollweg, J.A., Daniels, J.A.., 1986. Supercritical fluid extraction - Fundamental principles and modelling methods. Food Technology, 40(6) 55-65.

Rodriguez-Spong, B., Price, C. P., Jayasankar, A., Matzger, A. J. & Rodriguez-Hornedo, N., 2004. General principles of pharmaceutical solid polymorphism: a supramolecular perspective. Advanced Drug Delivery Reviews. 56, 241-274.
Rossi, S., Sandri, G., Caramella, C., 2005. Buccal drug delivery: A challenge already won?. Drug delivery/formulation and nanotechnology, 2(1) 59-65.

Roy, S., Pal, K., Anis, A., Pramanik, K. and Prabhakar, B., 2009. Polymers in Mucoadhesive Drug-Delivery Systems: A Brief Note', Designed Monomers and Polymers, 12(6), 483-495.

Ruiz, G., Ghaly, E. 2006. Mucoadhesive delivery system using carrageenan and eudragit RLPO. Vitae, 13, 1-2.

Ruiz M., Reyes I., Parera A., Allardo V.1998. Determination of the stability of omeprazole by means of differential scanning calorimetry; J. Therm. Anal.; 51: 29-35.

Malke, S., Shidhaye, S., Desai, J., Kadam, V., 2009. Oral Films - Patient Compliant Dosage Form For Pediatrics. The Internet Journal of Pediatrics and Neonatology, 11(2).

Sahena, F., Zaidul, I. S. M., Jinap, S., Karim, A. A., Abbas, K. A., Norulaini, N. A. N., Omar, A. K. M.., 2009. Application of supercritical CO2 in lipid extraction - A review. Journal of Food Engineering, 95(2) 240-253.

Sandri G, R. S., 2004. Assessment of chitosan derivatives as buccal and vaginal penetration enhancers. Eur J Pharm Sci., 351-359.

Sarisuta, N., Tourtip, T., Chuarcharoern, S., 1998. Chemical stability and mechanism of degradation of omeprazole in solution. Thai. J. Pharm. Sci., 22, 81-88.

Senel, S., Hincal, A.A. 2001. Drug permeation enhancement via buccal route: possibilities and limitation, J. Control. Release, 72. 133-144.

Schachter, A., Ramoni, M., 2007. Paediatric drug development. Nature reviews. Drug Discovery.6, 429-430.

Schirm, E.1., Tobi, H., de Vries, T.W., Choonara, I., De Jong-van den Berg, L.T., 2003. Lack of appropriate formulations of medicines for children in the community. Acta Paediatrica, 92(3) 1486-1489.

Senel, S., Hincal, A.A. 2001. Drug permeation enhancement via buccal route: possibilities and limitation, J. Control. Release, 72. 133-144.

Setty, C., Babubhai, S., Pathan, I., 2010. Development of valdecoxib topical gels: Effect of formulation variables in the realese of valdecoxib. International Journal of Pharmacy and

Pharmaceutical Sciences, 2(1) 70-73.

Shaikh, R., Singh, T.R.R., Garland, M.N., Woolfson, A.D., Donnelly, R.F., 2011. Mucoadhesive drug delivery systems. Journal of Pharmacy and BioAllied Science , (1)89-100.

Shinkar D. M., Dhake, A. S., Setty, C. M., 2012. Drug delivery from the oral cavity: a focus on mucoadhesive buccal drug delivery systems. Pub , 66(5), 466-500.

Shivonen M, Jarvenpaa E, Hietaniemi V, Huopalathi R., 1999. Advances in supercritical carbon dioxide technologies. Trends in Food Science and Technology. 10, 217-222.

Shoaib, M, H., Tazeen, J., Merchant, H. A. and Yousuf, R. I., 2006. Evaluation of drug release kinetics from ibuprofen matrix tablets using HPMC, Pakistan journal of pharmaceutical science, 19(2), 119-24.

Shojaei, A., 1998. Buccal Mucosa As A Route For Systemic Drug Delivery: A Review. Journal of Pharmacy and Pharmaceutical Sciences , 1(1), pp. 15-30.

Siddhiqui, N., Garg, G. & Sharma, P., 2011. A Short Review on "A Novel Approach in Oral Fast Dissolving Drug Delivery System and Their Patents". Advances in Biological Research, 5(6) 291-303.

Siepmann, J., Siegel, A. R., Siepmann, F., 2012. Diffusion controlled drug delivery systems. Cont. Release Soc. 6-9.

Singh, S., Singh, R.P., Gupta, S.K., Kalyanwat, R., Yadav, S., 2011. Buccal Mucosa as a route for Drug Delivery: Mechanism, Design and Evaluation. Research Journal of Pharmaceutical, Biological and Chemical, 2(3), 358-372.

Smart, J.D. 2005. Buccal drug delivery, Expert Opin Ther Pat, 2(3), 507-17.

Smart, J.D. 2005. The basics and underlying mechanism of mucoadhesion, Adv Drug Deli Rev, 57, 155-1568.

Squier, CA, Kremer, M.J., 2001. Biology of oral mucosa and esophagus. J Natl Cancer Inst

Monogr., 7-15.

Stephenson, G.A., Forbes, R.A., Reutzel-Edens, S.M. 2001. Characterization of the solid state: quantitative issues. Adv Drug Deliv Rev, 48, 67-90.

Stroyer, A., McGinity, J. & Leopold, C., 2006. Solid State Interactions between the Proton Pump Inhibitor Omeprazole and Various Enteric Coating Polymers. Journal of pharmaceutical science, 95(6) 1343-1353.

Sudhakar, Y., Kuotsu, K. & Bandyopadhyay, A., 2006. Buccal bioadhesive drug delivey - A promising option for orally less efficient drugs. Journal of controlled release, Volume 114, pp. 15-40.

Tangri, P., Khurana, S. & Madhav, S., 2011. Muchoadhesive drug delivery: Mechanism and methods of evaluation. International Journal of Pharma and Bio Sciences, 2(1), pp. 458-467.

Thirawong, N., Nunthanid, J., Puttipipatkhachorn, S. & Sriamornsak, P., 2007. Mucoadhesive properties of various pectins on gastrointestinal mucosa: An in vitro evaluation using texture analyzer. European Journal of Pharmaceutics and Biopharmaceutics, 67(1), pp. 132-140.

Thomson, A., Sauve, M., Kassam, N. & Kamitakahara, H., 2010. Safety of the long-term use of proton pump inhibitors. World journal of Gastroenterology, 16(19), pp. 2323-2330.

Tiloo S, R. V. (2011). Mucoadhesive Microparticulate Drug Delivery System. International Journal of Pharmaceutical Review and Research , (9)2011.

Toledo, M., Soared a Silva, M., Ramos, M., Salustio, P., Casimiro, T., Marques, H.C. 2006. $SCCO_2$-assisted preparation of Omeprazole/Cyclodextrin inclusion complexes. Comparative sudy with conventional methods. FCT. PTDC/QUI/66086/2006.

Tuovinen L1, Peltonen S, Järvinen K.., 2003. Drug release from starch-acetate films. Journal of controlled release, 345-354.

Turton, R., 2008. Challenges in the modeling and prediction of coating of pharmaceutical dosage forms. Powder Technology, 181(2) 186-194.

Vandenplas, v. et al., 2009. Pediatric Gastroesophageal Reflux Clinical Practice Guidelines:

Joint Recommendations of the North American Society for Pediatric Gastroenterology, Hepatology, and Nutrition (NASPGHAN) and the European Society for Pediatric Gastroenterology, Hepatology, a. Journal of Pediatric Gastroenterology and Nutrition, 49(4), 498-547.

Verma, N., Chattopadhyay, P., 2011. Polymeric platform for mucoadhesive buccal drug delivery system: a review. Int J Curr Pharm Res, 3(3), 3-8.

Verma, P., Thakur. A.S., Deshmukh, K., Jha, A.K., Verma, S., 2010. Routes of drug administration. International Journal of Pharmaceutical Studies and Research, 1(1) 54-59.

Veuillez, F1., Kalia, Y.N., Jacques, Y., Deshusses, J., Buri, P., 2001. Factors and strategies for improving buccal absorption of peptides. Eur.J.Pharm.Biopharm, 93-109.

Wagner, C., Barth, V., Oliveira, S. & Campos, M., 2011. Effectiveness of the Proton Pump Inhibitor Omeprazole Associated with Calcium Hydroxide as Intracanal Medication: An In Vivo Study. Journal of Endodontics, 37(9)1253-1257.

Walker, G.F.1., Langoth, N., Bernkop-Schnürch, A., 2002. Peptidase activity on the surface of the porcine buccal mucosa. Int J Pharm, 141-147.

Wang, Y., Dave, R., Pfeffer, R., 2004. Polymer coating/encapsulation of nanoparticles using a supercritical anti-solvent process. Journal of Supercritical Fluids, 28(1) 85-99.

Wertz, P. W., Squier, C.A., 1991. Cellular and molecular basis of barrier function in oral epithelium. Crit Rev Ther Drug Carrier Syst, 237-269.

Won, S.H., Kho, S.H., Kim, K.Y., Chung, S.C., Lee, S.W., 2001. Analysis of residual saliva and minor salivary gland secretions. Archives of Oral Biology, 46(7) 619-624.

Zia, W., Ko, Y., Zhu, W., Wong, A., Park, C.B. 2009. A study of the crystallization, melting and foaming behaviors of polylactic acid in compressed CO_2. Int J. Mol. Sci. 10(12); 5381-5397.

Zia, W., Yu, J., Ma, W., He, J. 2007. Cosolvent effect of water in supercritical carbon dioxide facilitating induced crystallization of polycarbonate. Polymer Eng and Sci. 1338-1343.

Zhou, T., Zhang, J., Jingfu, J. & Jiang, G., 2013. Poly(ethylene glycol) plasticized poly(vinyl alcohol)/poly(acrylamide-co-diallyldimethylammonium chloride) as alkaline anion-exchange membrane for potential fuel cell applications. Synthetic Metals, 167(1) 43-50.

Zimmermann, A.E.1., Walters, J.K., Katona, B.G., Souney, P.E., Levine, D., 2001. A Review of Omeprazole Use in the Treatment of Acid-Related Disorders in Children. Clinical therapeutics, 23(5) 660-679.

CHAPTER ELEVEN: APPENDIX

APPENDIX A: EXPERIMENTAL TECHNIQUES

A1 Texture Analyser (TA)

Texture analysis is an important attribute in determination of strength and flexibility of any product and it affects processing, handling, influences behaviour, and affects shelf life and consumer acceptance of products. Texture Analysers are used to measure many properties, such as 'hardness' or resistance to deformation (compression mode), spread-ability, adhesiveness and tensile strength, (brittleness, extensibility) on a vast range of products including films as can be seen in figure 1.24 (Estelle et al., 2006). In the case of films, durability, stress resistance, softness, flexibility, pliability and elasticity are the main mechanical properties measured and are important to maintain the integrity of the dosage form (Lehrsch et al., 2012).

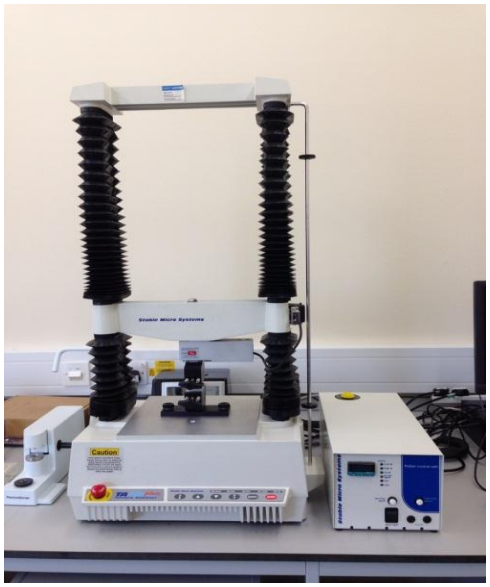

Figure 1.24 Texture analyser

Tensile test is designed to measure the forces required to elongate a specimen to its breaking point. The test has been authorised by the American society for testing and material (ASTM D882) for films with a thickness of less than 1 mm in diameter. It can be performed in two ways (i) static weighting constant rate of grip separation test where two grips holding the film are separated at a constant rate and (i) pendulum weighing constant rate of power grip in

which one of the grips is kept at a constant rate of motion, while the second has a variable rate of motion (Thirawong et al., 2007).

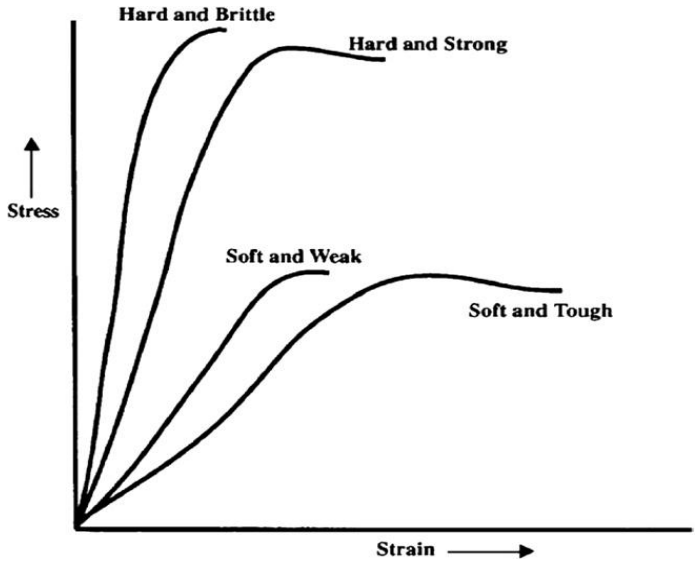

Figure 1.25 Stress verses strain behaviour of the texture analyser results (Jelesarov et al., 1999)

Several values can be obtained from a regular stress–strain curve (Figure 1.25) (Roy et al., 2010); however, most relevant to the study of buccal films are the tensile strength, the elongation at break, and the elastic modulus, also known as Young's modulus. The tensile strength of a film is defined as the resistance of the material to a force tending to tear it apart and normally identified as the maximum stress in the stress–strain curve (Hsieh et al., 2004). It is a complex function of the film's ultimate resistance to rupture and is obtained from the maximum stress value and is reported as the corresponding force (Gupta et al., 2011).

$$Tensile\ strength = \frac{Force\ at\ failure}{cross\text{-}sectional\ area\ of\ the\ film} \qquad \text{Equation 1.5}$$

The elongation at break is a measurement of the maximum deformation the film can undergo before tearing apart and is calculated using equation 1.6

$$Elongation\ at\ break = \frac{Increase\ in\ length\ at\ break}{Initial\ film\ length} \times 100 \qquad \text{Equation 1.6}$$

In general, elongation (or strain) will increase with an increasing content of suitable plasticizing agents. Young's modulus is an evaluation of the stiffness or how the film

deforms in the elastic region. It is defined in the initial elastic phase of deformation and is obtained from the ratio of applied stress and corresponding strain and can be computed from the slope of the linear portion of the stress–strain curve (Abdulla et al., 2009).

$$Young's\ modulus = \frac{slope\ of\ stres{-}strain\ curve}{Film\ thickness \times Cross\ head\ speed} \qquad \text{Equation 1.7}$$

Soft and weak polymers have a low tensile strength, low Young's modulus, and low elongation at break, while a soft and strong polymer exhibits a moderate tensile strength, low Young's modulus, and a high elongation at break. Desired mechanical properties will vary depending on the formulation goals and the method chosen, but in general, some examples of behaviours obtained from stress–strain curves can be depicted (Roy et al., 2010). A typical TA curve is shown in figure 1.26.

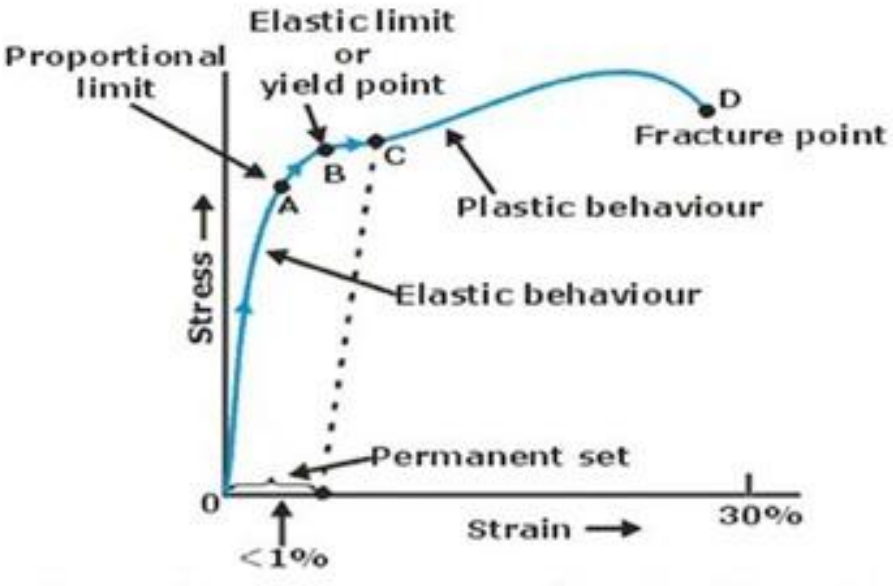

Figure 1.26 Characterisation of the texture analyser peak (Johnson., 2013).

Another functional film property determined by the texture analyser is mucoadhesion. The instrument measures detachment forces from its mobile arm, which after normalizing is considered as adhesive forces, and the maximum force is normally referred to as mucoadhesive force. The important parameters of mucoadhesion are peak adhesive force (PAF) required to separate the film from the mucosal surface was determined by the maximum force. The area under the curve (AUC) representing the total work of adhesion (TWA) is estimated from the force-distance plot whiles the cohesiveness of the sample

determined from distance of travel) which can be used to define the strength of adhesion and residence time of buccal films (Ayensu, PhD thesis, 2012)(Pawar, PhD thesis, 2013).

A2 Thermal analysis

A2.1 Hot stage microscopy (HSM)

In order to produce visually examinable types of thermal transitions of a sample, hot stage microscopy is used. The HSM enables us to understand the dynamics of a particular transition and helps to gain a much more accurate representation, producing valuable information on the compounds, in relation to their melting points and transformations during heating. It is used to explore a combination of both thermal analysis and microscopy, enabling a relationship of temperature and time to function, particle size and particle morphology (Chadha et al., 2012). HSM can be used for compound morphology, solid-solid transformations, interaction between different compounds, dissolution of one compounds in another, sublimation and evaporation, melting upon heating (solid-liquid transformations), solidification upon cooling (liquid-solid transformations) and crystal growth.

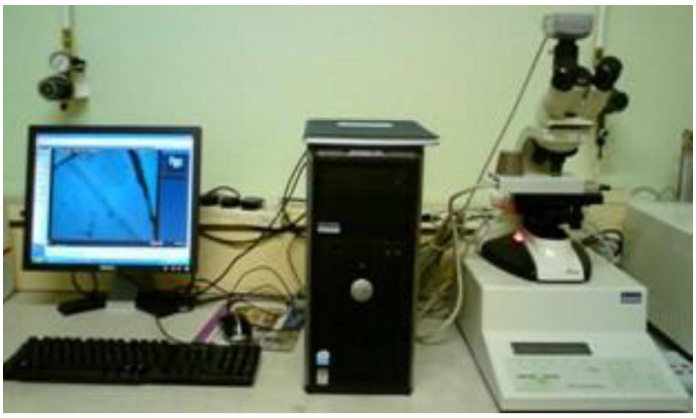

Figure 1.27 Hot stage microscopy instrument used in the current research

A2.2 Differential scanning calorimetry (DSC)

Differential scanning calorimetry (DSC), is a thermal analysis technique that determines how a material's heat capacity (C_p) changes with temperature. DSC measures the temperatures and heat flows associated with transitions in materials as a function of time and temperature in a controlled atmosphere (figure 1.28 and 1.29). It provides quantitative and qualitative

information about physical and chemical changes that involve endothermic and exothermic processes or changes in heat capacity (Chapman., 2004; Hans, 1999). DSC is used to measure melting/boiling temperature, percentage crystallinity, glass transition temperature, softening crystallisation, presence of recyclates/regrinds, enthalpy of melting, effects of plasticisers and polymer blends (presence, composition and compatibility) and polymorphic changes that can occur during formulation or storage. Such information helps formulators to design drug delivery systems with adequate stability and appropriate solubility *in-vivo* to obtain improved bioavailability at the site of the action (Boyd et al., 2008).

Figure 1.28 DSC instrument used in this research

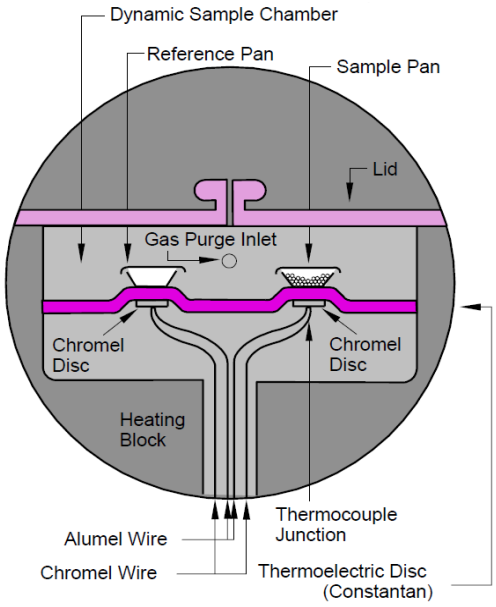

Figure 1.29 Sample and reference pan inside the DSC machine. Available at - <http://masters.donntu.edu.ua/2006/feht/borisenkov/lib/DCSE_2_clip_image002.jpg > [Accessed: 24/05/2013]

There are two main types of DSC, heat flux and power compensation DSC.

In a heat flux DSC, these same events cause the sample to absorb heat (endothermic) and be cooler than the furnace, so the peaks in a thermogram point downwards. The reverse logic applies to exothermic events where energy is released. The temperature of the calorimeter is increased linearly with the time (scanned) while the heating rate ($d_T/d_t = \beta$) is maintained constant. The same heating power is applied to the sample and reference pans and the temperature difference (ΔT) between those two pans is measured (Lousinian et al., 2013). The output signal is obtained by converting ΔT to ΔQ (heat difference). The International Conference on Thermal Analysis and Calorimetry (ICTAC) set the convention that curves should follow this pattern many years ago. Most modern software systems allow the analyst to flip the curves as required (Lousinian et al., 2013).

Power compensation systems require two separate but identical surfaces independently controlling the temperature of the sample and reference. The same temperature is supplied to both pans (sample and reference) and the difference in the amount of input energy to the two furnaces detected. (Johnson., 2013). This difference in the heat signals is a measure of the enthalpy or heat capacity difference in the sample in comparison to the reference (Figure 1.29). Because of this, power compensation DSC is based on the "Zero Balance Principle", by maintaining the sample and reference pans at the same temperature and measuring the difference in power supplied to them and then directly recording that as signal ΔQ (ΔQ = heat) (Johnson., 2013). An individual signal (d_H/d_t which is the normalized heat generated per time unit or normalised heat flow) is proportional to the difference of heat input between sample and reference (Boyd & Marsh., 2008).

DSC conducts results through heat flows into the two pans. Heat flow is always higher in the sample because of greater heat capacity (C_p). The variation in flow d_q/d_t creates a small temperature difference ΔT across the specimen which is measured by a thermocouple.
The heat capacity is measured by following equation:

$\Delta T = K\, d_q/d_t = KC_p\beta$ Equation 1.8

where the symbols represent the following:

d_q/d_t = heat flow ΔT = temperature variation

C_p = heat capacity T = temperature

K = heat resistance t = time

β = heating rate

Figure 1.30consist of the heat flow plotted against the temperature. By using data, the enthalpies of transitions can be calculated by integrating the peak using the following equation:

$$\Delta H = KA \qquad \text{Equation 1.9}$$

ΔH is the enthalpy of transition, K is the calorimetric constant and A is the area under the curve.

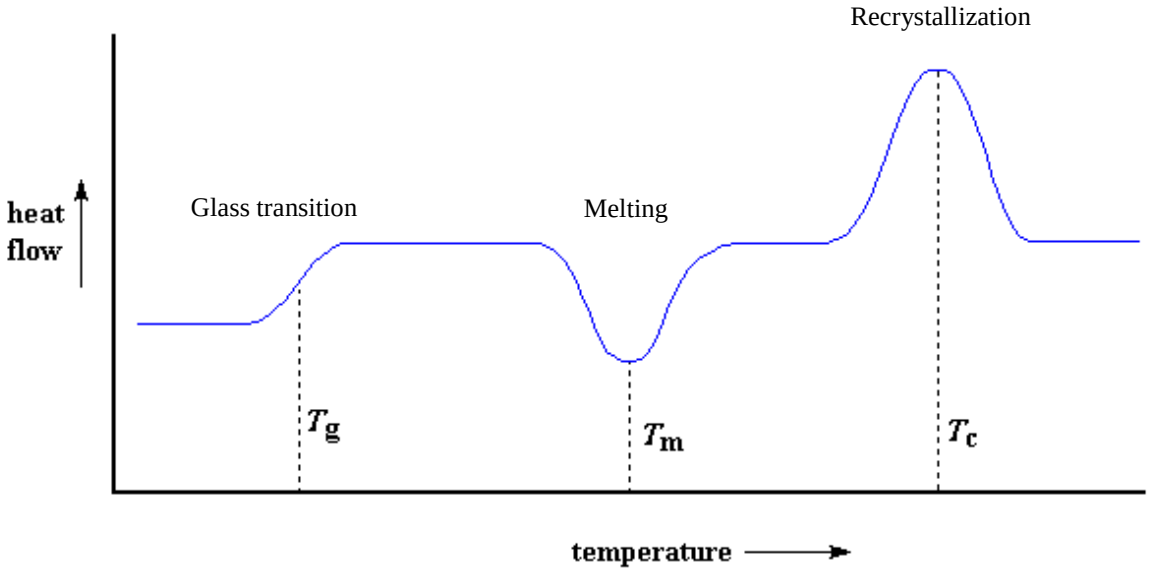

Figure 1.30 Peak behaviour of DSC results (Lousinian et al., 2013)

These curves (Figure 1.30) can be used to calculate the enthalpies of transitions, (ΔH), by integrating the peak of the state transition, where K is the calorimetric constant and A is the area under the curve (Johnson., 2013).

A2.3 Thermogravimetric analysis (TGA)

The thermogravimetric instrument is designed to assess the thermal stability of substances within the sample and a simple, yet accurate, way of measuring the thermal stability of samples, weight loss, moisture content and decomposition patterns. Many of these samples tend to exhibit changes in weight, producing characteristic curves when heated from an ambient temperature to approximately 900˚C. In order to explore the data from a quantitative approach, the gradient can be used in order to create a link to a thermal event such as a process of oxidisation or a reduction of water of crystallisation. With much more complex thermograms, it can be very useful to use a derivatogram (DTG) to interpret data. Samples are heated within a furnace, using temperature controlled programmes and are used to determine a samples hydration levels, moisture content, and decomposition stages. Absorbed and bound water can be differentiated by the different stages of weight loss and the temperature ranges (Chen et al, 1995). Within these types of processes, the TGA makes it possible, to manipulate chemical processes such as oxidation reactions. This can be done by controlling the atmosphere with elements such as oxygen or nitrogen (Rodrıguez-Spong et al., 2004; Zohuriaan et al., 2004). The different output of results given by the TGA serves as a quantitative tool for compound identification. A change in the sample mass is measured by temperature/time thermo balance function. Only changes that affect the mass of the sample size will have any effect on the measurements; thus, condensed phases that have no effect are those such as melting or crystalline transitions.

.

Figure 1.31 Thermogravimetric analysis instrument used in this research

A2.4 Scanning electron microscopy (SEM)

In scanning electron microscopy (SEM) images are formed by cathode ray tube synchronized with an electron probe as it scans the surface of an object. In a typical SEM an electron gun and multiple condenser lenses produce a beam and multiple condenser angles off the optic axis by the first electromagnetic scan coils. The second set of scan coils deflects the beam back across the optical axis. Both sets of scan coils are in the bore of the final lens (Frank et al., 2011). From this crossover, the rays, strike the specimen at various points one at a time. The scan coils and cathodes ray tubes are powered by the same scan generator, so that each scanned point in the specimen is unique as reproduced on the displaying or the recording cathode ray tube and video amplifier. To these amplifiers, one or more of the resultant signals - high-energy backscattered electrons; low-energy secondary and/or backscattered electrons, X-rays, and cathode-luminescent radiation in the UV, visible, and infrared regions - are fed. All the results can be monitored separately or simultaneously by means of the appropriate detectors (Jackman et al., 2013). Figure 1.32 shows the internal structure and mechanism of action of a typical SEM instrument.

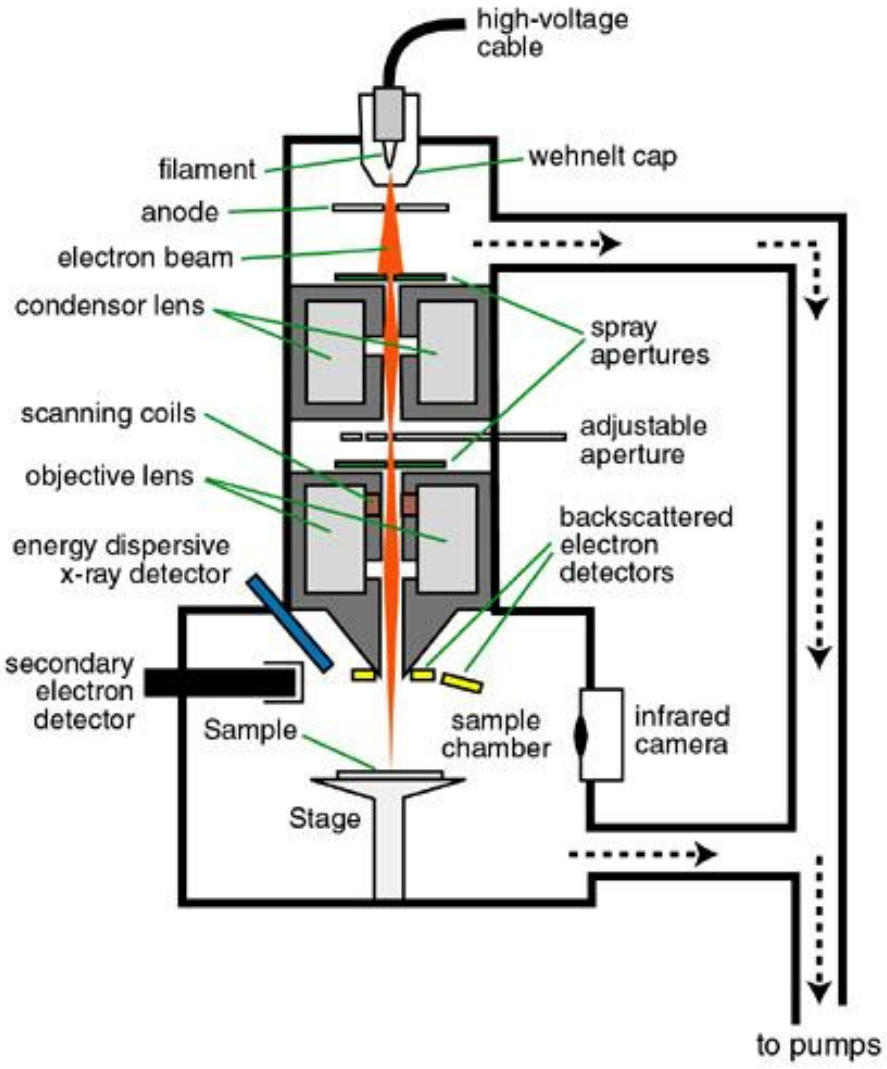

Figure 1.32 Internal structure of scanning electron microscope. Available at - <http://www4.nau.edu/microanalysis/Microprobe-SEM/Images/SEM_schematic.jpg > [Accessed: 27/05/2013]

Interpreting scanning electron micrographs is different from interpreting images obtained directly by bending light or electron rays from the object to image. SEM indirectly constructs a pattern or map that can be interpreted as an image of the object. It is facilitated by many other attributes including visibility, resolution, contrast, focus depth, morphology, apparent illumination and its three-dimensional aspect (Engel et al., 1993). SEM is generally used for different applications in pharmaceutical industries ((Engel et al., 1993) including: deposits and wear debris analysis, quality control checks, shape and distribution statistics of particles, failure analysis, contaminant analysis and particle sizing and characterisation.

A2.5 X-ray powder diffraction (XRPD)

About 95% of all solid materials can be described as crystalline and when X-rays interact with a crystalline substance a diffraction pattern is obtained. X-ray diffraction relies on the dual wave/particle nature of X-rays to discover information about the structure of crystalline materials. When an X-ray beam hits an atom, the electrons around the atom start to oscillate with the same frequency as the incoming beam (Dittrich et al., 2009). In almost all directions, there will be destructive interference, that is, the combining waves are out of phase and there is no resultant energy leaving the solid sample (Figure 1.34). However, the atoms in a crystal are arranged in a regular pattern, and in very few directions there will be constructive interference. The waves will be in phase resulting in well-defined X-ray beams leaving the sample in various directions. Hence, a diffracted beam may be described as "a beam composed of a large number of scattered rays mutually reinforcing one another" (Brügemann et al., 2004).

The peaks in an X-ray diffraction pattern are directly related to the atomic distances. For a given set of lattice planes with an inter-plane distance of "d" (Figure 1.33), the condition for a diffraction (peak) to occur can be simply written as equation 1.10 which is known as the Bragg's law, after W.L. Bragg, who first proposed it (Ayensu., 2012).

$$2\,d\sin\theta = n\lambda \qquad \text{Equation 1.10}$$

Where λ is the wavelength of the X-ray, θ the scattering angle, and n an integer representing the order of the diffraction peak.

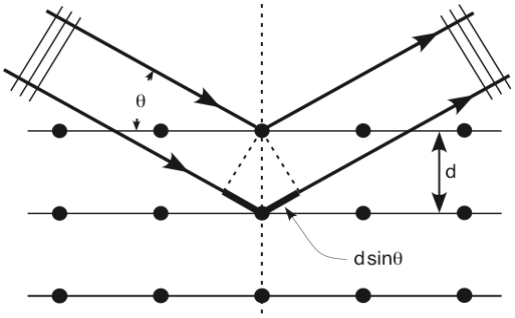

Figure 1.33 The relationship between atomic lattice planes and x-ray diffraction pattern (Ayensu, PhD thesis, 2012)

The main application of powder X-ray diffraction is to provide solid phase fingerprints that occasionally might be used to determine crystal structure (Dittrich & Bieniok., 2009). The non-destructive nature of XRPD makes it a useful technique for systematic drug-excipient

analysis in pre-formulation studies. To evaluate and determine the presence of solvent molecules in the lattice or change in density between polymorphs, a comparison between the cell volume and other crystalline forms will be beneficial (Geandier et al., 2012). Unique XRPD patterns of polymorphs and screening different polymorphs of a particular compound can differentiate one form from another. Determination of amorphous versus crystallinity by XRPD can be performed via calculation of percentage crystallinity. The measurement and determination depend on volume concentration of amorphous filler to crystalline active matrix in a drug's dosage form (Siddhiqui, et al., 2011). Percentage crystallinity is a critical parameter since it can influence a drug's processing behaviour and its pharmacological performance. All these tests provide information regarding drug stability (Dittrich et al., 2009). XRPD can also present unambiguous information about the formation of polymorphs or hydrates under different environmental (storage or processing) conditions since conditions such as increasing temperature and/or humidity during transport or storage could have a harmful effect on a drug's performance and toxicity.

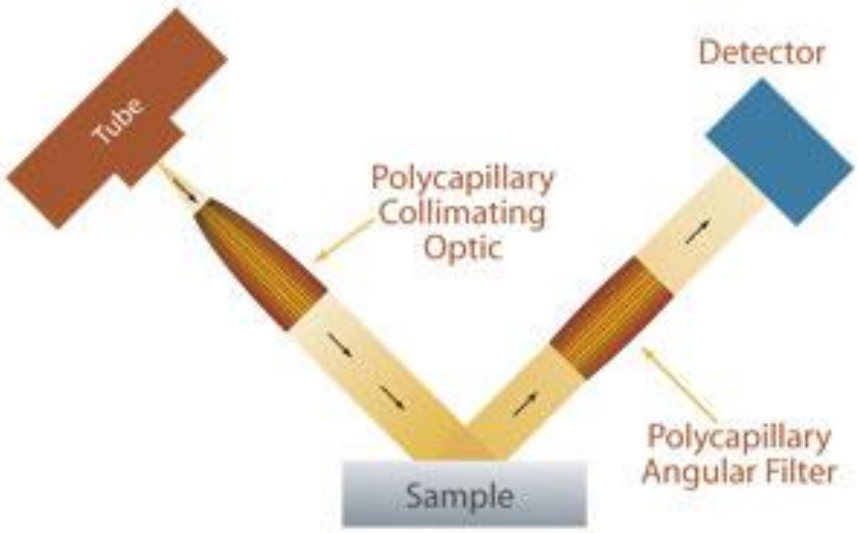

Figure 1.34 Characteristics of X-rays powder diffraction. Available at -
<http://www.xraydiffrac.com/images/xray04-221x318.jpg > [Accessed: 26/05/2013]

A2.6 Fourier transform infrared spectroscopy (FT-IR)

Infrared (IR) spectroscopy is a general term that describes the analysis of any varying signal into its constituent frequency components and is a vital technique used in the pharmaceutical industry. It works on the basis of identifying presence of specific functional groups in a molecule, it can also be used for unique collection of absorption bands to confirm the purity of a compound and subsequently detect the presence of specific impurities.

FT-IR spectroscopy was developed in order to overcome the limitations encountered with dispersive instruments. The main difficulty was the slow scanning process (Harrison et al., 2012). FT-IR offers great advantages such as all sources energy gets to the sample, improving the inherent signal. The distinctive changes that occurs in the wavenumbers of spectral peaks is mainly due the interaction that occur in specific location of the FT-IR. Between the proton-donor and proton-acceptor molecules hydrogen bonds are formed, which then shifts the bands to a lower wavenumber. One possible reason for this is due to the intensity of the hydrogen bond band which depends on the acidity of the hydrogen in the proton-donor and the alkalinity of the proton-acceptor in addition to their possible close contacts (Caykara et al., 2005). Covalent bonds both in donor and acceptor become weak as a consequence of hydrogen bonding whilst the energy barrier for angle deformation increases. The groups involved in hydrogen bond formation, show a decrease in the frequency valence vibration and a simultaneous increase in the frequency of deformation vibration. (Caykara et al., 2005).

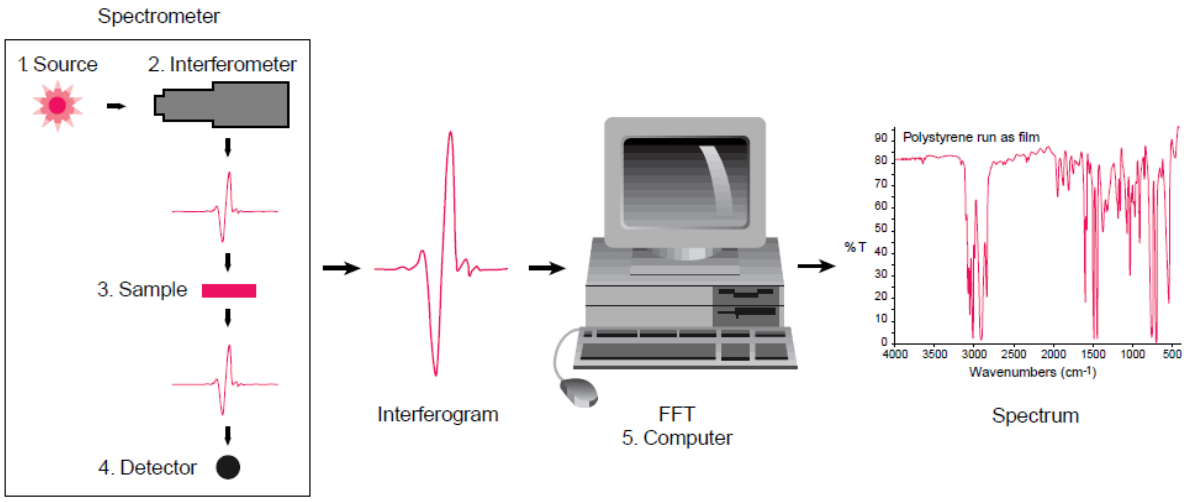

Figure 1.35 Mechanism of Fourier transform infrared spectroscopy. Available at - <http://www.afrinc.com/products/tgplus/fig1.gif> [Accessed: 24/05/2013]

Numerical Fourier analysis gives the relation of intensity and frequency, that is, the IR spectrum. The FT-IR technique can be used to analyse gases, liquids, and solids with minimal preparation (Harrison et al., 2012). The spectrometer may operate in transmission or reflection, but also in attenuated total reflection (ATR) mode, which has been widely used for the last two decades. There are three basic components in an FT-IR system: radiation source,

interferometer, and detector (Figure 1.35). The monochromator in a tradition IR is replaced by an interferometer, which divides radiant beams, generates an optical path difference between the beams (Diaham et al., 2011), and then recombines them in order to produce repetitive interference signals which contain infrared spectral information generated after passing through a sample (Sherazi et al., 2011) (figure 1.36).

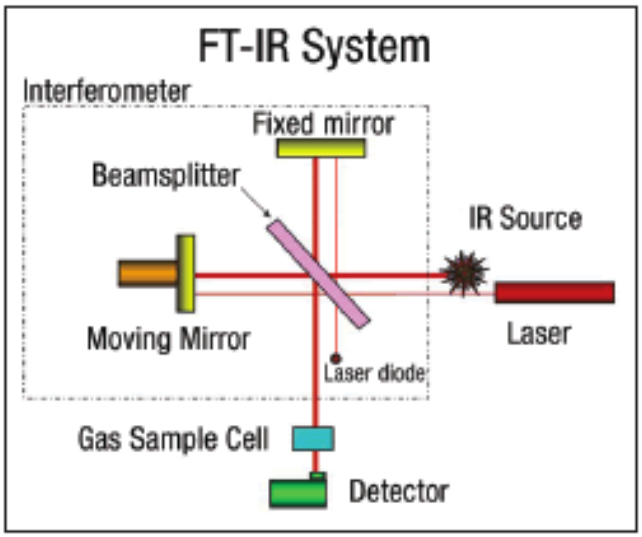

Figure 1.36 Simplified optical layout of a typical FT-IR spectrometer. Available at - <http://www.gasesmag.com/Assets/images/0109/art3fig10.gif> [Accessed: 26/05/2013]

A2.7 Supercritical fluid (SCF) processing

A process for polymeric film and encapsulation extraction is the supercritical carbon dioxide (Herrero et al., 2006). It explores the physical state of gases such as carbon dioxide which are fluids in higher temperatures and higher pressures in comparison to the critical point. At the critical point, distinct characteristic phases (liquid or gases) do not exist and therefore the supercritical phase is, in effect a single phase (Herrero et al., 2006). Unique characteristics of a supercritical liquid are that the density they hold is similar to that of a liquid; however, the diffusion and viscosity are that between a liquid and a gas (Rizvii et al., 1986). Table 1.7 is a comparative table exploring the relative values of such characteristics in terms of the liquid, gas, and supercritical phases of carbon dioxide. Carbon dioxide (CO_2) was chosen as the solvent, instead of an organic solvent, for many reasons (Gomez et al., 2000). CO_2 has minimal adverse health effects, has a low critical point of 73.8 bar and 31.1°C (Sahena et al., 2009). Because of its low critical points, supercritical CO_2 allows for extraction of compounds that may be thermally sensitive (Herrero et al., 2010). CO_2 would readily

evaporate from the extract at ambient conditions; whilst an organic solvent would leave a residual amount behind under the same conditions (Herrero et al., 2006). Supercritical CO_2 ($scCO_2$) has been used to decaffeinate coffee beans, extract aromas from spices, extract lipids, create porous polymers and in the cold sterilization of hydrogels (Baker et al., 2009; Cooper et al., 2001; Favati et al, 1988; Jimenez et al., 2008).

Table 1.7 Generalized physical properties for gas, liquid, and supercritical fluids

Mobile Phase	**Density (g/cm^3)**	**Viscosity (µPa-s**	**Diffusivity (cm^2/S)**
Gas	-10^3	$0.5\text{-}3.5 \times 10^{-4}$	0.01-1
SCF	0.2-0.9	$0.2\text{-}1.0 \times 10^{-3}$	$0.1\text{-}3.3 \times 10^{-4}$
Liquid	0.8-1.0	$0.3\text{-}2.4 \times 10^{-2}$	$0.5\text{-}2.0 \times 10^{-5}$

The density values of SCFs enable substantial solvation power. Table 1.7 shows that a supercritical fluid has the ability to have a higher mass transfer rate than a liquid solvent (Rizvii et al., 1986) due to the higher diffusivity through solutes because of their lower viscosity in SCF. The solubilising power of SCF can be altered by small changes in operating conditions or by the addition of co-solvent.

The mild operating conditions of low temperature and pressure make SCF attractive for pharmaceutical research, processing thermolabile or sensitive materials including biologics. SCF is also safe, environmentally friendly and economical. There are different SCF processes as shown below -

- SCF acts as a solvent: Rapid expansion of supercritical solvent (RESS) process.
- SCF acts as anti-solvent: Supercritical anti-solvent (SAS),
- Gas anti-solvent (GAS),
- Precipitation with compressed anti-solvent (PCA),
- Solution enhanced dispersion (SEDS) process.
- SCF acts as a plasticising/ swelling agent: Particles form gas saturated solution (PGSS) and related processes (CO_2- assisted aerolization processes)
- SCF can also act in coating processes.

Supercritical carbon dioxide instrument as seen in figure 1.37 can be divided in to three units. 1. CO_2 supply, 2. The reaction vessel and 3. The control unit.

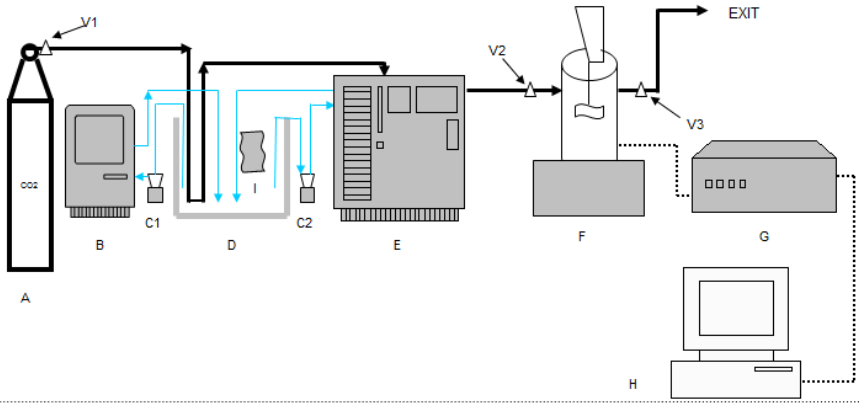

A- Liquid CO2 Cylinder
B- Cooling Unit
C1, C2- Water Pumping Units
D- Water Bath
E- Liquid CO2 Pumping Unit
F- Reaction Vessel
G- Control Unit
H- Display
I- Heating Unit
V1, V2, V3- Valves
CO2-
Water -

Figure 1.37 Schematic presentation of lab SCF instrument

The parameters of the experiment such as the temperature and pressure values can be assigned and monitored by the control unit (G) and display (H). The depressurisation of CO_2 is also controlled by the two units G and H.

APPENDIX B: AMORPHOUS AND CRYSTALLINE % RATIOS

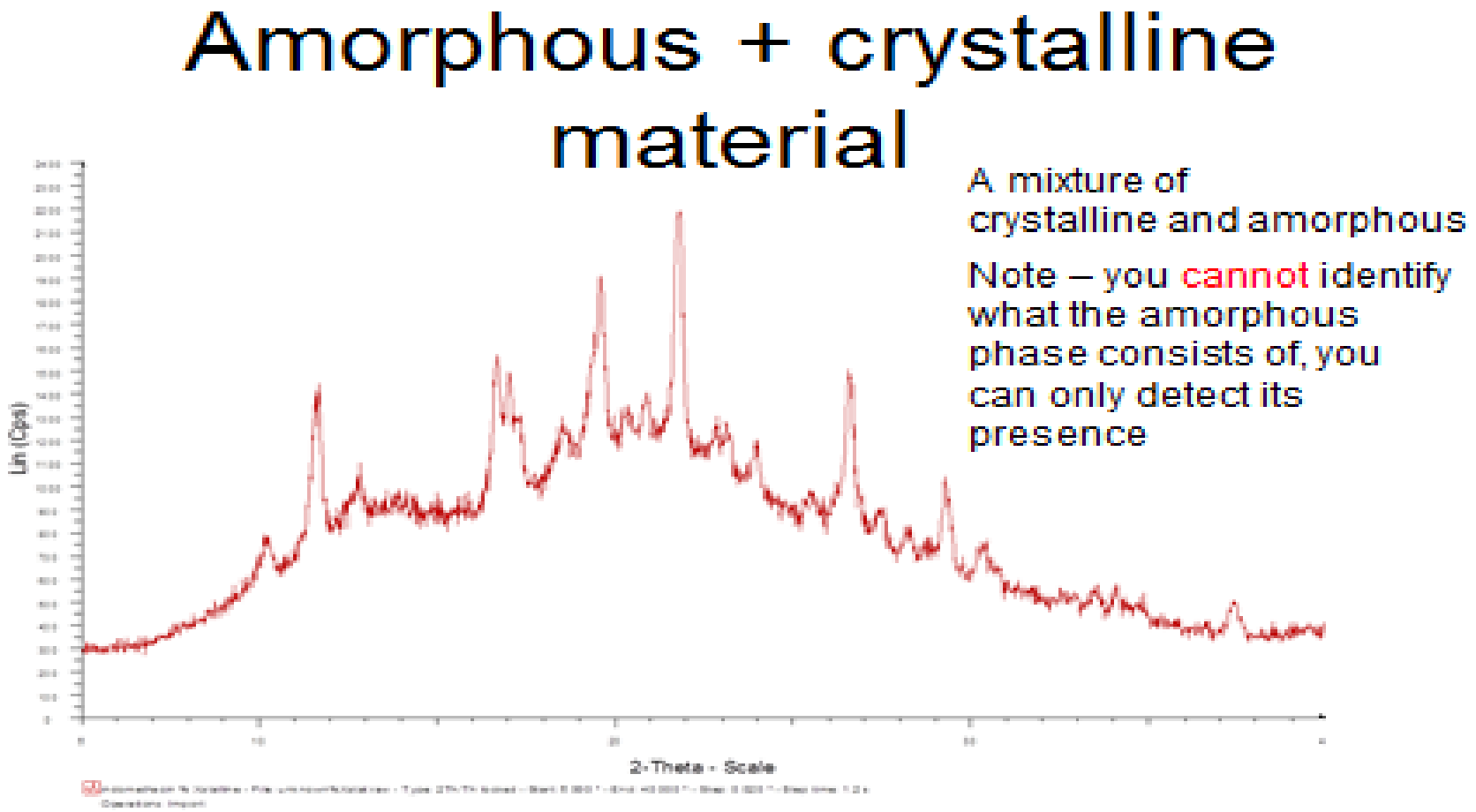

Quantification

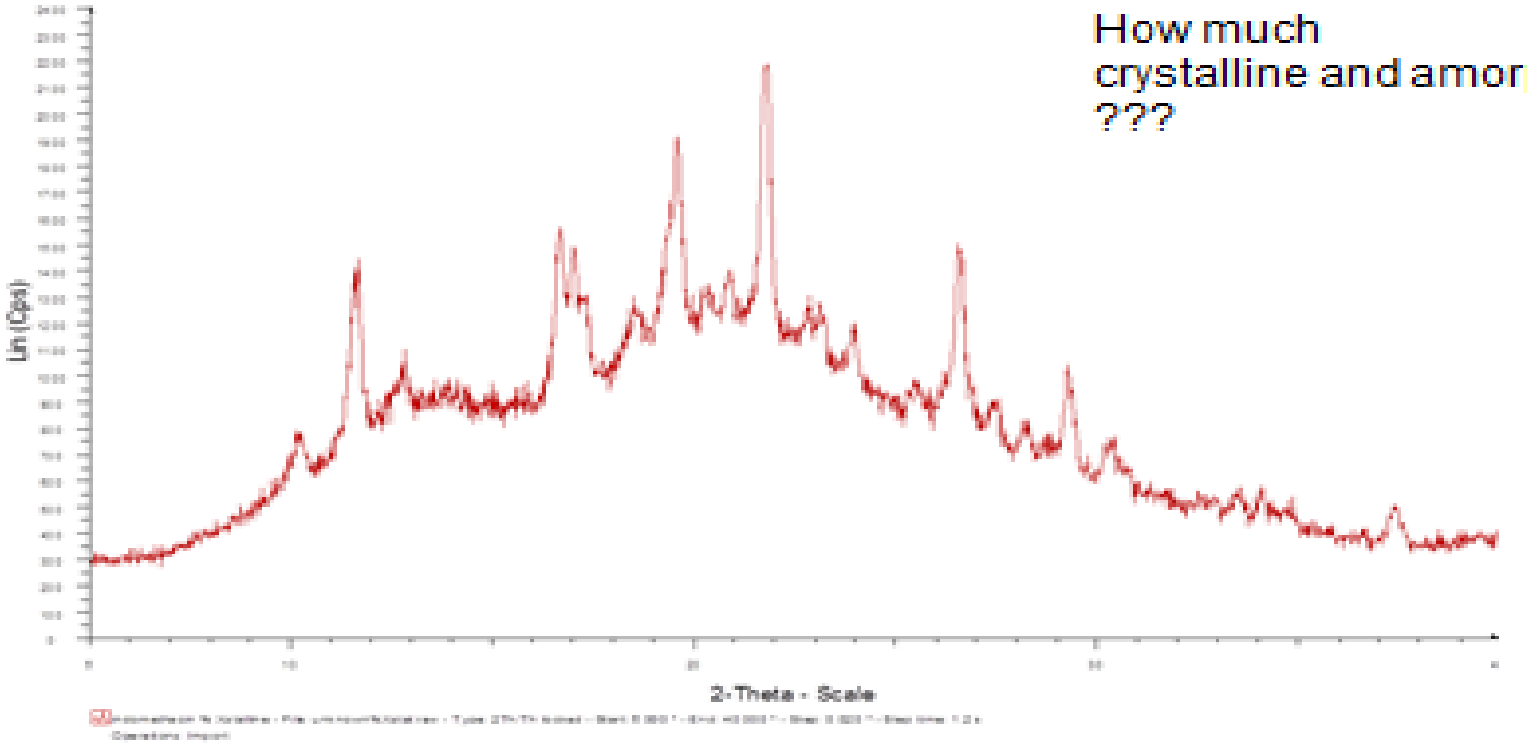

Quantification

- Method for quantifying % crystallinity
  - Measure the areas under the curves and ratio
    - The total area under the curve = amorphous+crystalline components
    - The area of the peaks only = crystalline component
    - Measure the total area, subtract amorphous background to give crystalline peaks
    - Measure crystalline area
    - Ratio the results to give % crystallinity

Quantification - ratios

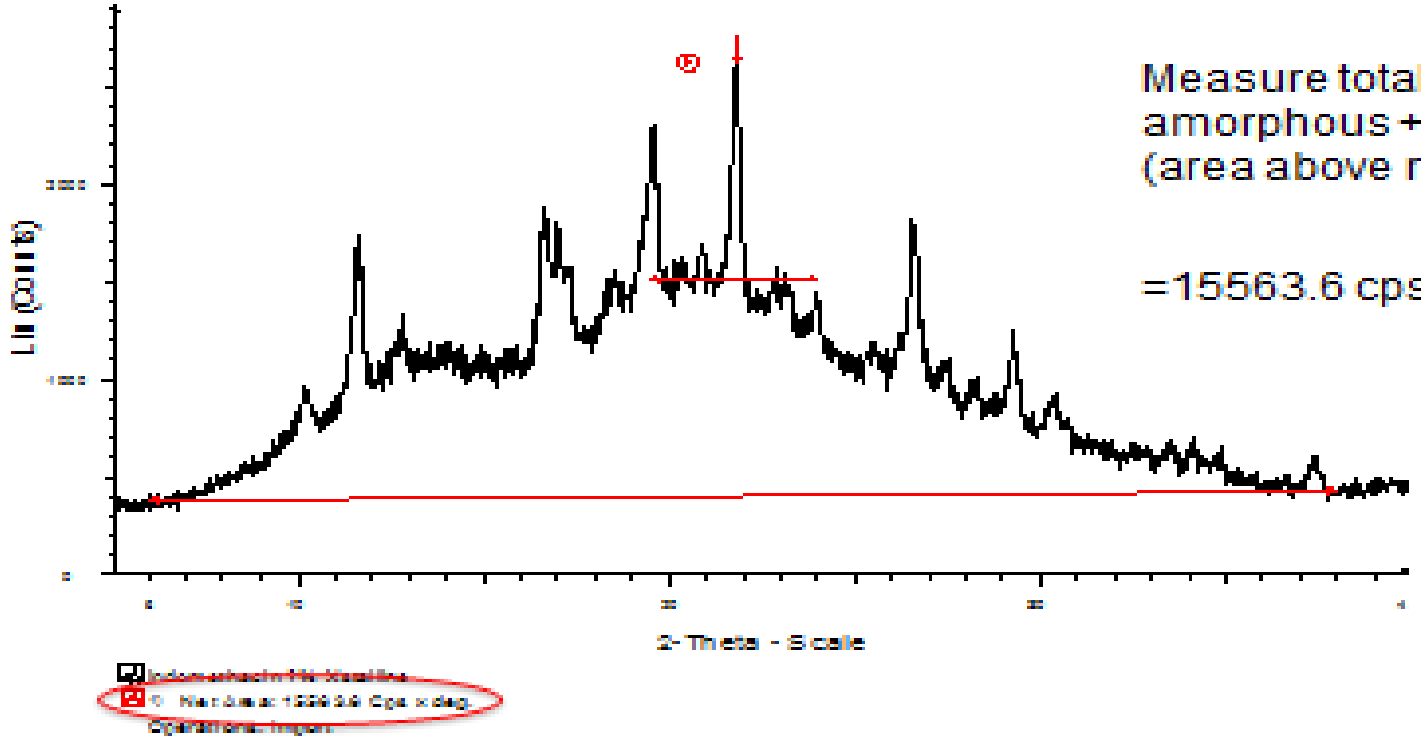

Measure total area amorphous + crystalline (area above red line)

=15563.6 cps x deg

Quantification - ratios

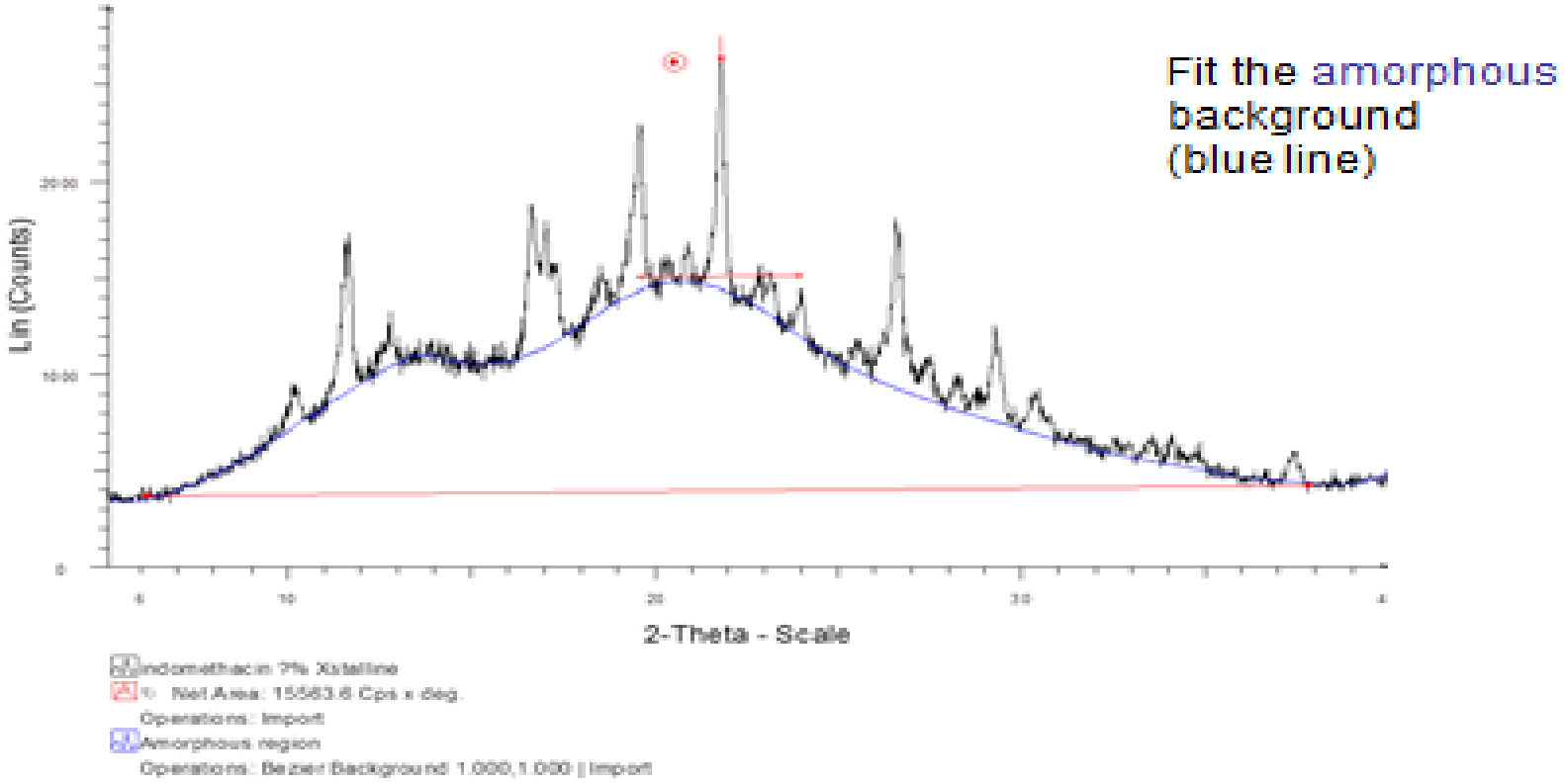

Quantification - ratios

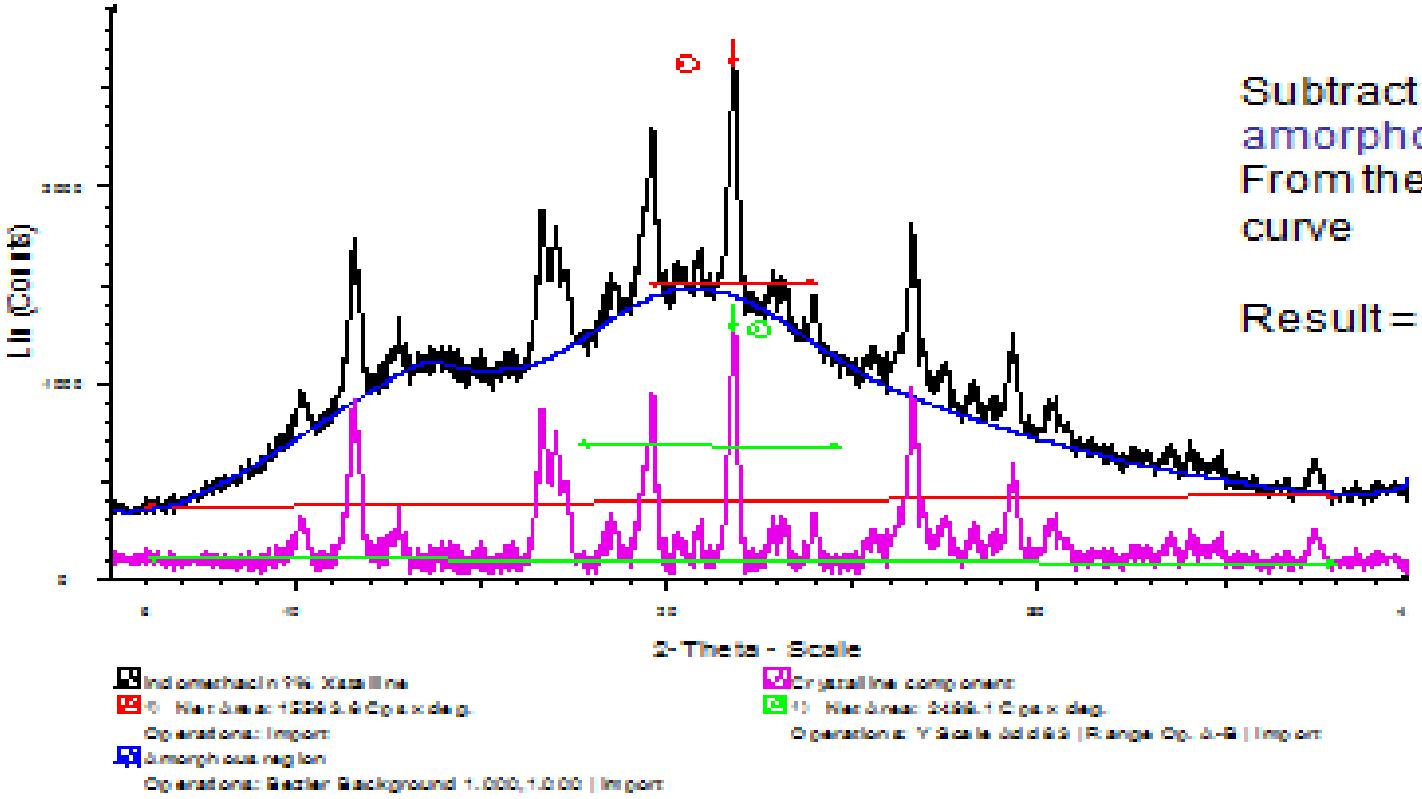

Quantification - ratios

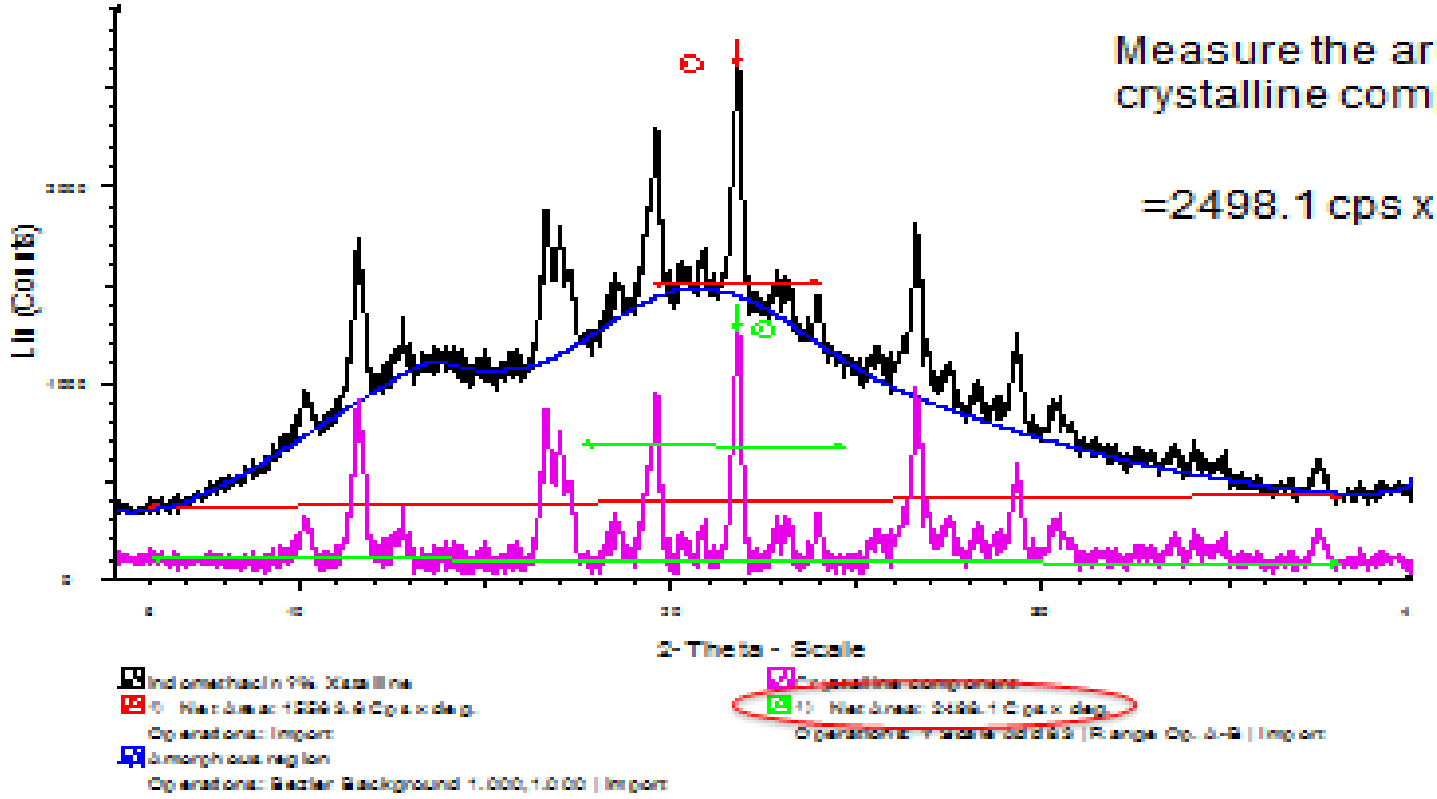

Quantification - ratios

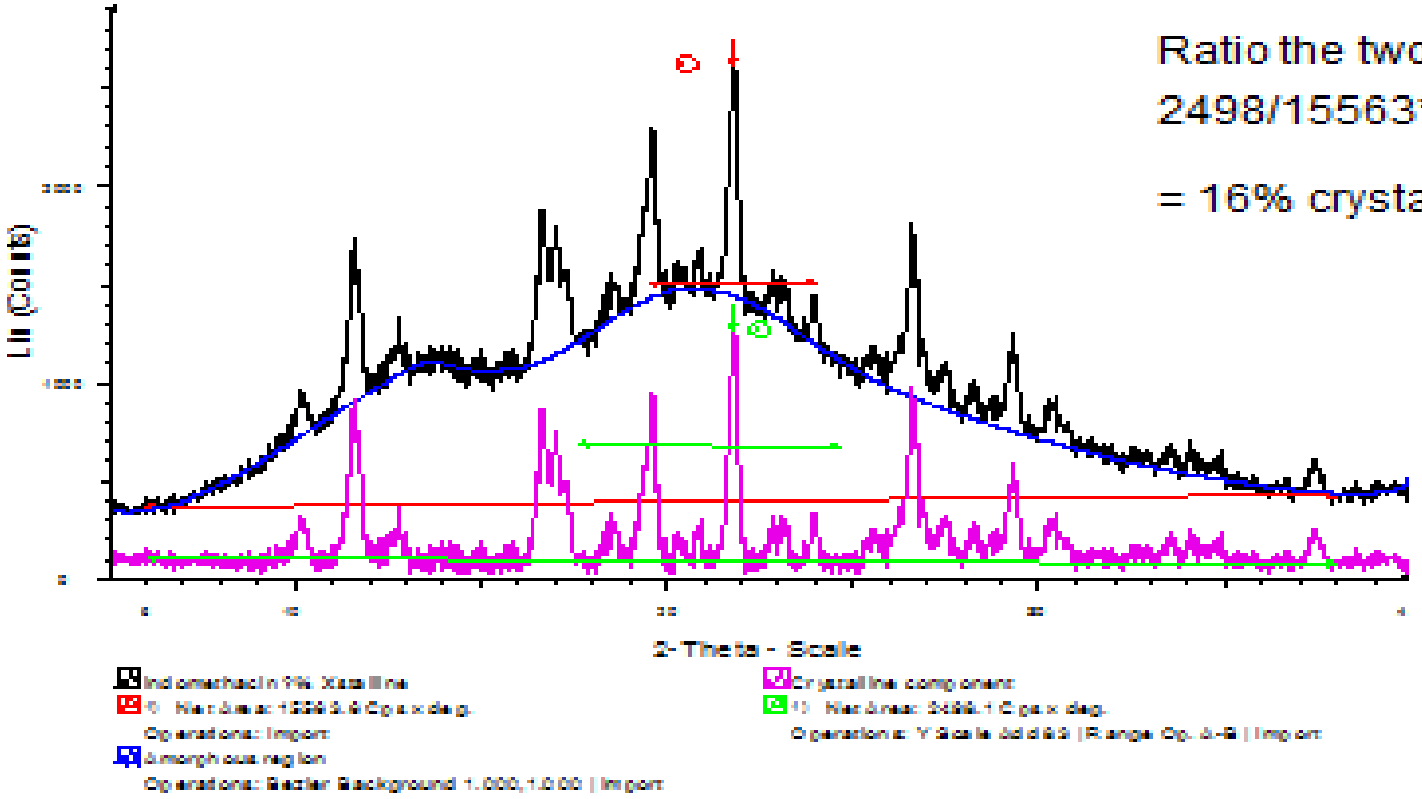

APPENDIX C: REPRESENTATIVE HPLC CHROMATOGRAMS SHOWING POTENTIAL OME BREAKDOWN IMPURITIES

Stability 0 days

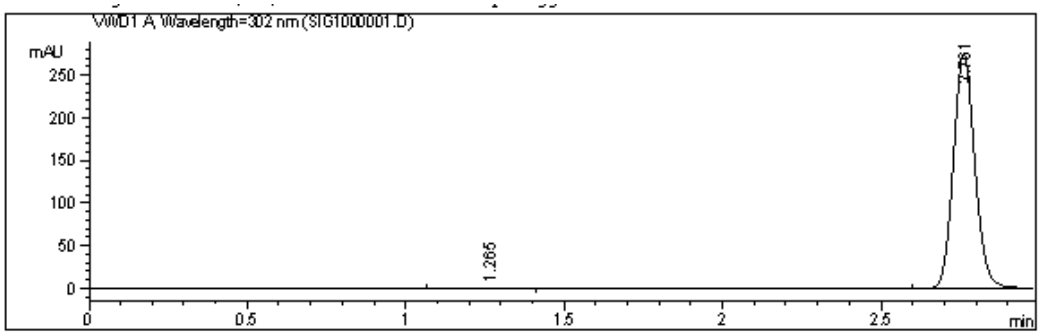

Stability 14 days (oven)

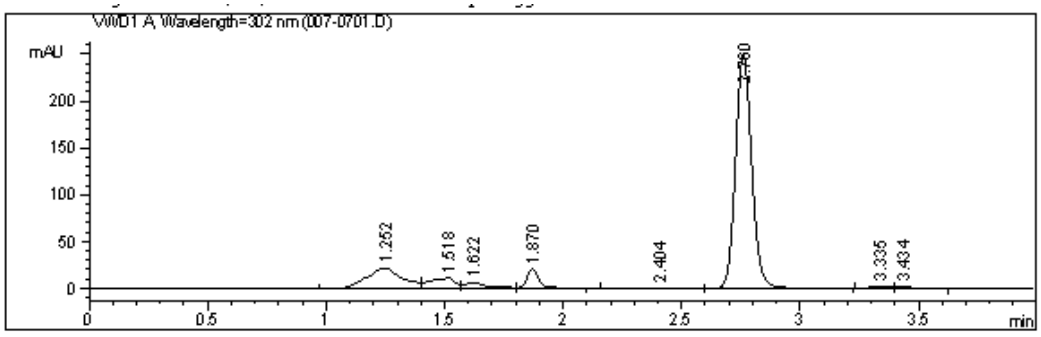

Stability 14 days (room)

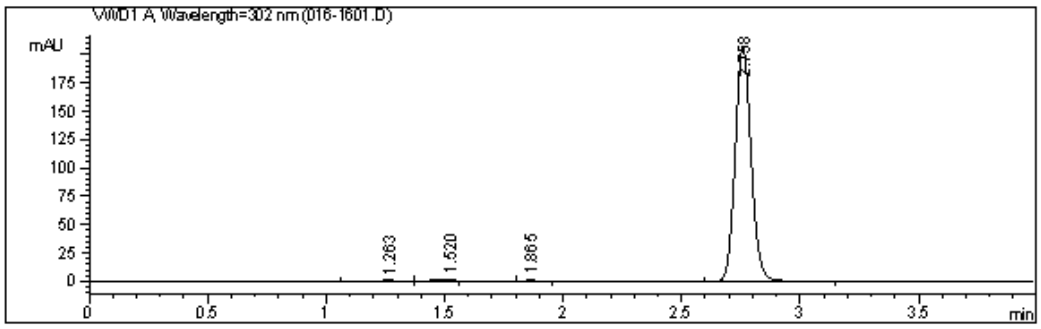

Stability 28 days (oven)

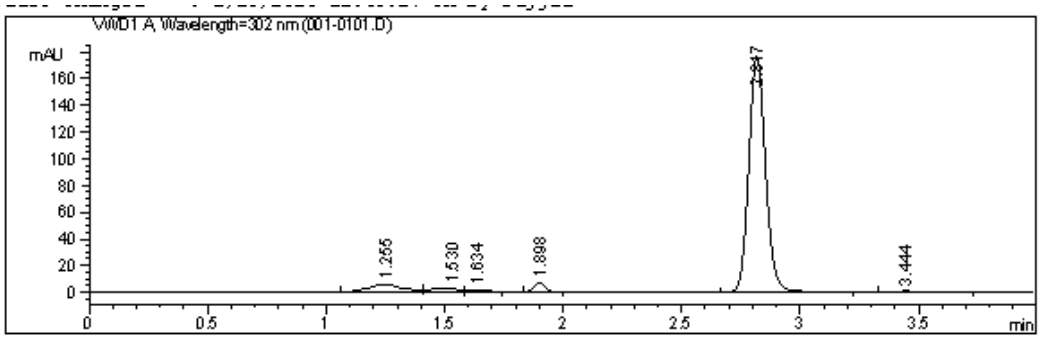

Stability 28 days (room)